No. 120
October 1971

Small Craft Engineering: Resistance, Propulsion, and Sea Keeping

Finn C. Michelsen
Joseph L. Moss
Joseph Koelbel
Daniel Savitsky
Howard Apollonio

Department of Naval Architecture

No. 120
October 1971
Reprinted January 1975
Reprinted March 1977

SMALL CRAFT ENGINEERING

RESISTANCE, PROPULSION, AND SEA KEEPING

Finn C. Michelsen/James L Moss
Naval Architecture & Marine Engineering
University of Michigan

Joseph Koelbel, Jr
Naval Architect

Daniel Savitsky
Davidson Laboratory
Stevens Institute of Technology

Howard Apollonio
Jacuzzi Brothers

Department of Naval Architecture
and Marine Engineering
College of Engineering
The University of Michigan
Ann Arbor, Michigan 48104

Page

The section on behavior in a seaway begins on page 179. The section on waterjet propulsion begins on page 256. Each of these sections has its own table of contents immediately preceding these pages.

FUNDAMENTALS OF RESISTANCE AND PROPULSION

Finn C Michelsen
James L Moss
The University of Michigan

1. GENERAL

Resistance in the present context may be defined as the force tending to resist the motion of a body through a fluid. Stated differently, the resistance is the component in the direction of motion of the total force acting on a body. Ships and small craft usually operate at the interface of two fluids, the air and the water. The major exception would be deeply submerged submarines. Air cushion vehicles and hydrofoil craft operate at the interface but will be specifically excluded from this treatise. We shall confine our attention to surface type displacement or planing craft. In these vessels, hydrodynamic forces predominate and will be given appropriate emphasis here.

In order to examine resistance in detail we shall consider two concepts: a) the forces acting on the body, and b) the modes by which energy is dissipated in the water. More simply, what is the effect of the water on the vehicle and what is the effect of the vehicle on the water?

Although it is not explicit in the title to this section, we shall be looking at lifting forces as well as resistance forces. Lift may be defined as the resultant force component that acts at right angles to the resistance force. The vector sum of resistance and lift is the total force.

For the typical boat, proceeding at a constant speed on a straight line in smooth water, the resistance force will be in the horizontal plane and the lift force will be in the transverse plane. Moreover, the lift force will be vertical if the boat geometry is symmetric port and starboard. We shall confine our discussion to this case, but there are other cases of importance. These include steady-state turning (where the lift force may no longer be vertical) and the non-steady-state case of the boat proceeding in waves.

2. HYDRODYNAMIC FORCES ACTING ON A BODY

Referring to Figure 1.1, the total hydrodynamic force, F, is acting on the elemental surface area, dA. The orientation in space of the force F is arbitrary relative to the coordinate system. The positive x-axis is in the direction of motion of the body of which dA is a part. The positive y-axis is to port and the positive z-axis is vertical upwards.

The total force, F, may be decomposed into two mutually orthogonal forces, T and N, where T is the component tangential to the surface, dA, and N is normal to the surface.

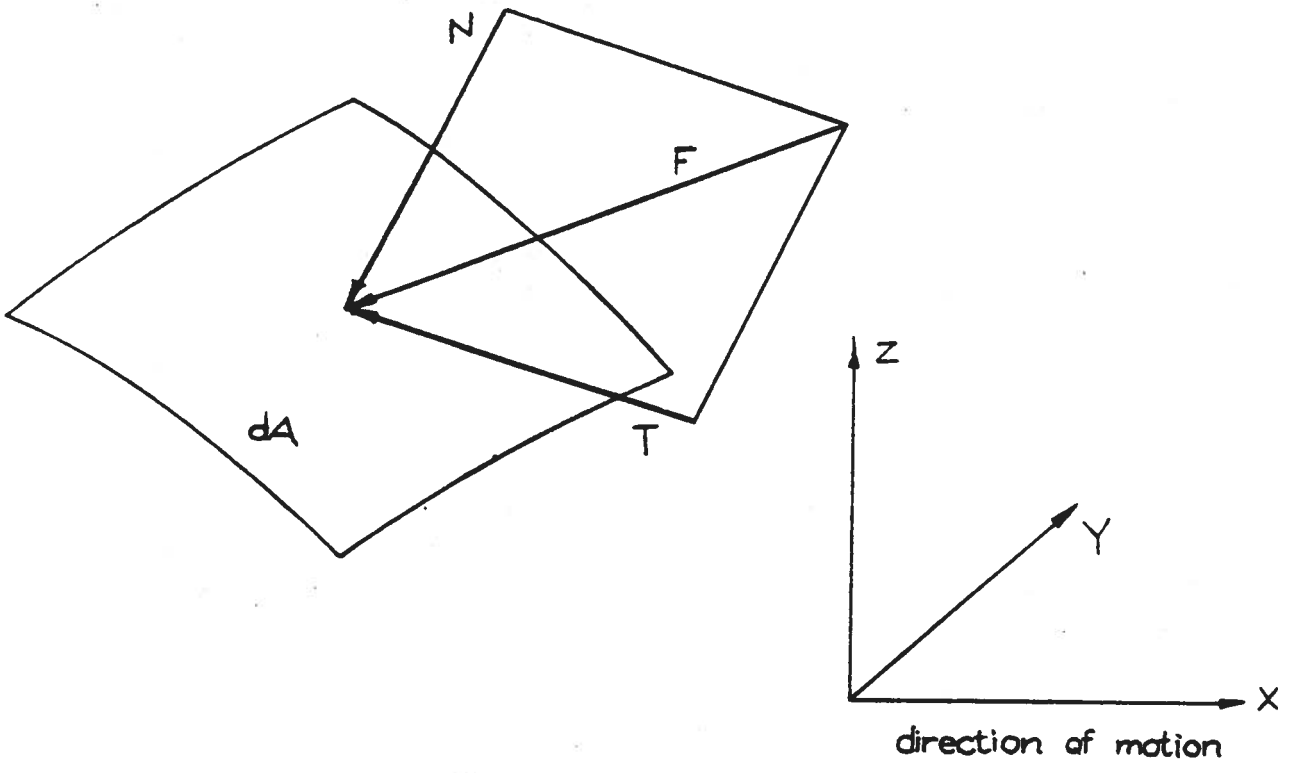

Figure 1.1. Tangential and Normal Force Components.

The sum of the components of N and T in the direction of motion integrated over the body must equal the resistance, R.

$$R = \int_A (T_x + N_x)dA \qquad (1.1)$$

For the symmetric case, the hydrodynamic lift becomes

3. FORMS OF RESISTANCE: MODES OF ENERGY DISSIPATION

3.1 GENERAL

The concept of forces acting on a body being either tangential or normal to the body lends itself to an understanding of the modes of energy dissipation. The force associated with a particular energy loss, taken in the direction of motion, is the resistance component of concern.

Resistance components may be listed as:

1. Eddy resistance: the force associated with the energy lost in generating eddies which move into the downstream flow.

2. Frictional resistance: the force associated with the shearing action of the water within the boundary layer.

3. Wave resistance: the force associated with the energy that is continuously supplied to the free wave system left behind by the boat.

Both the eddy and frictional resistances are due to the viscous properties of the water.

3.2 EDDY RESISTANCE

Eddies are shed abaft exposed appendages such as open shafts on power boats and may also be generated by too drastic a curvature or a discontinuity in hull form in the direction of the flow. The flow behind a transom stern on a conventional power boat proceeding at low speed is a good example of eddying.

In an ideal fluid,* Figure 1.2a, a body experiences only normal pressure forces. The components of pressure on the forebody taken in the direction of motion resist the motion while those on the afterbody assist the motion. When the pressures on both the forebody and afterbody are integrated, the result is that no net force opposes or assists the motion. That is, in an ideal infinite fluid it can be shown that the body experiences no resistance to motion. This is known as D'Alembert's paradox. However, when the viscous properties of the real fluid, Figure 1.2b, are taken into account, we find that a modification of the pressure field around the body takes place. A boundary layer is formed and possibly some eddies are shed. The effect of these viscous alternations to the pressure field is generally to reduce the pressures acting on the afterbody. The forebody pressures are altered only insignificantly. With

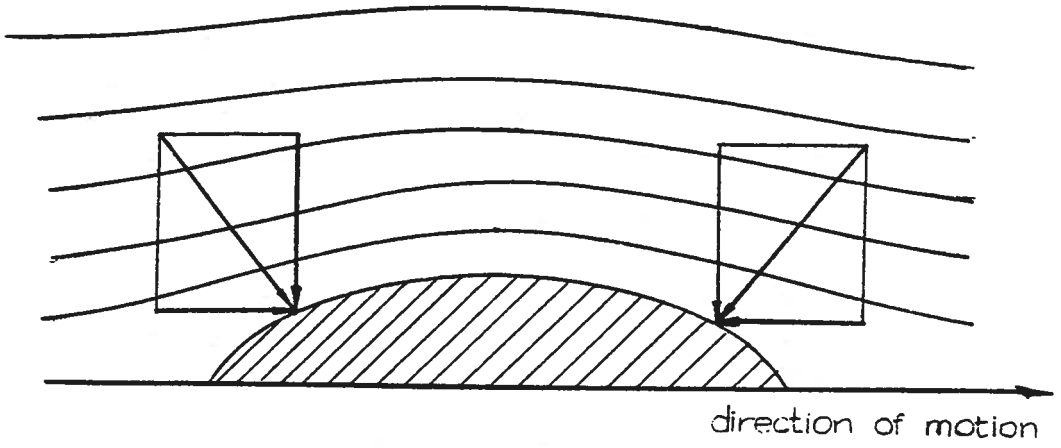

Figure 1.2a. Flow around a body in an ideal fluid.

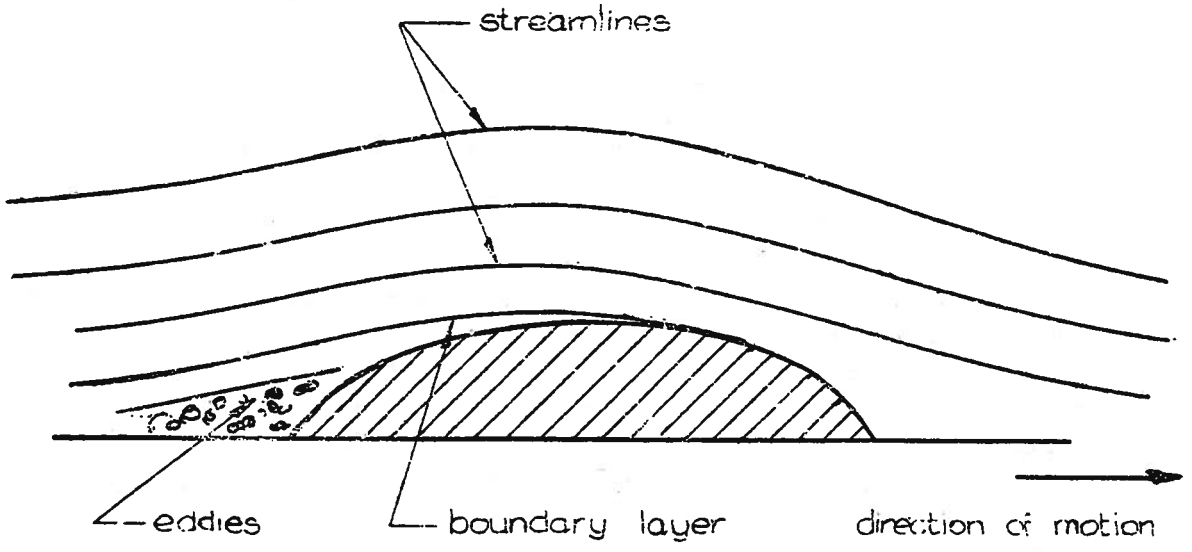

Figure 1.2b. Flow around a body in a real fluid.

reduced pressures on the afterbody and only small changes in pressures on the forebody, the integrated pressure component in the direction of motion leads to a resultant force tending to resist the motion of the body. This force is commonly called form drag or viscous pressure drag.

3.3 FRICTIONAL RESISTANCE

The force associated with the shearing flow in the boundary layer on an arbitrary body is difficult to obtain precisely. Simplifying assumptions and empirical equations are used to estimate the frictional or skin-friction resistance. These equations are based on measurements of forces on flat plates at zero angle of incidence to the flow and have been largely substantiated by comparison with frictional forces obtained theoretically. Since boundary layers on ships and small craft are known to be turbulent, only turbulent boundary layers need to be considered.

The skin friction force may be calculated by the method of von Kármán, using the principle that the shear force at the wall must equal the change in momentum within the control volume bounded by abcd in Figure 1.3. The result for steady flow on the flat plate is

$$\tau = \frac{d}{dx}\left[\rho \int_0^{\delta_o} u(U - u)dy\right] \qquad (1.4)$$

where
- τ is the shearing stress at the wall
- ρ is the density of water
- x is the distance along the plate from the leading edge
- U is the free stream velocity
- u is the velocity within the boundary layer at a distance y from the wall
- δ_o is the thickness of the boundary layer

It is clear that in order to solve Equation (1.4) the relationship between u and y, or the boundary layer velocity gradient, is required. Measurements of flat plate boundary layer velocity gradients have been made by many investigators in the past (Shultz-Grunow, Froude, Kempf, Gebers.) A comprehensive set of modern data was obtained by Smith and Walker (Reference 1) and was found to be in good agreement with the earlier data of Shultz-Grunow and Kempf. In using the Smith and Walker data one should make slight corrections, as recommended by Landweber (Reference 2).

Boundary layer theory has also provided functional relationships for the velocity gradient close to and farther away from the wall. These are known as the inner and outer laws of the boundary layer. For the inner law we have

$$\frac{u}{U_\tau} = f\left(\frac{U_\tau y}{\nu}\right) \tag{1.5}$$

and for the outer law

$$\frac{U - u}{U_\tau} = F(y/\delta) \tag{1.6}$$

where

$$U_\tau = (\tau/\rho)^{\frac{1}{2}}$$

ν = kinematic viscosity

Von Kármán assumed a velocity distribution function that satisfied both the inner and outer laws when the right conditions were imposed on the functions f, Equation (1.5) and F, Equation (1.6). With von Kármán's velocity distribution substituted into the momentum integral of Eqution (1.4) the expression for the skin friction resistance of a flat plate under turbulent flow becomes

$$C_F^{-\frac{1}{2}} = A + B \log_{10} (R_n C_F) \tag{1.7}$$

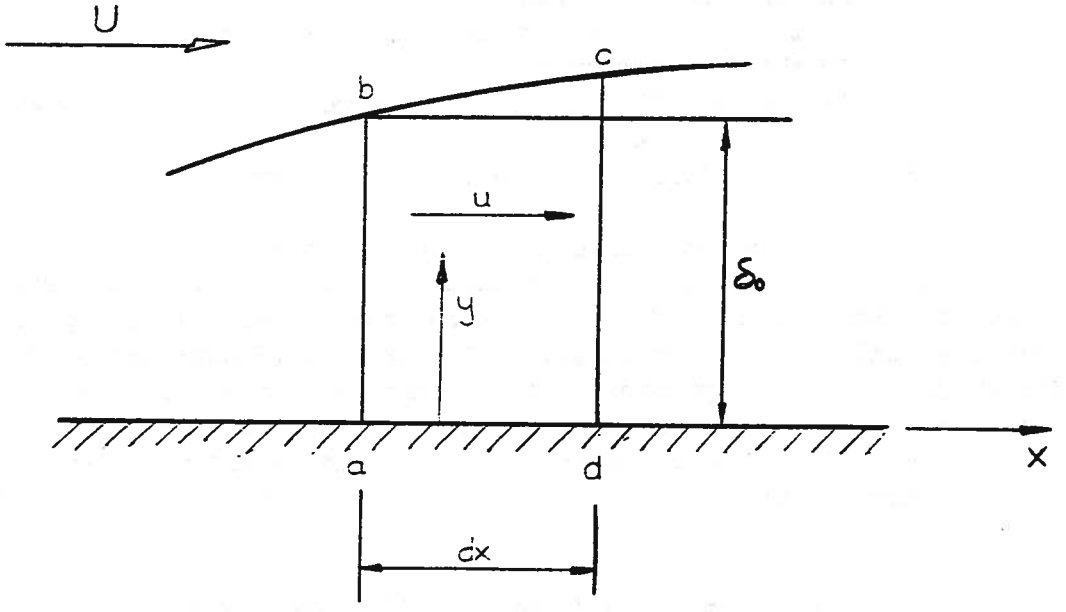

where A and B are constants to be determined experimentally,

C_F = frictional resistance coefficient = $R_F/\frac{\rho}{2} SU^2$

R_F = frictional resistance

S = wetted area of the plate

$R_n = UL/\nu$

L = length of the plate

The significance of the Reynolds number will be discussed in a later section.

Schoenherr (Reference 3) found that the data available in 1932 could fit Equation (1.7) well if A = 0 and B = 4.13. Accordingly, the now famous Schoenherr friction formulation is

$$\frac{0.242}{\sqrt{C_F}} = \log_{10} (R_n C_F) \qquad (1.8)$$

Other frictional resistance formulas have been proposed, but the Schoenherr formula is much used in ship and small craft design.

3.4 WAVE RESISTANCE

The subject of wave resistance has received intensive research for many years, going back to the now-classic work of Froude in the 1870's and the classical paper on the linear theory of Michell published in 1898. Wave resistance is the component of resistance over which the naval architect has the most control. On high speed craft, wave resistance often contributes the major share of the total resistance. Therefore, the incentive is great to find means of reducing this resistance component.

The nature of ship produced waves needs to be understood before one can analyze the resistance caused by the energy lost in these waves. Kelvin's classical explanation for the formation of ship-produced waves is as follows. Consider a pressure point moving on a straight line across the water surface. A wave pattern as shown in Figure 1.4 will result. In the figure, the pressure point is located at the origin of the

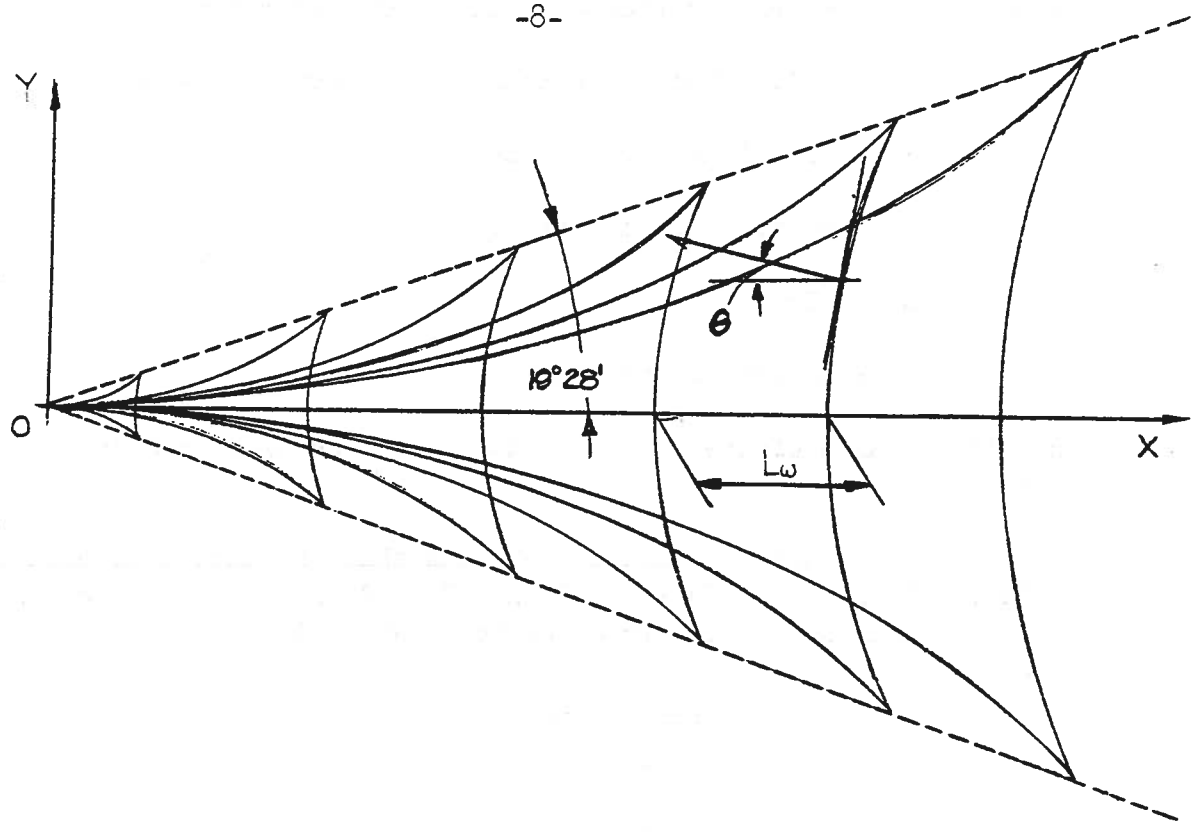

Figure 1.4. Kelvin Wave Pattern

coordinate system, the solid curved lines represent wave crests and the spaces between the lines are wave hollows. Two types of waves are present; the transverse waves which cross the x-axis at right angles, and the diverging waves. The intersections of the transverse and diverging waves form cusps, points at which the highest wave elevations occur. The cusp line, or dotted line in Figure 1.4, is oriented at an angle of 19°28' with the x-axis according to Kelvin's theory. The distance between successive crests on the x-axis, i.e. the transverse wave-length, is the same as that for a free wave traveling in deep water at the velocity of the moving pressure point.

$$L_w = \frac{2\pi V^2}{g} \qquad (1.9)$$

Kelvin's theory also showed that the amplitudes of each wave crest decrease proportionally to the square root of the distance from the pressure point.

Observations of the actual wave formations largely substantiate the theory of Kelvin, but with some modifications. First, a water-borne craft is not a pressure point moving on the free surface. It is rather, a pressure surface at and below the free surface. For conventional displacement hulls, such as cargo ships and passenger liners, waves are considered to emanate from four general areas of the hull; the extreme bow, the fore shoulder, the aft shoulder and the extreme stern. The resulting total wave system is confused. Nevertheless, the Kelvin wave pattern is often easily discernible, particularly in the waves generated by the bow and, to a somewhat lesser extent, in the waves generated by the stern. Wave observations also show that the relative predominance of the divergent and tranverse components is a function of hull speed and form. Slow speed barges generate tranverse waves almost exclusively and high speed hulls generate predominatly divergent waves. Angles as great as Kelvin's 19°28' are rarely observed.

Higher speeds usually produce smaller angles. Taylor (Reference 4) tells of Hovgaard's observations of angles as low as 11° for a high speed torpedo boat. Detailed measurments of the waves produced by prismatic planing surfaces have been made at the Davidson Laboratory (Reference 5) from which Figure 1.5 is typical. In the figure, the elevations are given only for the area aft of the step, but other waves produced by planing craft are usually insignificant by comparison. An intuitive feeling for the tremendous significance of the wave resistance of fast boats can be obtained from the figure when one considers that total wave amplitudes of nearly one-half beam are typical. For moderate sized boats this can amount to a wave several feet in height and a correspondingly great amount of energy that must be imparted to the water to produce such a wave.

There are four independent means of determining the wave resistance:

1. Determine the energy lost in the free wave system. Free waves are those that are left behind by the boat, which must do work upon the water in order to continuously supply the energy expended in the waves. There are also local waves, which are distortions of the free surface by the pressure field generated by the boat. These waves travel with the boat and do not require a continuous replenishment of energy. Therefore, the local waves do not contribute to the wave resistance. The energy lost in the free wave system can be determined experimentally, by measurement of the elevations of waves produced by

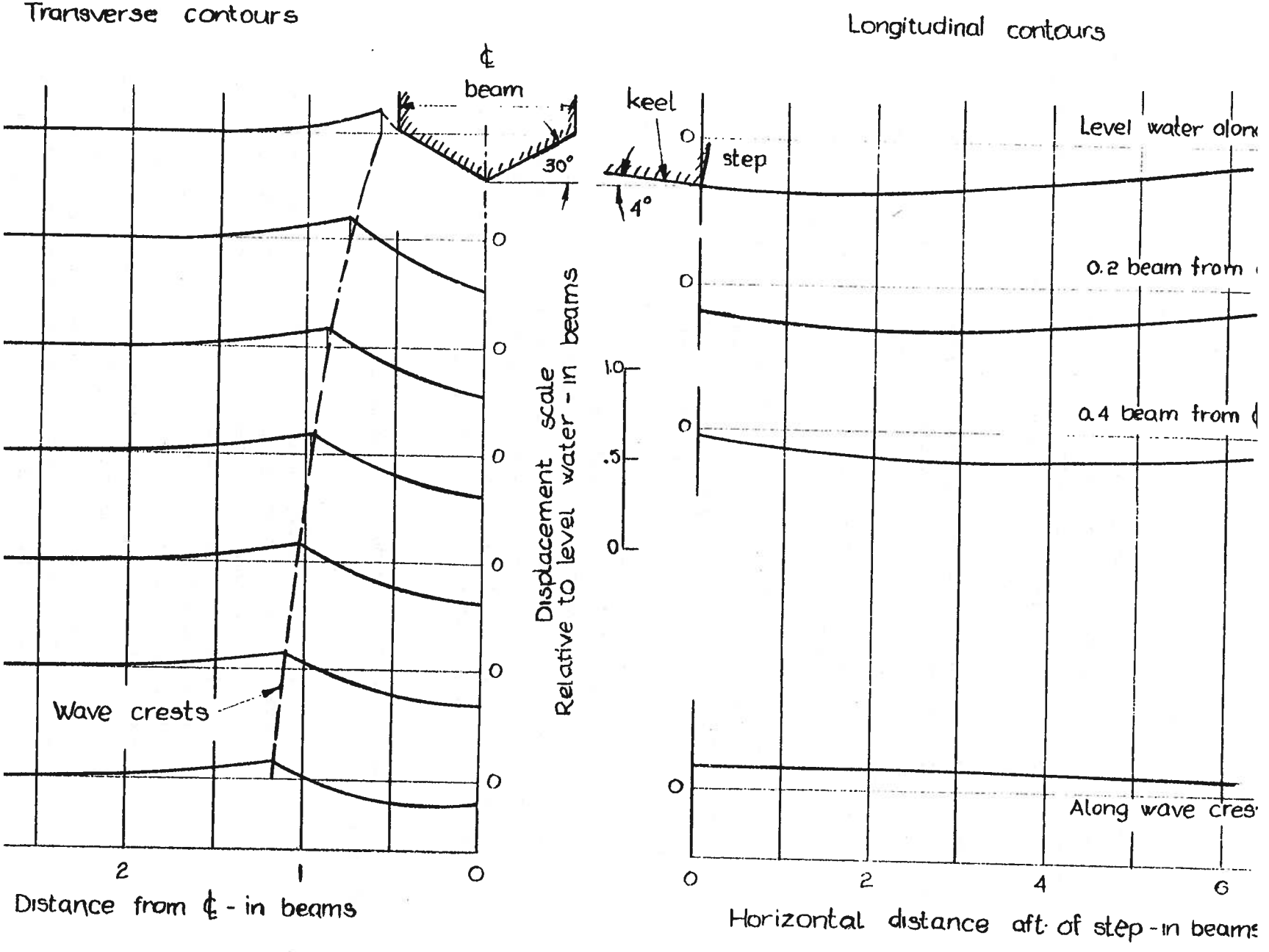

Figure 1.5. Experimental Wave Contours behind a planing prism.

2. Calculate the wave resistance using singularities such as sources and sinks* to express the shape of the hull. The most simple example of a body generated by sources and sinks is the ovoid shown in Figure 1.6. The source and sink are of equal intensity, or strength. That is, all of the fluid emitted by the source is taken in by the sink. When superimposed on the uniform velocity, the streamlines take the form shown in the figure where the heavy line indicates the boundary of the resulting closed body. One form of a wave resistance calculation is the equation of Havelock

$$R_w = \pi\rho V^2 \int_0^{\pi/2} A^2(\theta) \cos^3\theta \, d\theta \qquad (1.10)$$

where $A(\theta)$ is an amplitude function determined by the singularity distribution which expresses the hull. The integration variable, θ is oriented as shown in Figure 1.4. Calculations of this type are extremely difficult to perform even for simplified hull forms. They continue as the subject of extensive research.

3. Integrate measured pressures on the hull. We have seen that in an ideal fluid the value of the integral will be zero for the deeply submerged case. However, when the hull is on, or in the vicinity of the free surface, the integral will have a finite value to account for the wave energy being supplied. In a real fluid the value of the integral will also account for the eddy resistance, or viscous pressure resistance, as was shown in Figure 1.2. Therefore, in practice one determines not only the wave resistance but the viscous pressure resistance as well. Both taken together are known as the total pressure resistance and correspond to the N_x contribution in the integral in Equation(1.1). For the simplified planing hull, or planing prism, the total pressure resistance can be determined directly from our knowledge of planing mechanics. This point will be elaborated upon in the discussion of prismatic planing surfaces in Chapter 3. For more complicated hull forms, as most displacement craft are, it is necessary to conduct an experiment whereby a complete pressure survey is made over the underwater hull

* A source is an imaginary point that emits fluid in all directions simultaneously and at a uniform rate. A sink is the opposite of a source in that it takes in fluid uniformly from all directions.

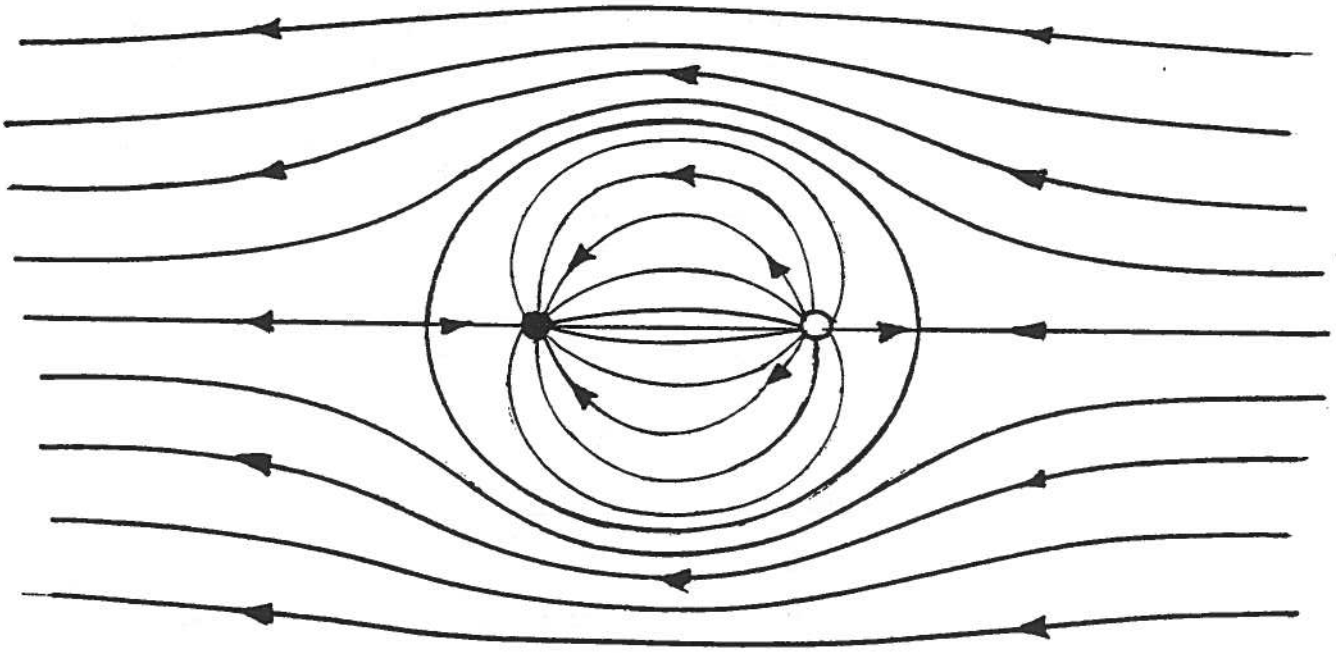

Figure 1.6. Source and Sink Superposed in a uniform stream

form. Normally such experiments are made on models and are expensive owing to the numerous measurements required to map the whole pressure field. As a result, only a relative handful of experiments of this type have been run in all model testing history. See for instance, Reference 16.

4. Deduce the wave resistance component from measurements of the total resistance on models. The means of accomplishing this will be discussed along with the subject of model testing in Section 5. For now, though, we can say that this method is the most common. It is the easiest, but it may also be the least accurate method in many cases and can lead to misinterpretations of model test results.

3.5 OTHER FORMS OF RESISTANCE

3.5.1 AIR AND WIND RESISTANCE:

Boats experience resistance forces due to air as well as those due to water. Since the density of water is roughly one thousand times that of air, we might expect the air resistance to be relatively small, which it usually is. However, when one considers that the above water hull and superstructures of most craft present a rather awkward appearance in comparison to the more streamlined appearance of the underwater hull, we might expect that resistance due to air ought to be considered.

Air resistance can be thought of in terms of three components:

i) resistance due to motion through still air
ii) resistance due to wind
iii) resistance due to the waves created by the wind (treated in Chapter 4)

Resistance in air is nearly all caused by eddies. Therefore, it is proportional to the square of the velocity, a fact that can be demonstrated using the principles of dimensional analysis. Eddy resistance can as well be related to fluid density and the area of the above water configuration projected onto the plane normal to the direction of motion.

$$R_A = \text{constant } \rho A_p V^2 \qquad (1.11)$$

The velocity term in Equation (1.11) is the velocity of the air relative to the boat, i.e.: the boat speed plus any wind velocity component in the direction of motion. The wind's velocity gradient in the vertical direction is not accounted for in Equation (1.11). See Figure 1.7 which is taken from Reference 8.

The variation in wind velocity over the relatively small vertical distance a small craft extends above the water may not be too important, but for large ships the gradient may be significant. For instance, modern high speed containerships typically have superstructure elements about one hundred feet above the water surface. At such heights the wind velocity may be half again that found only a few feet above the water surface.

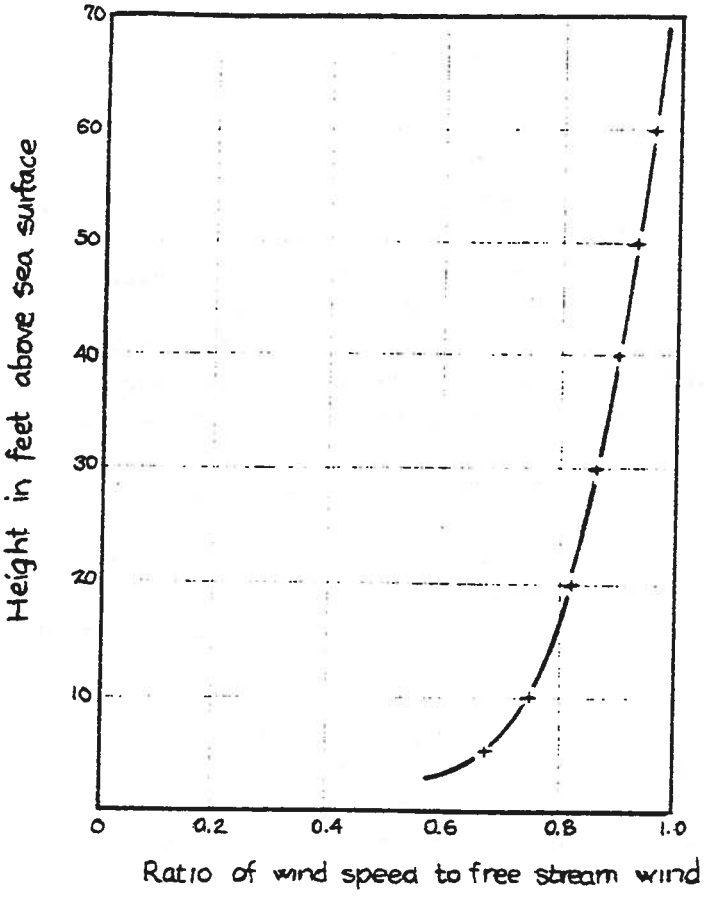

Figure 1.7. Wind Gradient above sea surface.

Taylor (Reference 4) gives an alternative form of Equation (1.11)

$$R_A = 0.002\ B^2\ V^2 \qquad (1.12)$$

where the area projected on to the transverse plane is assumed to be equivalent to a rectangle one beam of the ship wide and one-half beam high. The constant in Eqution (1.12) is derived from experimental measurements.

Although the influence of air resistance on high speed planing craft is not ordinarily accounted for in powering calculations, there is the possibility that this may be an important effect. Particularly for planing craft with tall superstructures, such as sport fishermen, the relatively high position of the aerodynamic forces may induce trimming moments large enough to influence hydrodynamic forces.

3.5.2 RESISTANCE IN RESTRICTED WATER

Although, strictly speaking, the effects of restricted water do not introduce another form of resistance, they do modify the forms of resistance already discussed. Waterways of limited width and depth cause two basic differences in flow, hence resistance changes. First, considering the boat to be stationary in a channel with the water in motion, it is necessary for the water to speed up in passing around the boat in order to satisfy continuity considerations. Also, there must be a corresponding decrease in pressures on the hull in order to satisfy the Bernoulli equation. The boat will tend to settle slightly due to the decreased pressures. In the case of the planing boat, the effects on boat attitude are most dramatic through the medium, or hump, speed range. Trim angles can be affected by a factor of two or more with a correspondingly large alteration in resistance, since the resistance of a planing boat is sensitive to trimming angle. Figure 1.8 (Reference 6) shows typical resistance, trim and CG rise for a Series 62* model in various depths of water.

In shallow water there is also a significant alteration in the wave patterns. The usual Kelvin pattern is markedly changed, this being related to the elementary wave speed as a function of water depth. Equation (1.9) gives the relationship between wave length and speed in water of unlimited depth. Solving for the wave speed, or wave celerity

$$c = \left(\frac{g\, L_w}{2\pi}\right)^{\frac{1}{2}} \qquad (1.13)$$

The more general expression for water of finite depth is

$$c = \left(\frac{g\, L_w}{2\pi}\right)^{\frac{1}{2}} \left(\tanh \frac{2\pi h}{L_w}\right)^{\frac{1}{2}} \qquad (1.14)$$

*Series 62 is a family of planing hulls model tested at the David Taylor Model Basin (now NSRDC). The results were published in Reference 7.

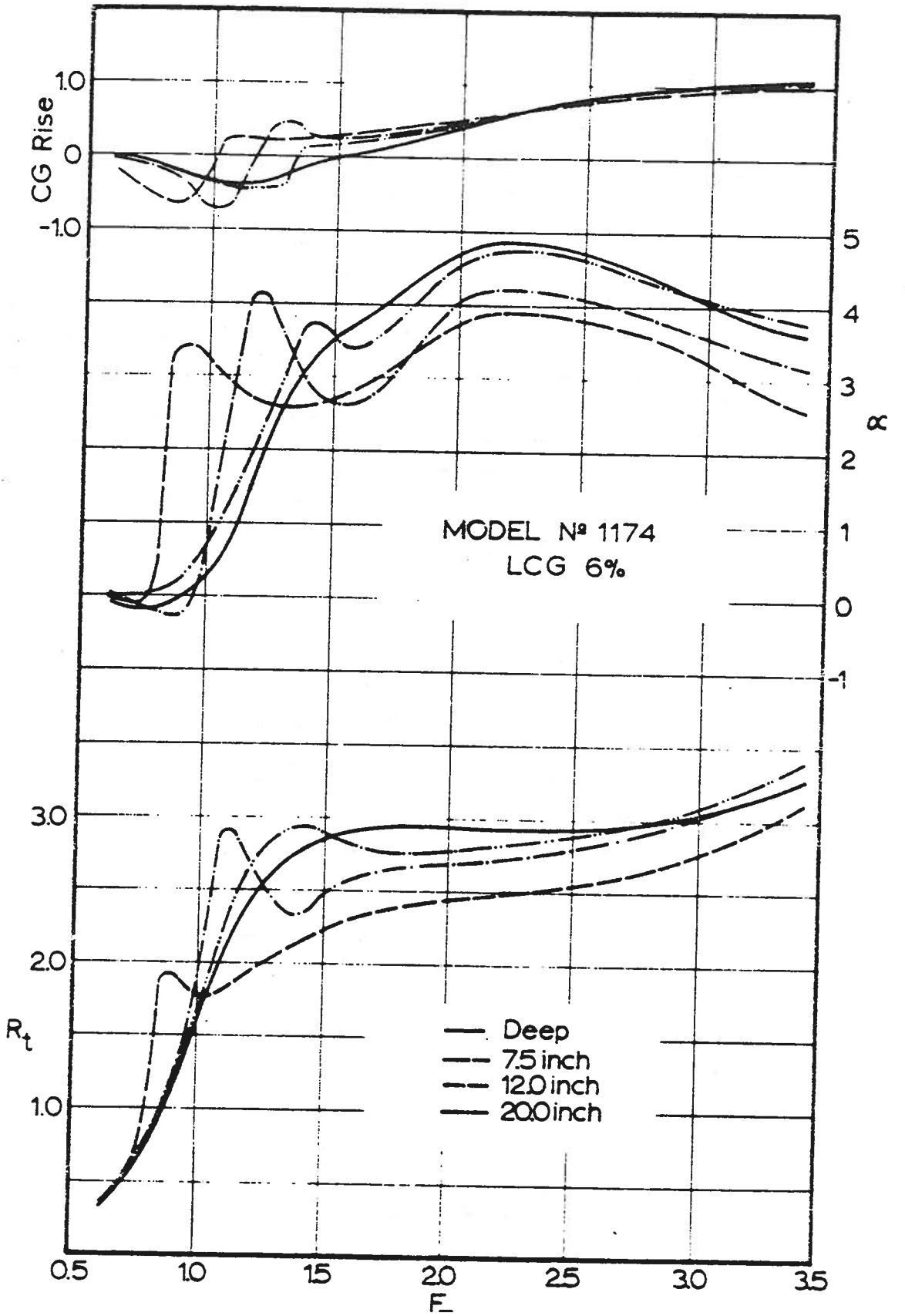
CG Rise
1.0
0
-1.0
5
4
3
2
1
0
-1
α
MODEL Nº 1174
LCG 6%
3.0
2.0
1.0
R_t
Deep
7.5 inch
12.0 inch
20.0 inch
0.5
1.0
1.5
2.0
2.5
3.0
3.5
F_∇

where h is the water depth. For deep water, or large values of h/L_w, Equation (1.14) degenerates to Equation (1.13) since the hyperbolic tangent approaches unity. In shallow water, or for small values of h/L_w, the value of the hyperbolic tangent approaches that of its argument, $2\pi h/L_w$, and Equation (1.14) becomes

$$c = \sqrt{g\,h}$$

or

$$c/\sqrt{g\,h} = 1$$

where $c/\sqrt{gh}$ is called the depth Froude number. At a value of unity it is called the critical depth Froude number.

At a depth Froude number considerably below unity the usual Kelvin wave pattern is maintained. Diverging and transverse wave components are present and the cusp line angle is about 19 degrees, or less, for high speed hulls. As the boat velocity approaches a speed corresponding to the critical speed, the wave pattern tends to orient itself at 90 degrees to the course of the boat. A single, rather large wave forms and is called variously the wave of translation, the critical wave, or the bore. Observations of this wave attest to its large size, which should be anticiapted since this single wave contains nearly all the energy associated with the wave resistance.

At supercritical speeds, transverse wave components largely disappear. The leading crest of the divergent waves tends to reorient itself back toward the Kelvin angle.

It is at the critical speed that the greatest effect on resistance occurs. Figure 1.9 is taken from Reference 6 and shows the residual resistance (which is the total resistance minus the frictional resistance, or the wave resistance plus the viscous pressure resistance) in shallow water compared to that in deep water. At the critical speed, the planing boat experiences greatly increased resistance, but at supercritical speeds there is an appreciable reduction in resistance. It is at the higher speeds where planing boats usually operate and normally have sufficient power available to accelerate through the hump at the critical speeds.

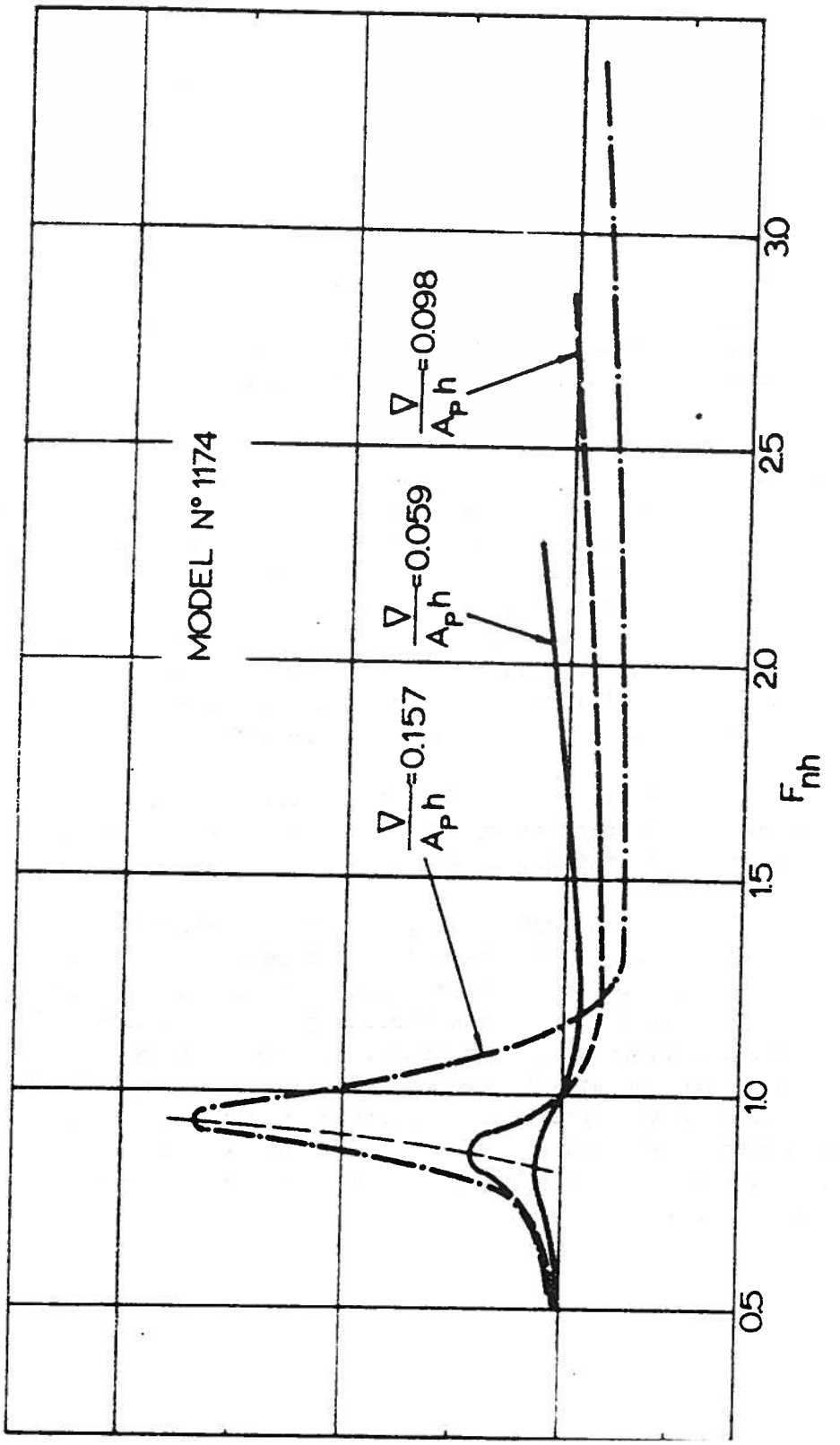

Figure 1.9. Residual resistance in shallow water.

The mechanisms of the individual components of resistance have been examined in a qualitative sense. It remains to discuss how we can quantitatively express the magnitudes of the resistance components. This will be the subject of the next section.

4. DIMENSIONAL ANALYSIS

4.1 GENERAL

Dimensional analysis is a method which allows us to determine groups of physical parameters that govern a particular physical system. In order to employ the analysis a prior knowledge of which physical quantities are to be included is required. This in turn leads to the definition of a functional relationship which the system must obey. The exact form of the function is not provided by the analysis. It does, however, give us the non-dimensional variables which should be used in the evaluation of the performance of the system, both to model scale as well as full scale. Dimensional analysis relies upon the principle that if a mathematical description is to be universally true it must be dimensionless. For the ship resistance problem the dimensional analysis is performed as follows:

$$R = f(\rho, V, L, \mu, g, p, k_1, k_2, k_3, \ldots)$$

where

	units*
ρ = mass density of water	$M\,L^{-3}$
V = velocity	$L\,T^{-1}$
L = length, measure of hull size	L
μ = viscosity of water	$M\,L^{-1}\,T^{-1}$
g = acceleration of gravity	$L\,T^{-2}$
p = pressure in the fluid	$M\,L^{-1}\,T^{-2}$
$k_1, k_2, \ldots$ = hull shape factors	

The shape factors are quantities that describe the geometry of the hull. For a ship they may be prismatic coefficient, length-beam ratio, etc. For a given hull form we can assume that they are taken care of by geometric similitude.

---

* M = mass
L = length
T = time

The resistance is assumed to be proportional to the product of all the variables each raised to a different exponential power.

$$R \propto \rho^a V^b L^c \mu^d g^e p^f \tag{1.15}$$

R must have units MLT^{-2} and since dimensional homogeneity must exist

$$[MLT^{-2}] = [ML^{-3}]^a[LT^{-1}]^b[L]^c[ML^{-1}T^{-1}]^d \times [LT^{-2}]^e[ML^{-1}T^{-2}]^f$$

From this equation three others can be determined, one each for M, L and T.

for M: $1 = a + d + f$
for L: $1 = -3a + b + c - d + e - f$
for T: $2 = b + d + 2e + 2f$

Solving for a, b and c gives

$$a = 1 - d - f$$
$$b = 2 - d - 2e - 2f$$
$$c = 2 - d + e$$

Substitution of the terms for a, b and c into Equation (1.15) gives

$$R \propto \rho^{(1-d-f)} V^{(2-d-2e-2f)} L^{(2-d+e)} \mu^d g^e p^f$$

Collecting terms of like exponent gives

$$R \propto \rho V^2 L^2 \left(\frac{\mu}{\rho VL}\right)^d \left(\frac{Lg}{V^2}\right)^e \left(\frac{p}{\rho V^2}\right)^f$$

or, taking into account that wetted area, S , is proportional to L^2, that kinematic viscosity, ν , is equivalent to μ/ρ , using the fraction 1/2 for the sake of convention and rearranging some terms

$$\frac{R}{\frac{1}{2}\rho S V^2} = f\left[\frac{VL}{\nu}, \frac{V}{\sqrt{gL}}, \frac{p}{\rho V^2}\right] \tag{1.16}$$

Each term in the equation is dimensionless. Therefore, Equation (1.16) states that when the resistance is made non-dimensional by the factor $\frac{1}{2} \rho SV^2$* it is a function of only the three parameters on the right side of the equation. We stated that shape factors could be accounted for by keeping these invariant, but we did not require the hull form to be of any particular shape of size. Therefore, Equation (1.16) also states that when two hull forms are geometrically similar, such as model and full scale hull, the flow around the two hulls will be similar and the left hand side of the equation will be the same for each hull when all terms in the right hand side are the same. This important principle is the basis of all model testing. Since nearly all our knowledge of ship hydrodynamics is based on model testing, careful consideration of Equation (1.16) is required. That then will be the subject of the next several sections.

4.2 FRICTIONAL RESISTANCE - REYNOLDS' LAW

The first term in the right hand side of Equation (1.16) VL/ν, is the only term dependent on the viscosity of the fluid. Therefore, the frictional resistance coefficient, $C_F = R_F/\frac{1}{2} \rho SV^2$, will be the same for geometrically similar bodies of different size when VL/ν is the same.** This statement is known as Reynolds' Law since it was Osborne Reynolds who first explained the significance of VL/ν, in 1883. VL/ν is known as Reynolds' number, R_n, the influence of which on flat plate flow we have already seen in Equations (1.7) and (1.8). For the arbitrary three-dimensional body Reynolds' Law governs the tangential forces illustrated in Figure 1.1 and expressed in Equations (1.1) through (1.3).

4.3 RESIDUARY RESISTANCE - FROUDE'S LAW

William Froude stated his law of comparison in 1868, by considering the resistance of ship hulls in the absence of frictional resistance, i.e., the second term in the right hand side of Equation (1.16) ignoring the third term temporarily. He arrived at his conclusions through observations of ships models of similar geometry, but of different sizes. He noted that the wave patterns generated were geometrically similar when the models were moving at identical values of $V/\sqrt{gL}$, or Froude number F_n . Froude's Law then, is that the residuary resistance coefficient, $C_R = R_R/\frac{1}{2} \rho SV^2$ will be the same for geometrically similar bodies when F_n is the same.

---

* $R/\frac{1}{2} \rho SV^2$ is called the [illegible]

Other forms of the Froude number are in common use. The most common is the speed-length ratio, $V_k/\sqrt{L}$, where speed is in knots and the gravitational acceleration term is dropped. Values of $V_K/\sqrt{L}$ are approximately three times those of F_n.

$$V_k/\sqrt{L} = 3.355\ F_n \qquad F_n = 0.298\ V_k/\sqrt{L}$$

For high speed planing craft, wetted length, L, varies with speed so that Froude number expressed in terms of length is not a particularly significant parameter since length variations with speed will be different from boat to boat. Therefore, two other types of Froude numbers for use with planing boats have come into popular acceptance. The first is known simply as a speed coefficient where beam replaces length in the usual Froude number. Accordingly

$$C_v = V/\sqrt{gb}$$

However, few planing craft have a constant beam so that the selection of some average value must be made. A second variation is the so-called volume Froude number

$$F_\nabla = V/\sqrt{g\nabla^{1/3}}$$

where ∇ is the static volumetric displacement of the boat the cube root of which gives a linear dimension.

An interesting aside to the discussion of various types of Froude numbers is that perhaps none is universally applicable to planing craft. F_∇ suffers when comparing planing catamarans, or other multihulls, with monohulls. One normally wishes to compare competitive designs at the same Froude number, in which case the total displacement of the catamaran would be used. However, in evaluating the performance of the catamaran as a planing device, one ought to use a Froude number based on half the displacement.

Note that the residuary resistance is equivalent to the wave resistance plus the eddy resistance. Also, Froude's Law governs the normal forces illustrated in Figure 1.1 and expressed in Equations (1.1) through (1.3).

5. MODEL TESTING

5.1 GENERAL

Since model test results are an important ingredient of nearly any successful small craft design, it is important to have a basic knowledge of model testing methods. Equation (1.16) shows that complete similarity between model and full scale requires simultaneous satisfaction of Froude's and Reynolds' Laws. This is impossible, however. With Froude, increasing length corresponds to increasing velocity. With Reynolds', the opposite is true. These two requirements quite obviously cannot be simultaneously accommodated. If the ratio between ship and model size is λ ,

$$\lambda = L_S/L_M$$

then the velocity must vary as $1/\lambda$ to satisfy Reynolds' Law and as $\lambda^{\frac{1}{2}}$ to satisfy Froude's Law.

The pressure term in Equation (1.16), $p/\rho V^2$, demands that the total pressure in the fluid be in proportion to the scale, ratio, λ, which would be the case if the atmospheric pressure were ignored. However, the atmospheric pressure is relatively much greater on the model. Fortunately, hydrodynamic forces are generally dependent on pressure differences, not total pressures, so that as long as the flow remains similar on model and ship it is not necessary to satisfy the pressure term. When the total pressure in the water drops to approximately water vapor pressure, cavitation occurs and gross flow dissimilarities develop. Therefore, we may no longer disregard the pressure term for purposes of model testing when cavitation may occur full scale. A more thorough discussion of cavitation is given in Section 5 of Chapter 2.

5.2 FROUDE METHOD

To avoid the seeming paradox of not being able to satisfy the conditions set forth by Equation (1.16), Froude proposed a method of extrapolating model resistance to full scale. It is based on separating from the total resistance the frictional resistance and extrapolating each to full scale according to different laws. In coefficient form

$$C_T = C_F + C_R$$

The residuary resistance coefficient is the same for model and full scale at identical Froude numbers according to Froude's Law.

$$C_{R_M} = C_{R_S}$$

Froude assumed that if the frictional resistance of both model and ship could be calculated, then the total resistance coefficient for the ship could be determined as

$$C_{T_S} = C_{T_M} - (C_{F_M} - C_{F_S}) \tag{1.17}$$

which is shown graphically in Figure 1.10 , ignoring the factor C_A temporarily. In order to determine the frictional resistance, the hull is assumed to have the same frictional resistance as a flat plate of equal wetted area, length and velocity. The hull and flat plate are assumed to be smooth. In order to facilitate computation of frictional resistance, Froude towed a series of flat plates of different lengths and surface textures and measured their total resistance, which he assumed was due only to skin friction. He assumed the resistance to be of the form

$$R = f S V^n$$

where f and n varied according to the length of plate and surface texture. The value of the maximum Reynolds number of the original Froude experiments was only about 5×10^7 which is considerabley less than applicable for most ships and high speed small boats. Froude's formulation has since been modified. In 1935 the International Conference of Ship Tank Superintendents adopted the Froude method, the essence of which is given in Equation (1.17) as well as the following equations for the frictional resistance of ship hull forms.

for fresh water

$$R_F = [0.00849 + 0.0516/(8.8 + L)]\ S\ V_k^{1.825}$$

for salt water

$$R_F = [0.00871 + 0.0530/(8.8 + L)]S\ V_k^{1.825} \tag{1.18}$$

These formulations of frictional resistance are still in use in some

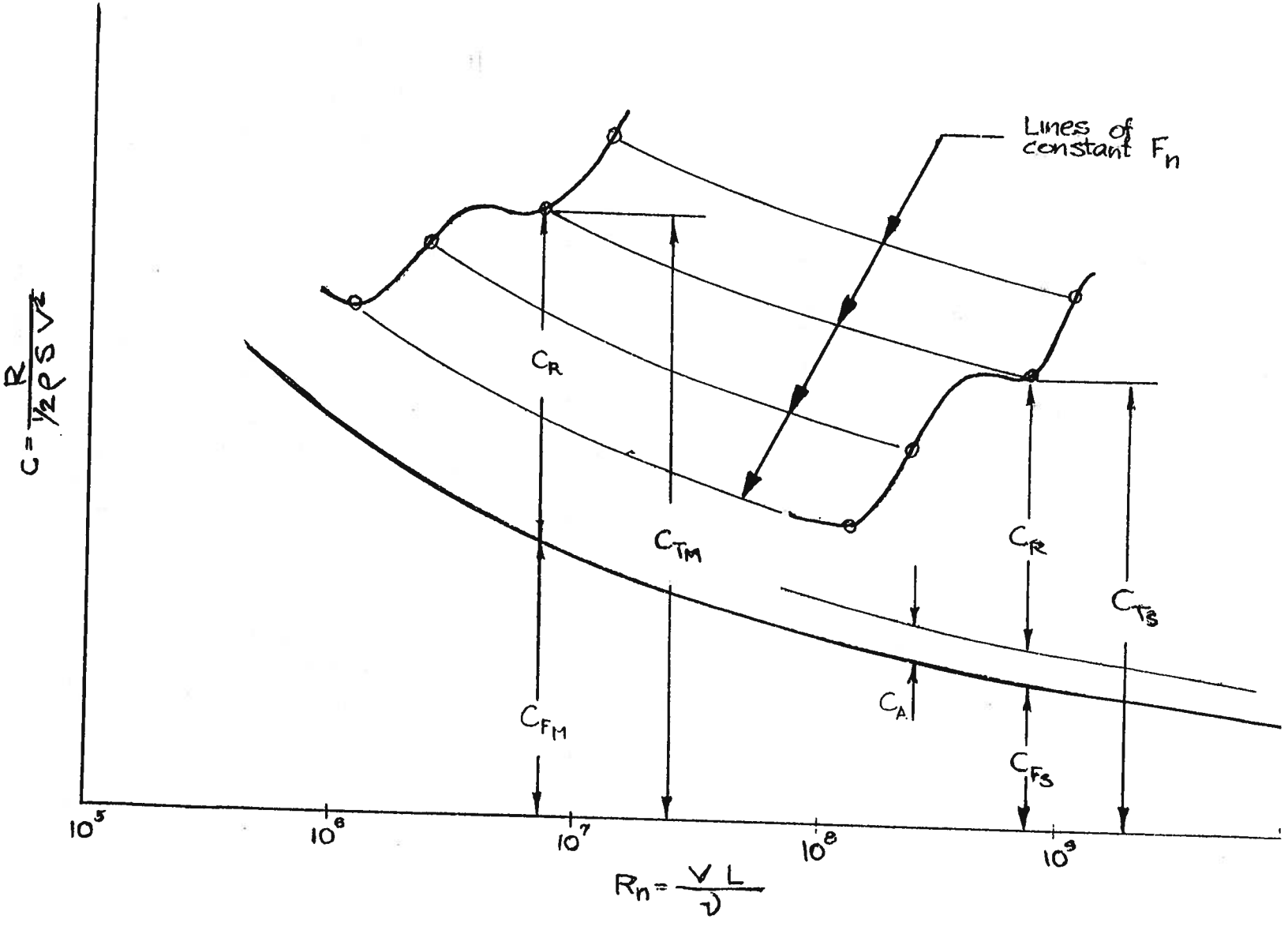

Figure 1.10. Froude Method of Extrapolation.

In 1947 the American Towing Tank Conference, officially adopted the Schoenherr frictional resistance formula for use with the Froude method. Equation (1.8)` gives the formula and it is repeated here.

$$\frac{0.242}{\sqrt{C_F}} = \log_{10} (R_n C_F) \qquad (1.8)$$

This formula was considered to be the best representation of the frictional resistance of smooth flat plates with fully turbulent boundary layer flow. To account for the relatively rougher ship surface, roughness allowance was also recommended by the ATTC. $\Delta C_F = 0.0004$ was recommended for newly painted ships.

In truth, the use of a roughness allowance was merely a means of bringing into better agreement model test resistance predictions and resistance deduced from full scale trials. There was no scientific evidence to support an increment of frictional resistance coefficient due to roughness of exactly 0.0004 at high Reynolds numbers. Consequently the International Towing Tank Conference later acknowledged the roughness allowance as a means of correlation and renamed it the correlation allowance, C_A. Values of C_A in use today differ widely according to ship type and hull coating. Some representative values are given in the following table.

SHIP TYPE	C_A
Cargo ships	0.0004
Super tanker	0 - 0.0002
Barge	0.0004
Naval vessels with special anti-fouling coatings	0.0005 - 0.0012
Naval vessels with conventional coatings	0.0004
Small commercial craft	0.0004
Small high speed craft	0

In 1957 the ITTC also adopted a so-called model-ship correlation line as a better engineering solution to the resistance prediction problem than the 1947 ATTC line. Its formula is

$$C_F = \frac{0.075}{(\log_{10} R_n - 2)^2} \qquad (1.19)$$

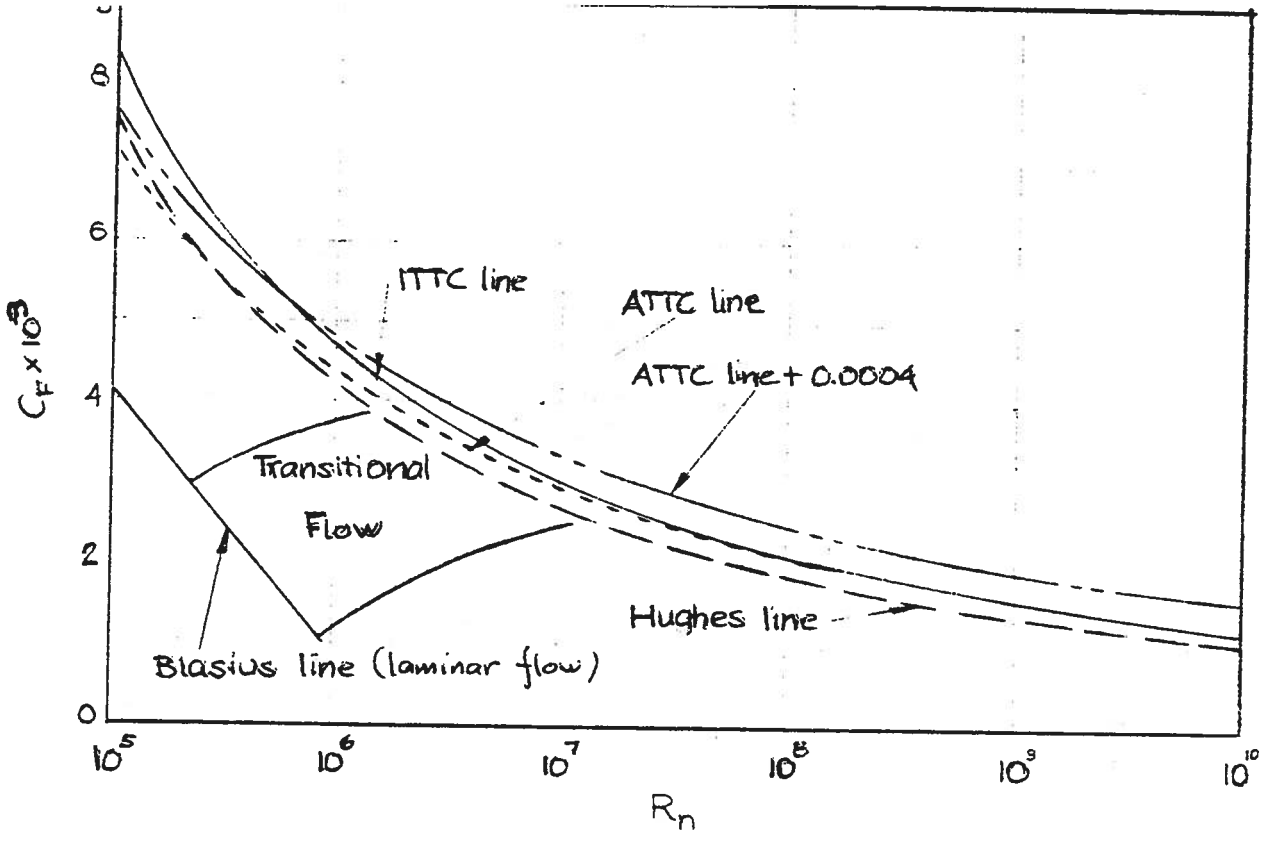

Figure 1.11. Friction coefficient formulations.

At Reynolds numbers greater than about 5×10^7 the 1947 ATTC and 1957 ITTC lines are virtually equivalent. At low Reynolds numbers the 1957 ITTC line gives somewhat higher values of frictional resistance. See Figure 1.11.

It is at these lower Reynolds numbers that most model tests are run. The ITTC was careful to explain that their recommendation was not proposed as a more accurate flat plate friction formula, but rather as a more accurate engineering solution to the problem of model resistance extrapolation to full scale.

An interesting narrative of the various towing tank conferences' actions regarding model testing procedures and extrapolation methods is given by Todd in Reference 8.

5.7 HUGHES METHOD

In 1954 Hughes (Reference 9) proposed a variation on the Froude method of extrapolation. Whereas the Froude method subdivides the total resistance into two components one of which is due to the tangential force component and the other to the normal component, the Hughes method subdivides the resistance into components of energy loss due to viscous properties of the water and to making waves. The wave resistance conforms to Froude's Law or

$$C_{W_M} = C_{W_S}$$

See Figure 1.12. Hughes reasoned that the wave resistance ought to be extrapolated by Froude's Law, and that the total viscous resistance is made up of the skin friction, analogous to that of a flat plate, plus the viscous pressure resistance which is caused by the three dimensional shape of the body. In order to establish a truly two dimensional frictional resistance formula, he tested pontoons and plates with proportions that were varied systematically so that corrections rendered the results two dimensional without edge and end effects. The maximum Reynolds number was about 3×10^8. The resulting formula (Reference 10) is

$$C_{F_o} = \frac{0.066}{(\log_{10} R_n - 2.03)^2} \qquad (1.20)$$

where C_{F_o} = frictional resistance coefficient for two dimensional turbulent flow over a smooth flat surface. See Figure 11.

The Hughes method may be written as

$$C_{T_S} = C_{T_M} - (1+k)C_{F_{o_M}} + (1+k)C_{F_{o_S}} \qquad (1.21)$$

where

$$(1+k)C_{F_o} = C_{PV} + C_{F_o} \qquad (1.22)$$

where C_{PV} = viscous pressure resistance coefficient

k = form factor representing a constant percentage increase over the two dimensional frictional resistance, accounting for the viscous pressure resistance.

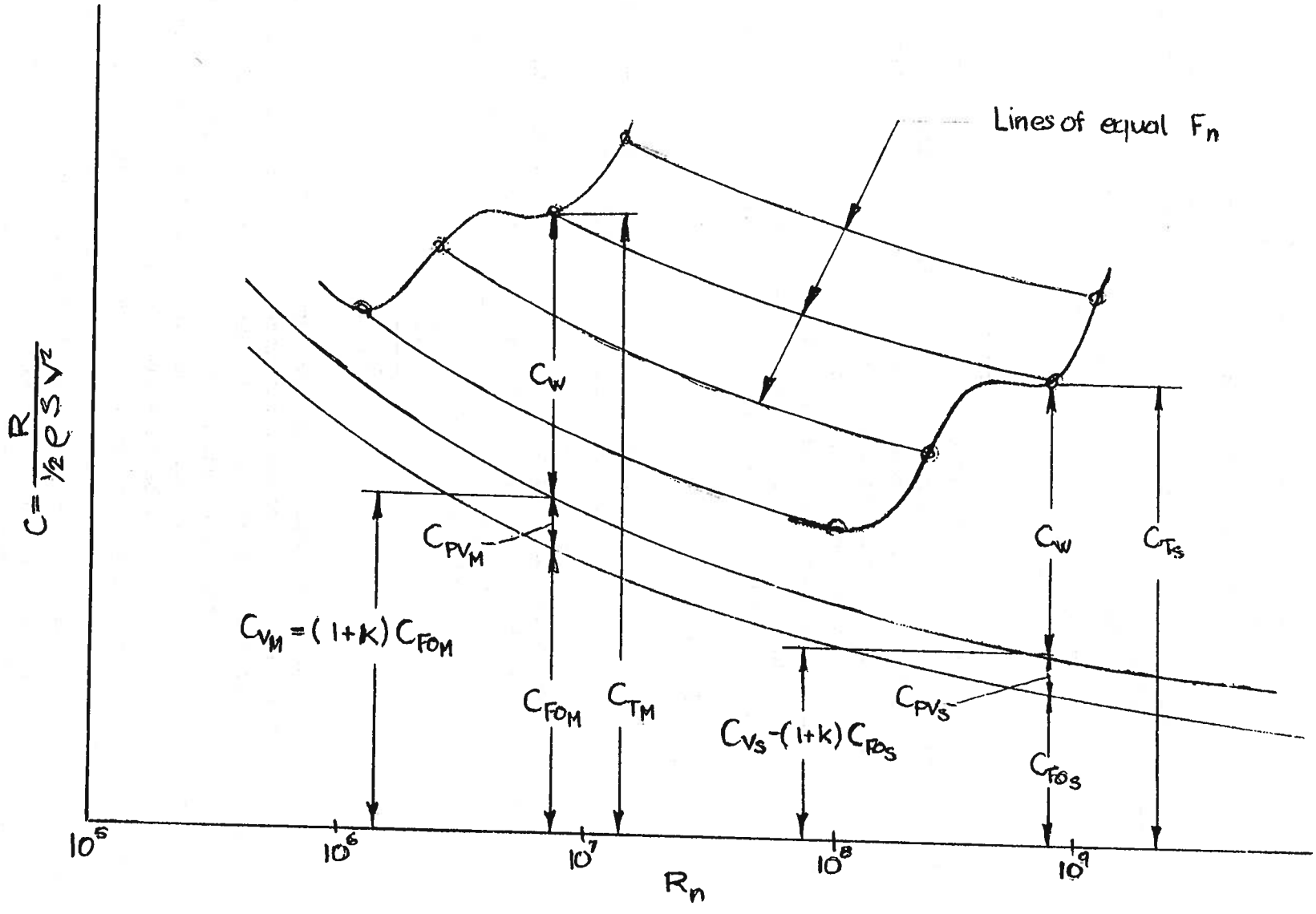

Figure 1.12. Hughes Method of Extrapolation.

The Hughes method has a particular attractiveness in that it provides a means of determining the wave resistance by deduction from the total resistance measurement. However, the rather low values of C_{Fo} compared to accepted values of C_F has been criticised. Hughes' friction coefficients are almost uniformly 12 percent less than those of the 1957 ITTC line. Therefore, many researchers have used the method for estimates of the wave resistance, but usually by applying a form factor to the 1947 ATTC coefficients, which are more generally acceptable as representing flat plate flow.

For purposes of full scale predictions, the Hughes method yields lower values of resistance than those of the Froude method. This is true even when the same friction coefficients are used, since there is an adjustment to a greater portion of the total resistance with the Hughes method than with the Froude method. Therefore, it would be necessary to devise larger correlation allowances in order to use the Hughes method and predict the same full scale resistance. Nevertheless, the Hughes method has supplied researchers with a valuable tool with which to estimate the three components of total resistance.

5.4 TURBULENT FLOW

When conducting model resistance or propulsion experiments, it is necessary to stimulate turbulent boundary layer flow. As illustrated in Figure 1.11, all the model-ship correlation lines assume the flow to be fully turbulent. However, at fairly low Reynolds numbers the flow may be partially laminar, or transitional. Fully laminar boundary layer frictional resistance follows the formula set forth by Blasius as indicated in the figure.

$$C_F = \frac{1.327}{\sqrt{R_n}} \qquad (1.23)$$

Various frictional resistance formulas for transitional flow on flat plates have been proposed, but large discrepancies between them exist. Besides, the degree of laminar or turbulent flow on arbitrary three dimensional forms is probably not a predictable quantity. Hypothetically, if laminar flow could be maintained on the model, accurate full scale predictions could be made even though the full scale boundary layer flow would be fully turbulent. However, practical difficulties prevent this. On reasonably sized models fully laminar flow is virtually impossible to maintain. There will always be some transitional, if not fully turbulent, flow. Also, the nature of separation is different under the influence of laminar or turbulent boundary layer flow. For

6. METHODS OF MODEL RESISTANCE TEST DATA PRESENTATION

So far all the figures used to illustrate model resistance have employed the $C - R_n$ system of presentation. For purposes of demonstrating the principles being explained in previous sections, this system is the most appropriate and it is non-dimensional, which is a prime requisite of any presentation system. For purposes of evaluating the relative merits of the resistances of competing hull forms, the system used thus far is hardly suitable at least without modification. To understand this one need only consider that the coefficient form of expressing resistance which has wetted area in the denominator, cannot correctly reflect the relative merit of two hulls of different wetted areas. Also, we are usually interested in using the Froude number as a speed parameter, since it reflects the wavemaking characteristics of a hull, rather than using the Reynolds number.

The resistance parameters in most common use when merit comparisons are desired are based on resistance per unit of displacement R_T/W, where displacement is usually measured in pounds for small high speed craft and in long tons for large ships, R_T/Δ. That is, superior hulls are generally considered to be those which have low resistance per unit displacement. This is equivalent to having high lift-drag ratios, terminology common to planing hulls. Therefore, we often use R_T/W vs Froude number in making merit comparisons between hulls. If the wave making characteristics are to be demonstrated adequately, the resistance parameter should be divided by a term involving the square of velocity as was demonstrated in the derivation of Equation (1.16). In order to preserve non-dimensionality, a division by the Froude number squared would be appropriate. One such parameter has been proposed by Telfer on various occasions (e.g. Reference 11) and has been designated C_{TL} by the ITTC.

$$C_{TL} = \frac{R_T L}{\Delta V_k^2} \tag{1.24}$$

Telfer has also shown that erroneous merit comparisons can be made if the data presentation systems are incompatible. If the resistance parameter chosen is to be a function of speed, such as C_{TL}, then the speed must be non-dimensionalized by the same quantities as those used on the abscissa of the graph. For instance, when plotting C_{TL}, the abscissa must be the speed-length ratio or Froude number based on length. Use of Froude number based on volume would result in an incompatible presentation.

An example illustrating compatible and incompatible systems compares a round bottom boat (Reference 12) to a hard chine boat (Reference 13) and is given in Figure 1.13. The upper portion of the figure shows C_{TL} plotted against F_v, but since C_{TL} is based on length, not volume as is F_∇, there is an incompatibility. The upper portion of the figure shows the hard chine boat to be superior above $F_\nabla = 2.4$. But when basing the comparison on R_T/W the hard chine boat does not become superior until $F_\nabla = 3.0$. Therefore, the choice of an incompatible presentation system led to an erroneous conclusion.

Had speed-length ratio (or Froude number based on length) been used on the abscissa, then the presentation would have been compatible. But, as we have already mentioned, speed parameters based on length are not particularly useful for planing craft. Therefore, it is logical to introduce a resistance parameter analogous to Telfer's C_{TL}, but based on displacement, i.e.,

$$\frac{R_T \, g \, \nabla^{1/3}}{\Delta \, V^2}$$

Converting volumetric displacement to pounds displacement, velocity in feet/second to velocity in knots and dropping the acceleration of gravity term

$$C_{TW} = \frac{R_T}{W^{2/3} \, V_k^{\,2}} \qquad (1.29)$$

This parameter is not in common use in planing craft literature. Had it been used in place of C_{TL} in Figure 1.13, the speed at which the curves crossed would have been the same in both presentations.

All the foregoing discussion on data presentation has assumed that the most suitable way to compare competing hull forms is on the basis of R_T/W. However, this may not always be the case. For example, modern container ships carry cargoes of very low density such that optimization of the design may be on the basis of internal volume or deck area. Even so, these quantities are not normally taken into account when evaluating the resistance of a hull form, probably since they are directly related to the economics of transportation, and somewhat less directly to hydrodynamic problems.

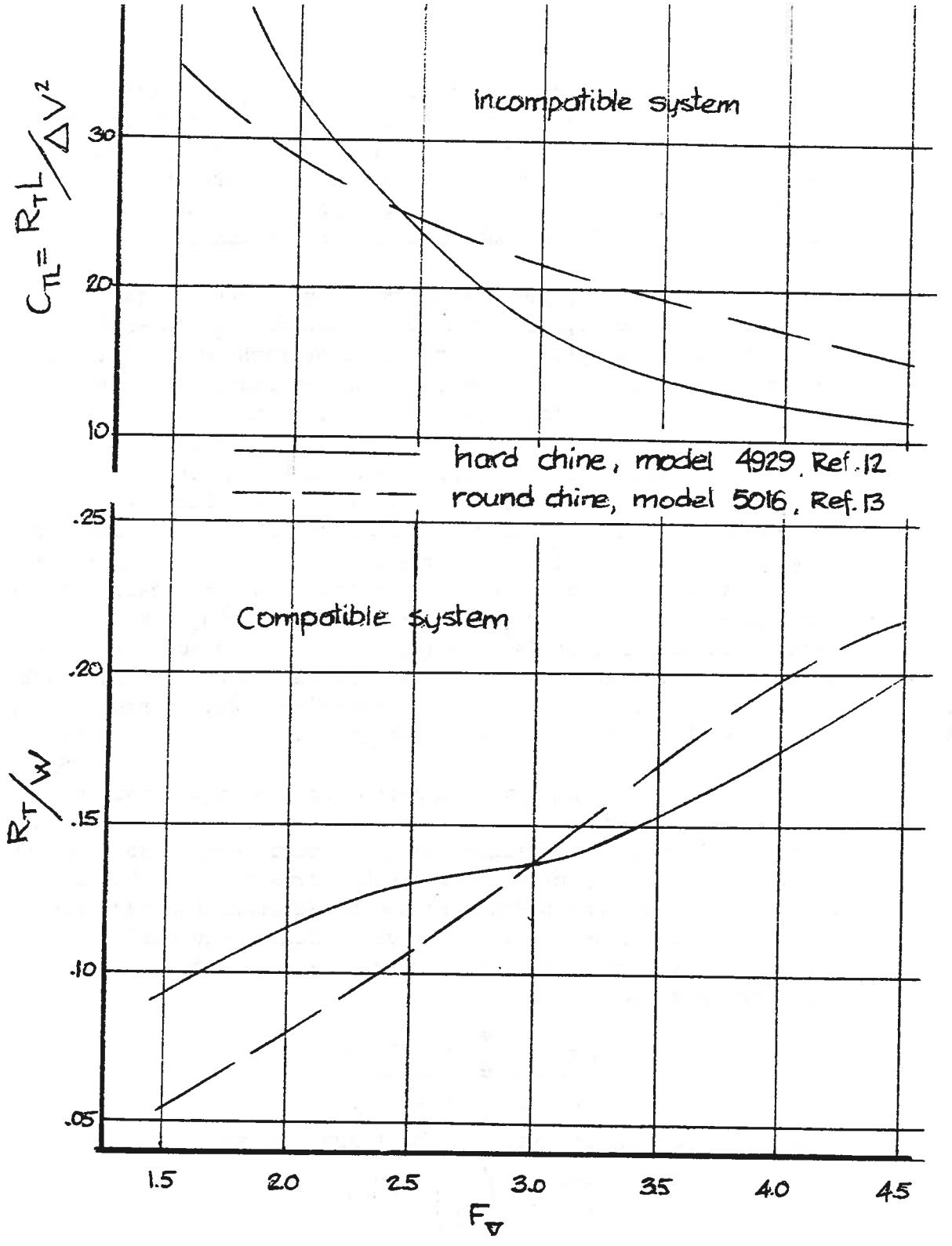

Figure 1.13. Compatible and Incompatible Data Presentation.

There are other commonly used data presentation systems. Instead of R_T/W, R_R/W plotted against a Froude number is often used when it is desired to examine the relative residuary resistances of two or more hulls. Since each hull being compared may have a different wetted area, hence frictional resistance, an erroneous impression of the total resistance comparison may be obtained.

The data presentation systems mentioned so far have all been non-dimensional except for constants such as the conversion of velocity from feet per second to knots or perhaps the elimination of the gravity acceleration term. In another sense, data presentation methods that combine total resistance with other quantities are not non-dimensional. The actual numerical values of R_T/W for a particular hull vary according to the size of the hull. As the size increases R_T becomes relatively smaller compared to W since W is related to model and full scale by the scale ratio cubed. But the effect of the frictional resistance correction in extrapolating R_T from one size to another is equivalent to scaling R_T by the scale ratio raised to some power less than three. Therefore, when using a resistance parameter involving R_T, it is important to state the hull size. With planing craft, specification of an aribtrary total weight, such as 10,000 lbs or 100,000 lbs is usual practice. With larges ships, lengths of 400 or 600 feet are commonly specified.

Another commonly used method of data presentation is the so-called circular notation devised by R. E. Froude. Its principal advantage is that the designer can make merit comparisons on the basis of the ability of different hull forms to carry the same displacement at the same speed. Froude non-dimensionalized speed by dividing it by the speed of a free wave of length one half the length of the side of a cube having the same volume as the hull. Accordingly the wave speed is

$$\left(\frac{g\, L_W}{2\pi}\right)^{\frac{1}{2}} = \left(\frac{g\, \nabla^{1/3}}{4\pi}\right)^{\frac{1}{2}}$$

Dividing this quantity into the hull speed gives

$$\textcircled{K} = \left(\frac{4\pi}{g}\right)^{\frac{1}{2}} \frac{V}{\nabla^{1/6}}$$

where (K) (called circular K) is the designation given by Froude to his speed parameter. If velocity is expressed in knots and displacement in long tons

$$(K) = 0.5834 \frac{V_k}{\Delta^{1/6}} \tag{1.26}$$

Froude's resistance parameter was obtained by dividing R_T/Δ by $(K)^2$ which yields a compatible system. A factor of 1000 was also introduced to avoid small numerical values. Hence

$$(C) = \frac{R_T}{\Delta} \frac{1000}{(K)^2} \tag{1.27}$$

where (C) is the resistance parameter symbol. When R_T and Δ are expressed in long tons

$$(C) = 2938 \frac{R_T}{\Delta^{2/3} V_k^2}$$

which, except for a constant, is equivalent to the previously proposed C_{TW}. (C) is normally expressed in terms of effective horsepower, P_E, where

$$P_E = \frac{R_T V}{550} = 0.00307 R_T V_k$$

Therefore

$$(C) = 427.1 \frac{P_E}{\Delta^{2/3} V_k^3} \tag{1.28}$$

As previously explained, values of (C) will be subject to ship length since the frictional resistance component varies according to the length. Therefore in the notation a subscript is usually added to indicate the length of hull for which the resistance was computed, e.g., $(C)_{100}$ or $(C)_{400}$.

We have examined the more common data presentation methods, but there are many less commonly used symbols. For instance, in a previous section the speed coefficient $C_v = V/\sqrt{g\,b}$ was mentioned. Also, resistance coefficients of the form $R/\frac{1}{2} \rho S V^2$, but with S substituted by L^2 or $\nabla^{2/3}$ are sometimes used. The reader can readily find it tedius to convert data from one source to the same form as that from another source.

presented as $\frac{R}{\Delta}$ and have been extrapolated differently. One of the goals of the ITTC is to try to standarize on the procedures and it has established its Committee on the Presentation of Data for that purpose. However, the committee has not found any presentation system acceptable to all and may never do so since the preference of the individual often dictates the method employed.

7. RESISTANCE OF METHODICAL SERIES OF HULL FORMS

A methodical series of hull forms is one in which geometric parameters have been varied in a systematic manner. By maintaining all significant parameters constant, such as L/B, B/T and LCB position, but systematically changing prismatic coefficient would constitute a limited series designed to reveal the relationship between resistance and C_p for the type of hull form in question. A series may be generated from one parent hull form, or several, as long as all parent hulls are systematically related to each other.

In an earlier section, when performing a dimensional analysis of ship resistance, factors expressive of the geometry, k_1, k_2 . . . , were eliminated from the first equation with the understanding that the resulting analysis would pertain to only one hull form, albeit an arbitrary one. It was necessary to make such a simplification since the intricate relationship between resistance and all possible geometric parameters is not fully understood and cannot be expressed analytically. Attempts have been made to find such relationships statistically using resistance data from model tests of loosely related hull forms of the same general type. The most notable of these attempts is Doust's work with trawlers (References 14 and 15.)

Over the years many methodical series of models have been tested. Recently the H-2 Panel of SNAME reviewed the open literature and non-proprietary model basin reports and found that results of approximately 150 series had been published. One of the main functions of Chapter 3 is to illustrate the use of such series, so that no further details need to be presented here. However, a bibliography of series publications that should be helpful to the small craft designer is included as an appendix to this chapter. It includes not only planing hulls, but also series of trawlers, coasters (on which there is a great deal of literature), high speed displacement ships and large conventional ships, all of which should be useful to the small craft designer.

REFERENCES

Chapter 1

1. Smith, Donald W. and Walker, John H., "Skin-Friction Measurements in Incompressible Flow," NASA TR R-26, 1959.

2. Landweber, L., "Reanalysis of Boundary-Layer Data on a Flat Plate," Iowa Institute of Hydraulic Research, Oct. 1960.

3. Schoenherr, K. E., "Resistance of Flat Plates Moving Through a Fluid," SNAME, 1932.

4. Taylor, D. W., The Speed and Power of Ships, U. S. Government Printing Office, Third Edition, 1943.

5. Korvin-Krouksky, B. V., Savitsky, D. and Lehman, W. E., "Wave Profile of a Vee-Planing Surface, Including Test Data on a 30-degree Deadrise Surface," Report No. 339, April 1949.

6. Toro, A. I., "Shallow-Water Performance of a Planing Boat," Southeastern Section, SNAME, April 1969. Also University of Michigan, Department of Naval Architecture and Marine Engineering Report No. 019, April 1969.

7. Clement, E. P. and Blount, D. L., "Resistance Tests of a Systematic Series of Planing Hull Forms," SNAME, Vol. 71, 1963.

8. Principles of Naval Architecture, by a group of authorities, SNAME, 1967.

9. Hughes, G., "Friction and Form Resistance in Turbulent Flow and a Proposed Formulation for use in Model and Ship Correlation," INA, 1954.

10. Hughes, G., "Frictional Resistance of Smooth Plane Surfaces in Turbulent Flow," INA, 1952.

11. Telfer, E. V., "The Design Presentation of Ship Model Resistance Data," NECI, 1962-63.

12. Chey, Y., "Model Tests of a Series of Six Patrol Boats in Smooth and Rough Water," Davidson Laboratory Report 985, August 1964.

13. Fridsma, G., "Model Tests of a Round Bottom Patrol Boat in Smooth

14. Doust, D. J. and O'Brien, T. P., "Resistance and Propulsion of Trawlers," NECI, 1958-59.

15. Doust, D. J., "Optimized Trawler Forms," NECI, 1962-63.

Chapter 2

1. Abbot, I. H. and vonDoenhoff, R. E., Theory of Wing Sections, Dover Publications, Inc., New York, 1959.

2. O'Brien, T. P., The Design of Marine Screw Propellers, Hutchinsson and Co., Ltd., London, 1968.

3. Principles of Naval Architecture, by a group of authorities, SNAME, 1967.

4. Kruppa, C. F. L, High Speed Propellers, The University of Michigan October 1967.

5. Gawn, R. W. L., "Effect of Pitch and Blade Width on Propeller Performance," INA, 1953.

6. Troost, L., "Open Water Test Series with Modern Propeller Forms," NECI, 1950-51.

7. Van Lammeren, W. P. A., Van Manen, J. D. and Oosterveld, M. W. C., "The Wageningen B-Screw Series," SNAME, 1969, to be published.

8. Burrill, L. C. and Emerson, A., "Propeller Cavitation: Further tests on 16 in. Propeller Models in the King's College Cavitation Tunnel," NECI, 1962-63.

9. Emerson, A. and Sinclair, L., "Propeller Cavitation: Systematic Series tests on 5 and 6-Bladed Model Propellers," SNAME, 1967.

10. Gawn, R. W. L. and Burrill, L. C., "Effect of Cavitation on the Performance of a Series of 16 in. Model Propellers," INA, 1957.

11. Newton, R. N., and Radar, H. P., "Performance Data of Propellers for High-Speed Craft," INA, 1961.

12. Shields, C. E., "Performance Characteristics of Several Partially Submerged Supercavitating Propellers," NSRDC Report 2723,

13. Caster, E. B., "TMB 2-, 3-, and 4-Bladed Supercavitating Propeller Series," DTMB Report 1637, January 1963.

14. Venning, Jr., E. and Haberman, W. L., "Supercavitating Propeller Performance," SNAME 1962.

15. West, E. E., and Crook, L. B., "A Velocity Survey and Wake Analysis for an Assualt Support Patrol Boat (ASPB) Represented by Model 5014," NSRDC T and E Report No. 149-H-05, Septemeber, 1967.

16. Hadler, J. B., "The Prediction of Power Performance on Planing Craft," SNAME, 1966.

APPENDIX

Bibliography of Methodical Series Useful to the Small Craft Designer

Planing Hulls

1. Davidson, K. S. M., and Suraez, A., "Tests of Twenty Related Models of V-Bottom Motor Boats EMB Series 50," ETT Report 170, Oct. 1941, revised Dec. 1948.

2. Clement, E. P. and Blount, D. L., "Resistance Tests of a Systematic Series of Planing Hull Forms," SNAME 1963.

3. Beys, P. M., "Series 63 Round Bottom Boats," DL Report 949, April 1963.

4. Chey, Y., "Model Tests of a Series of Six Patrol Boats in Smooth and Rough Water," DL Report 985, August 1964.

5. Fridsma, G., "Model Tests of a Round-Bottom Patrol Boat in Smooth and Rough Water," DL Letter Report 1074, June 1965.

High-Speed Displacment Ships

1. Van Mater, P. R., "Hydrodynamics of High Speed Ships," DL Report 876, Oct. 1961.

2. Yeh, H. Y. H., "Series 64-Resistance Experiments on High-Speed

3. Clement, E. P., "Merit Comparisons of the Series 64 High-Speed Displacement Hull Forms," DTMB Report 2129, Nov. 1965.

Conventional Displacement Ships

1. Nordstrom, H. F., "Systematic Tests with Models of Cargo Vessels with δpp = 0.575," SSPA Publications No. 16, 1950.

2. Edstrand, H., Lindgren, H., "Systematic Tests with Models of Ships with δpp = 0.525," SSPA Publications No. 38, 1956.

3. Gertler, M., "A Reanalysis of the Original Test Data for the Taylor Standard Seties," DTMB Report 806, March 1954.

4. Todd, F. H., "Series 60-Methodical Experiments with Models of Single-Screw Merchant Ships," DTMB Report 1712, 1963.

5. Lackenby, J. and Parker, M. N., "The BSRA Methodical Series An Overall Presentation, Variation of Resistance with Breadth-Draught Ratio and Length-Displacement Ratio," RINA 1966.

Fishing Vessels

1. Henschke, W., "Systematic Resistance Experiments with Models of Motor Fishing Vessels," Schiffstechnik, Bd. 4, 1957.

2. Ridgely-Nevitt, C., "The Resistance of Trawler Hull Forms of 0.65 Prismatic Coefficient," SNAME 1956.

3. Ridgely-Nevitt, C., "The Developement of Parent Hulls for a High Displacment-Length Series of Trawler Forms," SNAME 1963.

4. Ridgely-Nevitt, C., "The Resistance of a High Displacement-Length Ratio Trawler Series," SNAME 1967.

5. Patullo, R. N. M., and Thomson, G. R., "The BSRA Trawler Series (Part I) Beam-Draught and Length-Displacement Ratio Series Resistance and Propulsion Tests," RINA 1965.

6. Patullo, R. N. M., "The BSRA Trawler Series (Part II) Block Coefficient and Longitudinal Centre of Byouancy Variation

Coasters

1. Todd, F. H., "Further Model Experiments on the Resistance of Merchantile Ship Forms - Coaster Vessels," INA 1931.

2. Todd, F. H., and Weedon, J., "Further Resistance and Propellers Experiments with Models of Coasters," INA 1938.

3. Todd, F. H. and Weedon, J., "Experiments with Models of Cargo-Carrying Type Coasters," IME 1940.

4. Todd, F. H., and Weedon, J., "Further Experiments with Models of Cargo-Carrying Coasters," NECI 1942.

5. Haaland, A., "Noen Systematiske Formvariasjoner Med Modeller Av Lokalskip og Deres Innflytelese på Motstands-og Framdrifts forholdene (Some Systematic Form Variations on Resistance and Propulsive Results,") Skipsmodell takens Meddelesle Nr. 4, January 1951, (English summary).

6. Warholm, A. O., Lindgren, H., "Further Tests with Models of Coasters," SSPA Publications No. 35, 1955.

7. Dawson, J., "Resistance of Single-Screw Coasters, Part I," IESS 1952-1953.

8. Dawson, J., "Resistance of Single-Screw Coasters, Part II," IESS, 1954-1955.

9. Dawson J., "Resistance of Single-Screw Coasters, Part III," IESS, 1955-1956.

10. Dawson, J., "Resistance of Single-Screw Coaster, Part IV," IESS, 1959-1960.

11. Hansen, H. B., "Systematic Experiments with Models of Fast Coasters," Norwegian Ship Model Experiment Tank Publications No. 44, December 1966.

Catamarans

1. Schinke, A., and Puchstein, K., "Resistance Towing Tests with Catamaran Models," (in German) Schiffbautechnik, 16 Aug. 1966, p 423.

2. Schinke, A., and Puchstein, K., "A Contribution to the Study of

Miscellaneous

1. Koning, J. G., "E.H.P. of Small Seagoing Cargo Ships," Pub. 37, NSMB, 1938.

2. Nordstrom, H. F., "Some Tests with Models of Small Vessels," SSPA Publications No. 19, 1951.

3. Lindblad, A. F., "The Effect Upon Resistance of Large Beams on some Models with Block Coefficients between 0.65 and 0.60," INA 1953.

4. Helm, K., "Systematic (Model) Investigations on the Influence of (Hull) Form upon Resistance and Power Requirements, in Inland-Waterways Passenger Ships," (in German) Schiff u Hafen, 15 Feb., 1963, p. 98.

5. Helm, G.m "Systematic (Model) Investigations on the Resistance of Boats and Small Ships," (in German) Hansa, 101, No. 22, Nov. 1964, p. 2179, also HSVA Report No. 1300.

CHAPTER 2: FUNDAMENTALS OF PROPULSION

1. GENERAL

In Chapter 1, we discussed the resistance forces arising from moving the hull through the water. In this chapter we will deal with the means of supplying the propulsive force, or thrust needed to counteract the resistance.

Usually the hydrodynamic properties of the hull and propulsive device are easily separable. Normal screw propellers may be viewed as one hydrodynamic system and the hull as another. There are interactions between the two systems when they are brought together which may be quantified. Figure 2.1 shows this schematically.

Figure 2.1. Schematic Diagram of Hull and Propulsion Systems.

The individual features of the diagram may be discussed separately as was the "hull system" in Chapter 1. However, there are occasions when the small craft designer may be confronted with a situation where the resistive and propulsive properties are not easily separable. This would be true whenever buoyancy and propulsive force arise from the same part of the vehicle. For instance, the Archimedian screw shown in Figure 2.2 has a relatively large hub to supply buoyancy and the relatively small blades supply propulsive thrust.

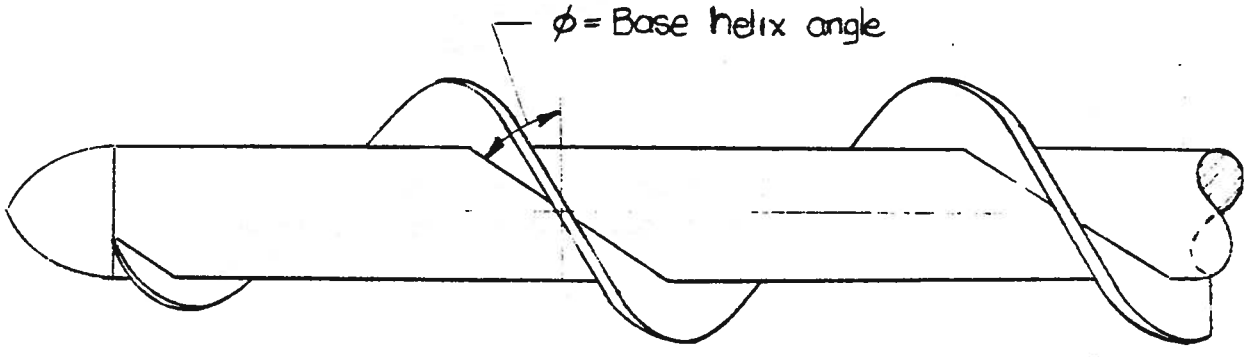

Two such pontoons with blades, spanned by a deck, would have resistance associated with the pontoons which could not easily be measured since the flow on the pontoons could be expected to be radically altered by the blades. Neither could the blade thrust be easily determined since the flow on the blades alone could be expected to be radically altered by the pontoon. Therefore, the resistance and propulsion systems cannot realistically be considered separately. However, we shall confine our discussion to arrangements as those depicted in Figure 2.1. Moreover, the discussion of propulsive devices will be confined exclusively to conventional screw propellers.

Achieving the maximum overall efficiency from the combinatio of hull and propulsive device is important. If the power developed by the propeller is denoted by P_D , then the overall efficiency, or propulsive coefficient, in the absence of mechanical losses in tran. - mission of the power to the propeller is

$$\eta_D = \frac{P_E}{P_D} \qquad (2.1)$$

where

$$P_D = \frac{2\pi Qn}{550}$$

Q = torque absorbed by the propeller
n = rotary speed of the propeller (R.P.S.)

and all quantities are in the ft-lb-sec units system. In addition, the propeller produces a thrust horsepower so that the efficiency of the propeller behind the boat, or in the behind condition, is

$$\eta_B = \frac{T\ V_A}{2\pi Qn} \qquad (2.2)$$

where

T = propeller thrust output
V_A = velocity of advance = average flow velocity through the propeller disc behind the boat.

The hull should have an efficiency associated with it, η_H, such that the product of the efficiencies of the two systems, hull and propeller, will equal the overall efficiency.

That is

$$\eta_D = \eta_B \cdot \eta_H \tag{2.3}$$

Hull efficiency has to do with the interaction mechanisms between the hull and propeller, which will be covered in a later section.

2. SCREW PROPELLER GEOMETRY

This discussion of propeller geometry is largely a matter of establishing defintions so that subsequent material may be more readily understandable.

2.1 SECTION GEOMETRY

The most important characteristics of the blade section are the chord-thickness distribution and camber. The chord is measured between nose and tail along the helical line that has a radius and pitch equal to that of the blade section. The following definitions refer to Figure 2.3.

Section types:

1) The segmental section has a flat face so that the chord line and face line coincide. The geometric pitch is measured from the same line. The maximum thickness is at the mid-chord point. The backs may be shaped parabolically, elliptically, or in the form of a circular arc (which is the most common and in which case the sections are known as ogival sections.)

2) Airfoil sections generally have curved faces as well as curved backs. The pitch datum line may be arbitrarily established. The face and back lines are established by measurements from the pitch datum line. The maximum thickness may occur at any point along the chord length. As with all blade sections, the thickness-chord ratio is defined as the ratio of the maximum thickness to the chord length, t/c.

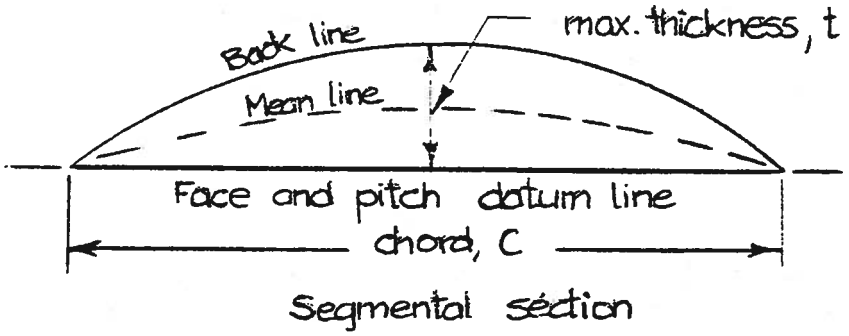

Segmental section

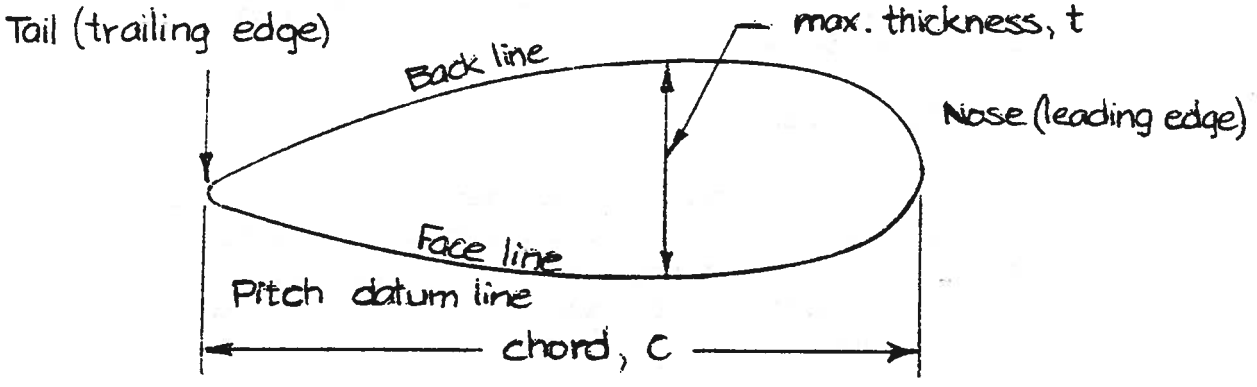

Airfoil section

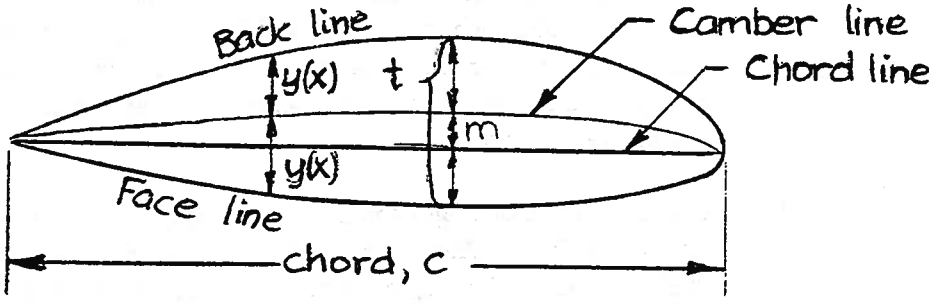

Composite section

Figure 2.3. Types of Propeller blade sections.

3) Composite sections may be similar in appearance to airfoil sections, but they are laid out in a different fashion and have basis in the theory of thin airfoils. Starting from the chord line a camber line is defined. The maximum offset from the chord line, m, is called the camber. The face line and back line offsets from the camber line are equal. Wind tunnel test results on many types of composite sections have been published by NACA and excellent summary of which is given in Reference 1. Among those sections, some are particularly suitable for marine propeller use.

NACA 63, 64, 65 - all have a camber-chord ratio, m/c, of 6 percent. The maximum camber, m, occurs at 0.3, 0.4, and 0.5 of the chord length from the nose, respectively.

NACA a =1.0 and a=0.8 mean lines - have chord-wise camber distribution theoretically derived to yield a constant flow velocity along the chord under conditions of shock-free entry. Shock-free entry implies that a section is working at the ideal angle of incidence. The stagnation pressure occurs at the nose of the section where the flow divides evenly over the face and back. The uniform velocity is a desirable feature for propellers that may cavitate. The a=1.0 mean line has constant velocity over the whole chord and the a=0.8 mean line for 0.8 of the chord.

NACA 16-06 to 16-21 - have constant velocity over 0.6 of the chord and thickness-chord ratios of from 0.06 to 0.21.

2.2 BLADE GEOMETRY

Definitions of the geometry of the complete propeller blade are given in the following list and in Figure 2.4.

D	=	diameter
P	=	pitch
Pitch ratio	=	P/D
R	=	maximum radius = D/2
r	=	radial distance from axis to section of interest
r_h	=	hub radius.
x	=	r/R = 0.2, 0.3, ... etc. Used as a subscript to denote a value at a particular radial location, e.g., $P_{0.7}$ is the pitch 0.7 of the distance from the axis to the tip.
Z	=	number of blades
t_o	=	maximum blade thickness projected to axis.
BTF	=	blade-thickness fraction = t_o/D .
A_o	=	disk area = πR^2.
A_p	=	projected area = area of all blades outside the hub when simply projected onto the plane of the propeller disk.
A_D	=	developed area = area of all blades resulting from rotation of the blade outline in the projected view onto the plane of the disk.
A_E	=	expanded area = area of all blades resulting from expansion of circular arc lengths at each radii in the developed view onto straight lines. On propeller drawings blade sections are normally shown in the expanded view. Note that by first rotating the sections onto the plane of the disk and then "unwrapping (or expanding) them, the helical chord lengths are preserved.
DAR	=	A_D/A_o = developed area ratio
EAR	=	A_E/A_o = expanded area ratio
BAR	=	blade area ratio and may equal DAR or EAR
MWR	=	mean width ratio
	=	mean blade width/diameter
	=	$\frac{\text{blade area/blade length (root to tip)}}{\text{diameter}}$
		(usually based on developed blade area)
Skew	=	term used to describe sweep, or curvature, of the maximum thickness line in expanded view. A symmetric blade has no skew. A blade may have either forward skew (uncommon) or backward skew (common) as is shown in Figure 2.4. A blade with skewback has greater rake than one with no skew owing to the effect of pitch.
Rake	=	angle subtended from plane of propeller disk

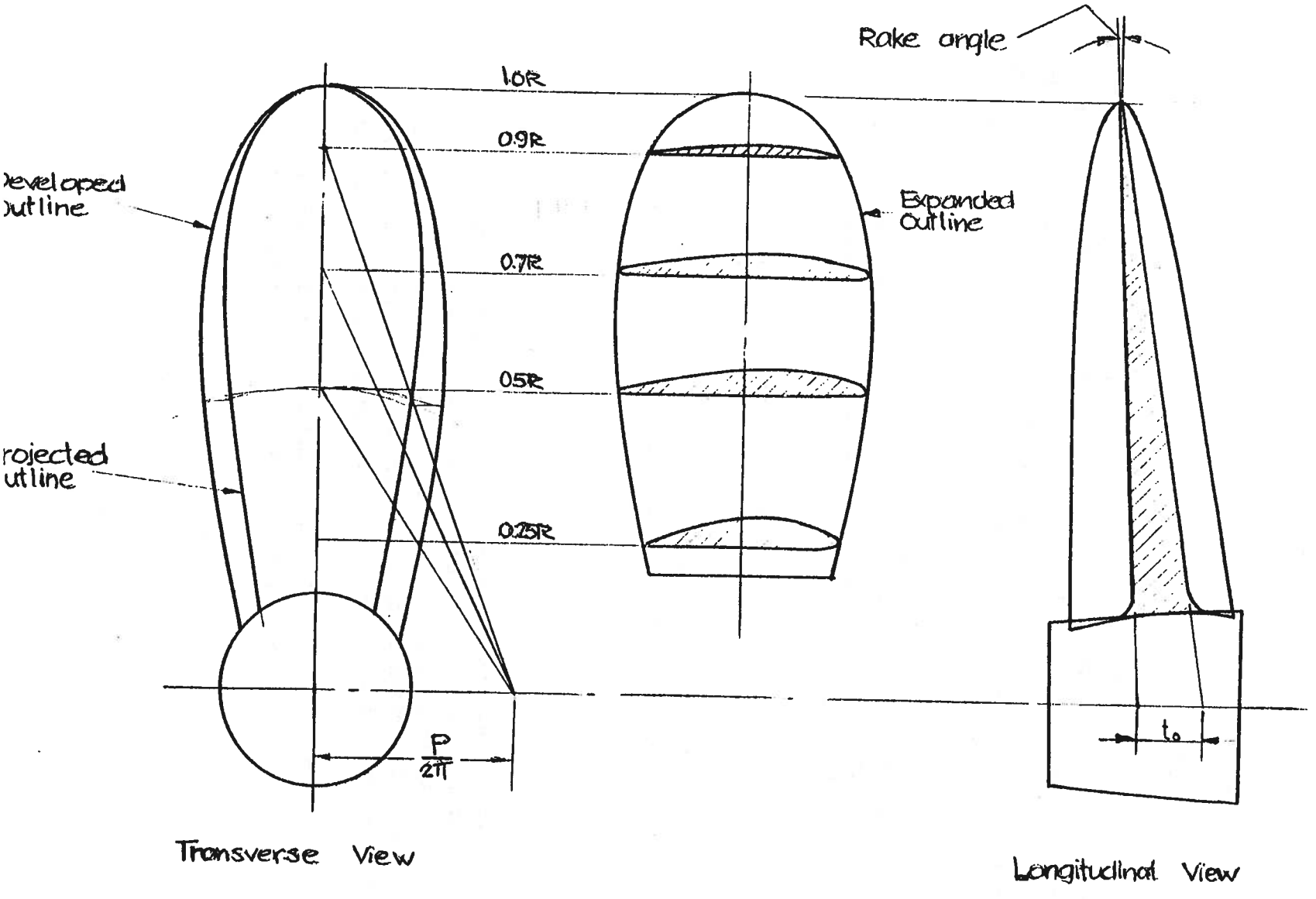

Figure 2.4. Propeller Drawing.

3. PROPELLER THEORIES

3.1 GENERAL

Early explanations of their behavior likened screw propellers to a bolt being threaded into a nut, in which case the propeller should advance through the water at a speed equal to its pitch times its rotary speed, P_n. However, the advance speed, V_A, was observed to be somewhat less, the difference being accounted for by the propeller slip, s.

At this point it is appropriate to digress some in order to define the two commonly used slips. The first, real slip, s_R, is the ratio of the difference in the ideal advance speed, Pn, and the actual advance speed, V_A, compared to the ideal speed.

$$s_R = 1 - \frac{V_A}{Pn} \tag{2.4}$$

The second, apparent slip, s_A, is the slip usually measured on boats and assumes that the speed of water through the propeller plane is the same as the speed of the boat, V ,

$$s_A = 1 - \frac{V}{Pn} \tag{2.5}$$

Since the actual advance speed is usually less than the boat speed, the apparent slip is an erroneous measure of the propeller behavior. However, apparent slip is much more easily measured on full scale boats and comparison of different propellers of the same diameter on the same boat using apparent slip is a generally valid procedure.

The efficiency of a propeller might be defined as the ratio of the output thrust horsepowers at the two different speeds. Accordingly

$$\eta = \frac{T\ V_A}{T\ Pn} = 1 - s_R \tag{2.6}$$

and $\eta = 1.0$ when there is no slip.

Initially propeller theories developed along two lines. One considered the momentum imparted to the water by the propeller. The momentum theory explains efficiency dependency on propeller loading, but does not give the shape of the propeller. The blade element theory considers the forces acting on the propeller based on its geometry, but has produced unrealistic results for design purposes, probably because the theory fails to account for the flow modifications due to the propeller.

Modern theories are based on the concept of circulation, or vortex action, and hence the term circulation theory. The relation between the forces on the blades and the momentum changes in the fluid are treated. The latest refinements in the theory have made it possible to employ it in practical design work although the computations are rather complicated and usually done by digital computer. Introduction of some simplifications makes the calculations manageable by hand. Some numerical example can be found in Reference 2.

3.2 MOMENTUM THEORY

The propeller is regarded as a disk and imparts a change in pressure to the fluid as it flows through a circular column of changing diameter. In order to maintain continuity, the velocity in the column must increase in the downstream direction as the column shrinks in size. See Figure 2.5.

The forces at the disk, or propeller thrust, must equal the change in pressure times the area

$$T = \delta p \, A_o \tag{2.7}$$

This reaction force must also equal the change in momentum

$$T = \rho \cdot q \cdot \delta V \tag{2.8}$$

where q is the volume of fluid flowing through the disk per unit time. If the pressure across the disk is constant, then so is the velocity and

$$q = A_o \cdot V_1 \tag{2.9}$$

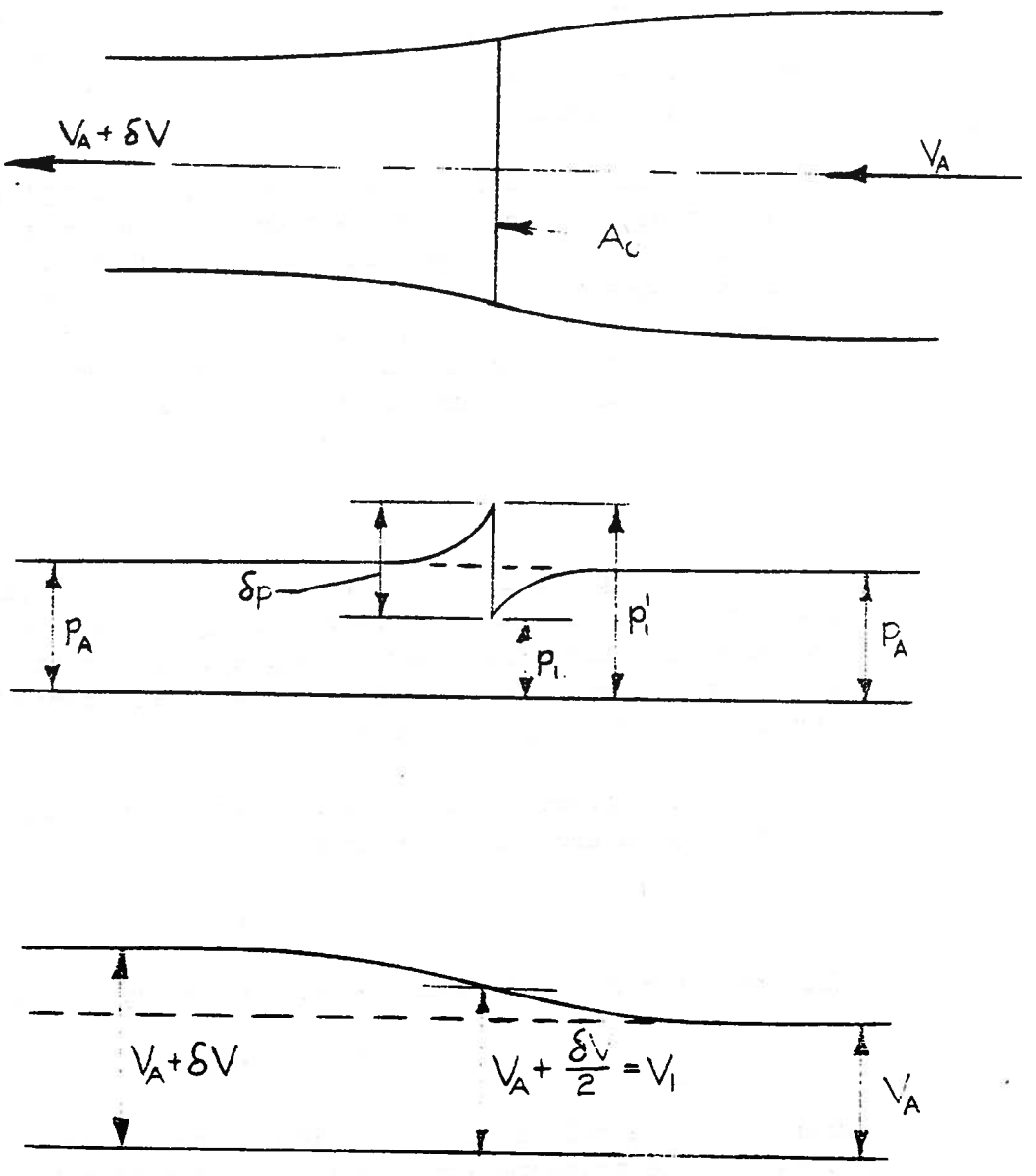

Figure 2.5. Momentum Theory.

Noting that the pressure in the fluid far downstream must be that of the free stream and the same as that far upstream, and applying the Bernoulli equation from the disk to a downstream point and from the disk to an upstream point we get

for upstream of the disk

$$\tfrac{1}{2}\rho V_A^2 + p_A = \tfrac{1}{2}\rho V_1^2 + p_1 \qquad (2.10).$$

for downstream of the disk

$$\tfrac{1}{2}\rho(V_A + \delta V)^2 + p_A = \tfrac{1}{2}\rho V_1^2 + p_1' \qquad (2.11)$$

Solving Equations (2.10) and (2.11) for $p_1' - p_1 = \delta p$ yields

$$\delta p = \tfrac{1}{2}\rho\,\delta V(2 V_A + \delta V) \qquad (2.12)$$

Also from Equations (2.7), (2.8) and (2.9)

$$\delta p = \rho \cdot V_1 \cdot \delta V \qquad (2.13)$$

Eliminating δp from Equations (2.12) and (2.13) gives

$$V_1 = V_A + \tfrac{1}{2}\delta V \qquad (2.14)$$

or at the disk the increase in velocity is half the total increase.

Using Equations (2.8), (2.9) and (2.14) the thrust becomes

$$T = \rho \cdot A_o (V_A + \tfrac{1}{2}\delta V)\,\delta V \qquad (2.15)$$

In the absence of frictional losses, the efficiency of the propeller may be defined as the thrust horsepower delivered by the screw, $T V_A$, divided by the power absorbed by the screw, $T V_1$,

$$\eta = \frac{T V_A}{T V_1} = \frac{V_A}{V_A + \tfrac{1}{2}\delta V} \qquad (2.16)$$

From Equation (2.16) it follows that propellers of high efficiency accelerate the water as little as possible (small δ V), while accelerating as large a mass as possible (large V_A). This last statement seems to suggest that large, slow turning propellers would be more efficient than small, high speed ones, a fact that is borne out in practice.

Later developments in the momentum theory include the effect of rotary velocities in the screw race, which deteriorate the efficiency somewhat, but do not detract from the overall conclusions just drawn. As with the induced axial velocity, the induced rotary velocity at the screw disk is half the total.

3.3 BLADE ELEMENT THEORY

In the blade element theory each blade of the propeller is divided into a number of annular strips and each is assumed to act as a two dimensional foil of infinite span. The lift and drag forces are obtained from data such as that available from NACA (mentioned in Section 2.1). A velocity and force vector diagram for a typical element is shown in Figure 2.6.

For a blade element with span dr the drag force on the foil will be dR and the lift dL, where dR is the same direction as the flow velocity V. V is the vector summation of the rotary and advance velocities. The total force, dF, acting on the foil is the vector summation of the lift and drag. In turn dF can be decomposed into the force vectors dS and dM where dS is the thrust supplied by the blade element and dM is the force giving rise to the torque absorbed.

The total thrust output of the propeller is

$$T = Z \int_0^R dS \cdot dr = Z \int_0^R (dL \cos\beta - dR \sin\beta)\, dr \qquad (2.17)$$

and the total torque is

$$Q = Z \int_0^R dM \cdot r \cdot dr = Z \int_0^R (dL \sin\beta + dR \cos\beta)\, r\, dr \qquad (2.18)$$

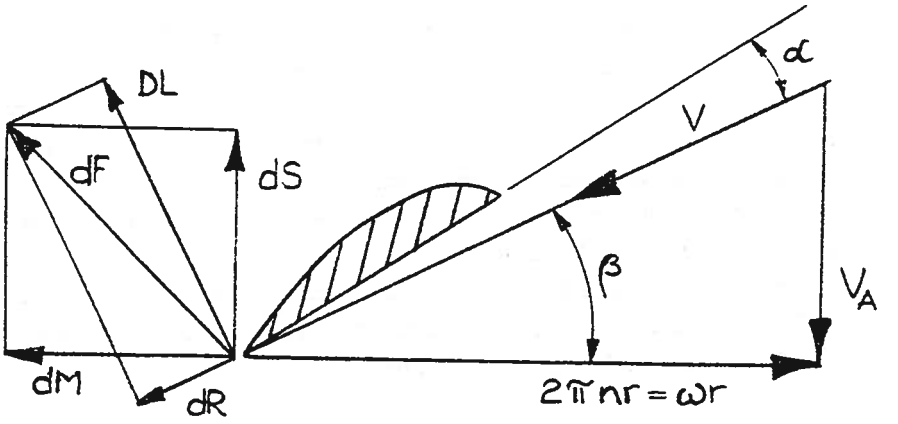

Figure 2.6. Section forces and velocities without induced velocities.

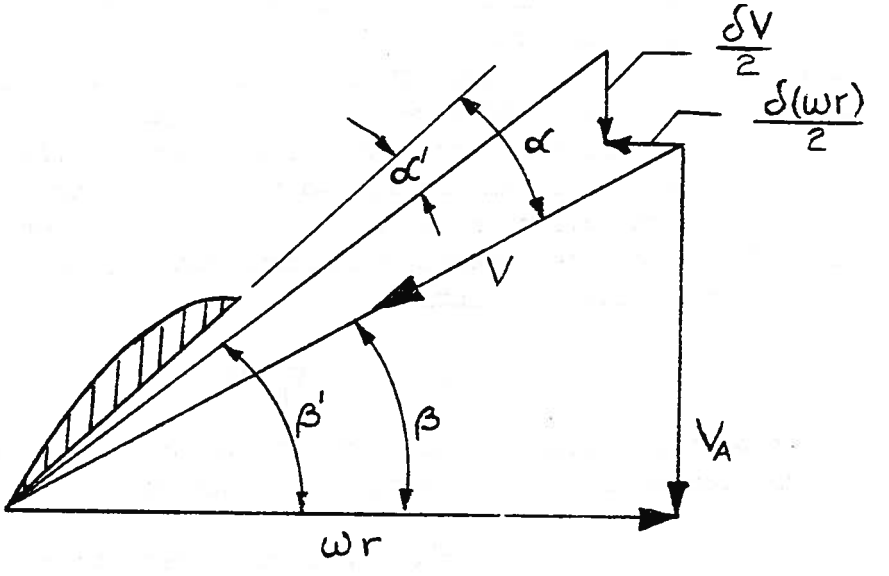

Figure 2.7. Induced velocities and angles of attack.

Equations (2.17) and (2.18) in conjunction with Figure 2.6 represent rather primitive blade element theory. The effect of the induced velocities has been ignored, which can have a dramatic effect on the angle of incidence. Figure 2.7 shows the velocity vector diagram including both the axial and rotary induced velocities. The angle α' is considerably less than the angle α, and since the lift and drag properties of foil sections are highly dependent on incidence angle, neglect of the induced velocities in the blade element theory can lead to serious inaccuracies. This is true even though the induced velocities are small relative to the advance and rotary speeds of the propeller.

The improved blade element theory takes into account the induced velocities that are a product of the momentum theory, but three dimensional effects such as "spilling" of the lift at the blade tips and mutual interference between the blades are not accounted for. The basic circulation theory and its many refinements do however, largely account for these factors.

3.4 CIRCULATION THEORY

The circulation theory, or vortex theory, is the basis for modern theoretical propeller design methods. Circulation is the value of the line integral on a closed curve in a flow field. As an example consider the streamlines in Figure 2.8 where rv = constant and each streamline is circular. The innermost radius, r_o, defines a cylinder with its axis normal to the streamlines V. If r_o is very small, the cylinder is called a vortex tube or filament. If we perform the line integration around any closed path in the flow field we have the circulation,

$$\Gamma = \oint V_s \, ds$$

It can be shown that Γ has a finite value only if the path of integration encloses the origin, O. Otherwise Γ is zero.

For the cylinder and when the free stream velocity U is superimposed, the total velocity on the top of the cylinder is U + V and on the bottom U - V. According to the Bernoulli theorem the pressure will decrease where the velocity has increased and vice versa. The difference in pressure is

$$\delta p = \tfrac{1}{2}\rho \left[(U + V)^2 - (U - V)^2\right] = 2 \rho \cdot U \cdot V$$

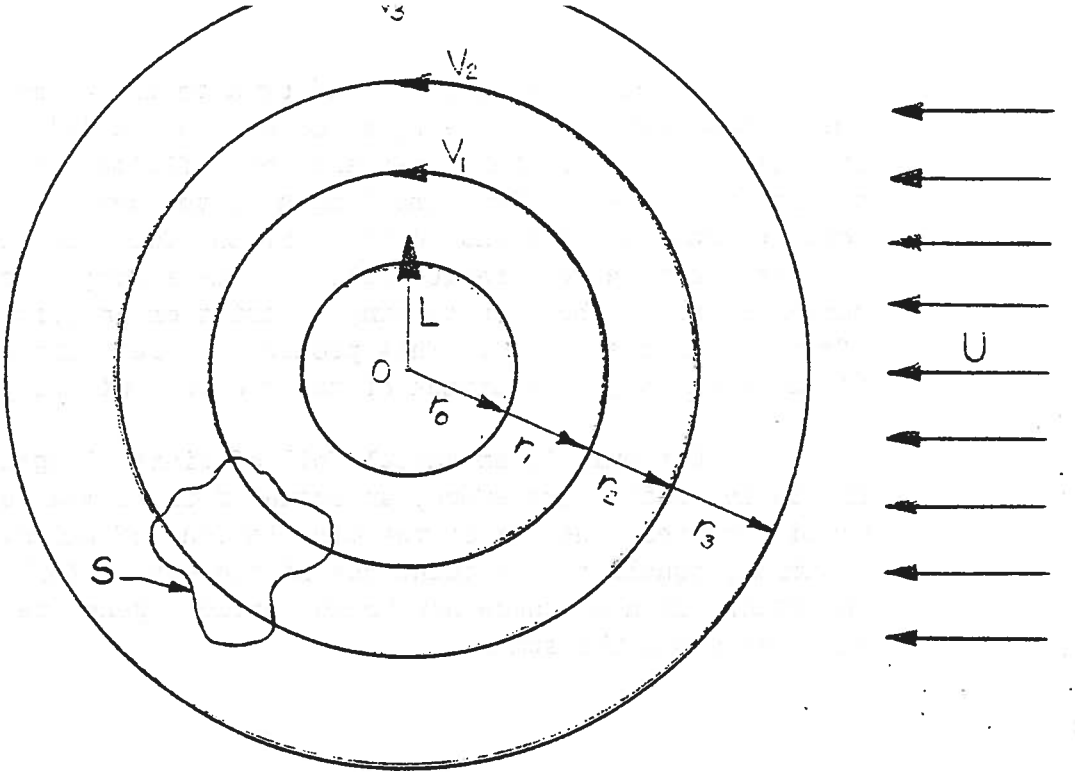

Figure 2.8. Vortex Filament.

The lift per unit length of the cylinder will be the integrated pressure difference around half the cylinder, top or bottom, or half the value of the line integral of the pressure difference around the complete cylinder.

$$L = \tfrac{1}{2} \oint \delta p \cdot dS = \rho U \oint V \, dS$$

or

$$L = \rho \cdot \Gamma \cdot U \tag{2.19}$$

Equation (2.19) is known as the Kutta-Joukowsky equation and is of fundamental importance for the calculation of the lift on a foil section. If the lift is to be calculated, the circulation must be known.

Circulation is generated by a foil. We may therefore replace the actual propeller blade by a vortex line called the lifting line. This is the core of the vortex and for a finite foil is called the bound or lifting vortex. Along the length of the bound vortex the circulation could be constant and indeed it is if the foil span is infinite. But for the finite aspect ratio foil, such as a prop blade, there is a flow component along the span causing a variation in lift along the span (from hub to blade tip). This produces a free vortex sheet which influences the angle of attack of the sections of the propeller blade.

Not only is an actual foil of finite length, but its chord is finite in width. Therefore, an actual foil is made up of a series of bound vortices, the sum of the circulations of which, at any span-wise location, equals the circulations of the entire foil at that point on the span. Each of these new bound vortices generates its own free vortices along the span.

4. DIMENSIONAL ANALYSIS AND PROPELLER MODEL TESTING

In Section 4 of Chapter 1 the detailed dimensional analysis was carried out for the resistance of any given hull form. For propellers, knowledge of the parameters that influence both thrust and torque is desired. In a manner analogous to that for resistance, the thrust could be a function of the following:

a) density of water, ρ
b) viscosity of water, μ
c) acceleration due to gravity, g
d) pressure in the water, p
e) propeller size represented by the diameter, D
f) inflow speed represented by V_A and n

As with resistance

$$T \propto \rho^a, \mu^b, g^c, p^d, D^e, V_A^f, n^g$$

or

$$\frac{T}{\rho D^2 V_A^2} = f\left[\frac{V_A}{\sqrt{g D}}, \frac{V_A}{n D}, \frac{V_A D}{\nu}, \frac{p}{\rho V_A^2}\right] \qquad (2.20)$$

where the propeller thrust coefficient is

$$C_T = \frac{T}{\rho D^2 V_A^2} \tag{2.21}$$

Similarly for torque

$$\frac{Q}{\rho D^3 V_A^2} = f\left[\frac{V_A}{\sqrt{g D}}, \frac{V_A}{nD}, \frac{V_A D}{\nu}, \frac{p}{\rho V_A^2}\right] \tag{2.22}$$

and

$$C_Q = \frac{Q}{\rho D^3 V_A^2} \tag{2.23}$$

Equations (2.20) and (2.22) state that, if the four quantities on the right-hand side of each equation are equivalent for two geometrically similar propellers of different sizes, then the flow patterns will be similar and the values of C_T and C_Q identical for both propellers. This statement applies to propellers tested in open water, i.e., without the hull model in proximity to the propeller model. The first term, $V_A/\sqrt{g D}$, is a Froude number based on diameter and the third term, $V_A D/\nu$, is a Reynolds' number. As with ship model tesing, both Froude's Law and Reynolds' Law cannot be satisified simultantously. However, in contrast to ship model testing, a correction is seldom required for failure to satisfy Reynolds' Law. This is because at a Reynolds' number of about

$$R_n = \frac{MWR \cdot D \sqrt{V_A^2 + (0.7\Pi\, nD)^2}}{\nu} = 3 \times 10^5$$

the values of C_T and C_Q are observed to be constant. Therefore, model tests are run at high Reynolds' numbers where compliance with Reynolds' Law is safely neglected.

The fourth term, $p/\rho V_A^2$, can be neglected as long as cavitation will not occur on the full scale propeller for the same reason cited in the discussion of ship models, i.e., the forces on the propeller are due to pressure differences in the water, not total pressure. However, many high speed propellers may be expected to cavitate in which case the model must be tested in a water tunnel where the total pressure in the water can be regulated by partially evacuating the atmosphere from the tunnel.

The second term in Equations (2.20) and (2.22) states that the slip of both model and full scale must be the same since

$$s_R = 1 - \frac{V_A}{P \cdot n} = 1 - \frac{J}{P/D}$$

where $J = V_A/n \cdot D$= advance coefficient and, since the two propellers are geometrically similar, P/D must be the same.

If the model test results are plotted as C_T and C_Q against a base of J the values would be applicable to the full scale propeller in open water provided that the model Reynolds number was sufficiently high and, further, that the full scale propeller does not cavitate. Should cavitation occur, an additional requirement is that the pressure be regulated in the model test.

In practice Froude's Law seldom needs to be satisfied since the propeller is sufficiently immersed to avoid wavemaking due to the propeller. For this reason, when model propellers are oper water tested, they are at a depth of two or three diameters. However, since cavitation must nearly always be taken into account in designing propellers for high speed craft, model propeller data obtained in water tunnels are required. Usually, propeller tests in water tunnels are conducted in the absence of a free surface so that Froude's Law may be ignored if the full scale propeller is not expected to operate in the vicinity of the free surface. For most boats this will be the case, but in cases such as some race boats, the propellers will operate near the free surface. Reference 12 contains test data on four fully cavitating propellers operating only partly submerged as well as deeply submerged. The torque and thrust characteristics were found to be greatly dependent on depth of submergence. When the propellers were partially out of the water, however, the torque and thrust coefficients were essentially constant above a Froude number of 3.0 based on diameter. For a two-foot diameter propeller F = 3.0 corresponds to a boat speed of about 15 knots, a very low speed for a race boat. Therefore, when model testing propellers to be used near the free surface, it is necessary to simulate the water depth to obtain the correct torque and thrust coefficients, but it appears that Froude's Law may be violated if the Froude number is kept high enough.

5. PROPELLER CAVITATION

5.1 GENERAL

Cavitation is a flow phenomenon caused by reduced pressure in the water. If the local pressure is reduced to a sufficiently low value, cavities or bubbles of water vapor will form. Some of these may be shed downstream but others may collapse on the surface of the propeller blades. When this happens over a period of time, physical errosion of the blade material may result. In severe cases the propeller strength may be reduced to the point of blade failure.

Cavitation occurs on highly loaded propellers, i.e., propellers that are required to produce a great deal of thrust, considering their size. The immediate effect is a breakdown in thrust and a resulting loss in efficiency. In severe cases a boat may not attain the desired speed. Even though the bubbles formed contained water vapor, the local pressure in the water need not necessarily be reduced to that of water vapor. Small particles in the water or small air bubbles can serve as nuclei to encourage bubble formation. The following table shows vapor pressure for distilled water at various temperatures:

Temperature Degrees F	Vapor Pressure psia	psfa
32	0.09	1.3
40	0.12	1.8
50	0.18	2.6
60	0.26	3.7
70	0.36	5.2
80	0.51	7.3
90	0.70	10.1
212	14.70	2117

However, propeller cavitation may occur when the local pressure is as great as 2.5 psia. As the table shows, one atmosphere of pressure, 14.70 psia, is about 50 times the vapor pressure of water, 0.26 psia, at normal ambient temperatures. Therefore, the common occurance of air drawing by propellers when the local pressure would be 14.70 psia cannot be a phenomenon similar to cavitation.

Besides blade damage and loss of propeller efficiency, other deleterious effects of cavitation are noise, vibration, and errosion damage to rudders and struts upon which cavitities may impinge and collapse.

5.2 TYPES OF CAVITATION

There are several types of cavitation each of which is called by a fairly descriptive name. They are listed and described here in the order of increasing propeller loading.

Face cavitation - occurs on lightly loaded propellers on the face and near the leading edge when the angle of attack becomes negative due to an adverse local velocity component in the wake.

Tip cavitation - appears as a helical spiral shed from the blade tips and is caused by intense tip vortices, the pressure in the core of which is sufficiently reduced.

Sheet cavitation - occurs as the loading increases and the tip cavities spread along the leading edge. The sheets are generated from the leading edge across the backs of the blades.

Bubble cavitation - forms on the backs downstream from the sheet cavitites.

Hub cavitation - is similar to tip cavitation since a vortex must form at the hub end of each blade.

Finally, if the loading is severe enough, the sheet completely envelopes the blade backs and the propeller is said to be fully cavitating. Propellers designed to be fully cavitating are discussed in Section 7.

5.3 CAVITATION NUMBERS

In general there are two types of cavitation numbers, or indices that suggest the likelihood of cavity flow. One deals with local pressures and is called the section cavitation number. The other considers the propeller as a whole and is usually simply called the cavitation number. In order to distinguish between the two, we shall call the latter the propeller cavitation number. Each type of number has more than one definition. In fact, O'Brien (Reference 2) points out seven different defintions. We shall be concerned with only two, one for each type.

Cavitation numbers are the ratio of the maximum pressure change in the fluid to the stagnation pressure. They can be derived by considering Figure 2.9.

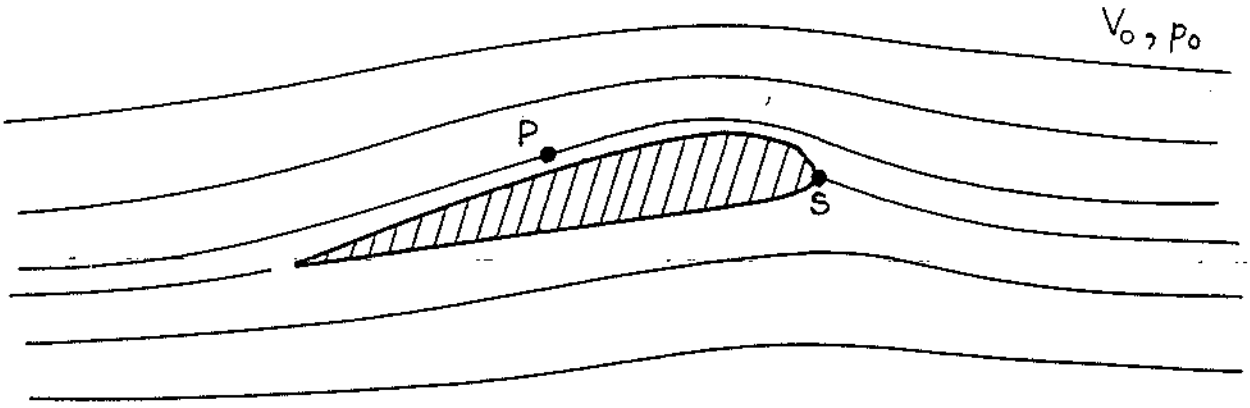

Figure 2.9. Streamlines around a foil.

On any streamline the Bernoulli equation gives

$$p_o + \tfrac{1}{2} \rho V_o^2 \approx \text{constant}$$

At any point P on the streamline with pressure p and velocity V

$$p + \tfrac{1}{2} \rho V^2 = p_o + \tfrac{1}{2} \rho V_o^2$$

and the change in pressure will be

$$\delta p = p - p_o = \tfrac{1}{2} \rho (V_o^2 - V^2) \qquad (2.24)$$

At the stagnation point S the velocity is zero so that the stagnation pressure is

$$\delta p = \tfrac{1}{2} \rho V_o^2 \qquad (2.25)$$

From Equation (2.24)

$$p = p_o + \delta p$$

Cavitation will occur when p is equal to the vapor pressure p_v

$$p_v = p_o + \delta p$$

Or, cavitation will begin when

$$\delta p \geq p_o - p_v$$

Dividing by the stagnation pressure gives the expression for cavitation number

$$\sigma = \frac{p_o - p_v}{\tfrac{1}{2} \rho V_o^2} \qquad (2.26)$$

5.3.1 PROPELLER CAVITATION NUMBER, σ_o

The propeller cavitation number is useful for the presentation of model data and for use in empirical methods to determine the likelihood of cavitation. It is not particularly useful for determining local cavitation conditions. It is based on the stagnation pressure of the speed of advance and the hydrostatic pressure at the propeller axis.

$$\sigma_o = \frac{p_a + \rho g h - p_v}{\frac{\rho}{2} V_A^2} \qquad (2.27)$$

Figure 2.10 gives the relation between σ_o and advance speed in knots in salt water for $\rho gh \ll (p_a - p_v)$, which is usual for high-speed craft.

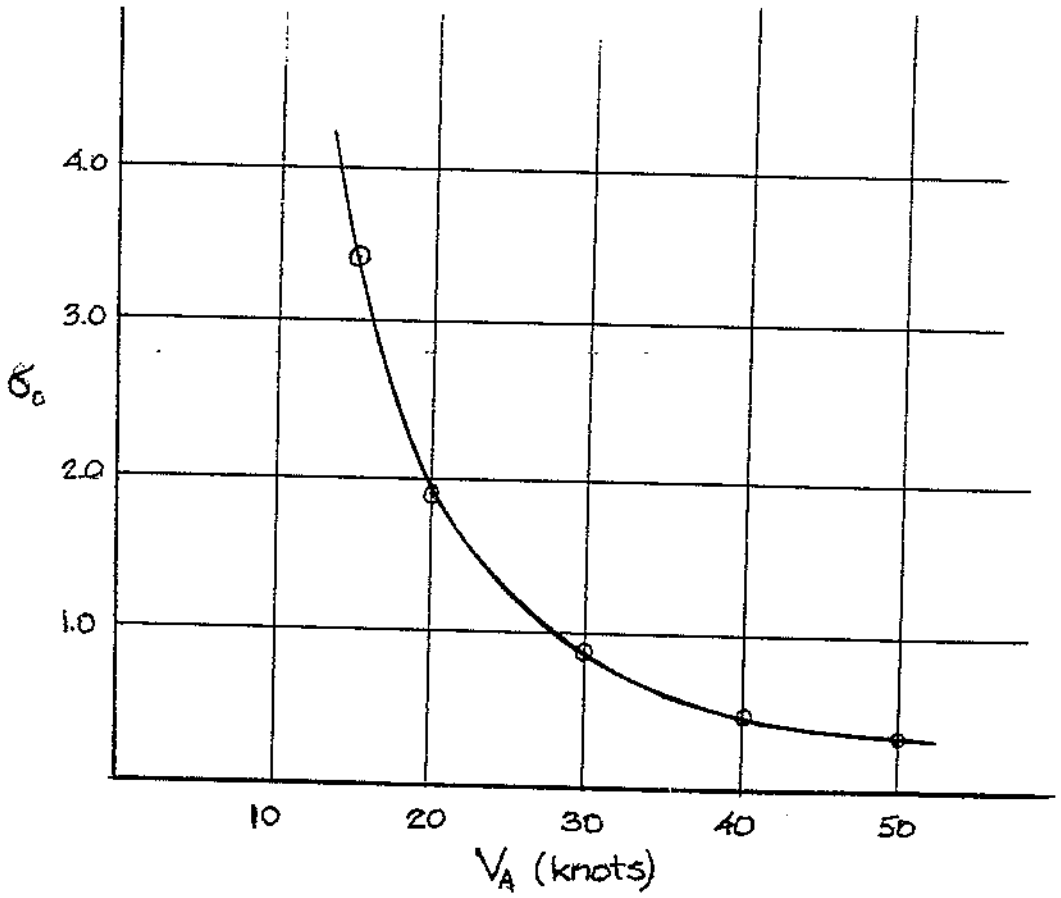

Figure 2.10. Approximate relationship between σ_o and V_A.

5.3.2 SECTION CAVITATION NUMBER , σ_x

The section cavitation number is based on the local inflow velocity, ignoring the induced velocity. Therefore, it is useful for determining cavitation conditions for individual blade elements. The hydrostatic pressure term is based on the depth of water to the blade section of interest when the blade is in the upright position.

$$\sigma_x = \frac{p_a + \rho g(h - xR) - p_v}{\frac{\rho}{2}\left[V_A^2 + (2\pi n\, xR)^2\right]} \qquad (2.28)$$

where h = the depth of submergence of the xR radius when the blade is upright

For deeply submerged propellers ($h \gg R$)

$$\sigma_x \simeq \frac{\sigma_o}{1 + (\frac{x\pi}{J})^2} \qquad (2.29)$$

where $J = V_A/nD$

Commonly, $x = 0.7$ is used as the design radius since the greatest thrust is produced at the section located about 0.7R from the propeller axis. Hence, $\sigma_x = \sigma_{0.7}$ is commonly the section cavitation number of interest.

5.4 CAVITATION CRITERIA

It is important to know the likelihood of cavitation when designing blade sections or selecting a propeller type from among those available in the literature. There are in the literature numerous charts that give some guidance to the extent and type of cavitation that may be expected as functions of thrust loading, cavitation number, blade area ratio and slip. Most of these charts are empirically derived from observations of cavitation patterns on model propellers and other practical experience. Of these, perhaps the most widely known is the Burrill chart, first published in 1943 and subsequently widely reproduced in the literature. See Figure 2.11.

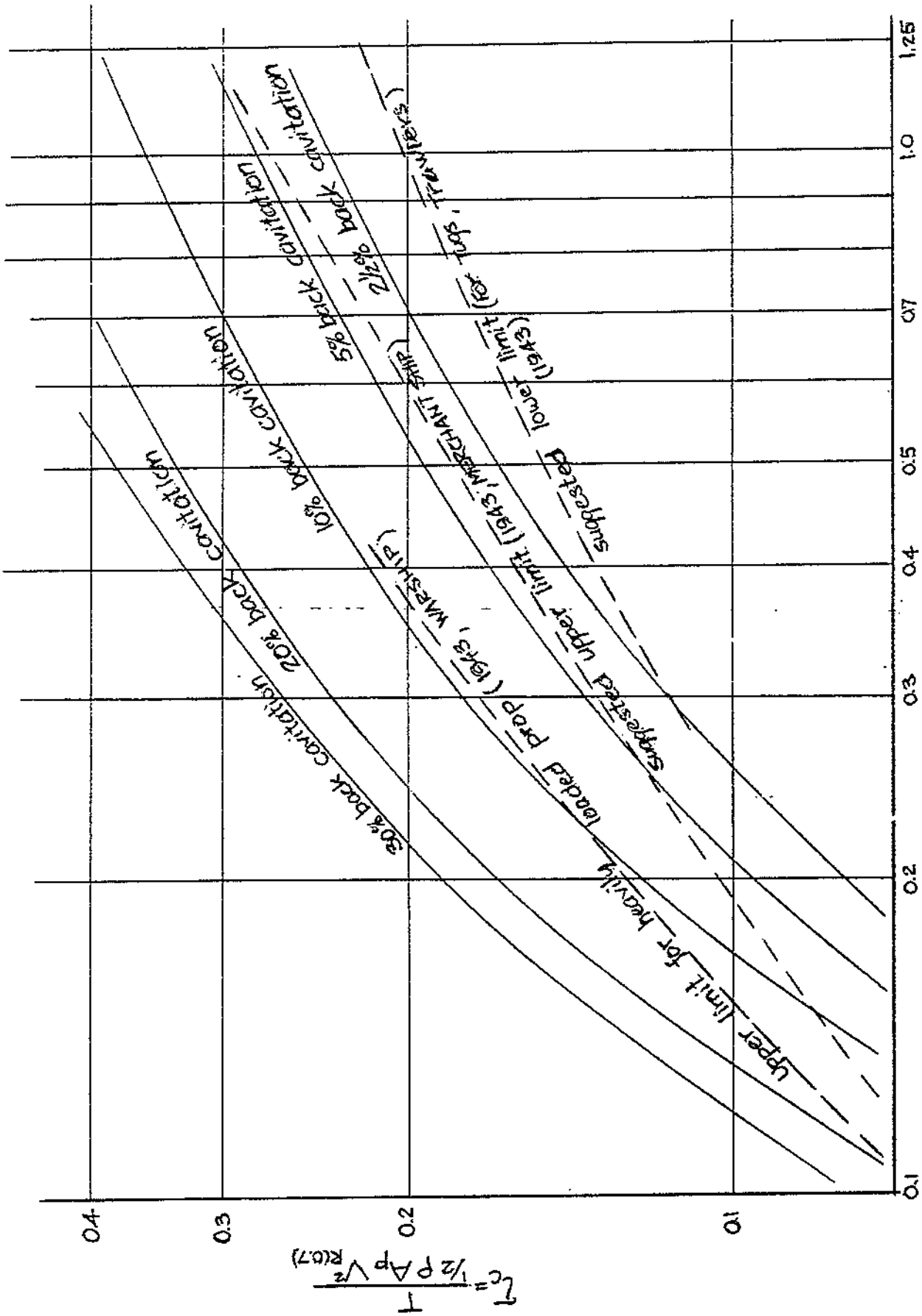

Figure 2.11. Cavitation Criteria.

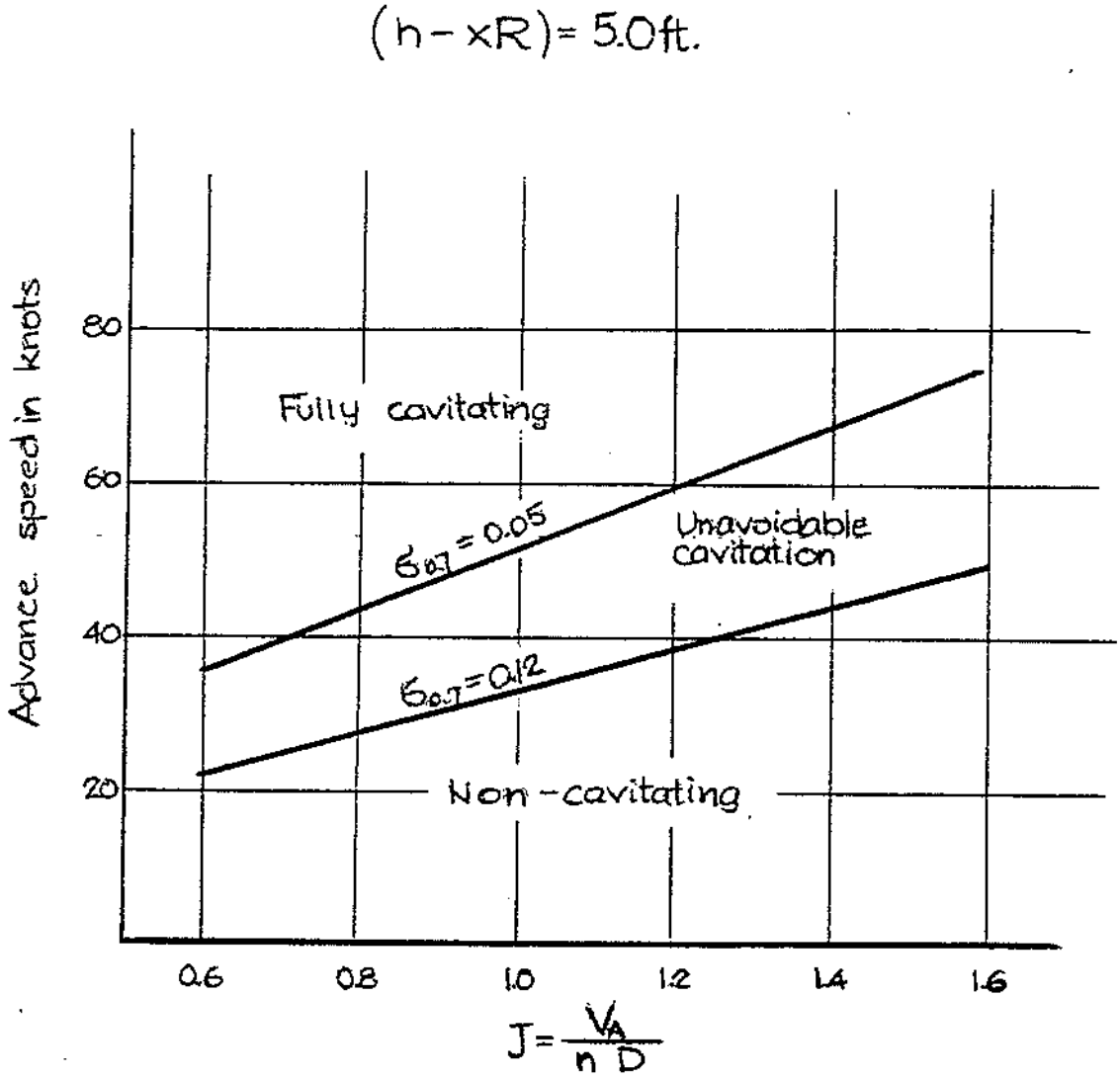

Figure 2.12. Design ranges for high speed propellers.

Most of the empirical charts make little or no allowance for propeller section type that may be a mandatory requirement of any cavitation criteria for propellers to be used on planing craft. For extremely high speeds, fully cavitating sections may be required because severe cavitation is unavoidable. For lower speeds, there may be the possibility of some cavitation and at even lower speed fully wetted conditions may be assured. Kruppa (Reference 4) has devised a chart based on assumptions of uniform inflow conditions and relationships between pressure differences and section properties from thin airfoil theory. The chart is reproduced in Figure 2.12. In the upper left-hand region of the figure, fully cavitating propellers will be required while in the lower right-hand region there is little chance of any cavity flow. The section cavitation number must have a value less than about $\sigma_{0.7} = 0.12$ for cavitation to occur. If $\sigma_{0.7} \leq 0.05$, fully cavitating conditions may be expected. In the central region on the chart in Figure 2.12, one may have to tolerate some cavitation and may select a propeller type designed to maintain efficiency under such conditions.

6.0 PROPELLER TEST DATA PRESENTATION

6.1 K - J SYSTEM

In Section 4 it was noted that open water test data or water tunnel test data could be presented as C_T and C_Q against J. However, at low advance speeds the denominator of these coefficients becomes small and the values of the coefficients correspondingly very large. For tugboat bollard conditions the advance velocity is zero and the coefficients are infinitely large. To avoid this disadvantage we can replace V_A by nD since $J = V_A/nD$ is the same for model and full scale. New coefficients result.

For thrust

$$K_T = \frac{T}{\rho n^2 D^4} \tag{2.30}$$

for torque

$$K_Q = \frac{Q}{\rho n^2 D^5} \tag{2.31}$$

The efficiency in open water is

$$\eta_o = \frac{T V_A}{2\pi Q n}$$

or

$$\eta_o = \frac{J}{2\pi} \frac{K_T}{K_Q} \tag{2.32}$$

When the quantities in Equations (2.30), (2.31) and (2.32) are plotted against J we have a graph of the "open water characteristics" in probably the most common format, called the K-J system. An illustration is given in Figure 2.13 for the NSMB B-Series with 4 blades and 0.55 area ratio. (See section 7 for a description of the NSMB B-Series). As the figure shows, one of the principal advantages of the K-J system is the apparent display of the effects of pitch-diameter ratio. . When design conditions are related to values of torque or thrust, instead of delivered or thrust horsepowers, the K-J system is quite suitable.

The effects of cavitation on thrust and torque characteristics of a single propeller operating at different cavitation numbers are easily seen in the K-J data presentation format. An illustration for one of the KCD series propellers (description given in Section 7) is given in Figure 2.14. For higher values of slip, or lower values of J, when the propeller is more heavily loaded, the thrust coefficient decreases for lower values of σ_o more than for less severe cavitation conditions. This substantiates the remarks made in earlier sections to the effect that caviation causes thrust breakdown.

6.2 B - δ SYSTEM

Another common data presentation system is the B-δ system first used by Taylor. Its chief advantage is that design conditions related to horsepower values, either thrust or delivered, are accommodated by the B-δ system. Equations for the pertinent quantities are

For thrust

$$B_u = \frac{N\, U^{0.5}}{V_a{}^{2.5}} \tag{2.33}$$

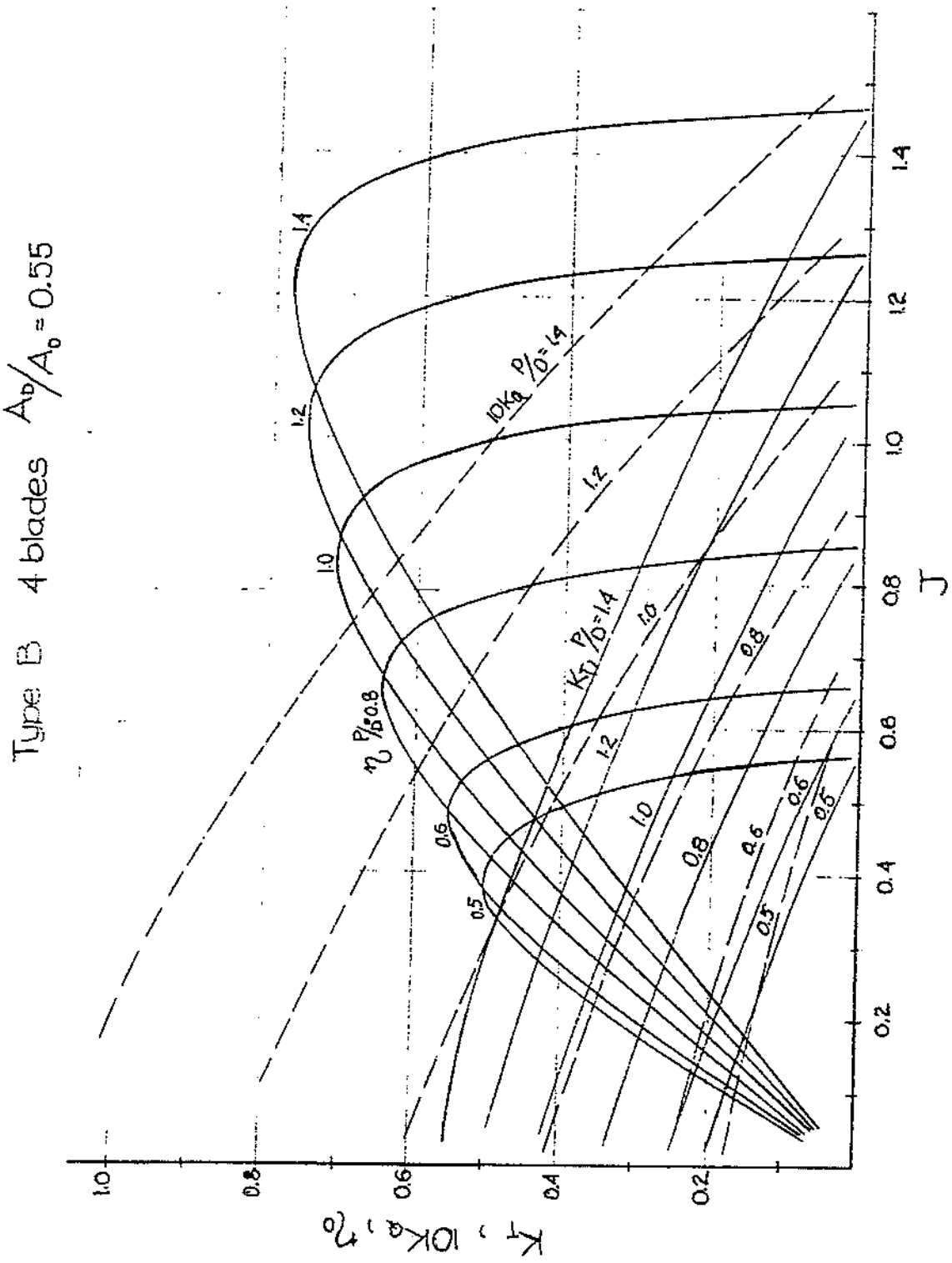

Figure 2.13. Troost Type B-4.55 propeller open water chart.

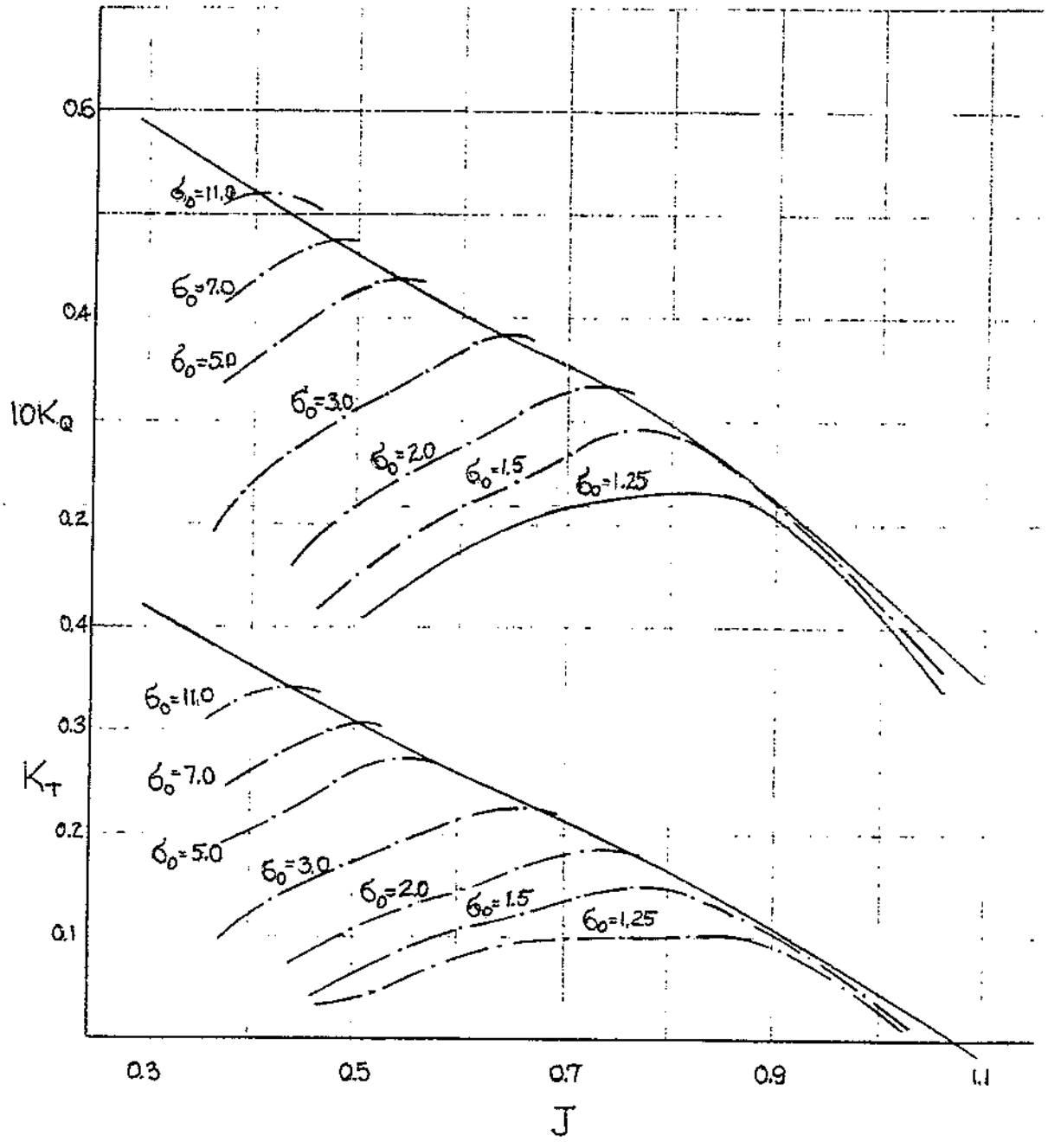

Figure 2.14. KCD 6.65 propeller open water chart for p/o = 1.0.

For torque

$$B_p = \frac{N\ P^{0.5}}{V_a{}^{2.5}} \tag{2.34}$$

For slip

$$\delta = \frac{N\ D}{V_a} \tag{2.35}$$

The open efficiency is

$$\eta_o = \left(\frac{Bu}{B_p}\right)^2 \tag{2.36}$$

where

N	=	revolutions per minute
U	=	thrust horsepower
P	=	delivered horsepower
V_a	=	advance speed in knots

Figure 2.15 shows the $B_p - \delta$ chart for the data of the same propellers used for Figure 2.13

There are alternative presentation systems to those mentioned, but usually the data of propeller series is presented in either the K-J or B-δ system and possibly in a second system. One example is the $\mu - \sigma$ system where

$$\phi = V_A \left(\frac{\rho\ D^3}{Q}\right)^{\frac{1}{2}} = \frac{J^{\frac{1}{2}}}{(K_Q)^{\frac{1}{2}}}$$

$$\mu = n\left(\frac{\rho\ D^5}{Q}\right)^{\frac{1}{2}} = \frac{1}{(K_Q)^{\frac{1}{2}}}$$

$$\sigma = \frac{D\ T}{2\Pi Q} = \frac{K_T}{2\Pi K_Q} = \frac{\eta_o}{J}$$

Convenient conversions between the K-J and B-δ systems are:

$$B_p = 33.09 \left(\frac{K_Q}{J^5}\right)^{\frac{1}{2}}$$

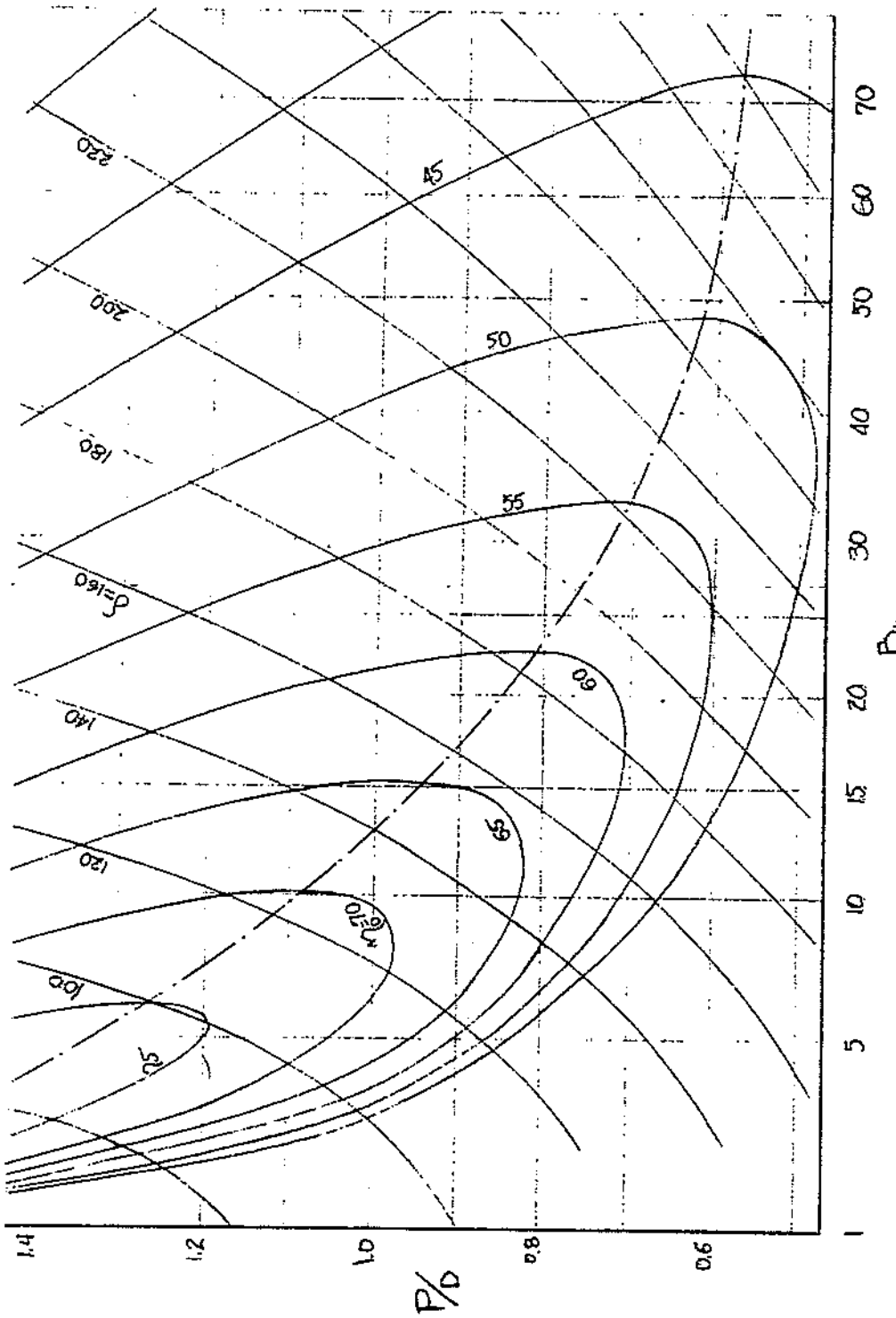

Figure 2.15. Troost type B-4.55 B_p - δ chart.

$$B_u = 13.20 \left(\frac{K_T}{J^2}\right)^{\frac{1}{2}}$$

$$\delta = \frac{101.3}{J}$$

7. SYSTEMATIC SERIES OF PROPELLERS

Over the years many methodical series of model propellers have been tested. Mainly the effects on thrust and torque of propeller blade area ratio and pitch-diameter ratio have been investigated, but some series work has included limited systematic studies of the effects due to variations in skew, blade thickness, radial pitch distribution, etc. The data from these series are applicable only for the cavitation conditions that existed during the tests. Therefore, the designer cannot apply data from a series of models tested at σ_o = atm (the pressure on the surface of the water for the tests was one atmosphere) if he anticipates cavitation will occur on the full scale propeller, at least not without some empirical adjustment of the data. Most propeller series have been model tested at σ_o = atm, but some have been tested over a range of values of σ_o.

No systematic series of models of fully cavitating propellers has yet been tested. However, some isolated test results are in the literature. See, for example, Reference 12. Theoretical methods of designing supercavitating, or fully cavitating, propellers have proved to be reasonably accurate. Thrust and torque characteristic for a series of theoretically derived supercavitating propellers may be found in Reference 13 while Reference 14 explains a design method based on theory.

Table 1 lists some of the more useful model series in the literature. The data from the first two series, AEW and NSMB, can be applied only when there are assurances of no cavitation. The KCD series data are applicable to boat speeds of about 25 to 30 knots according to the curve in Figure 2.10. Similarly, the KCA series data may be used for boat speeds up to 40 knots and the Newton-Hadar series data up to perhaps 60 knots. For higher speeds, supercavitating propellers will be required.

The Newton-Radar propellers are of special interest to the high speed boat designer since they were specially designed to operate under cavitating conditions even though they are not supercavitating propellers in the usual sense of the term. Norma

fully cavitating sections are somewhat wedge-shaped. They have very sharp leading edges, required to induce the cavity, and blunt, squared-off tails, required mainly so that the section will have enough material for adequate strength. The requirement of a sharp leading edge eliminates the possibility of much material in this region and this is a problem as far as strength is concerned. Owing to the blunt trailing edge, the propeller blades have very high form drag at speeds less than required for the fully developed cavity. Consequently supercavitating propellers have inferior efficiency at low speeds. Since the Newton-Rader propeller sections are similar to those used in the design of non-cavitating propellers the efficiency is acceptable over a broad speed range. As noted in Table 1, Reference 11 contains only a tabulation of the test results for the Newton-Rader series. To serve as a design aid, Figures 2.16 and 2.17 show the Newton-Rader data in the K-J presentation system.

TABLE I

Summary of Model Tests of Systematic Propeller Series

Series	Data Applicability	DESCRIPTION: Blade Outline	Section Type	Rake deg.	Z	Blade Thickness Ratio & Distribution	Remarks	P/D Range	BAR Range	σ_0 Range	Data Presentation System	Ref. No.
AEW(Gawn)	fully wetted	elliptic	flat-face segmental	none	3	0.060 linear		0.40-2.00	0.20-1.10	atm.	K - J	5
NSMB(Troost)	fully wetted	skewed	airfoil @ inner radii, segmental @ outer radii	15	2-7	0.040 - 0.055 linear	B-series described here was preceded by A-series which was somewhat more susceptible to cavitation.	0.50-1.40	0.30-1.05	atm.	K - J B - δ η - σ	6 & 7
KCD	partially cavitating	skewed	airfoil @ inner radii, segmental @ outer radii	8-12	4-6	0.040 - 0.060 linear	includes effects of radial pitch distribution and amount of skew	0.68-1.60	0.58-0.80	1.25 -11.0	K - J B - δ	8 & 9
KCA(Gawn)	partially cavitating	elliptic	flat-face segmental	none	3	0.045 linear	similar to AEW (Gawn) series	0.60-2.00	0.50-1.10	0.50- atm.	K - J	10
Newton-Rader	partially cavitating	elliptic	composite	none	3	0.060 non-linear (hook at tip)	sections developed from NACA a = 1.0 mean line, with quasi-elliptic thickness form and modified nose.	1.05-2.04	0.48-0.95	0.25- atm.	tabulated	11

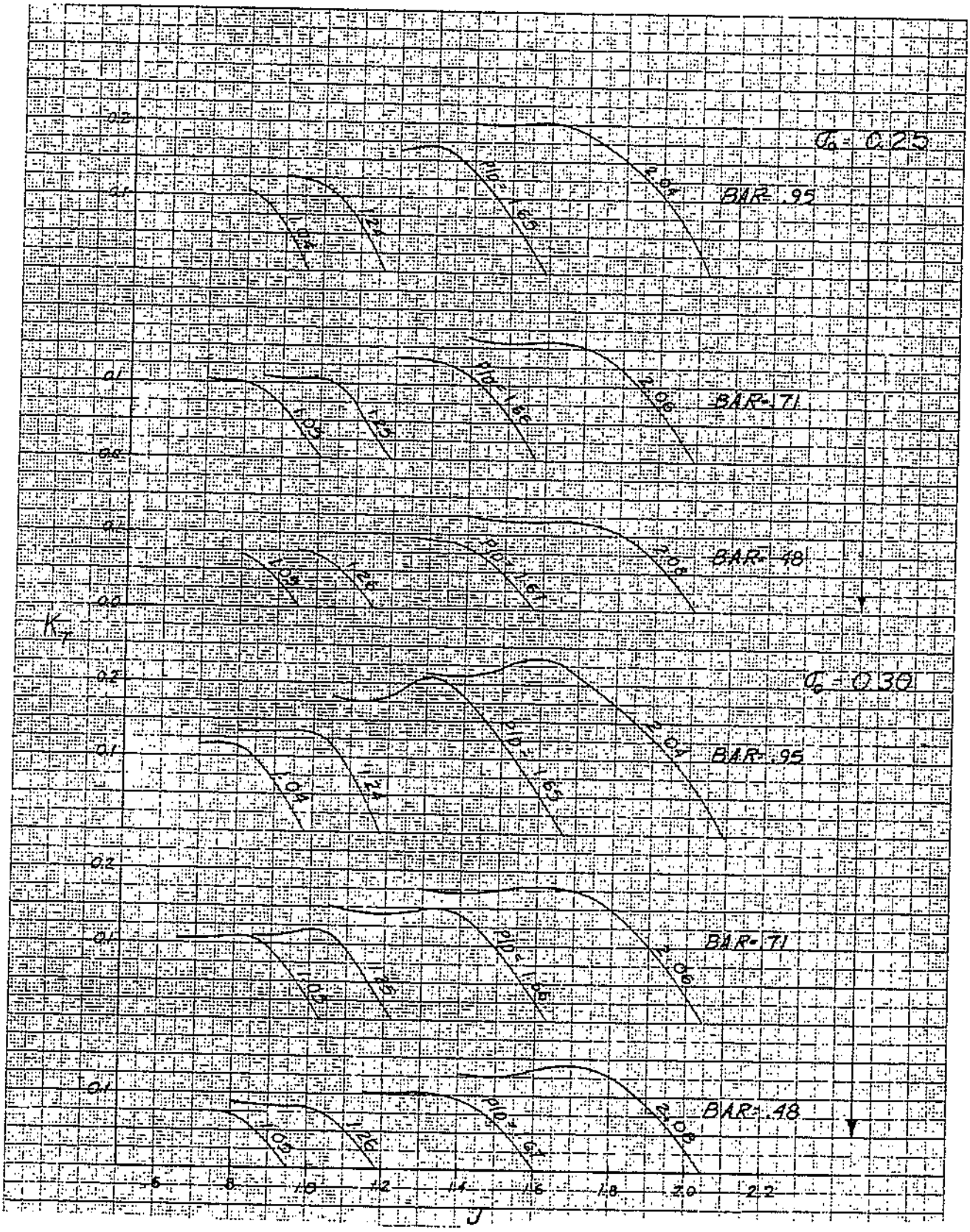

Figure 2.16 (a). K_T vs J for Newton and Rader propellers in open water (Reference 11).

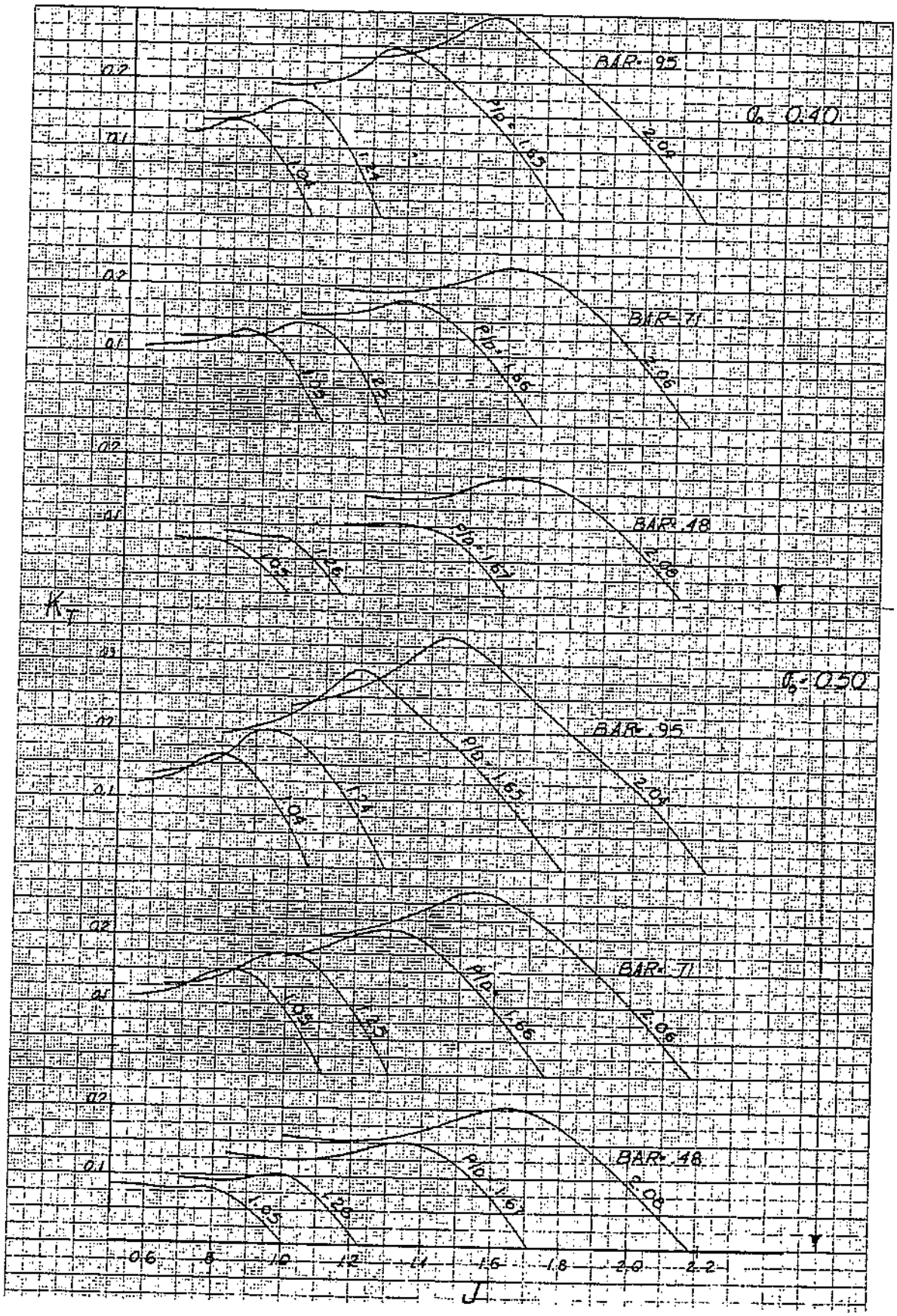

Figure 2.16 (b). K_T vs J for Newton and Radar propellers in open water (Reference 11).

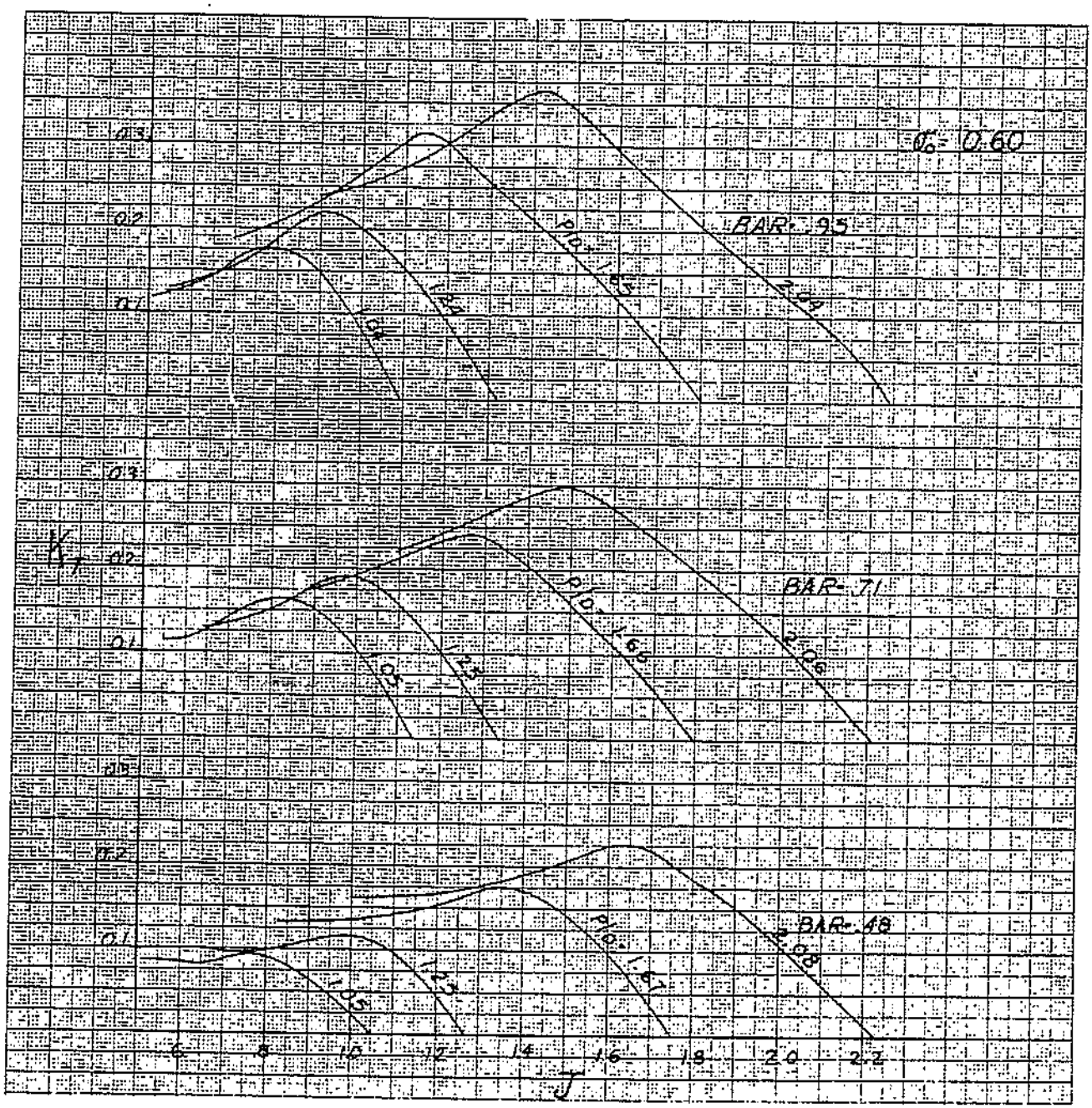

Figure 2.16 (c). K_T vs J for Newton and Radar propellers in open water (Reference 11).

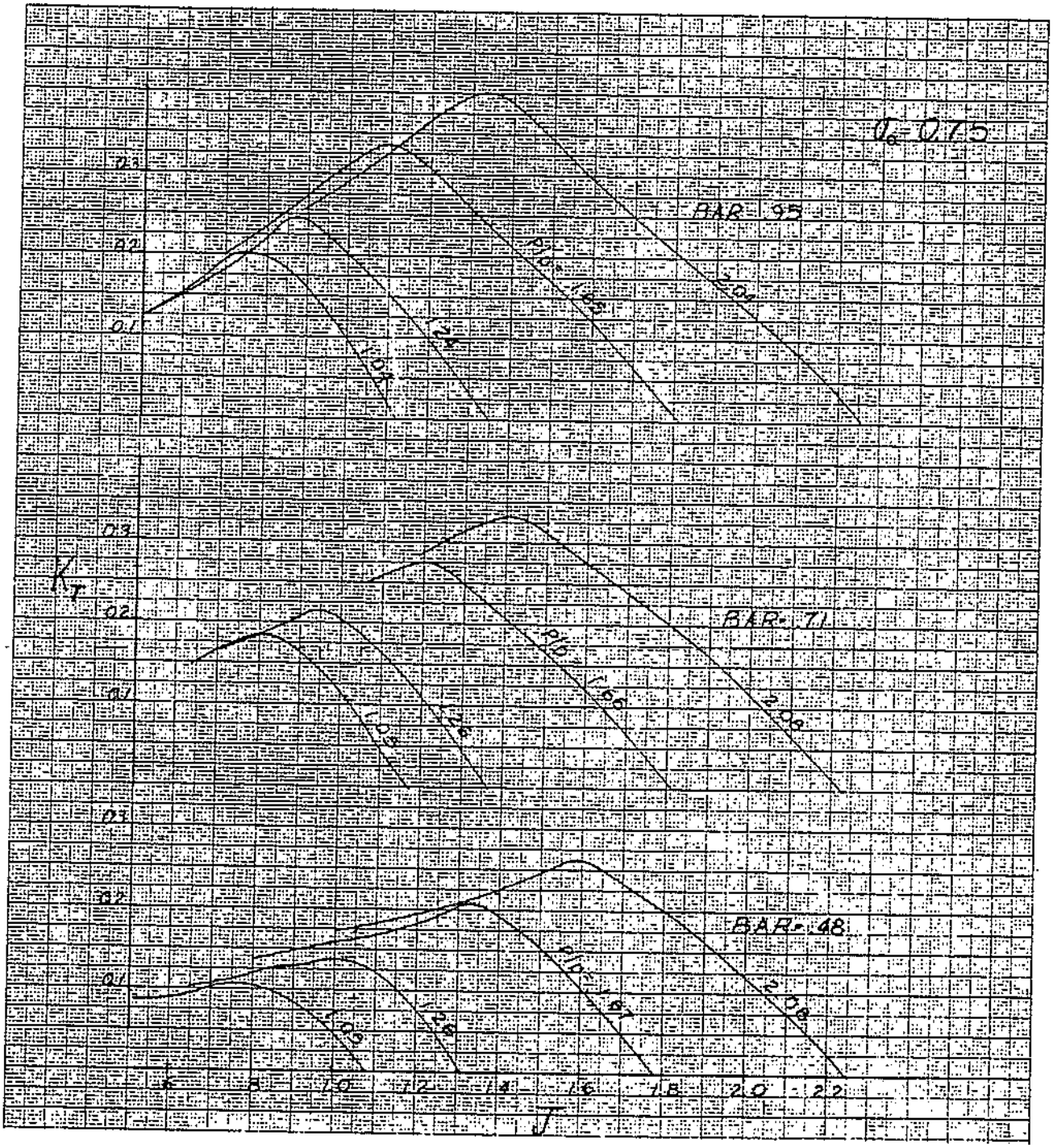

Figure 2.16 (d). K_T vs J for Newton and Radar propellers in open water (Reference 11).

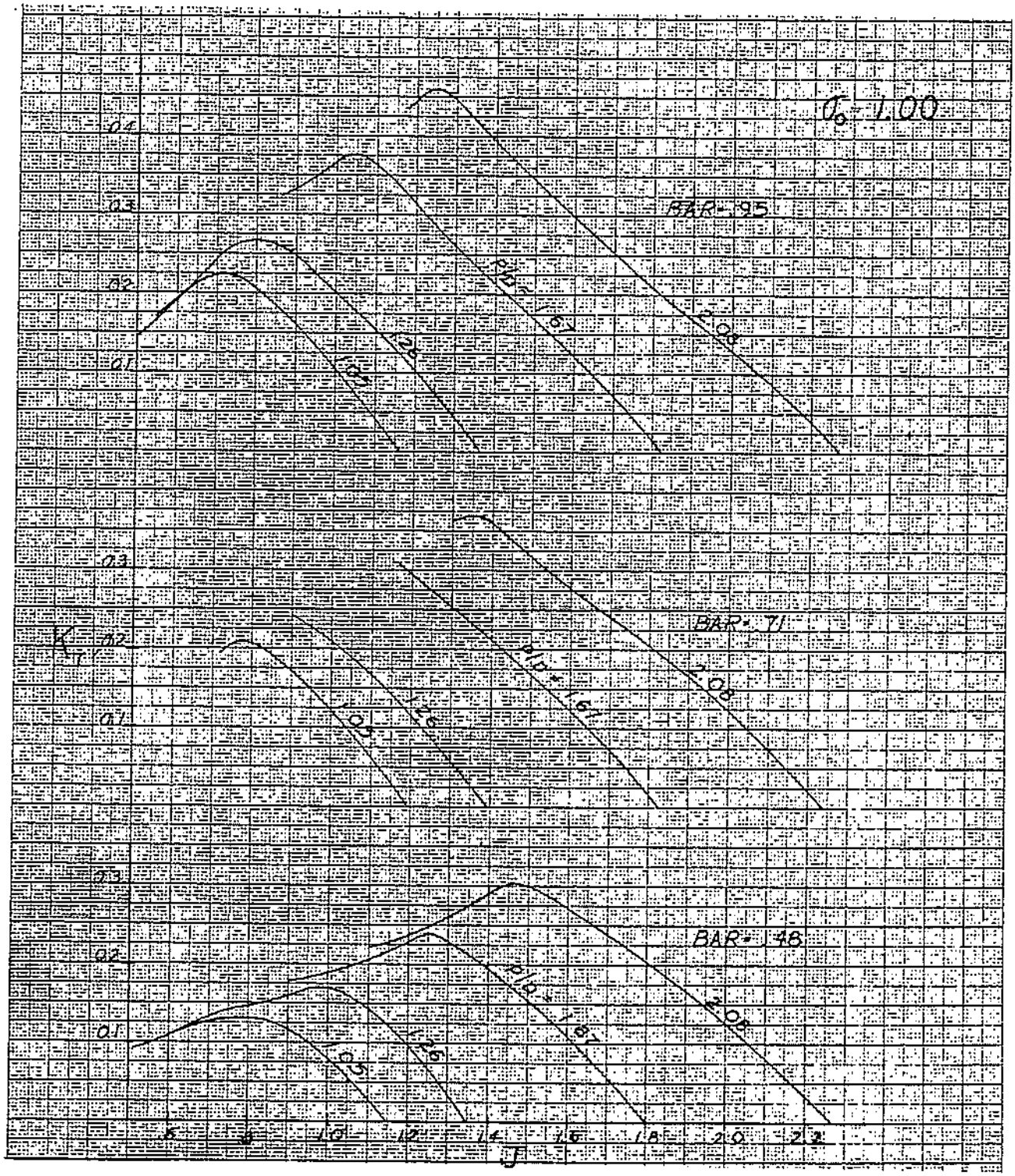

Figure 2.16 (e). K_T vs J for Newton and Radar propellers in open water (Reference 11).

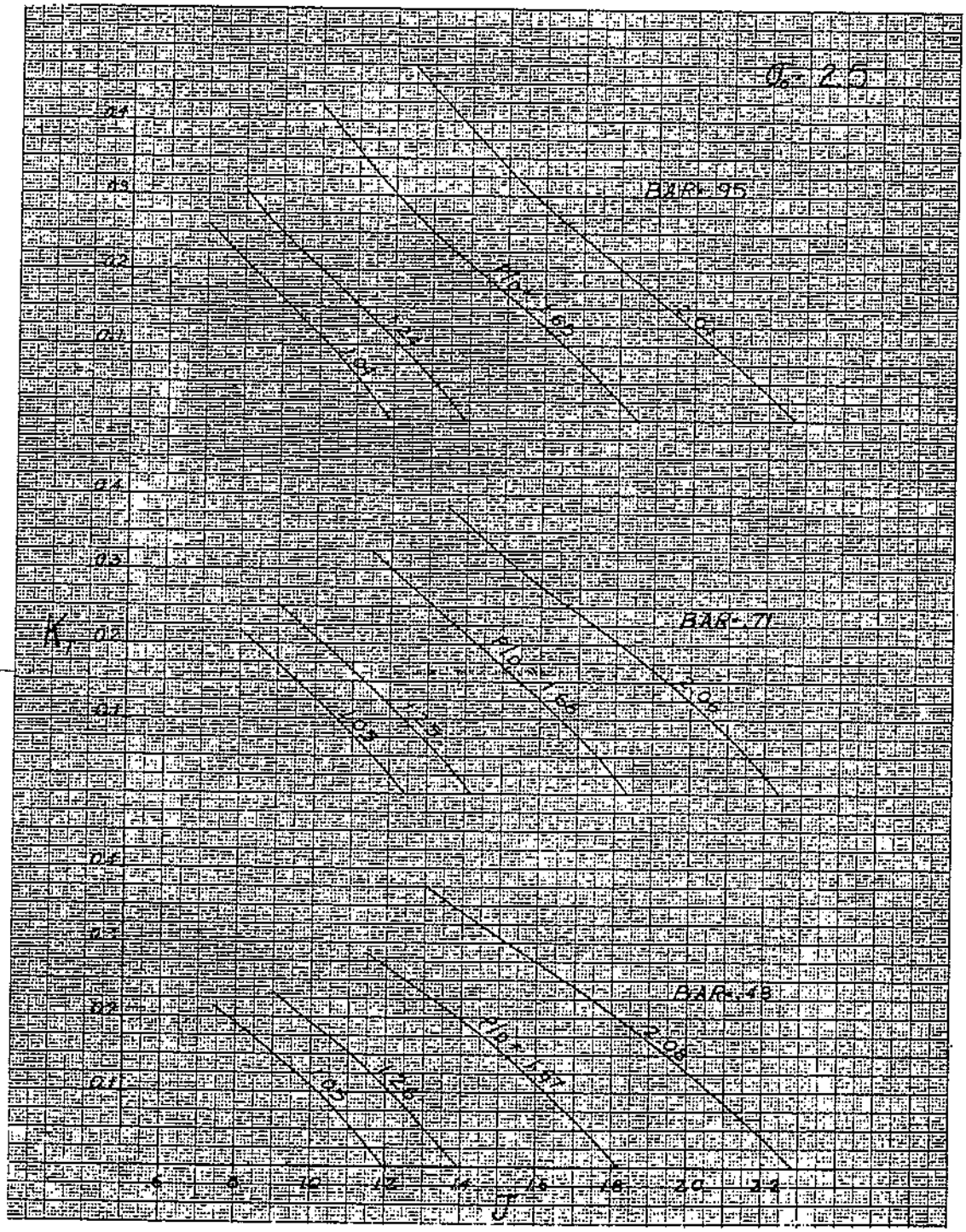

gure 2.16 (f). K_T vs J for Newton and Radar propellers in open water (Reference 11).

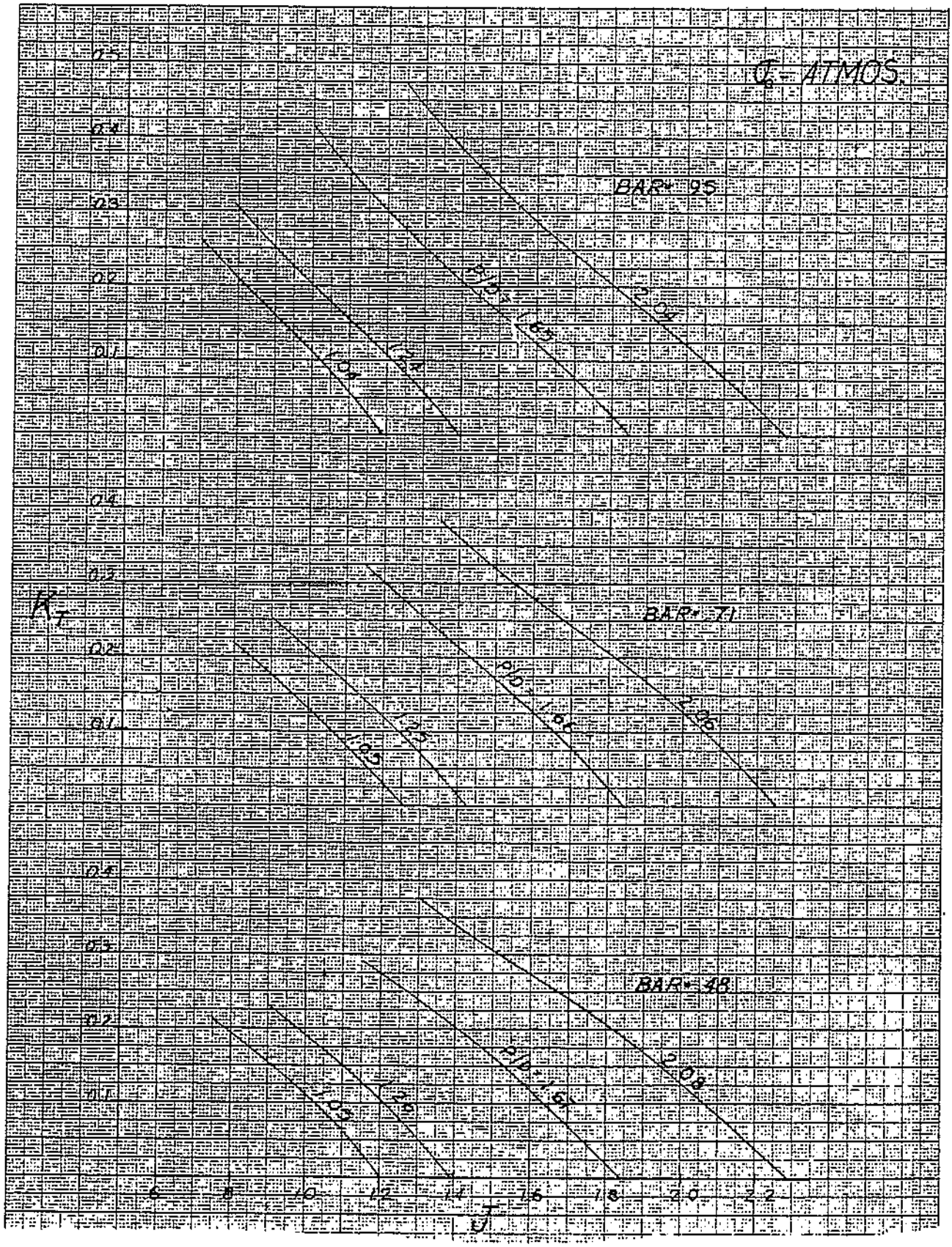

Figure 2.16 (g). K_T vs J for Newton and Radar propellers in open water (Reference 11).

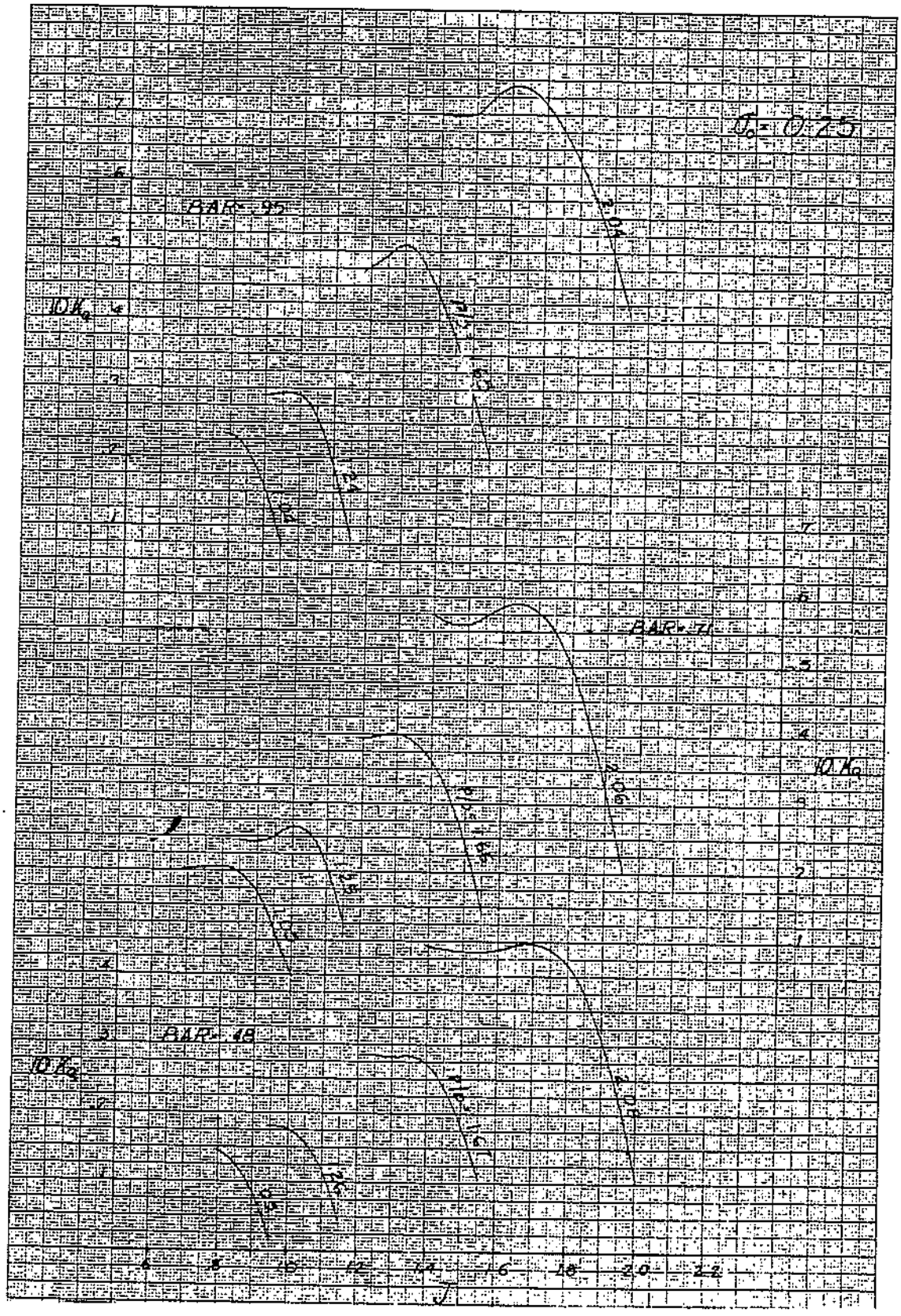

Figure 2.17 (a). 10 K_Q vs J for Newton and Radar propellers in open water (Reference 11).

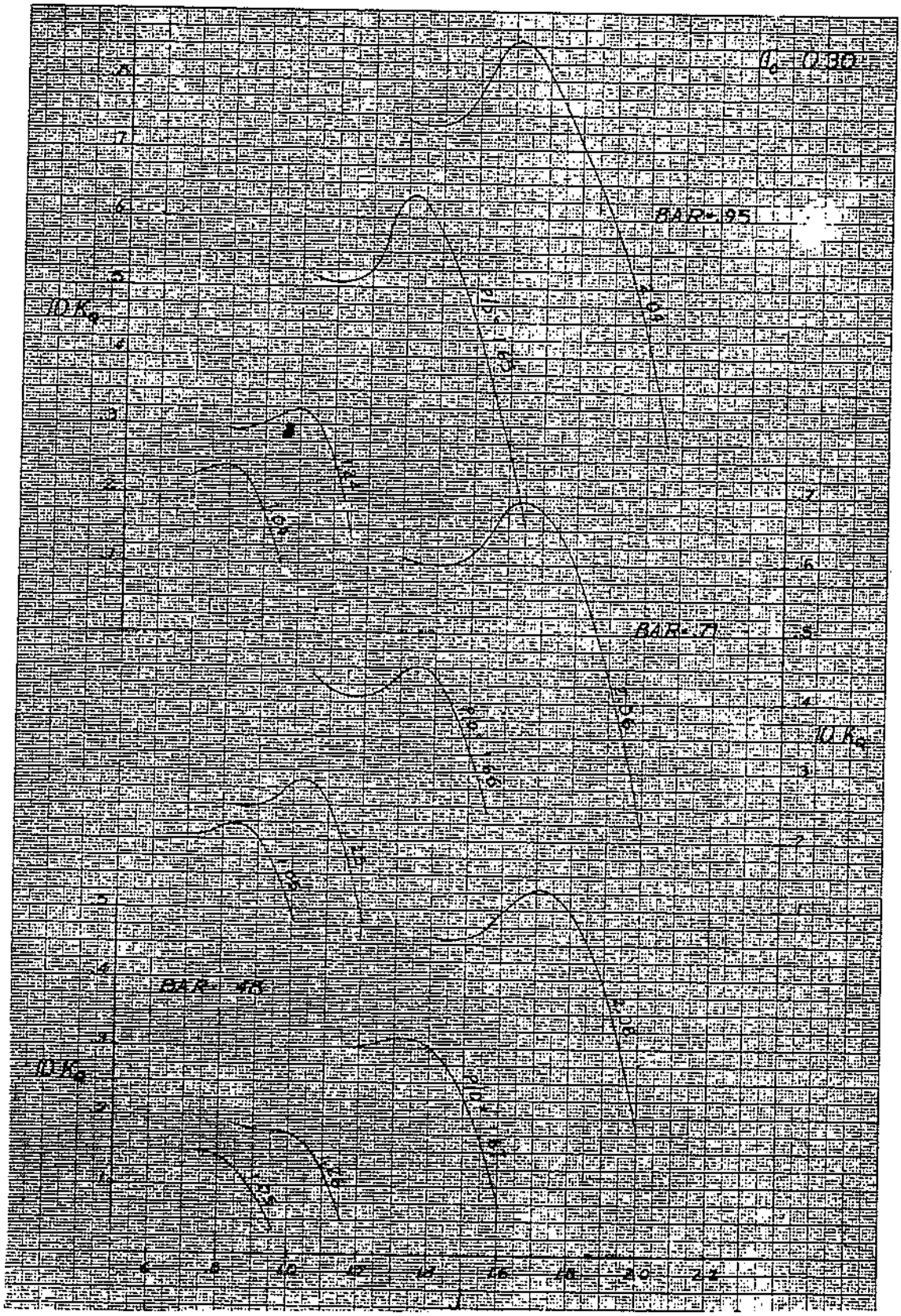

Figure 2.17 (b). 10 K_Q vs J for Newton and Radar propellers in open water (Reference 11).

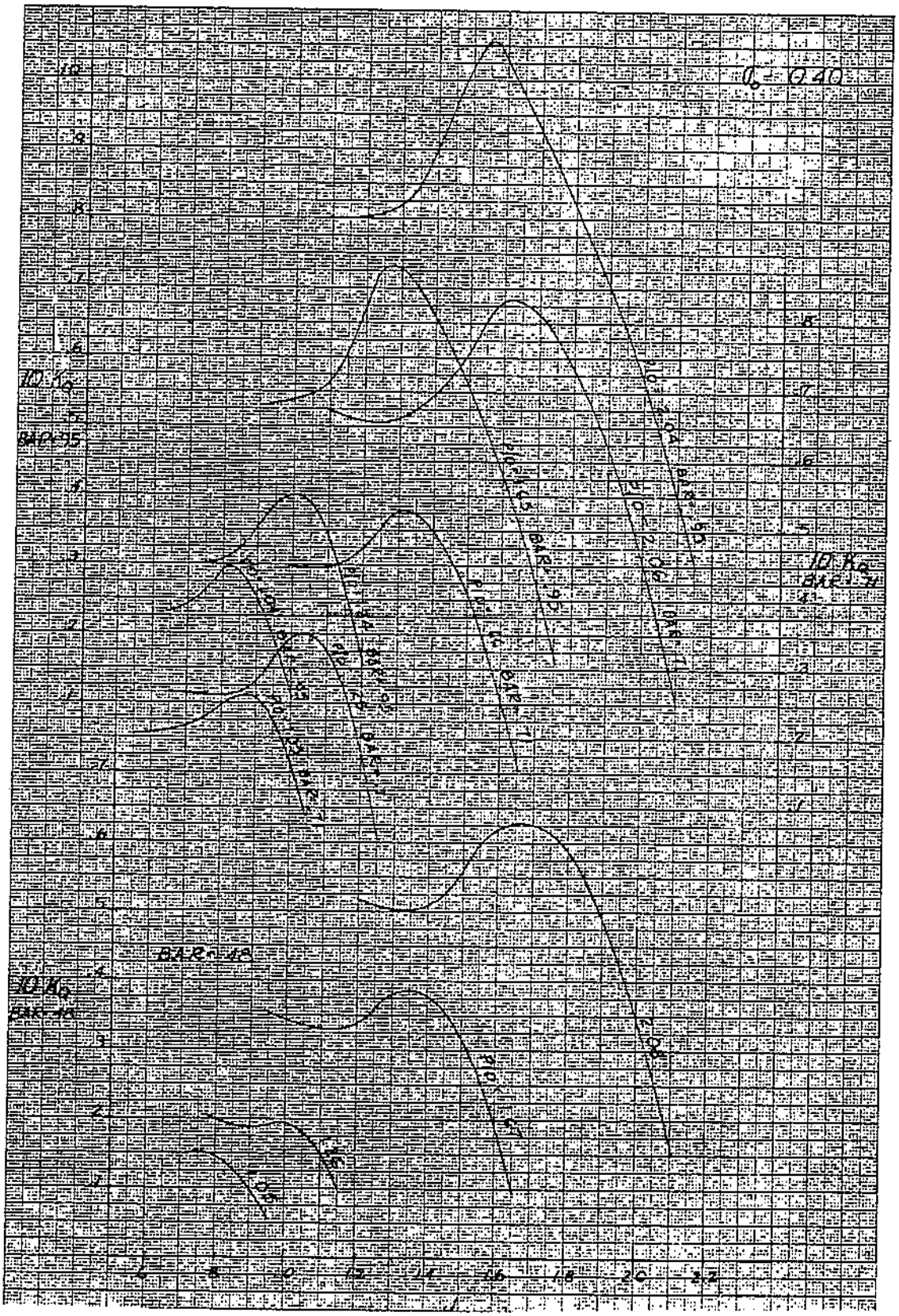

Figure 2.17 (c). 10 K_Q vs J for Newton and Radar propellers in open water (Reference 11).

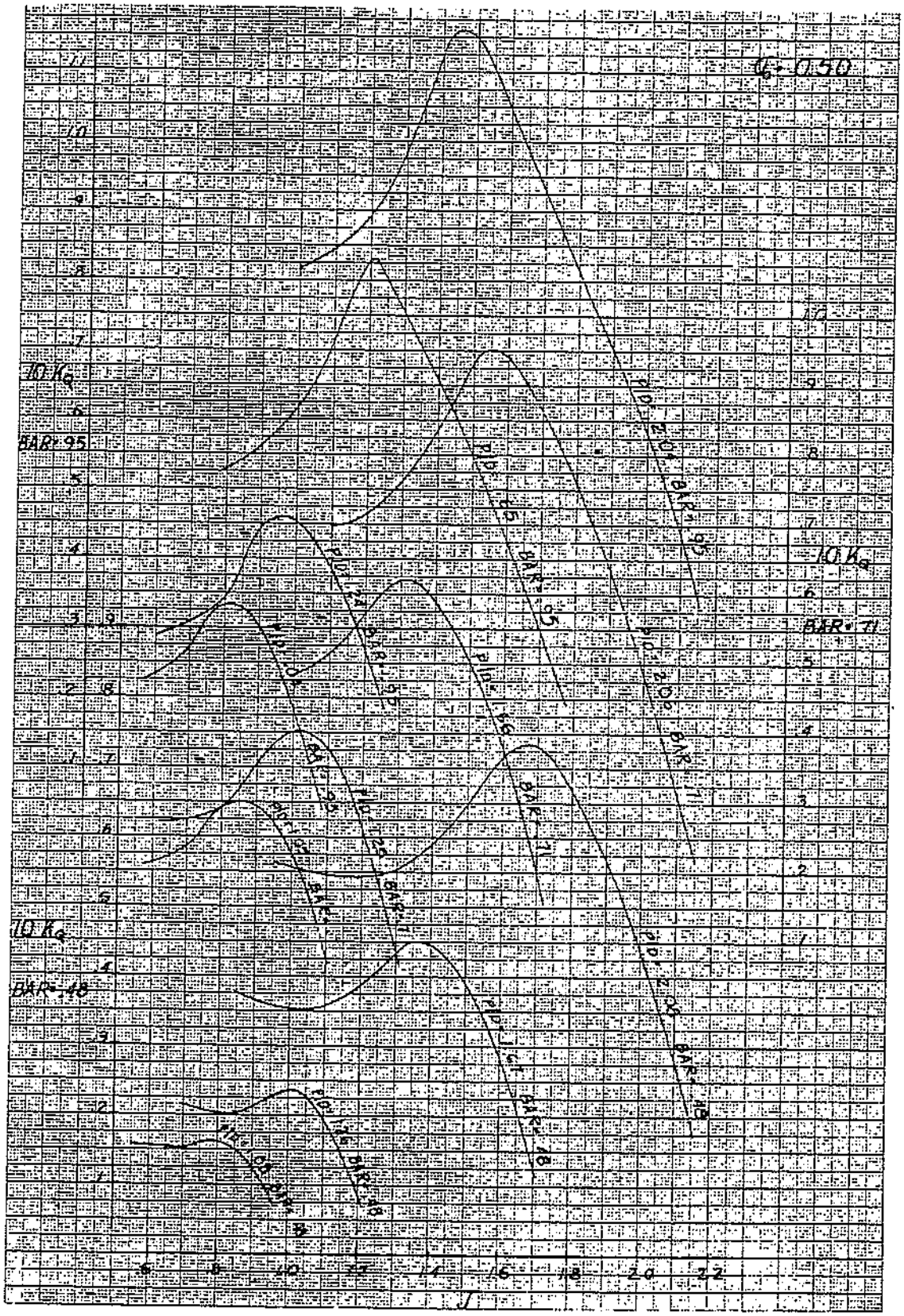

Figure 2.17 (d). 10 K_Q vs J for Newton and Radar propellers in open water (Reference 11).

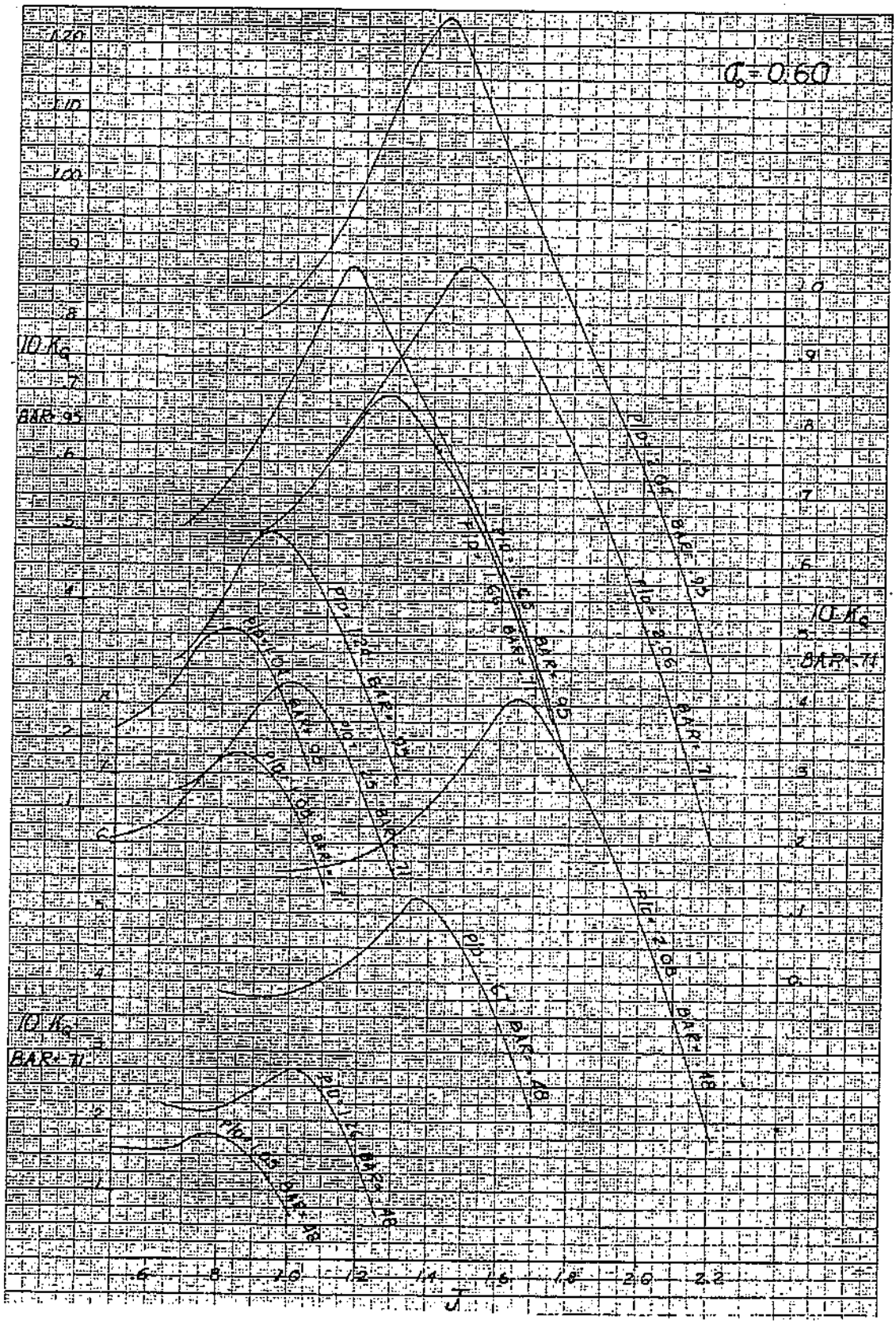

Figure 2.17 (e). $10\,K_Q$ vs J for Newton and Radar propellers in open water (Reference 11).

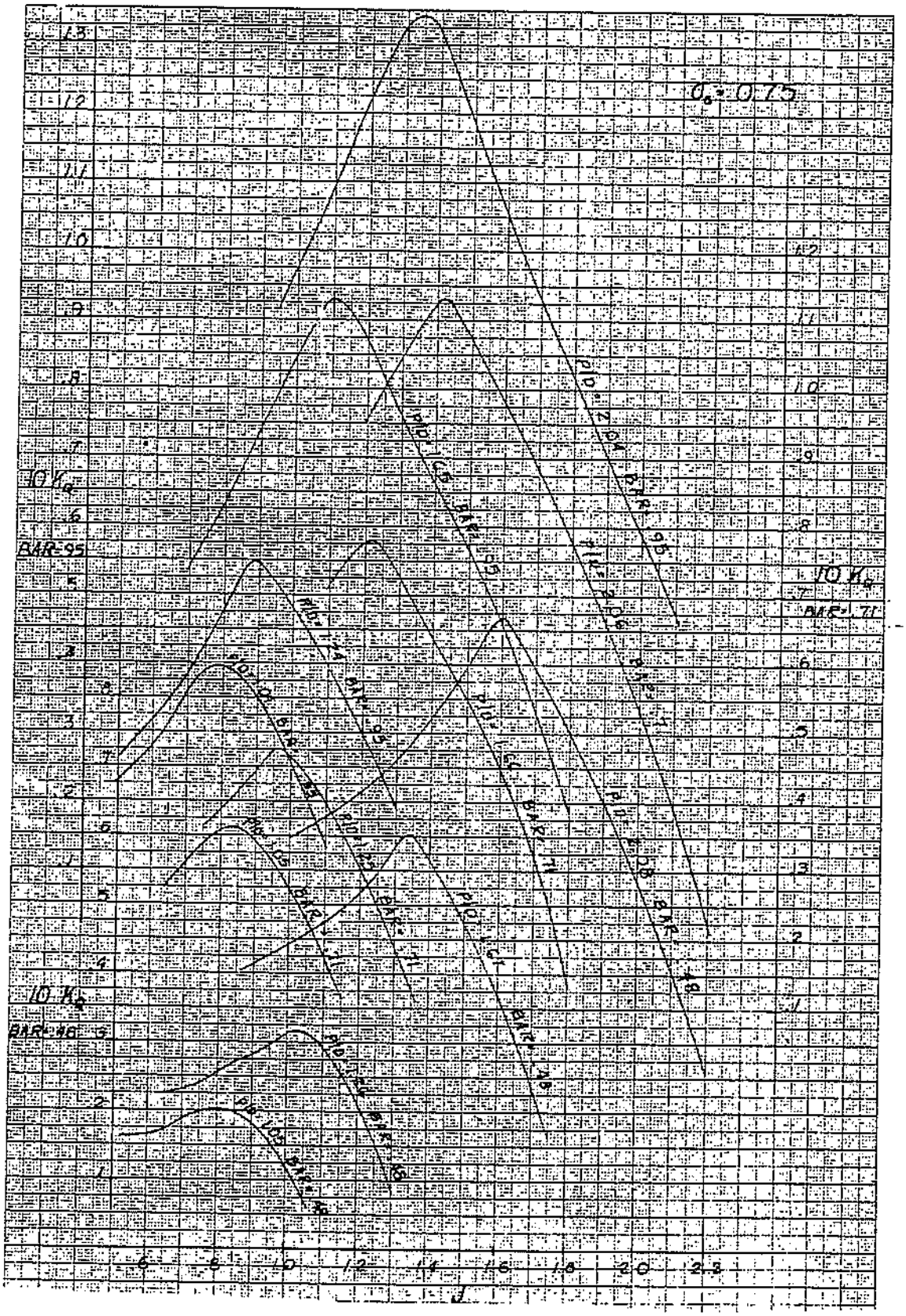

Figure 2.17 (f). 10 K_Q vs J for Newton and Radar propellers in open water (Reference 11).

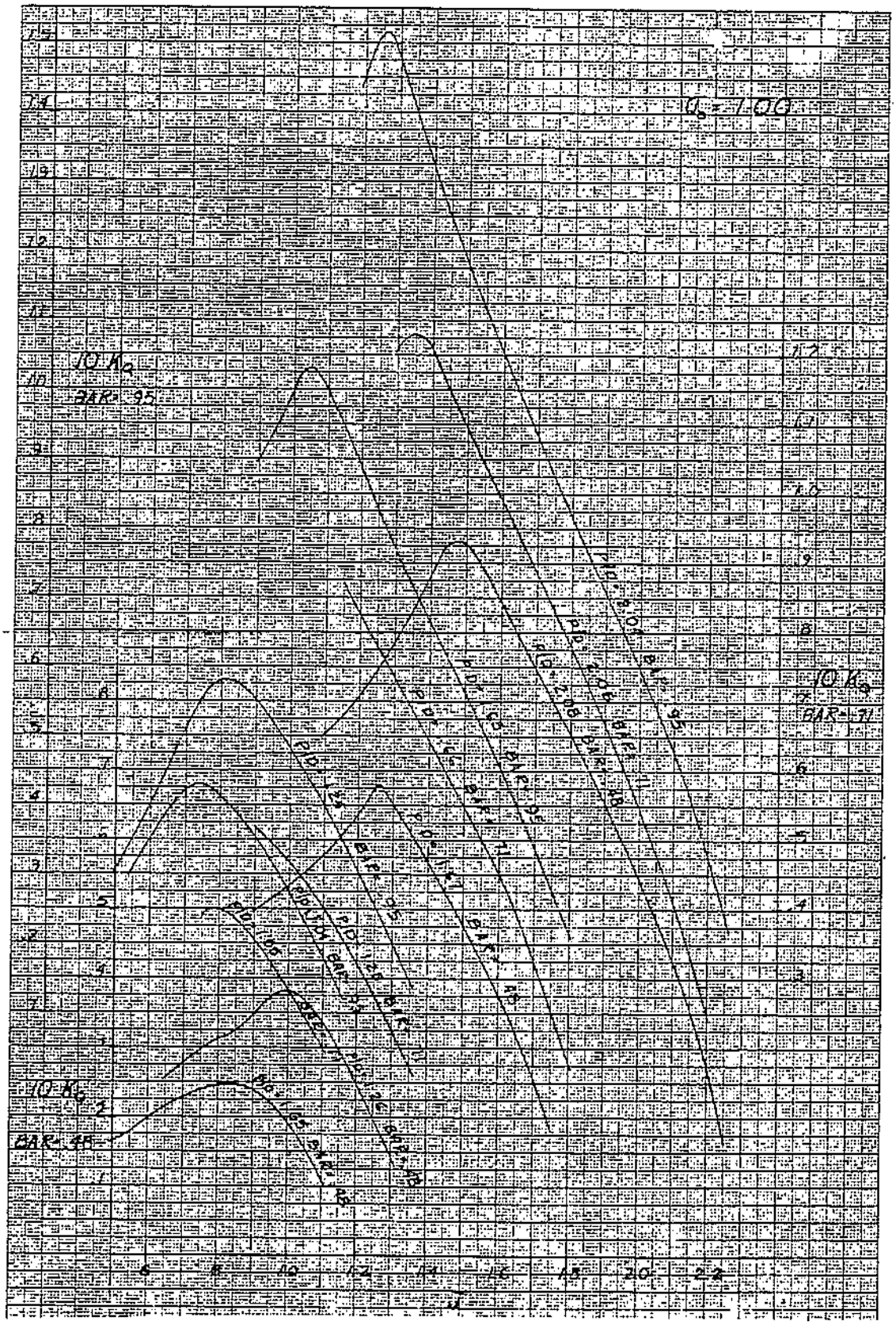

Figure 2.17 (g). 10 K_Q vs J for Newton and Radar propellers in open water (Reference 11).

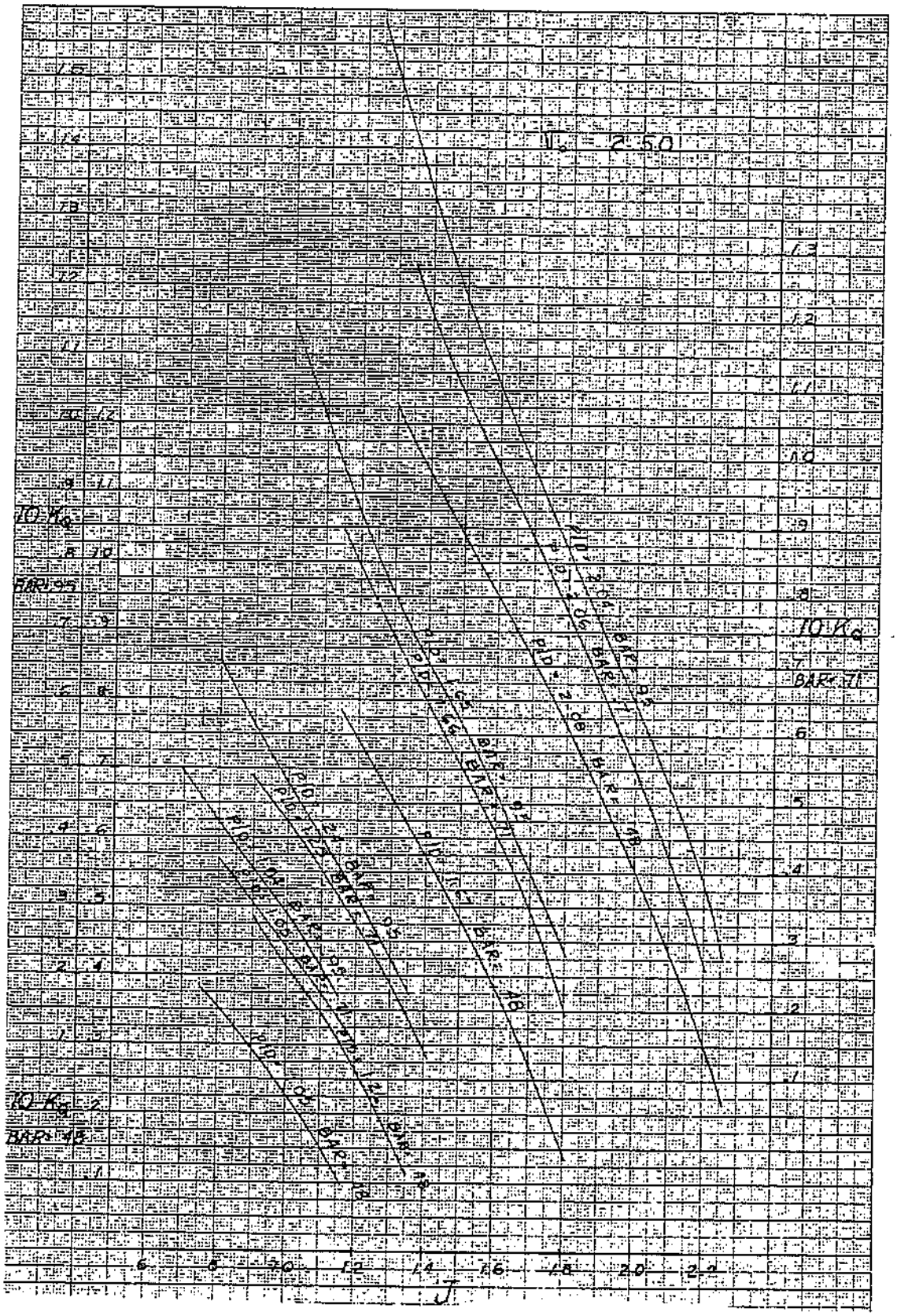

Figure 2.17 (h). 10 K_Q vs J for Newton and Radar propellers in open water (Reference 11).

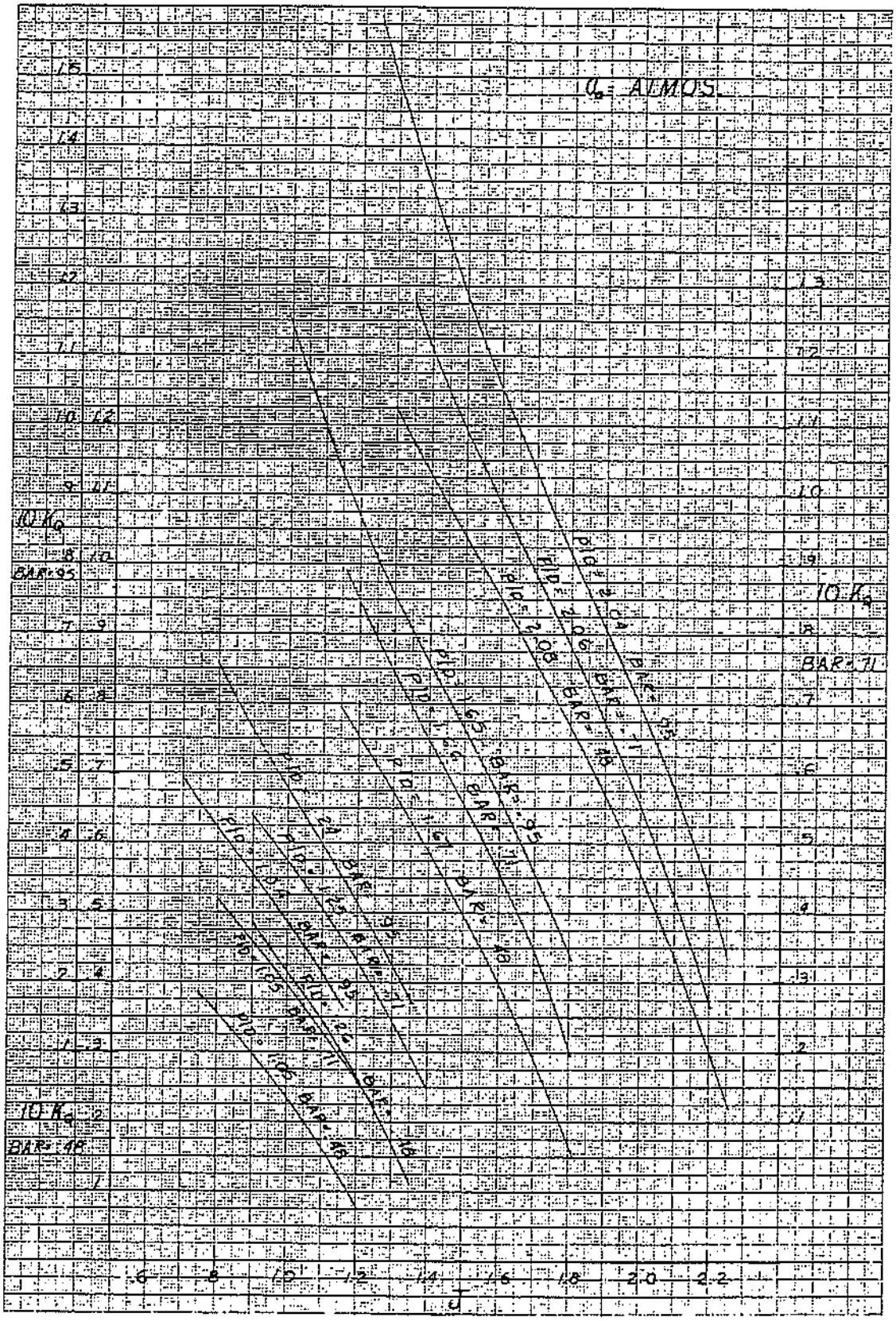

Figure 2.17 (i). 10 K_Q vs J for Newton and Radar propellers in open water (Reference 11).

8. HULL-PROPELLER INTERACTIONS

So far in this chapter we have discussed only propellers, whereas Chapter 1 was devoted exclusively to the hull. The two systems, hull and propulsive device, may be expected to interact. Specifically, the flow the propeller experiences when placed behind the hull is non-uniform and has an average speed usually less than that of the boat. In this new flow field the propeller torque and thrust properties differ from those in open water. The resistance of the hull form is also modified somewhat due to the influence of the propeller on the flow around the hull. Usually the effect is to increase the resistance, hence the term resistance augment. Viewed from the standpoint of the propeller, the thrust output must be greater than the resistance of the hull without the propeller, hence the term thrust deduction fraction.

8.1 WAKE

The difference in the hull speed, V, and the average speed of advance into the propeller behind the boat, V_A, is called the wake speed. The wake fraction is the ratio of the wake speed to boat speed.

$$w = \frac{V - V_A}{V}$$

or

$$1 - w = \frac{V_A}{V}$$

If the wake speed exceeds that of the boat speed, the wake is said to be negative. This rarely occurs in practice and when it does, the wake is only slightly negative. Wake fractions may be as high as 0.50 on some types of ships, but on high speed planing boats with exposed shafts the wake fraction is usually small.

Wake flows on hull forms consist of three components.

a) The frictional wake is the fluid slowdown caused by the boundary layer downstream from the hull.

b) The potential wake is caused by the streamline flow around the hull. According to the Bernoulli theorem reduced pressures cause increased velocities and vice-versa.

c) The wave wake is caused by the orbital velocities contained within the waves created by the hull form. Crests create forward velocties and troughs sternward velocities.

The propellers on high speed planing craft are usually only slightly within the boundary layer and are not near waves so that the wake is largely a potential wake due to the pressure distribution on the hull. However, the influence of the pressures a short distance from the hull is relatively small, which accounts for the low wake fraction values associated with the planing hull.

There are two commonly used types of wakes: nominal and effective. The nominal wake is obtained by actual measurements of velocities either point-by-point with a multi-hole pitot tube or by an impeller with vanes at some radius. The impeller gives the average velocity in the axial direction whereas the pitot tube gives local velocity components in three dimensional space. See Reference 15 for pitot tube data on a planing craft.

The effective wake is obtained with the propeller in place and from measurements of torque or thrust and RPM on the propeller. From these measurements we can calculate K_T and K_Q. Corresponding advance coefficient values, J_T or J_Q, can be determined from the open water characteristic curves. Finally, effective wakes based on thrust or torque can be calcualted.

$$w_T = 1 - \frac{J_T}{J} \tag{2.37}$$

$$w_Q = 1 - \frac{J_Q}{J} \tag{2.38}$$

where

$$J = V/nD$$

and

$$V = \text{boat speed.}$$

Hadler (Reference 16) gives values of effective wakes and other propulsive quantities for two different planing hulls as follows:

	$(1-w_T)$	$(1-w_Q)$	η_H	η_R	η_D^*	$\eta_D^\ddagger$
Hull No. 1	0.99	0.97	0.95	0.90	0.65	0.51
Hull No. 2	0.96	0.98	0.93	1.08	0.69	0.59

* based on resistance with appendages
‡ based on bare hull resistance

8.2 RELATIVE ROTATIVE EFFICIENCY

The fact that effective wakes based on thrust and on torque are not identical should come as no surprise since propellers many be expected to behave differently in different flow fields. The propeller efficiency in the behind condition, η_B, is not identical to that in open water, η_o, and the ratio of the two is known as the relative rotative efficiency, η_R,

$$\eta_R = \frac{\eta_B}{\eta_o} = \frac{\frac{TV}{2\pi Qn}}{\frac{T_c V}{2\pi Q_o n}} = \frac{T\,Q_o}{T_o Q} \qquad (2.39)$$

when thrust and torque are measured at the same slip. Relative rotative efficiencies rarely deviate more than several percent from unity. Values of relative rotative efficiency from Reference 16 are given in the table in Section 8.1.

8.3 THRUST DEDUCTION

When the propeller is placed behind the hull, the flow is accelerated as was explained by the momentum theory of propellers. Modifications to the boundary layer, the potential field and the wave induced velocities result and there is a corresponding change in resistance. For equilibrium to exist, the new resistance must be equal to the propeller thrust output, or the component in the direction of motion in the case of inclined shafting and or boat trim. Normally the thrust is greater than the resistance measured in the absence of the propeller. The difference in thrust and resistance is called the resistance augment. The resistance augment fraction is

$$a = \frac{T - R_T}{R_T}$$

Viewing the problem in the reverse fashion, we say that we must make a deduction from the thrust equal to the resistance augment. Or, the thrust deduction fraction is

$$t = \frac{T - R_T}{T} \tag{2.40}$$

or

$$1 - t = \frac{R_T}{T}$$

8.4 HULL EFFICIENCY

In view of the remarks in the preceding section we may define the efficiency of the hull as the resistance horsepower, or effective horsepower, P_E, required to tow the hull as a ratio to a thrust horsepower, P_T, based on the "average" velocity of flow in the plane of the propeller. Thus

$$\eta_H = \frac{\frac{R_T V}{550}}{\frac{T V_A}{550}} = \frac{R_T}{T} \cdot \frac{V}{V_A}$$

or

$$\eta_H = \frac{1 - t}{1 - w} \tag{2.41}$$

Values of hull efficiency from Reference 16 are given in the table in Section 8.1.

8.5 PROPULSIVE COEFFICIENT

The introductory paragraphs to this chapter defined overall efficiency, or propulsive coefficient as the product of the efficiencies of the propeller and hull.

$$\eta_D = \eta_B \cdot \eta_H$$

But

$$\eta_B = \eta_R \cdot \eta_o$$

So

$$\eta_D = \eta_o \cdot \eta_H \cdot \eta_R \tag{2.42}$$

which is also

$$\eta_D = \frac{P_E}{P_D}$$

The reader is cautioned to distinguish between the resistance of the appended and unappended hull. Since the delivered horsepower is that required to overcome the resistance of the appendages as well as that of the hull, and since most resistance data available to the planing hull designer are for the bare hull, the table in Section 8.1 contains η_D's based on both resistance measurements. Chapter 3 contains much more useful information in this regard for the small craft designer.

9. SELF-PROPELLED MODEL TESTS

There are two reasons for conducting self-propelled model tests. They are a) to gain an accurate prediction of the horsepower developed by the propeller, and b) to determine the wake fraction and hence the velocity of advance into the propeller. Without the aid of propelled model tests, the propeller designer can only estimate the wake fraction. There are several helpful empirical equations for wake fraction, but model tests are required for accurate estimates. For example, see Reference 3 for equations developed by Taylor and Schoenherr, and others. Common practice is to base a preliminary model propeller selection, from among the stock of the model testing establishment, on empirical means of determining wake fraction. Once the test results are in hand the propeller design can be refined if required.

The similitude conditions that must be satisfied for the self-propelled test are the same as for resistance testing since the model moves through the water in the same way except that it is propelled rather than towed. Cavity flow conditions cannot be accurately represented. Therefore, models of high speed craft with propellers that are likely to cavitate cannot be accurately self-propelled. Fortunately, wake fractions are usually low on planing hulls so that the absence of self-propelled model data does not seriously affect the accuracy of the advance speed used in propeller design. More appended planing hull model resistance tests should be conducted however, since the lack of knowledge of appendage resistance probably creates more inaccuracies in planing boat powering predictions than lack of knowledge of wake speed. In spite of the difficulties of conducting high speed self-propelled model tests, many small craft can still be so tested if no cavitation on the full scale propeller is expected.

If the model was completely propelled by its propeller then it would supply a specific thrust equivalent to the model specific resistance plus augmentation. This would require a

specific propeller thrust loading, K_T, on the model greater than on the ship and a corresponding inferior model propeller efficiency would result. The full scale specific resistance is less than that for the model according to the equation

$$C_{T_S} = C_{T_M} - [C_{F_M} - (C_{F_S} + C_A)] \qquad (2.43)$$

where the terms in the bracket are the hull friction correction. The right-hand side of Equation (2.43) when evaluated for the model, is termed the "ideal resistance." Possibly this term is a misnomer since it connotes an ideal fluid, rather than a viscous fluid that does not require a friction correction for model tests. (Admittedly, the latter case would be an ideal situation.) Therefore, in order for the model propeller to have the correct specific thrust loading, it need overcome only the ideal resistance plus augmentation. The towing carriage supplies the balance of the force required to maintain the desired speed. The towing force is

$$D_f = \frac{\rho}{2} S V^2 [(C_{F_M} - (C_{FS} + C_A)]$$

evaluated for the model.

PERFORMANCE PREDICTION

Joseph G. Koelbel, Jr.

Naval Architect

CHAPTER 3: PERFORMANCE PREDICTION

1.0 PERFORMANCE PREDICTION

1.1 GENERAL

This chapter will be devoted almost entirely to planing boats. Virtually every bottom type, round, V, etc., will be considered, and information on the resistance of some of these at semi-planing and displacement speeds will be given. The calculation of appendage and wind resistance is the same for all types under consideration.

In a broad sense performance prediction encompasses the determination of not only the resistance, running attitude, and spray formation in steady state planing, but also motions and acceleration in six degrees of freedom, as well as the stability of rotation about the three axes. Moreover, this should all be done for smooth and rough water, in symmetrical and unsymmetrical planing conditions.

Not many of these matters are subject to numerical evaluation. The mathematical techniques are available but in many cases there is little or no experimental evidence with which to work. Therefore, some of the factors which influence the performance of planing boats depend solely on the designer's experience and judgment. Examples of items in this category are roll stability while planing, and bank angle in turns. There are some factors which are subject to varying degrees of approximation such as turning radius, resistance and trim of non-planing boats, etc. The calculations in which we have the greatest confidence are those for resistance and trim in the full planing condition of prismatic or nearly prismatic hulls, and predictions from model tests, and even these, of course are not really exact.

Many of the references present experimental data. Some of the authors fit curves to the data and derive equations; others draw conclusions regarding the relative merits of designs. The reader is urged not to take too much on face value, including this chapter. He should examine the references, their data, and their conclusions very carefully. There is scatter in the data, and sometimes more than one curve can be drawn with equal justification. In addition there are other problems with model testing as well as full scale testing. Unexpected model results are sometimes charged to improper turbulence stimulation, for example, and trim prediction from small and large models differ. Model testing people have spoken seriously of "tank storms" and "Monday morning results", the latter presumably because turbulence in the water is at a minimum after a week-end of inactivity. Factors of this type contribute to the need for careful examination and interpretation of data, no matter how meticulously it was gathered. However, it should be emphasized that much useful data has been gathered from model tests including prismatic planing surface data which is widely applicable to planing boat power prediction.

But the reader is not left completely on his own in these matters. Many of the references discuss these problems, some reexamine old data and correlate it with new data, etc. A great deal of the recommended examination and interpretation has been done by experienced men, and most of the material in the references is trustworthy. Nevertheless there are differences of opinion among the experts, and there is still much to be learned. It is good to see the subject in perspective, and to have a true appreciation of the present state-of-the-art of performance prediction.

There is a great deal of controversy over the relative merits of round and V-bottoms. This is a good example of why the reader must use good judgment in interpreting the material presented. In Reference 37, Marwood and Silverleaf give the results of model tests which compare a round bottom boat and a V-bottom boat for smooth water resistance and rough water behavior. Their conclusion was that the round bottom design was superior. It didn't require thousands of dollars worth of tank time to find that they are comparing a good round bottom design with a poor V-bottom design. As pointed out by Savitsky in his discussion of the paper, the performance differences are due, not to round versus hard-chine per se, but to other factors such as fineness of the bow and deadrise distribution which could be the same for either type. In general, as a round bottom type is developed for greater speed, and as a V-bottom type is developed for better seakeeping, the two become very much alike. This will be illustrated later.

Our intention is not to go into great detail in covering material which has been adequately presented before. Instead, this chapter will primarily be a guide to the use of the references.

Reference 16 is a good one to start with because of its approach to the subject, while References 1 and 12 are essential because of their treatment of the subject. Four different viewpoints on the understanding and calculation of planing phenomena are presented in these works. For other calculations, such as appendage resistance, Reference 3 is necessary and Reference 9 provides much additional data. Reference 3 is also essential because of its broad and thorough treatment of hydrodynamics and the many references it cites. In addition to the above, it is very important to have References 4, 5, 11, 15, 20, 21, 22, 25, 30, 57, 60, 61, 68 and 70. The relative importance of each of the remaining references depends to some extent on the designer's needs. For numerical data the various series reports are a great help, particularly Series 62, Reference 6, Series 63, Reference 7, and the patrol boat series, Reference 27.

From the standpoint of the practicing small craft designer the works which are least important to have at hand are References 2, 18, 34, 35, 39, 43, 45, 46, 50, 53, 54, 55, 62 and 63. The reader should consider the references and bibliographies cited in this chapter's references for further information. The most complete list of works on power boat design (more than 1000 titles) is given in Reference 76 and its companion volume, Reference 77.

2.0 DISCUSSION

2.1 ELEMENTS OF TRIM

2.1.1 Basic Planing

The mechanics of planing have been treated in great detail in the references, and no more of it will be repeated than necessary. There is no uniform definition of planing, and in practice there are many borderline cases in which it is difficult to decide on the basis of any definition. For the purpose of performance prediction by means of the planing equations, (there are other means of performance prediction which will also be covered) we are concerned with prismatic or nearly prismatic surfaces. That is, the buttocks must be straight, and the variation of the beam and deadrise in the planing area must not be great. When a surface of this type moves with a positive angle of attack and the flow separates cleanly from the chines and transom, it is planing. Another criterion, given in Reference 1, considers a boat to be planing when $C_V/\sqrt{\lambda} > 1$. This a good criterion but is not practical for field observation.

For steady state planing all the forces and moments acting on the boat must be in equilibrium. The simplest case is that of a flat plate planing at trim angle, τ, on a frictionless fluid. See Figure 3.1a. The only force acting on the surface is the normal force N, which is made up of hydrodynamic and hydrostatic pressures. Its vertical component is the lift, Δ, and its horizontal component is the pressure drag, D_p. In this case $D_p = \Delta \tan\tau$. When friction is added the forces are as shown in Figure 3.1b. There is still a normal force as before but there is also a tangential force, the friction drag, Df. Now the total drag is $D = \Delta \tan\tau + (Df/\cos\ )$.

In the case of a planing boat with a fixed longitudinal center of gravity location, the trim angle will adjust itself to place the center of pressure under the center of gravity. We need, therefore, to determine the trim angle which produces equilibrium. There are two methods of direct calculation. One was developed by Clement from the equation of Shuford (Reference 18) and is presented in References 12 and 13. This method is suitable only for high speeds where the buoyant contribution to lift is negligible. The information is presented in the form of design charts for easy application. Reference 13 applies only to planing catamarans. The other method was developed by Savitsky, Reference 1, and takes into account the buoyant forces and is therefore applicable to very low speeds. The resistance prediction is not quite as accurate at semi-planing speeds as at full planing speeds, primarily because of side wetting, but the trim prediction is good through the applicable speed range. This is a significant fact because in many practical design problems trim in the hump region is much more important than resistance. There is usually ample power to get over the hump but excessive trim can block the helmsman's vision, create a dangerous wake, and aggravate other problems. The use of this material will be explained in Section 3, but for the present it will suffice to explain that the basic trim calculation assumes the forces to act as shown in Figure 3.2. These assumptions

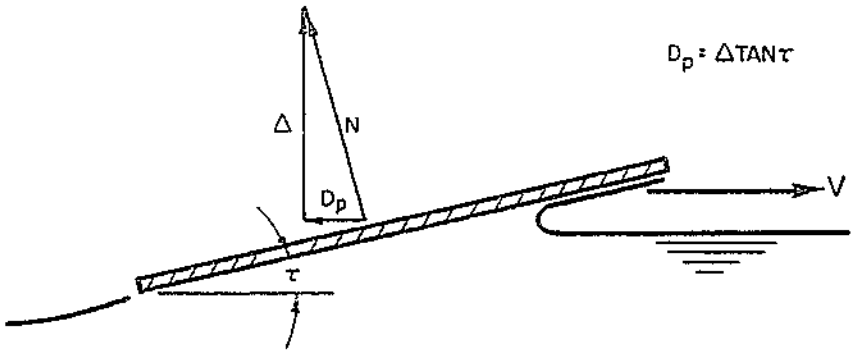

a) FRICTIONLESS FLUID

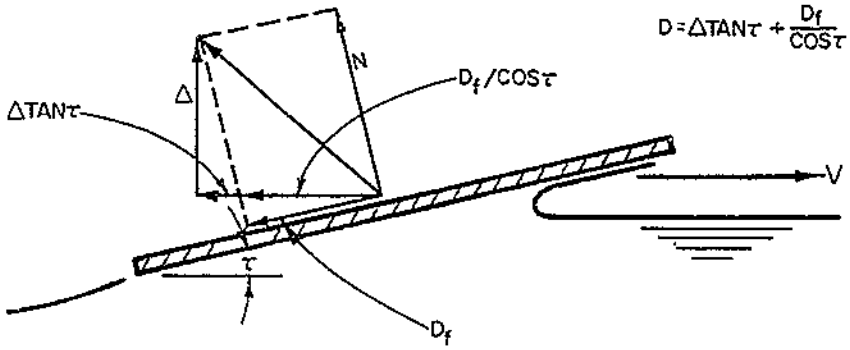

b) VISCOUS FLUID

Figure 3.1. Drag Components on Planing Surface

are implicit in the work of Clement, Murray (Reference 15), and Koelbel (Reference 16), and in many cases they provide a sufficiently close approximation. In Reference 71, Peter Brown of the Davidson Laboratory has modified the Shuford equation for planing lift to provide greater accuracy, that is, better agreement with experimental data. This new work has not yet come into general use.

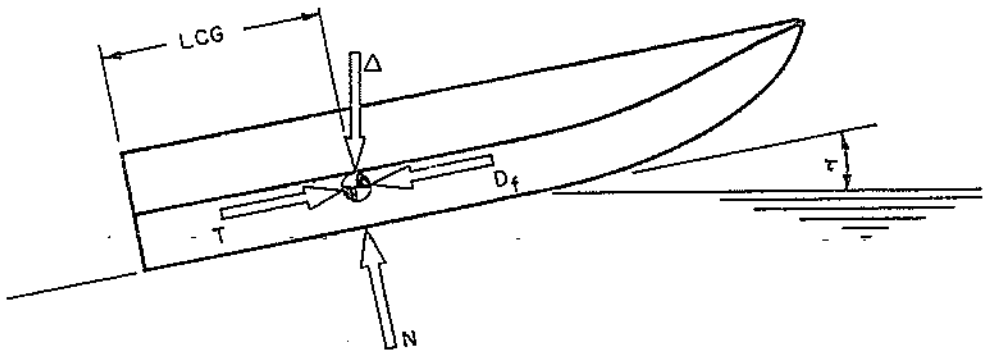

$LCG = C_p b\lambda$

Figure 3.2. Forces acting through center of gravity

2.1.2 Factors Which Influence Trim

There are additional factors which influence trim besides N, D_f, Δ and T (the thrust). Savitsky has developed a computational procedure which takes most of these into account. As shown in Figure 3.3, they are:

a) The thrust does not usually act through the center of gravity, and it is not always parallel to the keel. This creates an additional vertical force and a trimming moment.

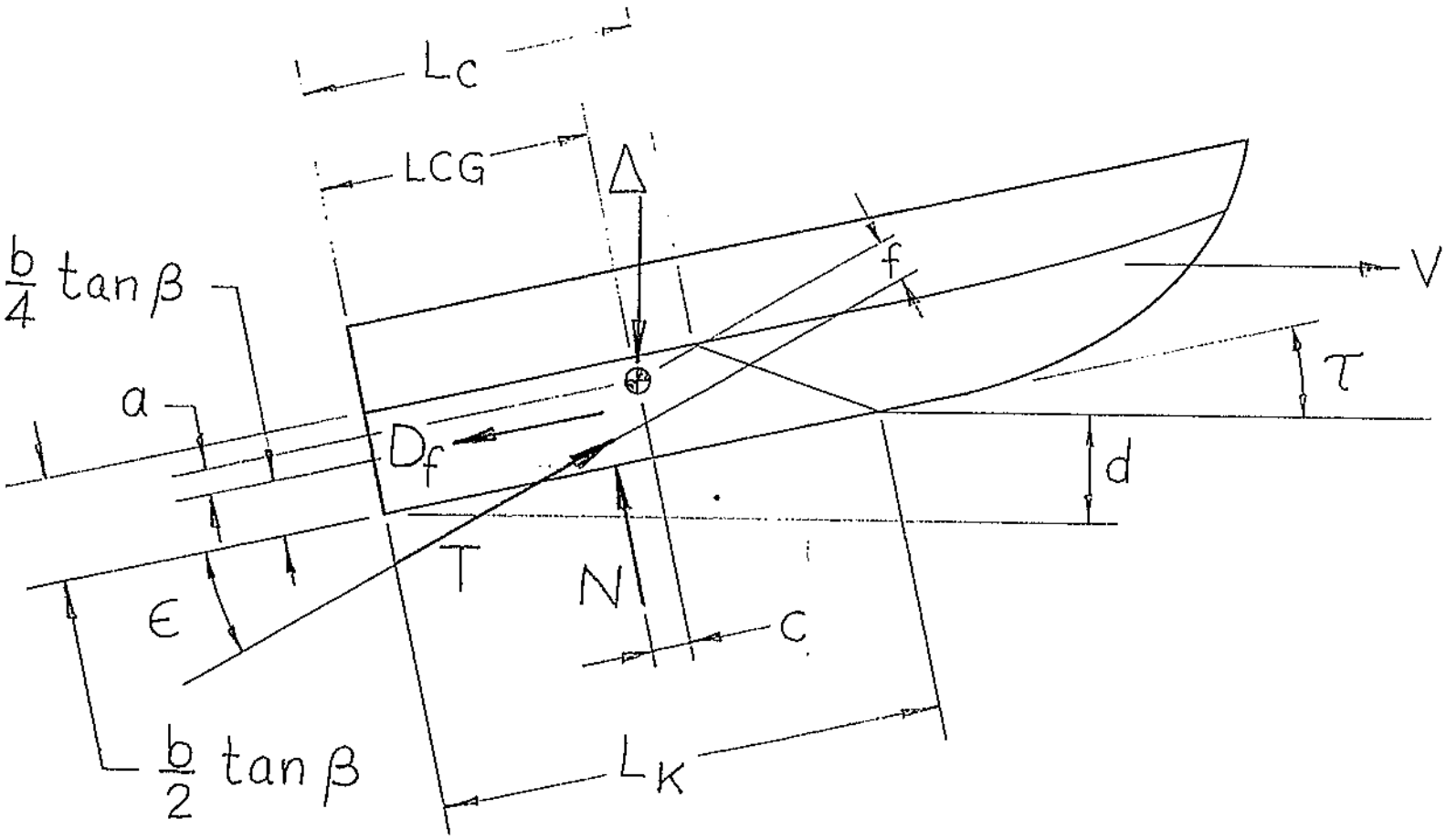

Figure 3.3. Forces not acting through the center of gravity

b) The frictional drag force does not act through the center of gravity and therefore creates a trimming moment.

c) Because of these trimming moments the normal forces on the bottom cannot act through the center of gravity, in order to maintain equilibrium.

As well:

d) The Savitsky calculations have been programmed for the computer by a number of people, and in at least some of thre programs, an additional factor is considered. It is the frictional drag on the centerline skeg and its trimming moment.

e) Wind resistance has not been included in the planing boat program. It is usually considered as an additional drag item, but in some cases of very high superstructures it could have a noticeable trimming moment.

f) The propulsion device has two influences on the boat's trim in addition to that of the thrust line. One is due to the pressure field around the propeller. The reduced pressure caused by the increased velocity tends to drop the stern. The second, for propellers inclinded to the flow, is an additional blade force acting at right angles to the shaft line, in an upward direction. In the case of a jet pump installation, only the influence of the inlet will be felt. There is no quantitative information on the effects of jet pumps but the case of screw propellers has been investigated by Hadler and reported in Reference 11, complete with design charts.

2.1.3. Longitudinal Stability

This refers primarily to porpoising. In his calculation method, Clement gives no criteria for determining longitudinal stability but in his report on Series 62, Reference 6, he presents a chart which gives porpoising limits for boats of that series. Savitsky, Reference 1, gives another chart of porpoising limits for prismatic surfaces of several deadrise angles. Both are useful guides and should be checked. Porpoising is an important consideration because it is the principal feature which limits the speed potential of a stepless planing hull. This matter is further discussed by Stoltz in Reference 16, and by Clement in Reference 17.

2.2 ELEMENTS OF RESISTANCE

2.2.1 Frictional Resistance

In calculating the frictional resistance of a planing boat, it is necessary to make the same assumptions as described in Chapter 1 for displacement vessels, except that the actual wetted area is calculated at each speed, instead of using the static wetted area. However, we assume the frictional resistance is the same as that of a rectangular flat plate the length of which is equal to the average of the wetted keel and wetted chine lengths. It is also tacitly assumed that the frictional resistance acts horizontally, except in the case of the detailed calculations described by Savitsky in Reference 1. Plots and/or tables of the frictional resistance coefficient versus Reynolds number may be found in References 2, 3, 4, 5 and 16. The usual roughness (or correlation) allowance is 0.0004, although there are other opinions on this, e.g. Baier's discussion of Reference 15. There should be some increase for shorter surfaces and decrease for longer surfaces but usually the smaller the boat the better chance there is for a uniformly smooth surface so in the absence of specific and accurate information for a particular case, the standard allowance is satisfactory.

In the planing calculation of Reference 1 the spray resistance is treated as an increment of the wetted area. It has been demonstrated that the water in the whisker spray (forward of the spray root) comes from a thin film on the still water surface ahead of the boat, and that its direction of flow across the bottom is a reflection of the direction of inflow to the spray root. It was therefore simply a matter of geometry to determine the spray wetted area and the direction of flow, which depend only on the deadrise and trim angle. (See Figure 3.4). It is only the aft component of the spray velocity which contributes to the drag. Using the assumptions that the friction coefficient of the spray is the same as that of the solid wetted area, and that the velocity across the spray wetted area is equal to the inflow velocity to the spray root (that is, the speed of the boat) then the spray contribution to the resistance is easily calculated. This contribution becomes smaller with a reduction in deadrise and increase in trim. For those combinations of trim and deadrise which cause the direction of the spray velocity to be transverse, $\Delta\lambda$, the effective increase in wetted area, is zero (even though there may be a large spray wetted area) because there is no additional drag from the spray. In some cases spray drag can be negative because the velocity vector has a forward component. When using these calculation methods, which are derived from prismatic data, for warped bottoms the local values of deadrise and trim (mean buttock angle of attack) in the spray area should be used rather than the afterbody values used in the principal planing calculations. The derivation of this method of calculation is given in References 1 and 54. Additional information is contained in the discussion of Reference 6. This method of calculating spray drag has been criticized because of the assumptions regarding friction drag coefficient and velocity. It is nevertheless a good approximation and may be the best we can do at the present time. However, it seems probable that the energy.

required to maintain the spray formation comes from the $\Delta \tan \tau$ component of resistance, so perhaps the spray drag should be Froude scaled. Reference 1 has a good picture of spray formation on a prismatic model and Reference 16 has a number of pictures of spray formation on a non-prismatic hull.

It should be mentioned that the flow directions shown in Figure 3.4 are for a heavily loaded model at high trim. Full scale observations of the flow under a relatively lightly loaded planing hull (with a translucent bottom) running at trim angles of 2 - 3 degrees show flow lines just about parallel to the keel over the entire bottom, except perhaps within a few inches of the chine.

2.2.2 Wave Resistance

For the full planing conditions of a prismatic (or nearly prismatic) surface, calculation of the wave resistance, D_p, is a simple matter because the pressure force, N, acts normally to the bottom and it must necessarily be of such magnitude that its vertical component is equal to the weight, Δ, of the boat. The normal force itself can be eliminated by geometric considerations, and the wave resistance is $D_p = \Delta \tan \tau$, as shown in Figures 3.1a and 3.1b.

When the curved portion of the bow is immersed, particularly at lower speeds and heavy loadings, the wave resistance is a much more complicated matter and is not subject to direct calculation. It must be estimated from the results of model tests or other empirical data.

Wave resistance is sometimes called residual resistance because of the standard procedure in model testing of measuring the total resistance and subtracting from this the calculated frictional resistance of the model based on the wetted area. What remains is the residual resistance and the usual practice is to scale according to Froude's Law, the entire residual resistance.

In the case of some important model data, e.g. Series 63, References 7 and 8, no spray rails were fitted (it is a round bilge design) and at the higher speeds the bow spray runs right to the sheer before separating. These large wetted areas above the static waterline are not given in the model data and therefore it is not possible to accurately determine how much of the model resistance to scale according to Froude's Law and how much to scale by Reynolds's Law. In addition, a full size boat of this type would be fitted with spray rails near the design waterline and most of the topside wetting would be eliminated. It is impossible to estimate the true wetted area from the photographs of the models, and in addition the friction coefficient and flow direction in the spray area are not known. This is further complicated by the fact that, even if the spray contribution to model drag could be eliminated on the assumption that the full size boat will have spray strips, the presence of the spray strips will cause a change in running trim and consequently in the wave resistance of the boat, thereby introducing another unknown of perhaps greater magnitude. So it seems that for the present we must use the standard method of expansion. The

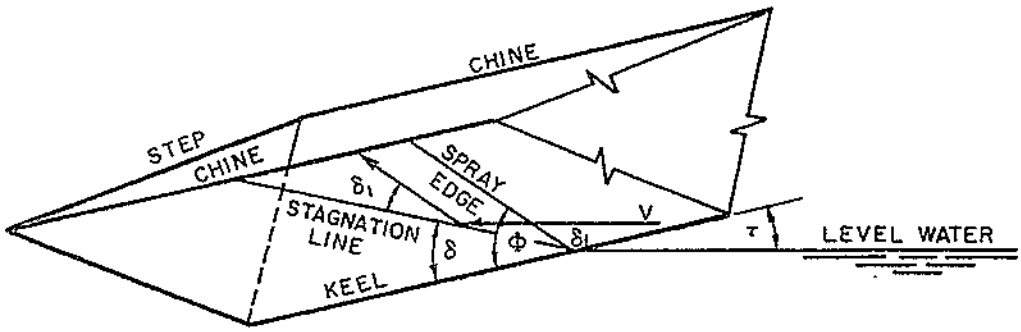

$$\tan\theta = \tan\Phi \cos\beta$$

$$\tan\alpha = \frac{\pi}{2}\,\frac{\tan\tau}{\tan\beta}$$

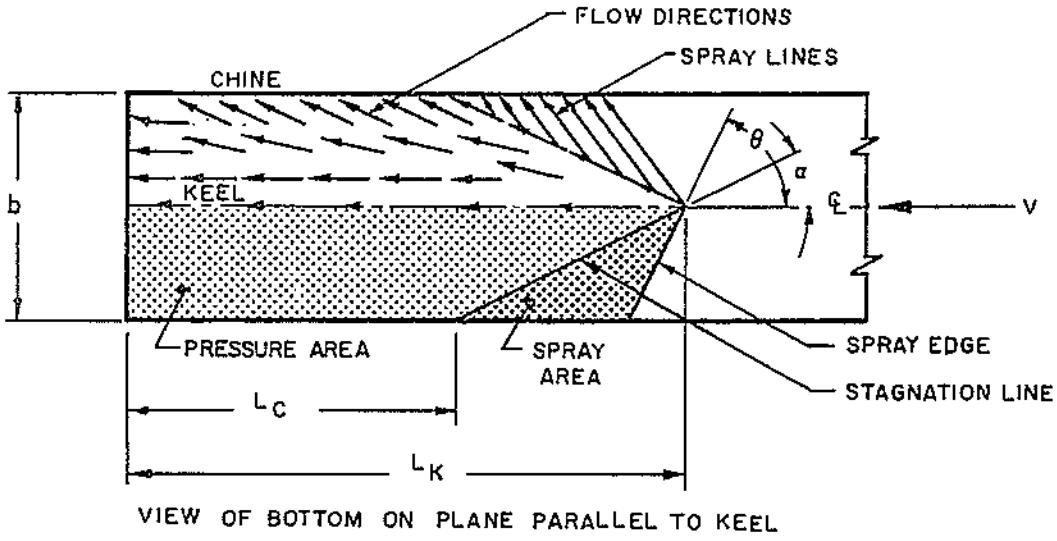

VIEW OF BOTTOM ON PLANE PARALLEL TO KEEL

Figure 3.4. Flow directions along planing prism and extent of spray area

spray resistance is therefore included in the residual resistance and considered proportional to the displacement. Probably it would have been better to apply spray strips to the models. However, at lower speeds, below a F_∇ of about 1.5, depending on loading, the bow wave is not so high and the residual resistance calculation is satisfactory. Some further information on this problem, in connection with hard chine models, is contained in Koelbel's discussion of Reference 6. Additional information on spray strips is given in Reference 19.

The use of trim flaps has an influence on the residual resistance. They have a direct pressure drag of their own but by far their greatest influence on drag is through their influence on the running trim of the hull. Edwin Monk published the results of some early full scale experiments with trim flaps. See Reference 56. While interesting and informative, the material cannot be used to predict the effects of flaps on other boats. In 1970 John C. Angeli wrote a technical note, Reference 72, on an investigation he made into the use of trim flaps on boats of his own design. It includes both experimental and analytical work and is generally applicable to boats in the full planing condition, provided they are similar in design to the models Mr. Angeli tested. This work has not yet been published.

A more recent investigation by Peter Brown was published this year. See Reference 71. The use of this material will be covered below under "Methods of Calculation".

2.2.3 Appendage Resistance

Appendages which have their greatest dimention in the direction of ship motion, and which are thin and lie substantially in the flow lines with the boat in steady motion, such as the external keel or skeg, can be considered to have primarily frictional resistance and can be simply included in the wetted area. Other appendages of higher aspect ratio, such as rudders, struts and shafts have more pressure drag than frictional drag and their resistance should be calculated according to methods given in References 3 or 9. Additional information can be found in References 5 and 10.

The prediction of appendage resistance from model tests is not easy because the size and speed of the hull are scaled by Froude's Law, whereas the appendages, which create no gravity waves, should be Reynolds scaled. This, of course, is out of the question because it would require the model appendages to be larger than the full scale appendages. So model appendages are always made to the same scale as the hull. Methods of predicting full scale resistance vary and the designer should rely on the establishment doing his testing for the best prediction methods. A report on the scale effect of model appendages is given in Reference 42.

In making direct calculations of the appendage resistance they should be considered in fairly small parts but there is a practical limit to the detail that is useful. For shafts, strut arms, and rudders the free stream velocity can be used for the whole part,

but for the strut palms, scoops, etc., consideration can be given to the velocity gradient in the boundary layer. Velocity augment due to the propeller slip stream should also be taken into account when appendages are influenced by it.

In calculating the drag of projecting intake scoops, it is satisfactory to consider the stagnation pressure of the average local velocity to act over the exposed frontal area, but for flush inlets it is necessary to consider the change of momentum in the intake water.

2.2.4 Air Resistance

Because of its relatively low magnitude air resistance does not require the care given to appendage or hull resistance (except in very high speed boats) but it is worthwhile to consider separately the above water hull, the superstructure, and items such as large masts or tuna towers, using appropriate drag coefficients for each. The trimming moment of the air drag on very high structures should be checked because its effect on the trim angle of the hull could have a large effect on the hull resistance. If the boat is required to make its design speed in a specified sea state, the wind speed required to produce that sea state should be added to the boat speed in calculating air drag. Usually no allowance is made for the variation in wind velocity with distance above the water. References 3, 4 and 9 give useful design information.

2.2.5 Rough Water Resistance Increment

This subject will be treated in Chapter 4. In addition, some qualitative remarks on the effects of hull shape will be made in Section 2.3 of this chapter.

2.2.6 Influence of Propulsion Device on Resistance

On any vessel with upward or inward sloping bottom surfaces forward of the propeller, such as ships and displacement boats, there is an increase in resistance because the low pressure field ahead of the propeller reduces the forward acting pressure force on the afterbody. In a planing boat afterbody surfaces are practically horizontal so this change in resistance is virtually zero. But the pressure field of the propeller has an indirect effect on resistance because of its effect on the trim. In addition there is a vertical side force (on a propeller at an angle to the flow) which tends to reduce the trim angle. Whether the net effect of these influences will be an increase or reduction in resistance depends on whether the change in trim is toward or away from the optimum. This matter has been investigated by Hadler and a complete discussion including design charts is given in Reference 11.

When outboard motors or sterndrive units are used, the trim of the boat can be altered by changing the tilt angle of the lower unit. This not only changes the direction of thrust but there is a significant lift force on the cavitation plate. It is principally through the effect on trim that sterndrive units influence the speed

of boats relative to that obtained with conventional inboard installations of equal power. Hadler has shown that a propeller inclined to the flow does not lose efficiency. Basically, thrust lost by the upward moving blade is gained by the downward moving blade. In addition, because of the lift to drag ratio common in planing boats, the reduction in the horizontal component of thrust due to the shaft angle is more than offset by the reduced load on the water due to the upward component of thrust.

In comparing the performance of various propulsion systems one cannot assume equal hull resistance because the change in l.c.g. from one installation to another will have a large effect on the resistance curve. Also, the complete weights of various installations are important considerations. These must include, for example, such items as the weight of inlet and exhaust silencing systems for gas turbine engines, the fuel load required for a given range or gas turbine engines, the fuel load required for a given range or endurance, which depends on the efficiency of the propulsion device (and on the specific fuel consumption of the engine).

There are other effects of the propulsion device which influence the resistance. The torque (of a single propeller) causes the boat to heel and the off center thrust (if the inflow velocity is at an angle to the shaft centerline, as in the case of conventional inboards) tends to turn the boat, which requires some rudder angle to keep the boat on course. The induced drag due to the side force on the rudder, and the increased resistance due to the resulting yawed attitude of the hull, are not usually calculated but their existence should be recognized. Reference 55 gives test results of flat and 20° deadrise prismatic surfaces planing in rolled and yawed attitudes but the lowest trim angle investigated was 6°. It is good background material but more work must be done before it becomes useful to the practicing designer.

2.3. HULL CHARACTERISTICS WHICH AFFECT PLANING PERFORMANCE

As with the other sections of this chapter, it is possible to give only a brief overview of the subject. Further information and other opinions are presented in References 20 through 31, as well as References 3, 5, 15 and 16. Particularly recommendable are References 20, 21 and 25.

2.3.1 Section Shape

A. V-Bottom. The most frequently used section shape is the V-Bottom, ranging from a few degrees of deadrise to around 30 degrees. In general, increasing deadrise reduces rough water pounding, improves directional stability, increases bank angle in turns, increases trim and reduces efficiency. There is one exception to the last point in the case high speed stepless boats, with more or less fixed l.c.g. positions; when the low deadrise hulls have "flattened out" to trim angles below the optimum, the deep V-hull running nearer the optimum trim will have less resistance. Excessive deadrise at the stern makes handling difficult at low speeds and reduces transverse stability while planing.

V-bottom hulls utilize a wide variety of section shapes.

a) Convex. This is inherently a wet section but by the proper use of spray rails the boat can be kept dry. The section pounds less than others of equal deadrise because there is less likelihood of its contacting the water on a large area at once. See Figure 3.5.

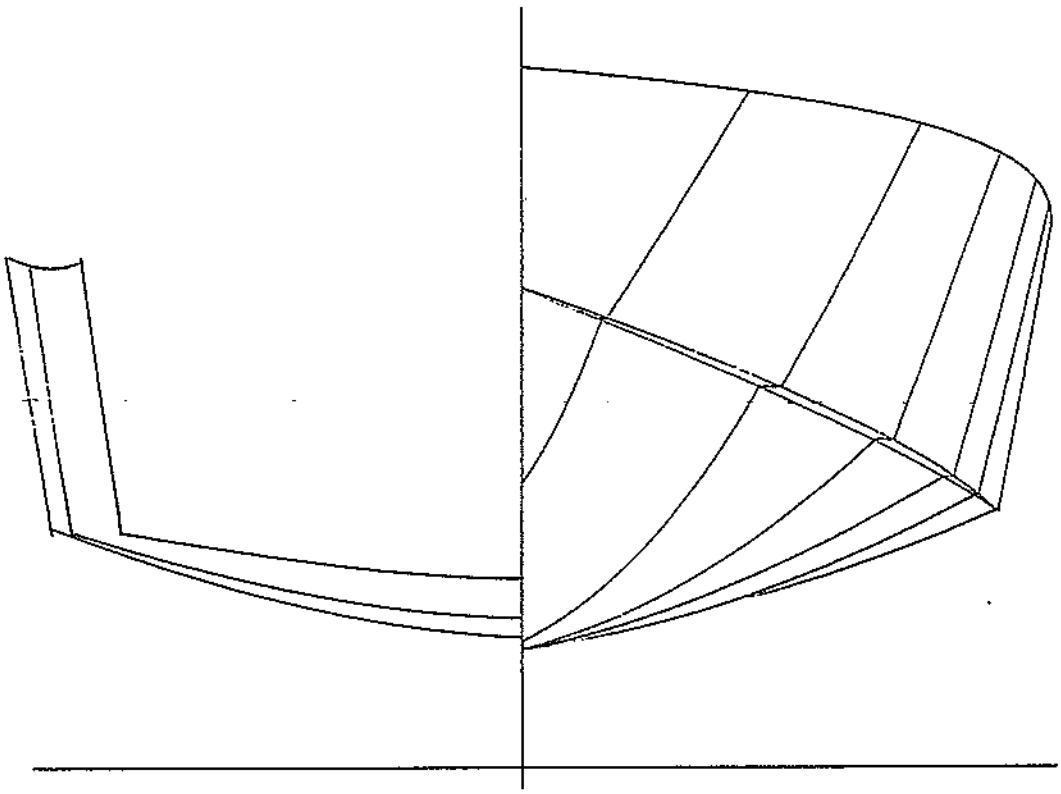

Figure 3.5. Convex sections

b) Concave. This is inherently a dry section but it is very hard riding because the hollow areas almost always "pocket" the water and produce impacts, sometimes over large areas at once. See Figure 3.6.

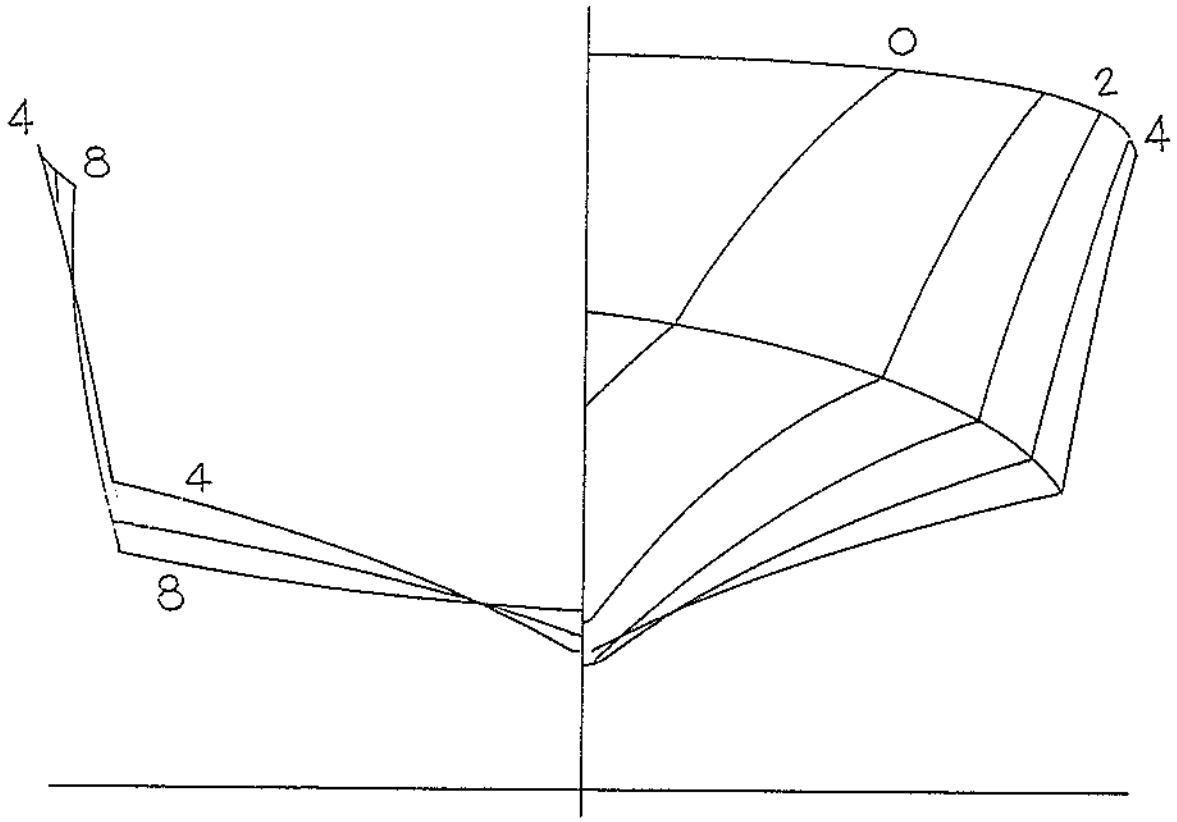

Figure 3.6. Cancave sections

c) Straight. Straight sections are considered by some to be about as good as any, and when considering only a transverse section this opinion has some degree of merit. But when considering the entire forebody surface produced by straight sections, it becomes apparent that they have all the faults and none of the virtues of both convex and concave sections. That is they produce a wet, pounding boat.

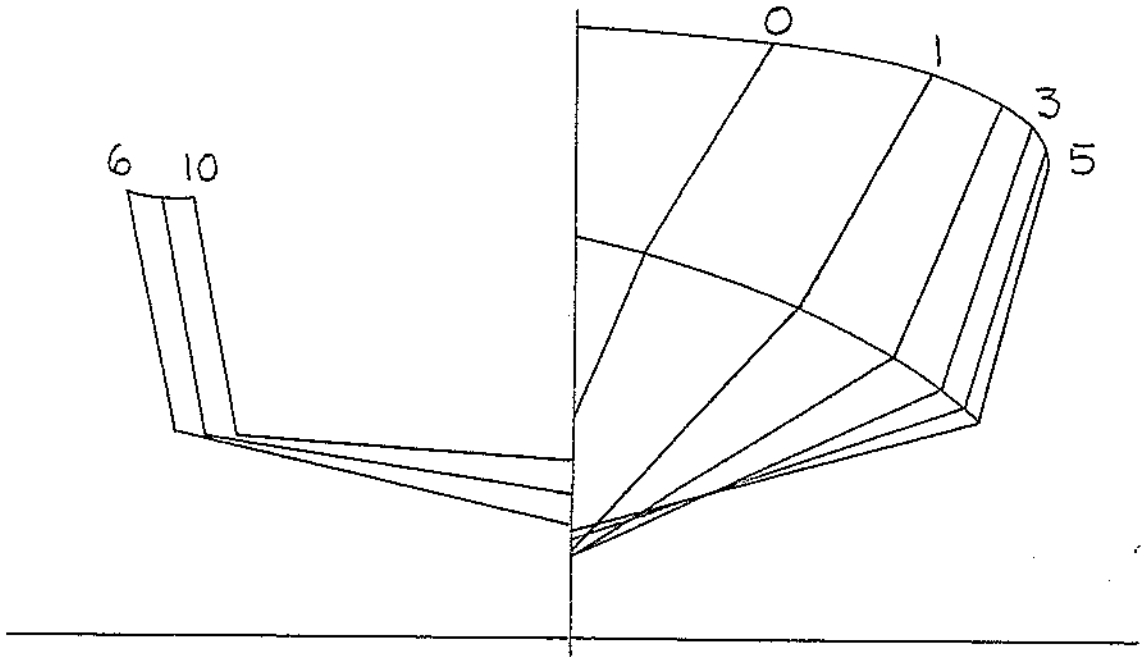

Figure 3.7. Straight sections

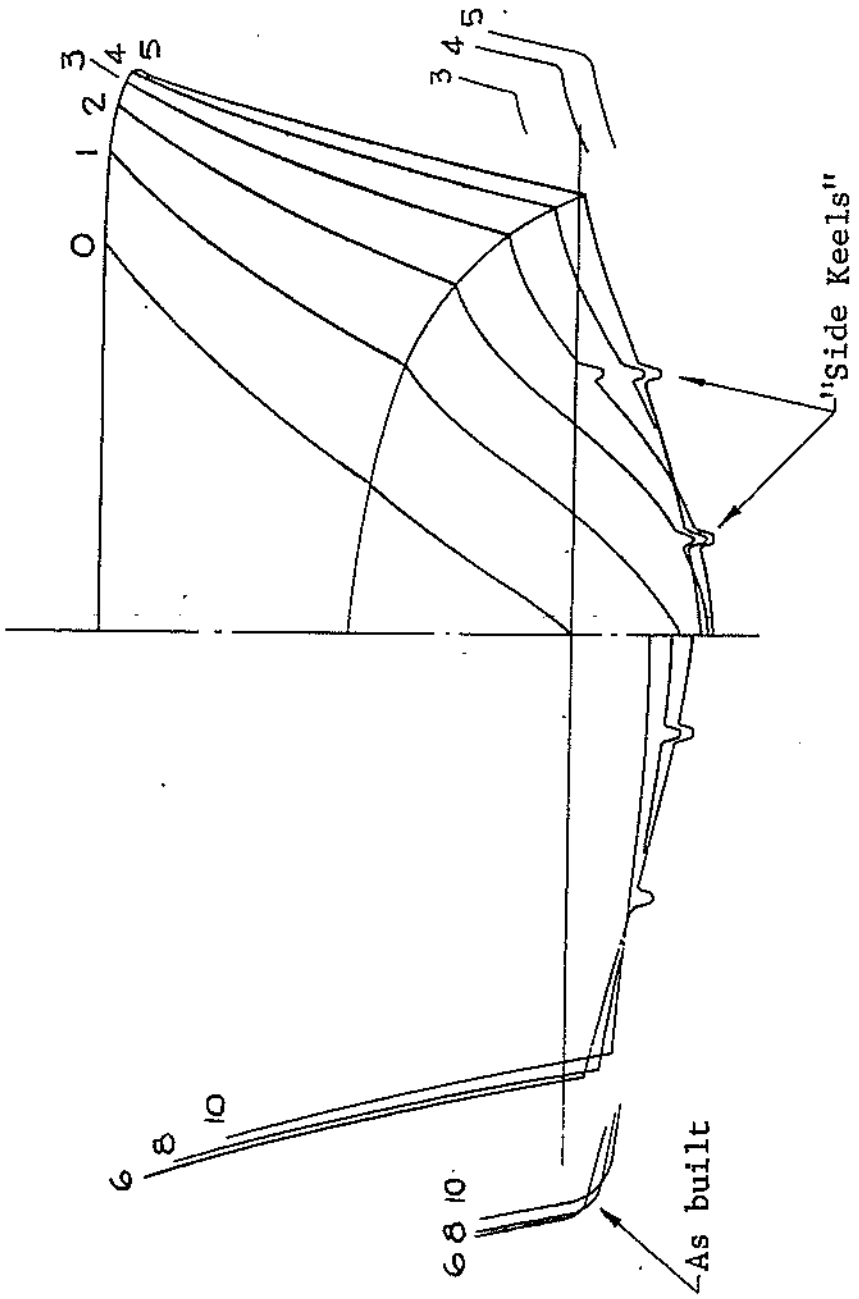

Figure 3.8. Inverted bell sections

d) Inverted Bell. These sections were designed as a "constant force" section and in an analysis of a two dimensional section immersing at constant rate into still water, they are. But a three dimensional boat operating in an irregular sea, especially bow seas, slaps very badly under the chine flare. The rounded keel does not pound, but produces a strong tendency to directional instability. It needs an external centerline keel or low spray strips to break up the cross flow when the forefoot becomes immersed in cross seas. See Figure 3.8.

e) An important aspect of the V-bottom design is the possibility, in high deadrise boats, of using spray strips on the bottom to separate the flow. In this way the boat can plane on a wide bottom at low speeds and a narrow bottom at high speeds. The same can be accomplished by means of a knuckle in the bottom withgreater deadrise outboard and less inboard. In a double chine design of this type an effective spray strip is required at the knuckle. These designs work out moderately well in practice, but notperfectly because the spray cannot be kept off the bottom as well as it appears on the drawing board. See Figure 3.9.

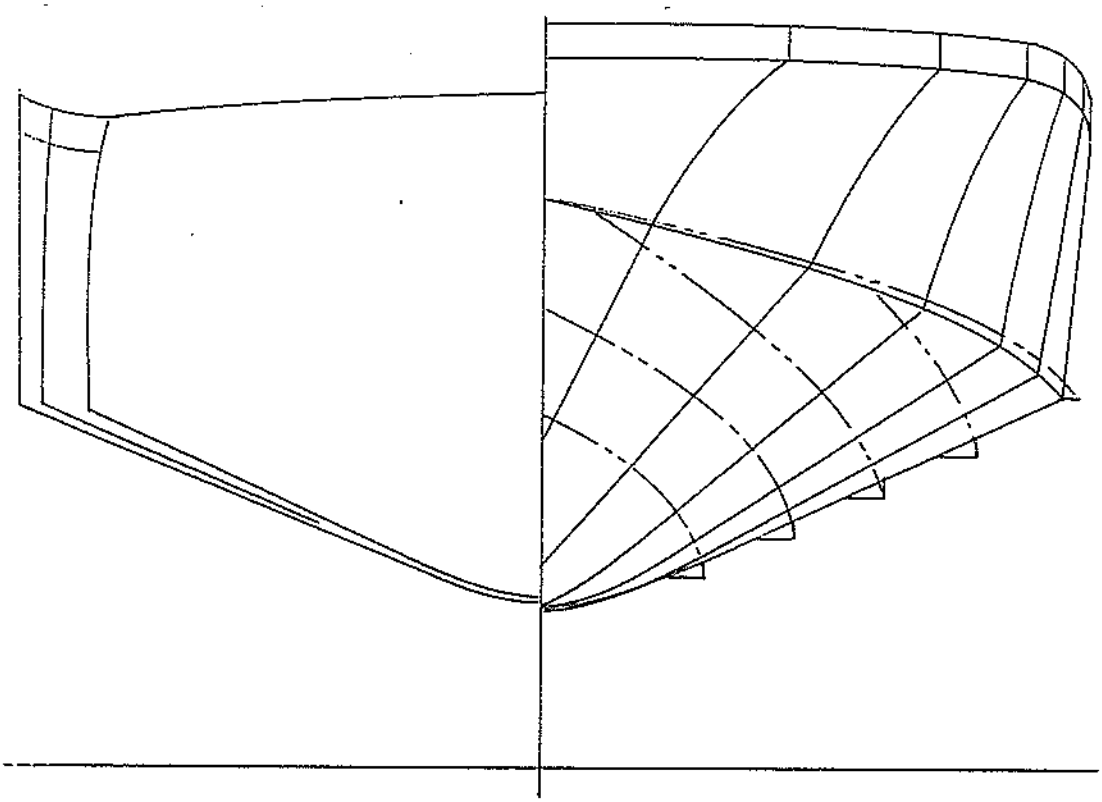

Figure 3.9. Deep V sections with spray strips

B) Inverted V-Bottom. This configuration has been popular with some designers ever since Hickman first introduced it, because of expected dryness and air cushioning of the ride. While the form has good hydrostatic stability, it also has an inherent tendency to capsize outboard on turns and therefore must be modified by beveling the chines. See Figure 3.10. The hull form provides some cushioning effect on the larger ripples, but in seas of any significance it is a hard pounder. Reference 32 presents test data on the planing characteristics of an inverted V prismatic surface with minus 10 degrees deadrise. Reference 33 reports that an inverted V model of minus 20 degrees deadrise has "significantly larger" impact loadings than a flat plate at some trim angles (high trims for a planing boat), but also, for nearly flat impacts, "a trend toward smaller loads relative to the flat bottom model". Additional test results are given in given in References 20, 21 and 24.

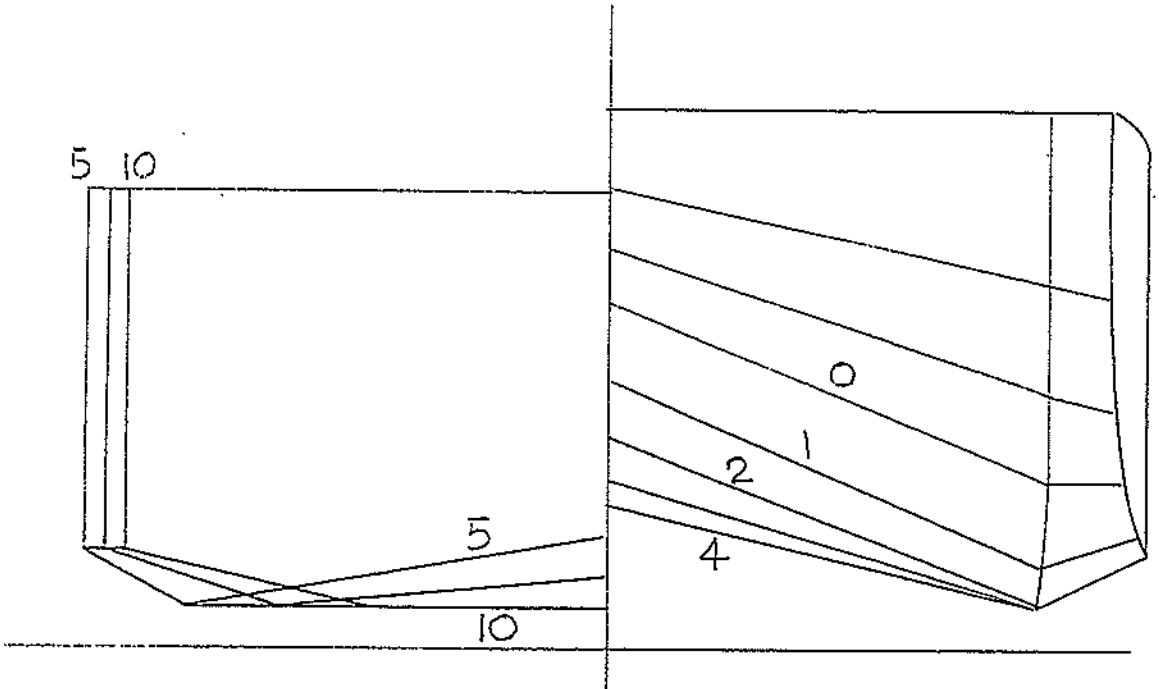

Figure 3.10. Inverted V sections

C) Variations of the Inverted V-Bottom. There are many variations of the inverted V besides the beveled or "non-trip" chines, such as the W-bottom and, with the addition of a second V on the centerline, an inverted W-bottom. Cathedral hulls and "whaler" hulls are good examples. Some of the configurations are incredibly complex and appear to have little engineering or architectural justification. One of the better of these forms is basically a moderately deep V hull with recurving chine flare which is designed to throw the spray down. In some of these designs it has has been observed that the spray is thrown down with such force that the rebound causes more spray to come aboard than if horizontal chine flare had been used.

These boats all have generally rectangular deck plans, and have, in varying degrees, the same virtues, and faults as the inverted V-bottom boat, namely static stability and a hard ride in rough water. The only quantitative information which is available for boats of this type gives little or no reason to suspect any superiority in load carrying or efficiency. See Reference 20. Apparently, no lines have been published on these designs.

D) Catamarans. The twin hull configuration offers an opportunity to increase the efficiency of a stepless hull. Porpoising stability limits the reduction in wetted area possible through an aft shift of the center of gravity, and, in a single hull, transverse stability limits the possible reduction in beam. But the catamaran form makes it possible to run on two very narrow hulls which together provide both longitudinal and transverse stability. Reference 13 gives a method for predicting the ideal high speed resistance of planing catamarans. It does not account for any interference effects between the hulls. The catamaran, like most of the hulls discussed in the previous section, provides a soft ride in small waves. But in waves large enough to contact the wing structure, the impacting is severe. This configuration is discussed in References 20 and 21. See Figure 3.11.

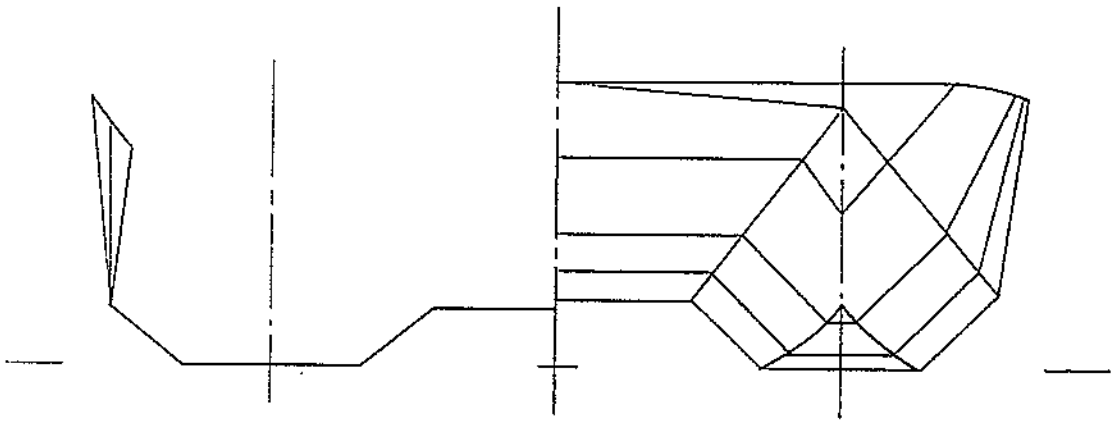

Figure 3.11. Catamaran sections

E) Round Bottom Boats. The performance of round bottom boats can be predicted with the planing equations when spray strips can be located to effectively separate the flow fairly low on the turn of the bilge. There are several reports of model tests on specific round bottom hull forms. Some of these are given in References 7*, 8, 27*, 28, 33, 34*, 35*, 36*, 39, 40 and 41. The references with asterisks present results for variations in the proprotions of the hull lines, in other words, a systematic series. The basic hull form for References 7 and 8 is shown in Figure 3.12. References 34 and 35 present a high speed displacement hull form (Figure 3.13) and Reference 36 presents a moderate speed displacement hull form.

There is a great deal of powering information which does not refer to specific hull forms. It is good for preliminary estimates of power and with experience can be fairly reliable. Sometimes it is the only information available. Some of the best sources of this information are References 3, 4, 15, 37, 38. It is in the form of equations or simple charts relating power to the speed, weight and perhaps a dimension of the boat. Each designer should make his own collection of this sort of information, constantly checking it against the most reliable information he can get. Some of this information, derived from some of the references and a number of unpublished sources will be presented in Section 3 of this chapter.

Aside from the problem of predicting resistance, spray rails are a necessity for a round bottom boat. One entirely conventional round bottom boat was observed in high speed turns to roll outboard and go down by the head badly. When spray strips were fitted along the waterline the boat banked inboard on turns and mainained normal trim.

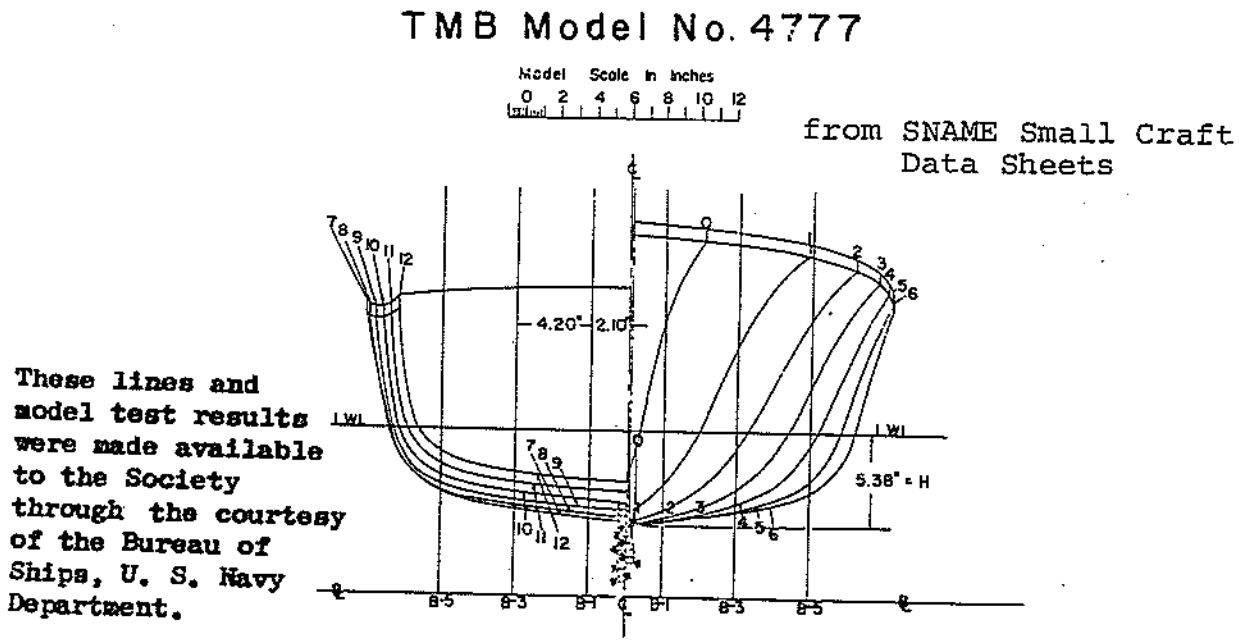

Figure 3.12. Round bottom sections

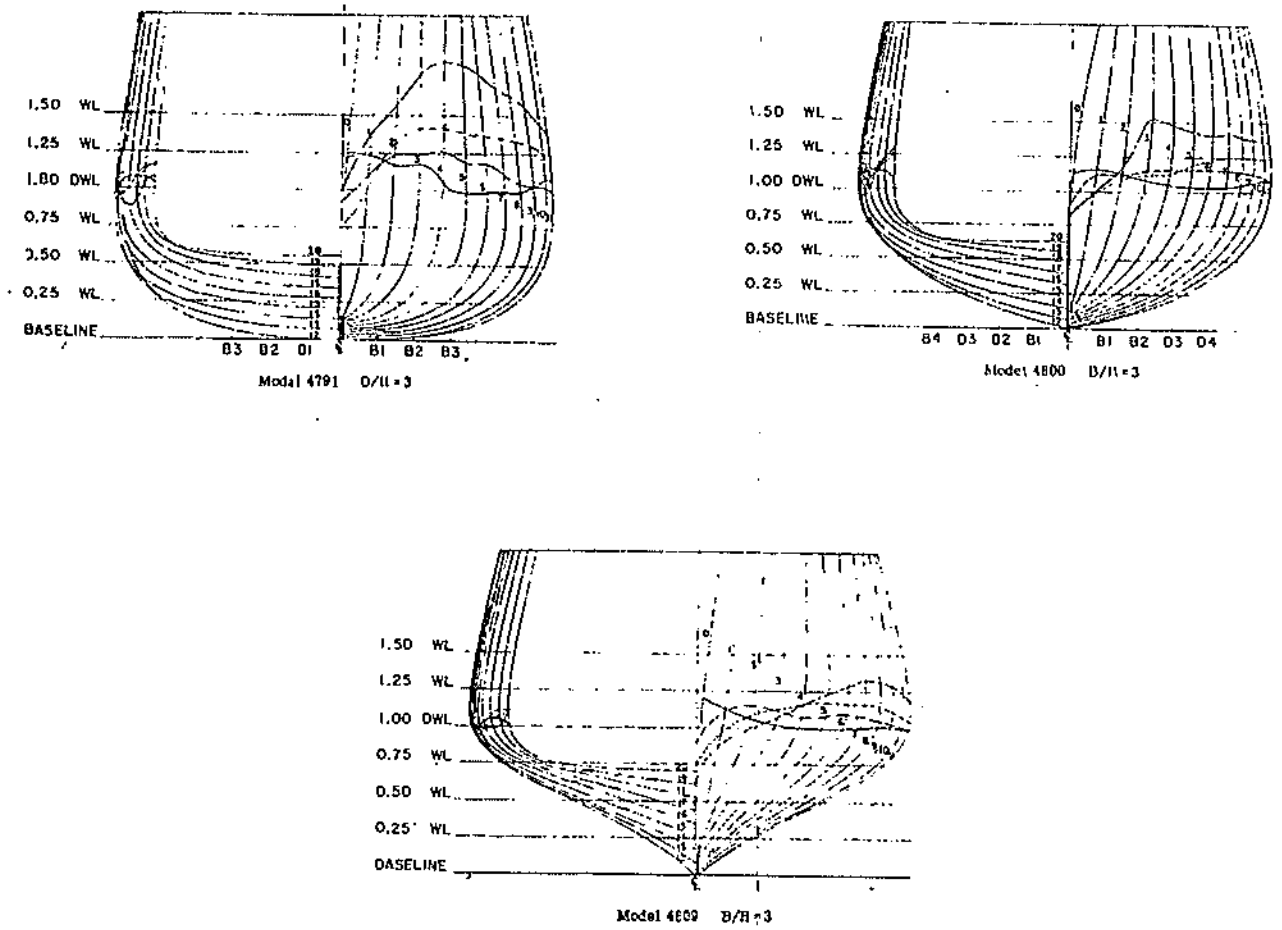

Figure 3.13. Body plans for three representative models of Series 64

The typical round bottom boat (Figure 3.12) is quite flat on the bottom and pounds badly when driven hard in rough water. Getting the turn of the bilge higher to increase the deadrise is a help. See Figure 3.14. However, excessively fine lines forward are to be avoided because of their tendency to dive and cause broaching in a following sea.

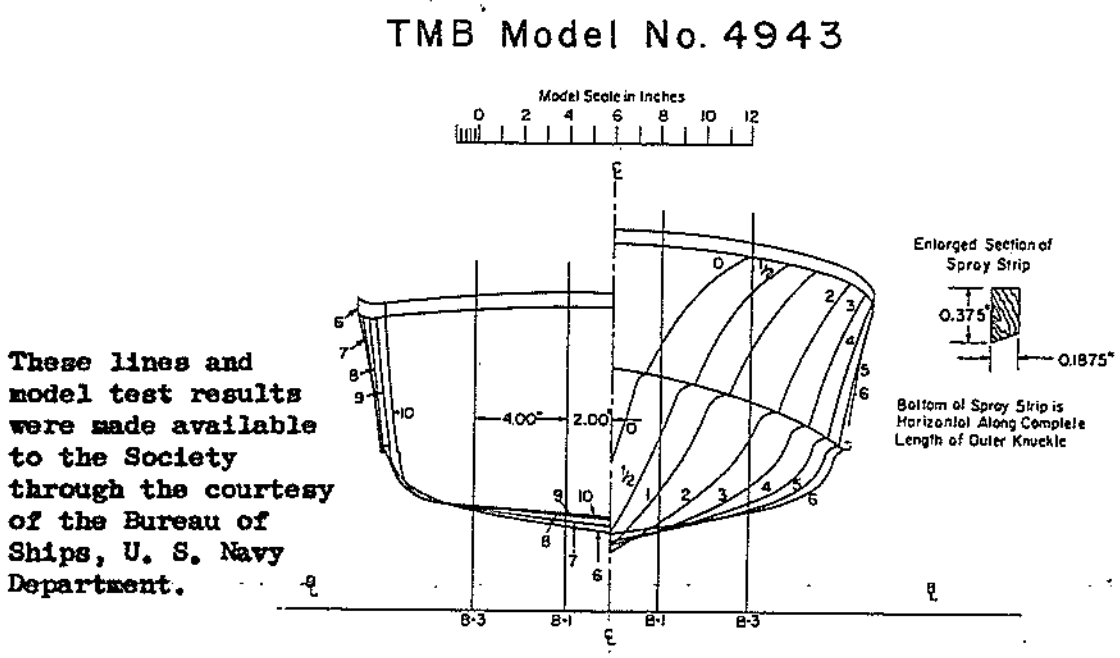

Figure 3.14. High deadrise, round bottom sections

An apparent anomally in round bottom boat resistance has been noted in Reference 27 and discussed in Reference 20. This is the fact that at high planing speeds a round bottom model was found to have less resistance in smooth water than a comparable V-bottom model. The reason for this is that the round bottom model ran at more nearly optimum trim which was higher than for the V-bottom model. However, this fact was a detriment at hump speeds and in rough water, particularly from the standpoint of accelerations.

2.3.2 Longitudinal Shape

A. Stepless. This form is the easiest for which to predict resistance and the easiest to build but has speed limitations because the trim is naturally reduced as speed is increased. It is often difficult to make a good compromise between the best dimensions for hump speeds and the best dimensions for high speed. In order to predict the trim the buttock lines must be straight in the afterbody, but when the maximum speed of the boat is in the hump region the trim and resistance can be reduced by hooking the buttock lines down slightly at the transom or by the use of wedges or trim flaps. But experience indicates that boats with hooked buttocks tend to broach more than boats with straight buttocks, although there is little or no quantitative information on this point.

The buttock shape at the bow deserves some consideration because it influences rough water behavior, as well as running trim at low speed. There are a number of NACA reports on seaplanes which can be used for guidance. Reference 43 is representative of these and Reference 25 is especially recommended. A systematic investigation of the influence of bow shape on planing boat performance is just beginning and this work will be covered in Chapter 4.

B. Stepped Hulls. Stepped hulls offer an opportunity to reduce wetted area, control trim angle, and increase the aspect ratio, but fixed stepped boats are not entirely free of stability problems... fixed stepped boats are not entirely free of stability problems because the after planing surface rides on the wake of the forebody and this wake changes shape with speed and loading. Collins Radio Company, in an unpublished report (Reference 44), describes the development of a single step runabout with a deep-V forebody and flat-V afterbody arranged so that only the outboard area of the afterbody would plane on the bow wave of the forebody, only a narrow portion of which was immersed. This seemed to produce better longitudinal stability.

The use of an adjustable stabilizer on a single step hull, the Plum-boat, is reported by Clement in References 17, 45 and 46. The concept has promise. Although a prototype has been built, testing has been limited and there has been no opportunity to see if it will produce a practical full scale boat. Clement has also investigated the use of bottom camber on stepped hulls to further improve their efficiency. This work is reported in References 47, 48 and 49. The effect of the bottom camber is to increase the pressure toward the trailing edge where it normally drops off, thereby creating greater total lift on a given wetted area.

Hobbs has discussed stepped boats in Referencd 31, and has had some success with two-step, moderately deep-V hulls. The claims for this type of hull compared with a stepless deep-V ocean racer type, are speed equivalent to 30 percent more power, controlled trim producing a softer ride in rough water, and greater maneuverability. While there is still little documentary evidence, his experience and that of a few others, going back to the British CMB's, indicates that the stepped hull can make an excellent rough water boat.

The two step hull eliminates some of the stability problems of single step boats, but there seems to be no additional benefit from more than two steps, although multiple steps and "shingled" bottoms, multiple longitudinal and diagonal shingles, etc., have been used. Reference 24 gives the results of model tests on several configurations of this type.

C. Warped Bottoms. The variation of deadrise with length, that is twist or warp in the bottom, reduces the planing efficiency, but only to a small degree for reasonable amounts of twist. It is a small penalty to pay when compared to the advantage gained. If the high deadrise required in the forebody is carried all the way to the stern, the boat will be difficult to maneuver at low speeds, and sometimes also at high speeds. Also, if an amount of deadrise which

is reasonable at the stern is carried forward of amidships, the boat will pound badly. So, some twist is good but excessive twist is very bad because it causes the forefoot to drag in the water, reducing directional stability and increasing skin friction. Fortunately, with convex sections a good compromise can be reached whereby a nearly prismatic surface can be used aft of the high speed stagnation line while the area outboard of and forward of this line can have increased deadrise and curvature, both of which help to reduce impact pressures. One such example, taken from Reference 25, is shown in Figure 3.15. This is obviously not the ideal solution to every design problem but for a small boat which must operate in a wide range of sea conditions and with a large variation in l.c.g. and displacement it has been very good. As with other designs, it is unfortunate that these claims are not better documented.

D. Forefoot Contour. As stated in other sections, a deep, fine forefoot will produce a strong tendency toward broaching. Usually, in a planing or semi-planing boat the fairbody line (the profile of the hull without appendages or hollow garboards) runs in a straight line forward from the transom. This line should begin curving up toward the stem at about 60 or 70 percent of the LWL forward of the transom. This, of course, is not a hard and fast rule and varies widely with the initial trim of the fairbody line, the expected running trim, and the amount of external skeg to be used. The problem is to achieve directional stability not only in smooth water, but also in a cross sea which has a tendency to throw the bow around, and in following seas, especially breaking surf, when it is imperative that the bow lift when being driven down the face of a wave. It is also important that the hull be directionally stable at displacement speeds. This type of forefoot is one of the features which contributes to the good directional stability of most of the cathedral and whaler type hulls. There is no quantitative information available for evaluating the effect of forefoot shape on boat performance. As with many other features, the designer must develop his own judgment based on careful observation of the performance of existing boats.

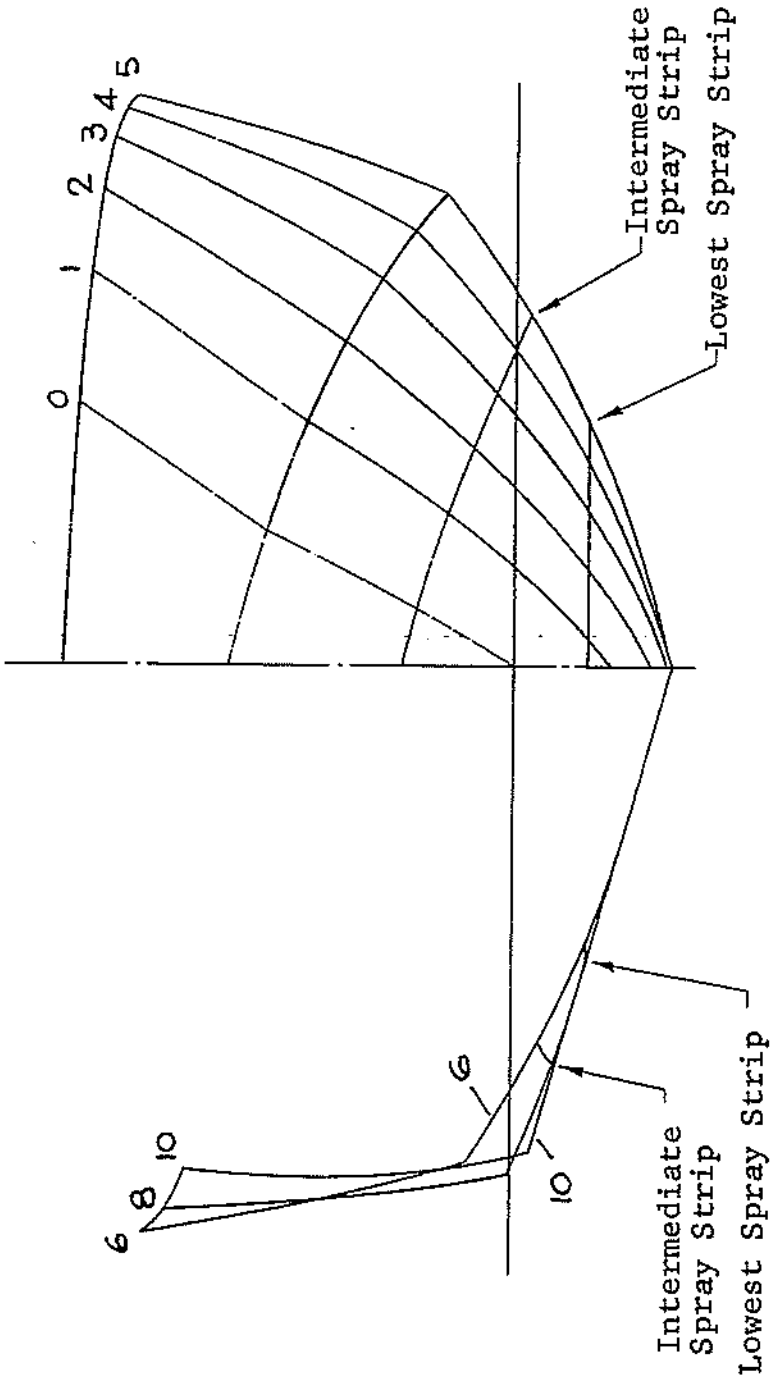

Figure 3.15. Warped Bottom

E. Trim Control. In many designs the variety of operating conditions imposes a large fore-and-aft shift of the center of gravity and/or a large variation in displacement. Usually the limitations on the principal dimensions preclude having the boat trim properly at all loads and speeds. In some ocean racers bow ballast tanks, the filling and draining of which can be controlled from the helmsman's station, are used for trim control, both in getting over the hump with a full load of fuel in the stern, and to reduce running trim in rough water. In many types of boats transom flaps are used for trim control. In very fast boats aerodynamic trim control is sometimes used, principally to keep the bow from lifting and flipping over. Aerodynamics, other than wind drag, are beyond the scope of this work, and fixed trim control devices, such as wedges and hooked buttocks are discussed under longitudinal shape. The principal point to make is that we have the tools for predicting the speed-trim curve for many boats. If it is known that certain combinations of speed, weight and center of gravity result in unacceptably high trims, and, if the dimensions of the boat cannot be changed to correct this, then there is good engineering justification for using trim control devices. In the case of ballast tanks, which may be free flooding, static trim and stability must also be considered. This is one area in which we are able to make good performance predictions. Calculations for the effect of trim flaps will be given below.

Limited trim control is also achieved by the use of two or more planing surfaces in tandem, that is, a stepped hull. A specialized version of the stepped hull is the Plum-boat with an adjustable stern stabilizer (References 17, 45 and 46).

The use of hydrofoils, either forward or aft, to control trim and damppitch motions has been proposed. It is believed some of these concepts have been experimented with, but there is no design information generally available. Reference 50 gives a little information on smooth water tests of a boat with partial hydrofoil support (the foils located near the bow).

Other means of controlling trim, which should at least be mentioned, are prop-riding for hydroplanes, and simply tilting the lower unit of outboard motors and sterndrives.

2.3.3 Planform

The principal features which characterize the planform of a lifting surface are aspect ratio, taper ratio and sweep-back. But these features of a planing surface cannot be determined simply by drawing an outline, as for an airplane wing or hydrofoil, because some of them are mutually dependent. The span of the lifting surface is equal to the chine beam. If the beam is fixed, the area and aspect ratio are simultaneously determined by the l.c.g. and for a given step shape, the taper ratio and sweep-back are both determined by the deadrise and trim angle. With all the foregoing fixed, the trim angle is determined by the weight and the speed. Actually, each factor is not fixed in the order stated, and in the preliminary

design stage there is some latitude in choosing a planform, but in a practical way the designer seldom has complete freedom of choice. Although a lifting surface approach is possible (one very good method is described in Reference 14), the usual treatment is concerned principally with beam and l.c.g. position, the rest of the factors falling out naturally. Nevertheless the designer should be familiar with the effects of the various factors. In the following discussion of planform the entire boat will be considered and not just the wetted (lifting) area.

A. Chine Shape. The length, and particularly the beam, of the chine area are determined by considerations of the space requirements of the boat's mission, buoyancy, stability, and hydrodynamic efficiency. In a boat which will operate in the hump region, or which will have difficulty getting over the hump, the chine beam at the transom should be wide to provide as much buoyant lift at the stern as possible. See the picture on page 9 of Reference 16. At full planing speeds, when dynamic lift predominates, the transom can be narrowed considerably to reduce frictional drag, without a noticeable loss in lift. The narrow stern also improves handling in a following sea, although with moderate deadrise (say 15°) the wide stern is not bad. The chine shape forward in plan view should not be very full because it reduces the deadrise and makes the bow blunt with consequent pounding and wetness. At speeds near the resistance hump, where so many boats operate, the bow makes a a significant contribution to the resistance and should therefore be made as fine as practicable, consistent with other requirements such as prevention of "routing" in a following sea. If the chine line is made narrow it is possible to develop a bow which does not pound badly, is dry (because of spray strips) and which will not bury in a following sea. Figure 3.16 shows a fair example of the application of these ideas. Photographs of this boat are shown on pages 7 through 20 of Reference 16.

B. Step Shape. Whatever the transom shape in planview, its intersection with the mean buttocks should be used in locating the center of pressure in the trim calculations. Pointed steps have been designed for better rough water handling, and re-entrant v-steps have been used in the lifting surface approach to planing hull design. None of these has a large effect on planing efficiency except perhaps through side effects such as improved step ventilation.

There are, of course, other considerations such as appearance, structure, arrangement, low speed drag, directional stability and turning which are all influenced by the planform of the steps and transom. References 24 and 26 give the results of model tests on stepped hulls. The latter shows that, from the standpoint of planing efficiency, the transverse step is as good as anything.

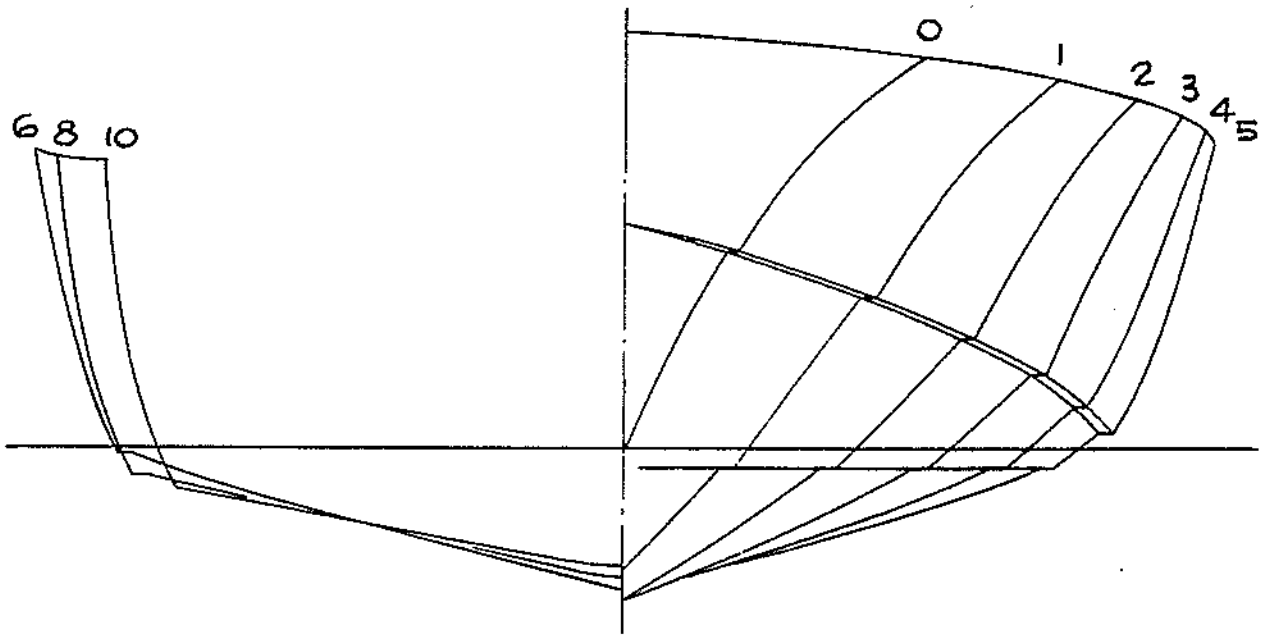

Figure 3.16. Recommended chine shape

NOTE THAT IN THE FOREBODY THIS IS VIRTUALLY
A ROUND BOTTOM BOAT

C. Aspect Ratio. In general the higher the aspect ratio (the wider the surface with respect to its length) the better the lift to drag ratio; but for planing surfaces there is little increase in L/D for aspect ratios above about 1. For a fixed aspect ratio, there is an optimum wetted area, the one which produces the optimum trim. But if one dimension of a planing surface is held constant and the other varied (such as in finding the best beam for fixed l.c.g. or the best l.c.g. for fixed beam), it will be found that the L/D does not necessarily increase with increasing aspect ratio. The best dimension will be the one which produces the optimum trim angle. The optimum trim angle varies with aspect ratio and deadrise. The effect on planing performance of variations in the aspect ratio are well documented and easily evaluated. See in particular References 1, 12 and 14.

2.3.4 Appendages

A. External keel, skeg, or fin. These appendages are used primarily to control directional stability and turning qualities and as usual, compromises are necessary, but there is seldom any difficulty

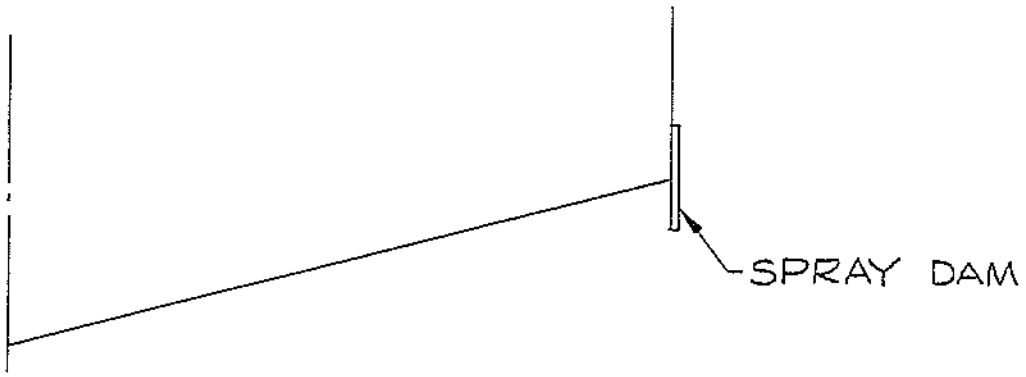

Figure 3.17. Spray dam

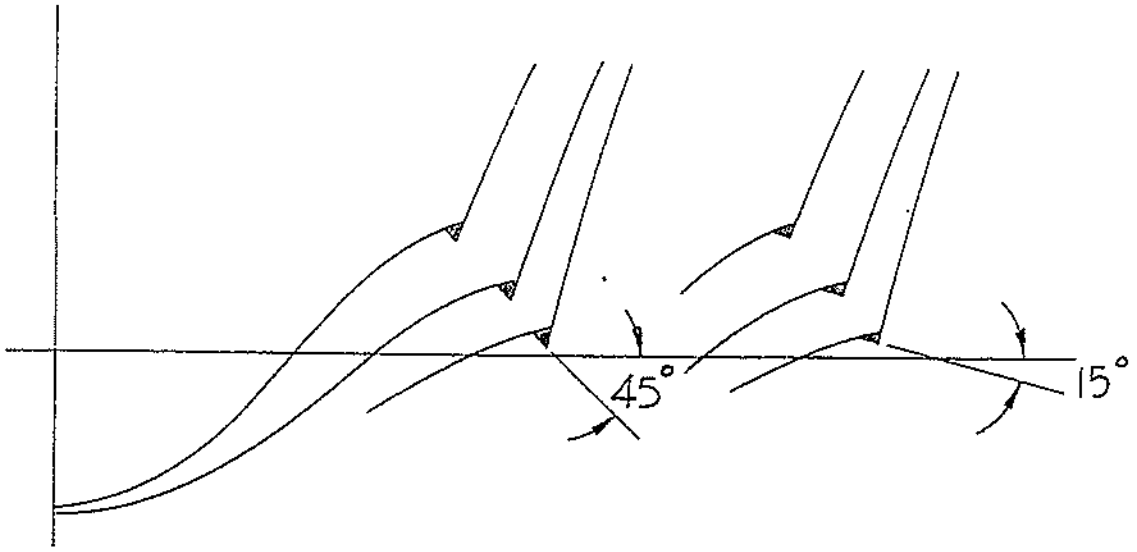

Figure 3.18. Spray rails

in getting a boat to be reasonably good in both course keeping and turning. For small fast cruisers and runabouts, the proper distribution of deadrise gives the boat the desired handling qualities without any appendages, except rudders and struts if inboard powered. For heavier, slower boats, which usually tend to have the greatest fairbody draft well forward, and for light, low-deadrise boats, a long skeg is essential. It is also a good idea in conventional inboard boats, to make the skeg deep enough to protect the propellers in case of grounding. The skeg should be long enough to get the center of lateral area aft of the center of gravity but it should nevertheless be cut away enough aft to permit the rudders to kick the stern around when maneuvering. Sometimes too large a skeg will prevent the side slipping in a turn to the extent that it will cause the boat to heel outboard. Reducing the skeg area in these cases restores the boat to proper banking on turns. Because of excessive side slipping of some racing runabouts, a fin is used forward to improve turning.

B. Spray Rails. Spray rails are perhaps the most important appendage on a planing boat because the essence of planing is flow separation. Spray rails, whether added on or built in, must be used along the chines and they must be sharp. Additional strips can be used above the chine forward for rough water operation, and below the chine to remove some of the whisker spray. References 51 and 52 present results of the analysis and testing of bottom spray strip locations.

A conventional spray strip has no effect on the main spray blister which can be eliminated only by a vertical "spray dam" (Figure 3.17) which would seldom be practical on a boat, primarily because of its vulnerability to damage, and because of its increased drag under all conditions except straight ahead motion of a prismatic surface with the chine parallel to the keel. Background information is contained in Reference 53. Reference 25 gives the results of some full scale experiments on the effects of varying the cross section (bottom angle) and location of spray strips. One important finding was that a steep angle (45°), Figure 3.18a, would throw the water down sharply causing it to splash back into the boat (as found with some cathedral hulls) whereas a small angle (15°), Figure 3.18b, will throw the water down and out, dissipating the energy horizontally, and making a much drier boat.

2.3.5 Loading

When the loading of a planing surface is changed from Δ_1 to Δ_2, all other factors constant, the trim angle, τ, varies as $(\Delta_2/\Delta_1)^{0.91}$, and the pressure drag D_p as $(\Delta_2/\Delta_1)^{1.91}$, as shown by the following analysis:

Referring to the calculation method described on pages 60 through 63 of Reference 16 (cited in Reference 1), and in particular to the charts and equations on page 61 of Reference 16, reproduced here as Figure 3.19, it can be seen that each of the factors on which

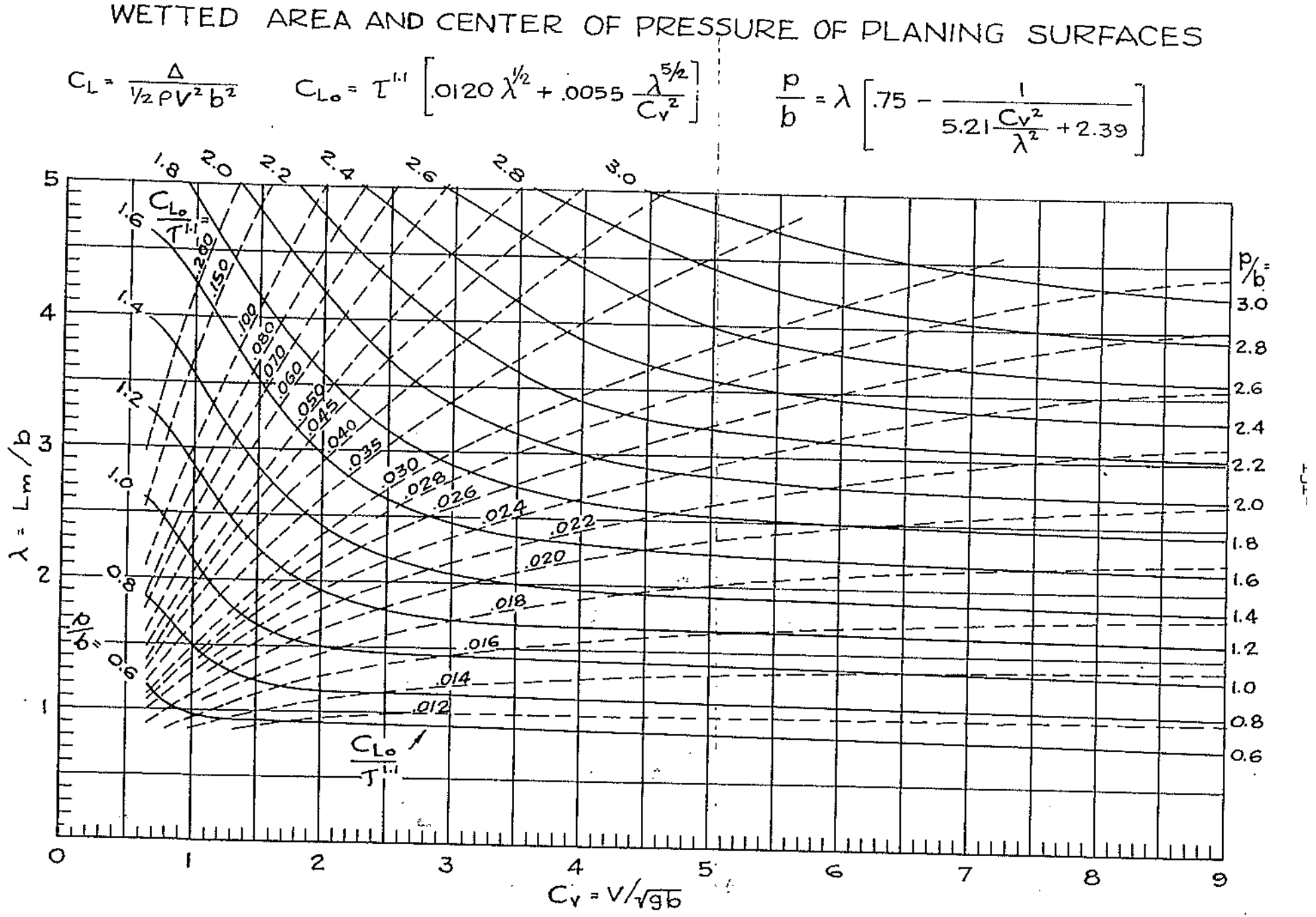

Figure 3.19. Wetted area and center of pressure of planing surfaces.

the resistance depends varies with a change in displacement as shown in Table I.

These simple relationships are useful when the trim and resistance curves of a boat must be corrected for a change in displacement, because they save running through the entire calculation for each point. It is necessary only to correct the wave resistance and add the previously calculated friction resistance to get the new total resistance. It does not matter if the curve was calculated from planing surface data or from model tests; the corrections are still valid for speed coefficients above 1.0. In the latter case (model test results) this will save time only if the expansion calculations are available.

The displacement of every boat changes with time, even if only by the weight of fuel consumed. Sometimes the variable weights (fuel and other consumables, payload, etc.) are a large percentage of the displacement. In every design due consideration must be given to the placement of variable weights. In boats which normally operate at full planing speeds it is desirable to have the center of gravity move forward as weight is added, provided that static trim and low speed handling are not adversely affected. In the case of very light boats which plane at a very flat trim angle at high speeds, it usually is good to have the weight added in the stern. Boats which will operate at displacement speeds in rough water should not be loaded heavily by the bow, even if this might be an advantage at planing speeds. In general a boat can stand to be out of trim more by the stern than the bow before becoming unsafe or unmanageable, but either extreme is bad. The complete range of displacement and l.c.g.'s should be checked for performance at all speeds from zero to maximum.

3.0 METHODS OF CALCULATION

3.1 GENERAL

Basically, there are three methods of performance calculation:

a) The use of simple charts or equations which relate the weight, the power, the speed and perhaps the length or beam of the boat. This method is quick and easy but has a number of drawbacks which will be explained in Section 3.2.

b) Direct calculation from planing equations which were derived from tests of prismatic (constant cross section) models. This method has the advantage of taking into account all the important factors which influence planing performance. It has the disadvantage that for boats with large variations in cross section with length and for conditions where much of the curved portion of the bow is in the water, the predictions are not exact. For most design work these disadvantages have not proven to be serious as long as care is taken in judging the effects of the variations from a constant section.

c) Prediction from tests of boat shaped (rather than prismatic) models, either a systematic series or an individual hull. In the latter case it may be a model of the new design or a similar design.

TABLE I

Resistance factor	For Δ_1	For Δ_2
$C_v = \frac{v}{\sqrt{g\,b}}$	C_{v_1}	Same
$C_{L_o} = \frac{\Delta}{1/2\,\rho\, v^2\, b^2}$	$C_{L_{o1}}$	$C_{L_{o2}} = C_{L_{o1}}\left(\frac{\Delta_2}{\Delta_1}\right)$
P/b	$(P/b)_1$	Same
λ, depends on C_v and P/b	λ_1	Same
$\frac{C_{Lo}}{\tau^{1.1}}$, depends on C_v and P/b	$\left(\frac{C_{Lo}}{\tau^{1.1}}\right)_1$	Same
$\tau^{1.1} = C_{L_o} \div \left(\frac{C_{Lo}}{\tau^{1.1}}\right)$	$\tau_1^{1.1}$	$\tau_2^{1.1} = \tau_1^{1.1}\left(\frac{\Delta_2}{\Delta_1}\right)$
$\tau = \sqrt[1.1]{\tau^{1.1}}$	$\tau_1 = \sqrt[1.1]{\tau_1^{1.1}}$	$\tau_2 = \sqrt[1.1]{\tau_1^{1.1}\left(\frac{\Delta_2}{\Delta_1}\right)} = \tau_1 \sqrt[1.1]{\frac{\Delta_2}{\Delta_1}} = \tau_1\left(\frac{\Delta_2}{\Delta_1}\right)^{0.91}$
$D_p = \Delta \tan\tau \sim \Delta\tau$	D_{p_1}	$D_{p_2} = D_{p_1}\left(\frac{\Delta_2}{\Delta_1}\right)\left(\frac{\Delta_2}{\Delta_1}\right)^{0.91} = D_{p_1}\left(\frac{\Delta_2}{\Delta_1}\right)^{1.91}$
$D_f \sim S \sim \lambda$	D_{f_1}	Same

Where:
- v = speed, fps.
- g = acceleration of gravity, ft./sec.^{2}
- b = beam, ft.
- p = l.c.g., forward of transom, ft.
- D_p = pressure drag (wave resistance)
- D_f = frictional drag
- S = wetted area
- λ = mean wetted length, beams
- $\Delta\lambda$ = effective wetted length increment due to spray drag

NOTE: The change in $\Delta\lambda$ due to the change in τ has been neglected. For $\tau < 3°$ and $\lambda < 1.5$ it should be checked and included. If the design has bottom spray strips which effectively eliminate the whisker spray, the correction need not be made.

It is only in the case of a model that is geometrically similar to the full scale boat that the prediction is a straight forward matter, and even then there are some questions about how to scale some components of resistance. When the model is different from the boat, care must be exercised to assure good results. As far as possible, guidelines will be given to assist the designer in exercising the required "care".

3.2 CHARTS AND EQUATIONS FOR PRELIMINARY DESIGN

There are a number of simplified methods in common use for the prediction of power boat performance. They consider only a few of the factors which affect a boat's performance and consequently cannot be used to good advantage except with a family of designs in which the missing factors are similar in all boats. For general performance predictions they are inadequate. This inadequacy has been illustrated for a number of these methods in Reference 59.

The methods compared in Reference 59 are all given in, or can be reduced to, the form of a curve of weight-horsepower ratio plotted against either the speed or the speed-length ratio. With these plots, not only is the basic comparison inadequate for most work but the method of plotting it is not the best. However, there are occasions in preliminary design work and in work on existing boats, when only limited information is available. For these cases it is desirable to have an easy method of estimating speed or power, but for best accuracy the information must be handled in a dimensionally correct manner. This matter will be taken up after brief discussion of the equations in common use for making speed-power estimates.

Bob Hobbs, in an unpublished report, lists 8 of these equations. Most of them can be found in References 4, 5 and 58. These equations can be put in the form $V = C(P^m/\Delta^n)$. The value of m varies from .333 to .572 and of n from .222 to 1.00. A brief study of the resistance curves presented in the references shows that they all have irregularities in them which would cause the exponents m and n to vary with speed, and from boat to boat. In fact, the speed-power curve of any given hull varies with loading. The only hope for an equation of this kind then, lies in the possibility that a number of boats considered normal for their type, the data will lie on a narrow enough band to permit a curve to be faired through it. The desirability of making quick preliminary powering estimates, the lack of good design data for many boat types, and the hope of finding some sort of hull efficiency index for judging the quality of a design, have prompted some recent investigations into this matter. Clement, in an unpublished report, compares the performance of 7 boats. The data for these boats is given in Table II. This information has been plotted in several ways, shown here as Figures 3.20 through 3.24. The figures show the difference in results produced by the different methods of plotting. In Figures 3.20 and 3.21 the data collapse well and a curve is faired through the points. Because of the simplicity of the functions used, Figure 3.21 is the more useful of the two, and the equation for its curve is shown in the figure. When put into the "standard" form it is:

$$V = 2.74 \frac{BHP^{0.551}}{\Delta^{0.476}}$$

Most of the data points lie within 10 percent of the curve. If more data points had been used, particularly at the ends, a different equation would have resulted. The fallacies in the assumptions of this approach are illustrated by plotting on Figures 3.20 and 3.21 the speed-power curves for boat 3, Table II, and for the parent form of Series 62 (from References 23 and 57 respectively). These 9 boats are all much the same type. To illustrate how far off the equation would be for another type, the curve for a 67-foot by 10-foot round bottom patrol boat (Reference 28) has also been added. In using the model data BHP/EHP was assumed equal to 2.0. In the opinion of the writer the equations are of little value but graphs such as Figure 3.21, when loaded with accurate data can be useful for preliminary design. Actually, the data collapse just as well in Figure 3.24, and the coefficients used there ($BHP/\Delta V$ and $V/\Delta 1/6$) are probably much more suitable for the collection and presentation of this kind of data.

Some of the best work that has been done in this area is presented in Reference 73. This work provides not only a tool for making preliminary power estimates but also a "yardstick" for evaluating a design. It is one of the few dimensionally correct methods that have been published. It also contains accurate full scale trial data on a large number of boats of many types from small runabouts to PT boats.

Once again, it is strongly suggested that the designer collect as much accurate data as he can, both model and full scale, and plot them on a suitable grid. In the case of model data it is necessary to keep notes on the assumed propulsive coefficient if BHP is plotted, and in both cases the size of the boat should be noted. The references will provide much useful information. Reference 66 (three volumes) will be especially helpful for low speed results. Reference 66 includes Reference 33.

3.3 DIRECT CALCULATION

Direct calculation means the determination of performance of a design directly from its dimensions, taking into account all of the important factors which influence planing performance: principally, displacement, beam, l.c.g. and deadrise. The charts discussed in Section 3.2 consider only displacement and perhaps length.

3.3.1 Clement

The design charts which Clement has developed from the equations of Shuford are very handy and permit easy visualization of the effect on performance of the various parameters. Their use is restricted to the full planing speeds. This method is presented in Reference 12, which also presents charts for the optimization of performance. The use of these charts is fully explained in the reference. The optimization charts are most useful when a stepped hull is to be designed and this approach is further developed in

TABLE II

Planing Boat Data

Ident. No.	Boat	W, lb.	Length, ft.	BHP	Max. V, knots	F_∇	$\frac{R}{W}\times\frac{BHP}{EHP}$	$\frac{R}{W}\times\frac{BHP}{EHP}\times 10F_\nabla$	Δ, tons	$\frac{BHP}{\Delta}$	$\Delta^{1/6}$	$\Delta^{7/6}$	$\frac{BHP}{\Delta^{7/6}}$	$\frac{V}{\Delta^{1/6}}$	$\frac{EHP}{\Delta^{7/6}}$
3	Elco Pt 622	111,000	76.4	4,440	42.3	3.6	0.308	11.7	49.6	39.5	1.916	95.0	46.7	22.1	2.13
3	Elco Pt 622	121,000	76.4	4,545	40.8	3.5	0.299	10.3	54.0	34.2	1.944	105.0	43.3	21.0	2.06
8	Brave	190,500		9,000	50.3	3.9	0.307	12.0	85.0	105.9	2.097	178.2	50.5	24.0	2.11
9	Mercury	219,500		10,500	52.	4.0	0.300	12.0	98.0	107.1	2.147	210.4	49.9	24.2	2.06
11	Jackie S.	13,450		900	50.	6.1	0.437	26.6	6.0	150.0	1.348	8.1	111.2	37.1	3.09
12	45' Rescue	32,000		900	33.	3.5	0.278	9.7	14.3	62.9	1.558	22.3	40.4	21.2	1.91
14	65' Picket	66,000		1,200	25.	2.4	0.237	5.6	29.5	40.7	1.758	51.9	23.1	14.2	1.63
17	Gee	18,000	40.	1,000	45.5	5.3	0.398	21.1	8.0	125.0	1.414	11.3	88.5	32.2	2.75

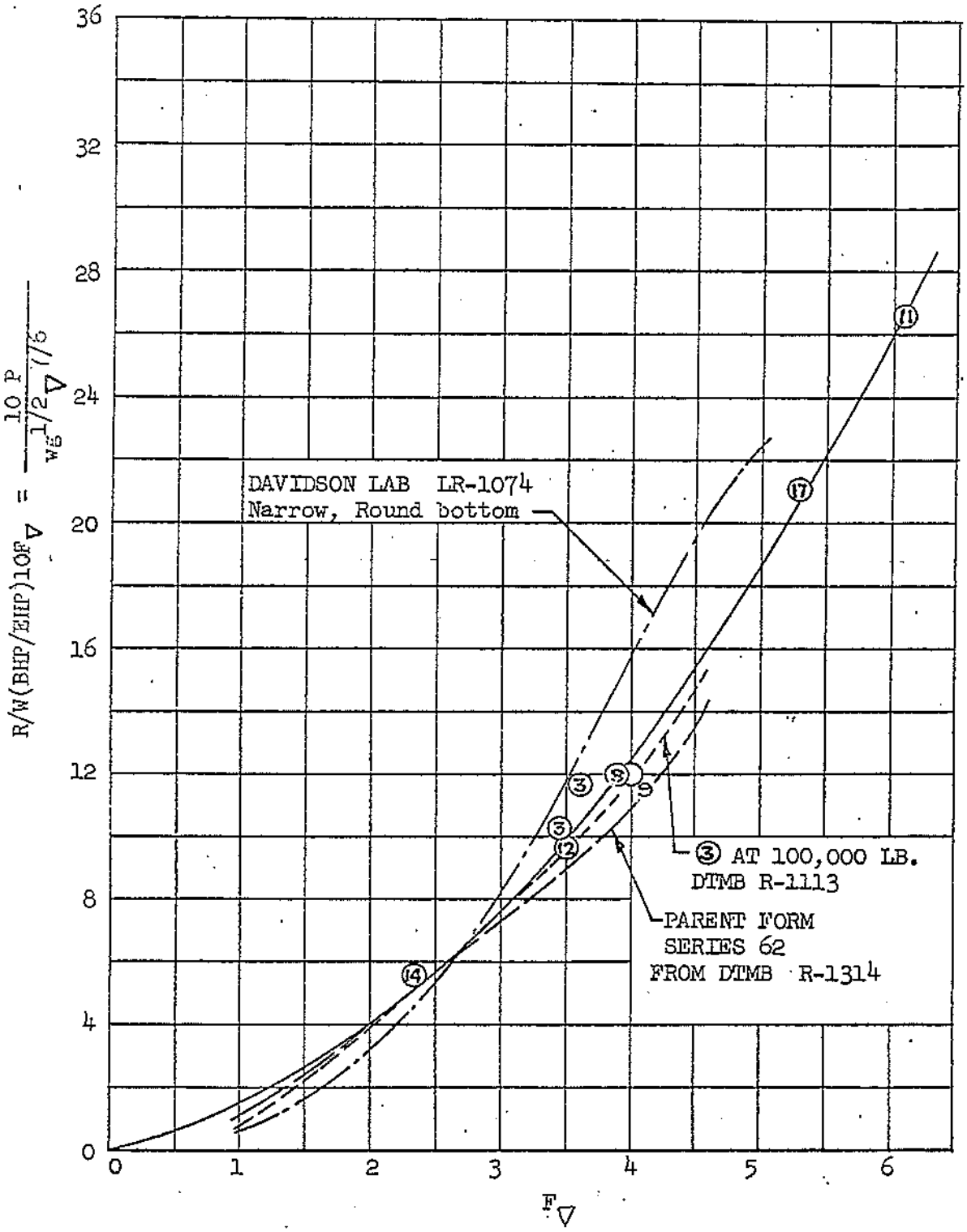

Fig. 3.20: $R/W(BHP/EHP)10F_{\nabla}$ vs. F_{∇} for several planing hulls

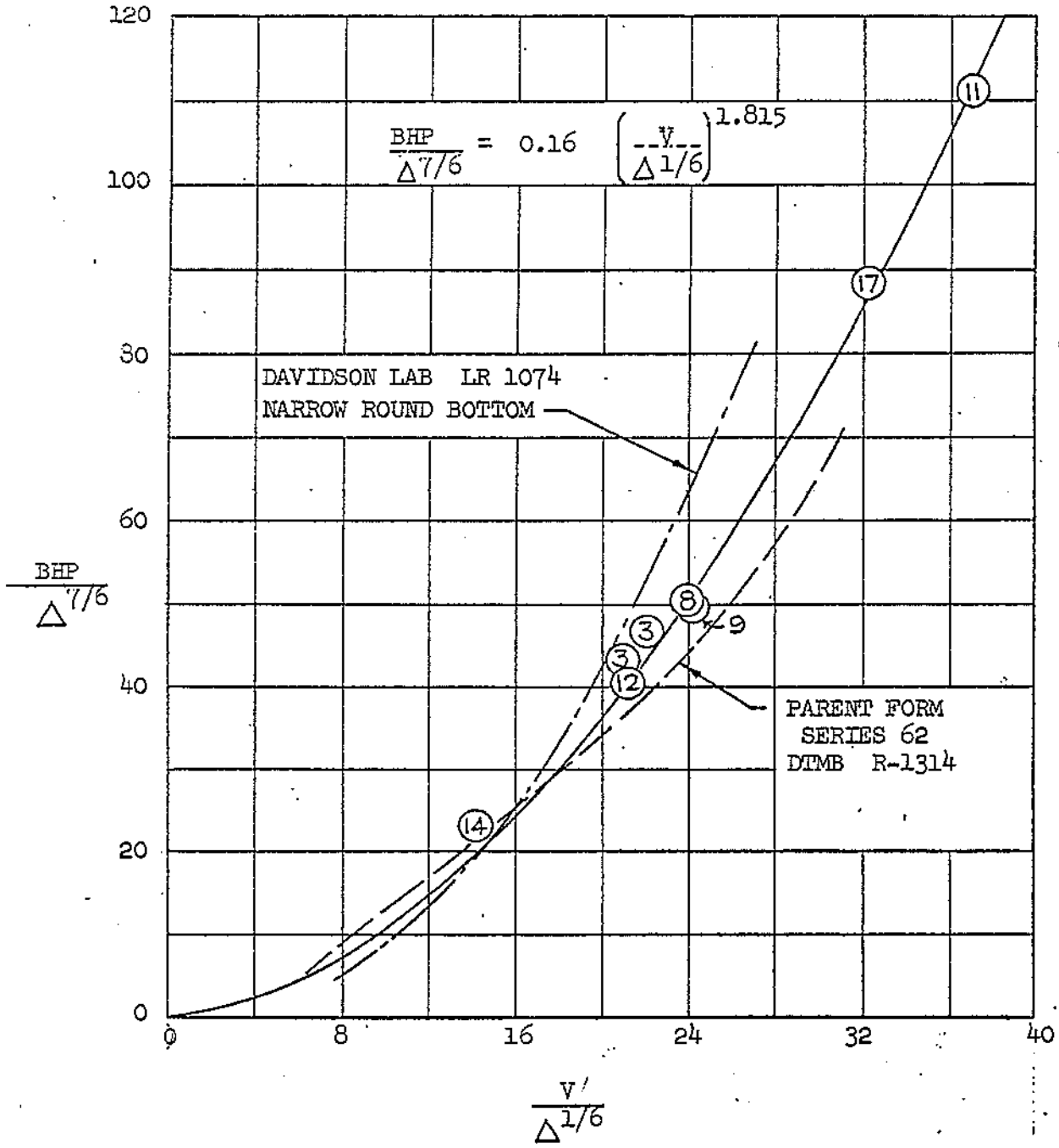

Fig. 3.21: $\frac{BHP}{\Delta^{7/6}}$ versus $\frac{V}{\Delta^{1/6}}$ for several planing hulls.

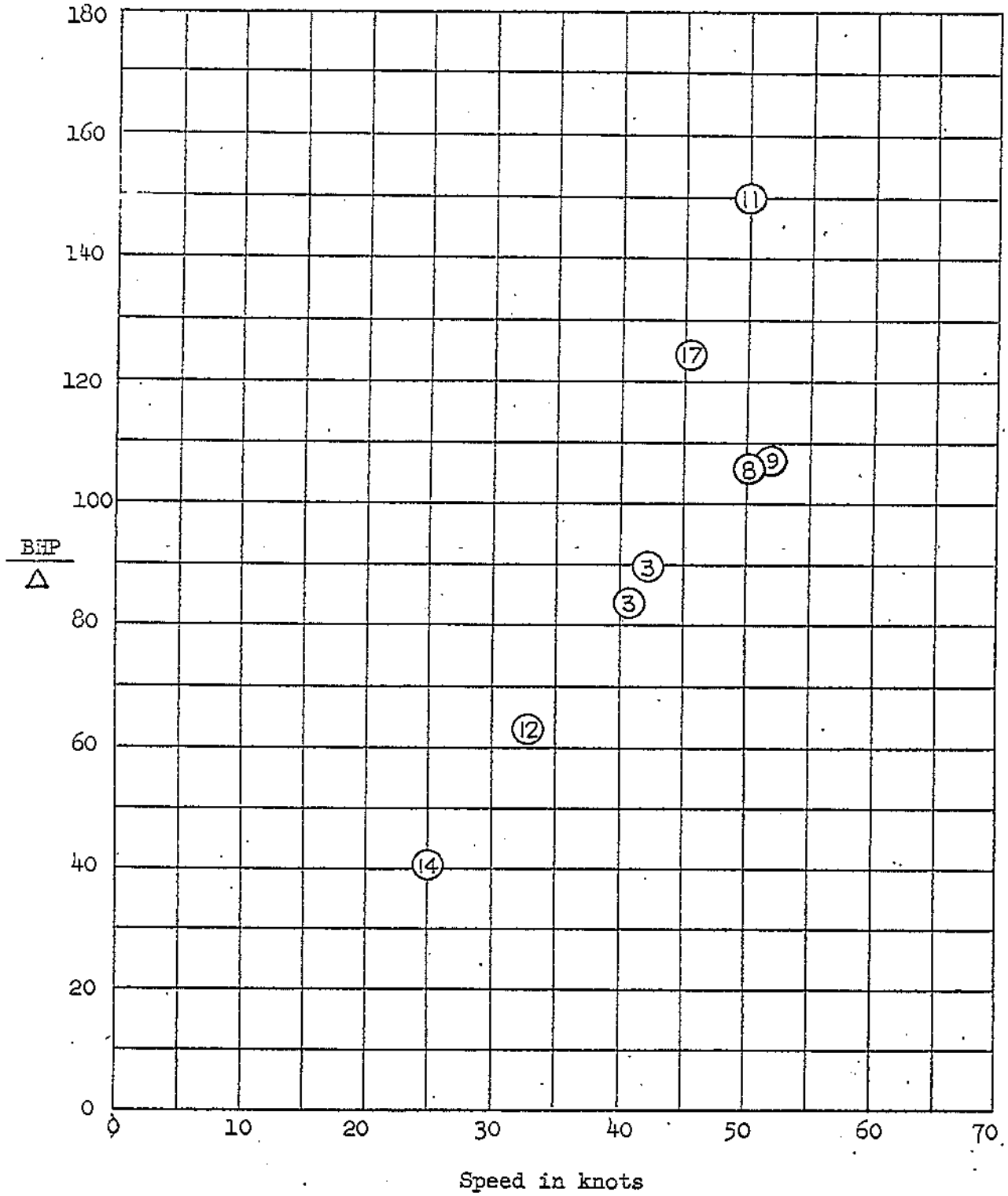

Fig. 3.22: BHP/Δ vs speed in knots for several planing hulls

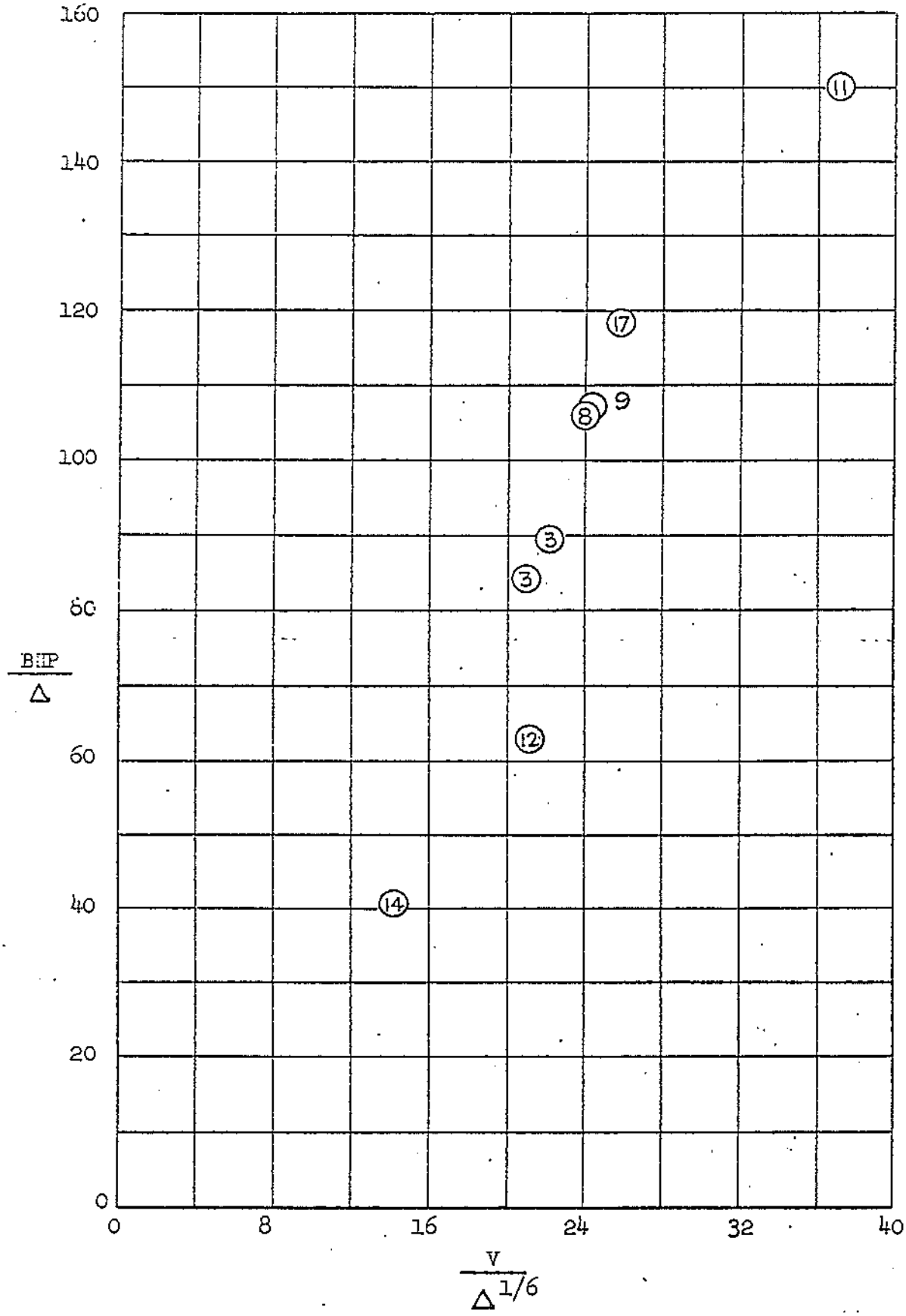

Fig. 3.23: BHP/Δ vs $V/\Delta^{1/6}$ for several planing hulls.

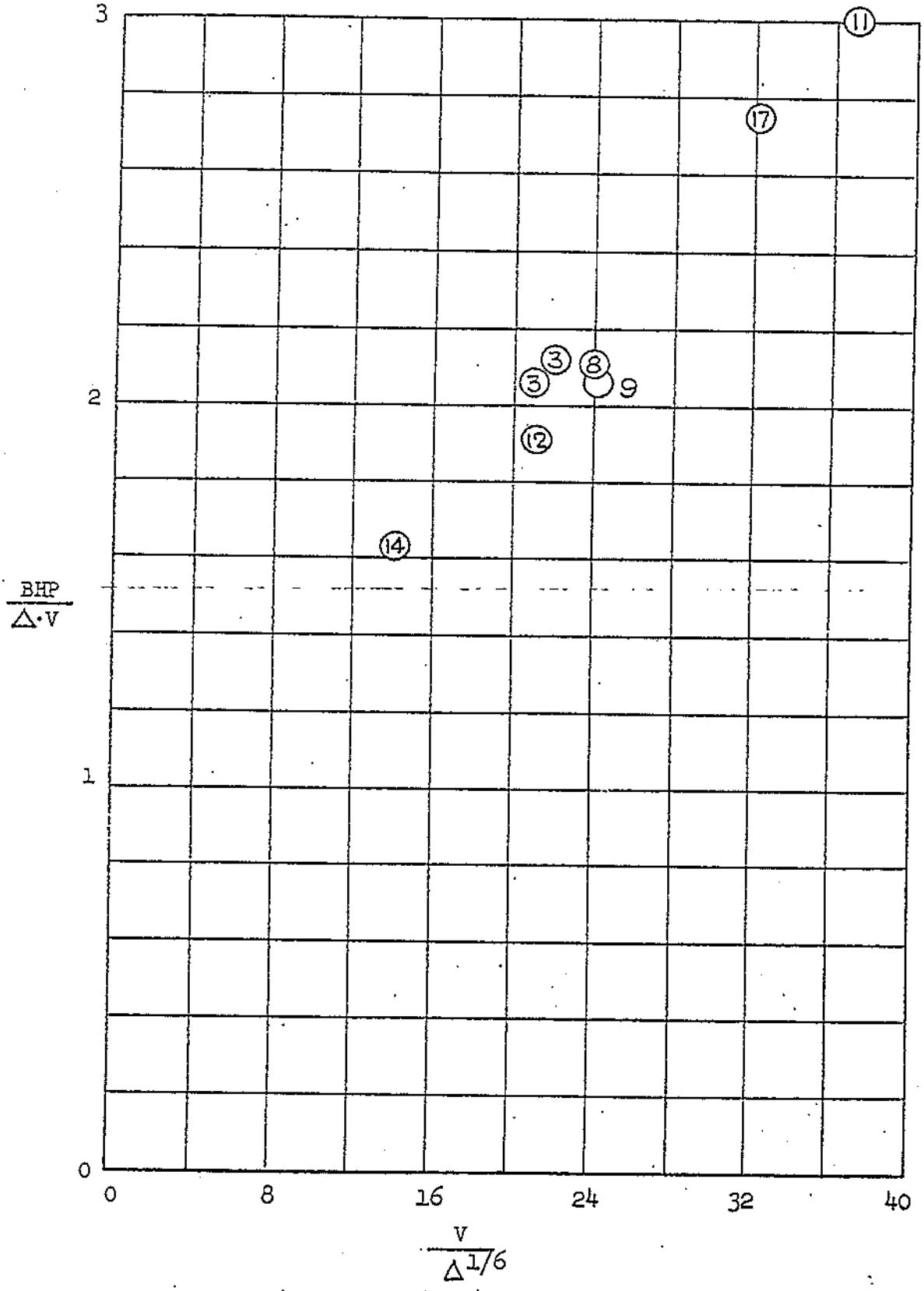

Fig. 3.24: BHP/Δ V vs V/ $\Delta^{1/6}$ for several planing hulls.

several references. Reference 12 presents a lifting surface approach to planing boat design. Reference 17 compares the 16 boats of the SNAME Small Craft Data Sheets (Refences 60 and 61) and 4 of the Series 62 models (Reference 6) with the Dynaplane; Reference 45 presents the results of extensive testing (variations in Δ, l.c.g., step depth, etc.) of a stepped hull with a (adjustable) Plum-stabilizer (named after the inventor John Plum); and Reference 46 investigates the effects of varying the length-beam ratio and the l.c.g. of the Plum-stabilized Dynaplane.

3.3.2 Savitsky

For most planing boat designs there is a need to calculate performance at low speeds and in the hump region. The planing equations developed by Savitsky from the results of many model tests, are valid down to speeds in the semi-planing range. They utilize the seaplane coefficients which is a very satisfactory way of handling planing phenomena.

It was seen, in Figure 3.21, that some powering data became more manageable when normalized on displacement in a dimensionally correct manner. Any dimension of the boat can be used for this purpose. In the case of the planing phenomena the beam has proven to be best. The reasons for, and use of, dimensionless coefficients have been explained by Stoltz in Reference 16, in References 3, 4 and 64, and in Chapter 1 of this volume.

In Reference 1 Savitsky details the derivation of the equations which give the lift, wetted area, and center of pressure of flat and V-bottom surfaces, and presents curves which greatly simplify their use. In addition he outlines the procedure for using the material and gives sample calculations.

A. Savitsky Short Form. Contact with the small boat community reveals that there are a number of well known designers and many unknown ones who feel that this approach is too complicated, and who fall back on the methods discussed in secion 3.2 above. It is hoped that after explaining the inadequacy of the simple powering equations we can now point out that the planing material is not only a powerful design tool but is also easy to apply. Even if the designer does not wish to understand the derivation of the equations he should study the design procedures well enough to see that most of the work has been taken out of them, particularly for the simple case which assumes all the forces to act through the center of gravity.

The forerunners of these equations were published in 1949 in Reference 62. The present equations, which were developed in order to get better agreement with the experimental data at low speeds were presented 1954 in Reference 63. Not only were the new equations more accurate but they were simpler in form enabling a direct

calculation be made rather than a series of iterations.* But the report itself was not handy to use in every day design work. The equations had been plotted in terms of the quantities that were to be calculated, rather than in terms of quantities that could be measured on the design. In Figure 3.25, taken from Reference 63, C_V is known since it can be calculated from the speed and beam, but λ and $C_{L_o}/\tau^{1.1}$ are unknowns. Likewise, in Figure 3.26, from the same reference, C_V is known but both λ and C_p are unknowns. In trying to make this material more tractable the author noted two facts: that both charts contain C_V and λ, and that the equation in Figure 3.26 could be multiplied through by λ to provide an equation for P/b (both of which quantities can be measured on the boat) in terms of C_V and λ. It was then possible to plot on a grid of C_V and λ curves of $C_{L_o}/\tau^{1.1}$ and P/b. This chart is shown in Figure 3.19. Its use has been explained in References 1 and 16, but because of the above mentioned reluctance to make use of it, some sample calculations will be given here.

The design used in this first example was to be a sport fisherman about 36' LOA to be produced by a local builder. Some fairly accurate weight information was available on other stock boats by the same builder so the displacement was accurately determined early in the design stage. But there was some latitude in choosing the chine beam and the l.c.g. The engines and fuel could be shifted forward or aft over a wide range. The deadrise was more or less fixed.

If one were to use the simple powering equations and charts discussed in Section 3.2 the horsepower for a given speed would be already fixed. But Figure 3.19 provides a chance to see how the power and trim will vary with changes in beam and l.c.g. and to choose these values for the design on a rational basis. Therefore, three values of each were chosen which would bracket the widest possible variations, namely b = 8-feet, 10-feet, and 12-feet, and l.c.g. = p = 10-feet, 13-feet, and 18-feet forward of the transom. The EHP and trim were calculated for these 9 combinations at each of 5 speeds from 15 mph to 35 mph. A sample calculation sheet for the 9 conditions at one speed is shown as Table III. It also shows the correction to resistance and trim for a change in displacement form 18,000 to 16,000 pounds, made by the simple method developed in Table I, and

*Reference 71 presents some very recent work which is still more accurate but which unfortunately is very complicated in form and has not yet come into general use. It also requires an iterative process to solve for the equilibrium trim angle.

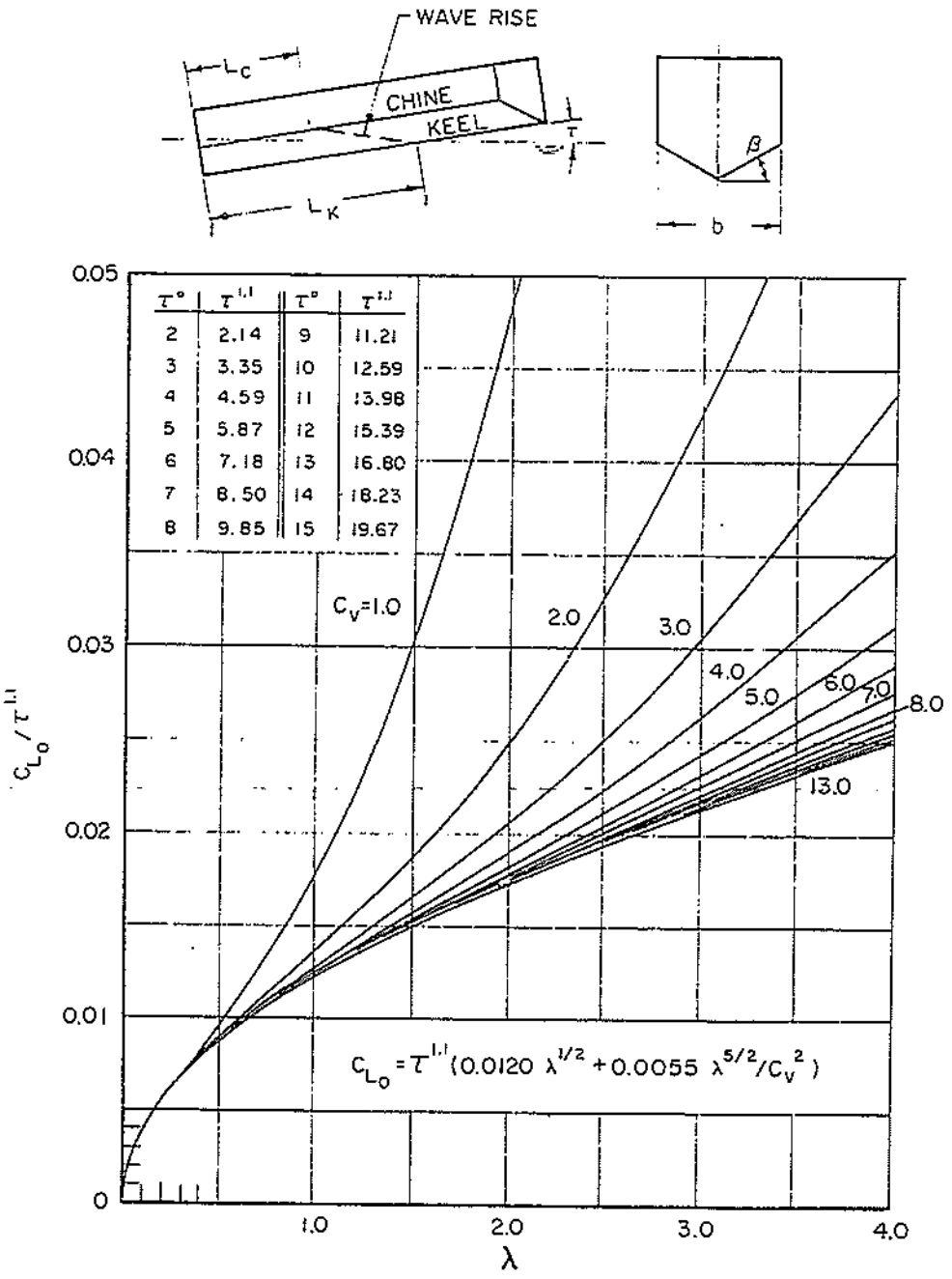

$\tau°$	$\tau^{1.1}$	$\tau°$	$\tau^{1.1}$
2	2.14	9	11.21
3	3.35	10	12.59
4	4.59	11	13.98
5	5.87	12	15.39
6	7.18	13	16.80
7	8.50	14	18.23
8	9.85	15	19.67

Figure 3.25. Lift coefficient of a flat planing surface; $\beta = 0°$.

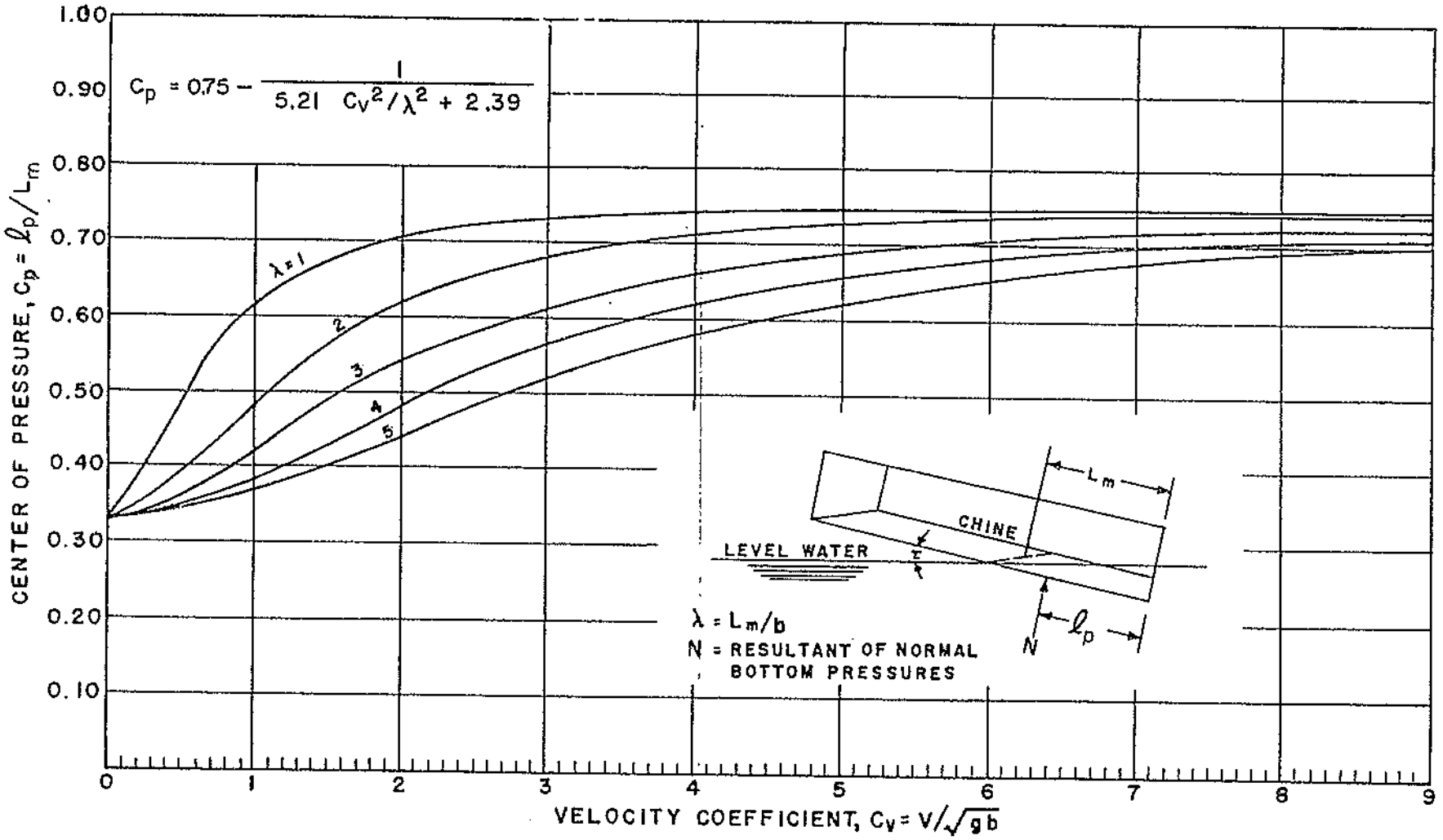

Figure 3.26. Center of Pressure of Planing Surfaces

TABLE III

36' SPORT FISHERMAN
BARE HULL EHP Calc.

$b = 8, 10, 12$; $\beta = 15°$
$p = 10, 13, 16$
$V = 15, 20, 25, 30, 35$ mph

$\Delta = 18,000$ LB
25 MPH = 36.7 FPS ; $V^2 = 1340$

b = BEAM	8' [illegible]			10' [illegible]			12' [illegible]		
p = LCG	10'	13'	16'	10'	13'	16'	10'	13'	16'
p/b =	1.25	1.62	2.00	1.00	1.30	1.60	.83	1.08	1.33
b^2	64	64	64	100	100	100	144	144	144
$C_{L\beta} = \Delta / v^2 b^2$	.21	.21	.21	.134	.134	.134	.093	.093	.093
C_{L_o} = (1)	.252	.252	.252	.180	.180	.180	.122	.122	.122
$C_v = v/\sqrt{gb}$	2.36	2.36	2.36	2.04	2.04	2.04	1.87	1.87	1.87
λ (2)	1.94	2.78	3.84	1.5	2.16	2.94	1.24	1.70	2.31
$C_{L_o}/\tau^{1.1}$ (2)	.022	.032	.050	.0186	.0263	.0345	.016	.0218	.031
$\tau^{1.1}$	11.4	7.9	5.04	9.7	6.7	4.55	7.65	5.60	3.94
τ (1)	9.1°	6.6°	4.35°	7.9°	5.6°	4.0°	6.36°	4.79°	3.48°
$\Delta\lambda$ (1)	.02	.10	.23	.04	.15	.26	.17	.35	.37
$\lambda + \Delta\lambda$	1.96	2.88	4.07	1.54	2.31	3.20	1.41	2.05	2.68
$S = b^2(\lambda + \Delta\lambda)$	125	184	260	154	231	320	203	295	415
$l_m = b\lambda$	15.5	22.2	30.7	15.0	21.6	29.4	14.9	20.4	27.7
$R_e = V l_m / \nu$ $[\times 10^7]$	4.74	6.79	9.40	4.58	6.61	9.00	4.55	6.24	8.47
$C_f + \delta$ = $[\times 10^{-3}]$	2.63	2.52	2.46	2.65	2.53	2.47	2.63	2.56	2.48
$R_f = (C_f + \delta) S v^2$	440	621	857	547	785	1060	715	1010	1380
$R_w = \Delta \tan \tau$	2880	2080	1365	2500	1758	1257	2010	1490	1090
$R_T = R_w + R_f$	3320	2701	2222	3047	2543	2317	2725	2500	2470
$EHP = R_T V / 550$	222	180	148	204	170	155	177	162	160
$L/D = \Delta / R_T$ =	5.4	6.7	8.1	5.5	7.1	7.8	6.6	7.2	7.3
$\Delta = 16,000$ LB	$\left(\frac{16}{18}\right)^{1.91} = .801$; $\left(\frac{16}{18}\right)^{0.91} = .90$								
R_f =	440	621	857	547	785	1060	715	1010	1380
R_w =	2305	1665	1091	2000	1410	1006	1610	1192	874
R_T =	2745	2286	1948	2547	2195	2066	2325	2202	2254
EHP =	183	152	120	170	146	138	155	147	150
$\tau°$ =	8.2°	5.94°	3.91°	7.1°	5.04°	3.60°	5.72°	4.3°	3.13°

(1) - FROM FIG. 32 ; (2) - FROM FIG. 19.

discussed in Section 2.3.5. Auxiliary charts necessary and/or useful for making these calculations (referred to by foot notes on the cauculation sheet, Table III) are shown in Figure 3.32.

In addition to plotting the results as the usual trim and power vs. speed, cross plots of trim and power vs. l.c.g. for several beams were drawn for each of the speeds. Plots for 4 speeds are shown in Figure 3.27 and Figure 3.28. This method seemed best to show the effects of varying these dimensions. Of course, the results can be plotted in any way that suits the particular problem best.

It can be seen that up to 25 mph it is good to keep the center of gravity forward and that in general the wide bottom has least resistance and the narrow bottom the greatest resistance. It can also be seen that there are crossovers (that is, as the c.g. goes ... forward the narrow beam becomes better) and that there are trends toward the optimum dimensions. Here we are not really concerned with optimizing the design but simply to do the best we can within the limitations of the design.

It was desirable not to have the running trim greater than about 6 degrees at any speed. This precluded putting the engine in the stern. The desirability of keeping a moderately fine bow prevented shifting the center of buoyancy much more than 13 feet forward, without lengthening the boat. For the narrow range of l.c.g. remaining, it is apparent that the narrowest beam is out of the question because it produces an increase in trim and EHP over the entire speed range. Except at 25 mph, 10 feet is just about the best beam. It was thought that most boats built to this design would be 30-milers and probably cruise at about 25 mph. There was then a conflict between widening the beam for cruising economy or narrowing it for better top speed. This was resolved by the additional consideration that most of the builder's customers are fishermen who regularly make long runs in the ocean. It was known, qualitatively, that increased beam would produce a larger rough water resistance increment which would at least partially offset the reduction in hull resistance. Also the wider boat would pound more in rough water. In addition to these considerations, the wider beam loses its advantage even in smooth water at the lighter displacement as shown by the dotted lines on the curves for 25 mph. Therefore a decision was made to keep the chine beam as near 10 feet as practicable. After that it was a matter of checking the requirements of buoyancy, stability and accomodations.

In other design problems there might be little interest in varying the beam (for instance) but it might be important to study the effects of large variations in displacemnt, or perhaps deadrise.

Another method of plotting boat performance for a wide range of parameters is shown in Figures 3.29, 3.30, and 3.31. It is interesting to note that at low speeds boat weight has a predominant influence, whereas at high speeds the weight makes less difference and beam has the greater influence.

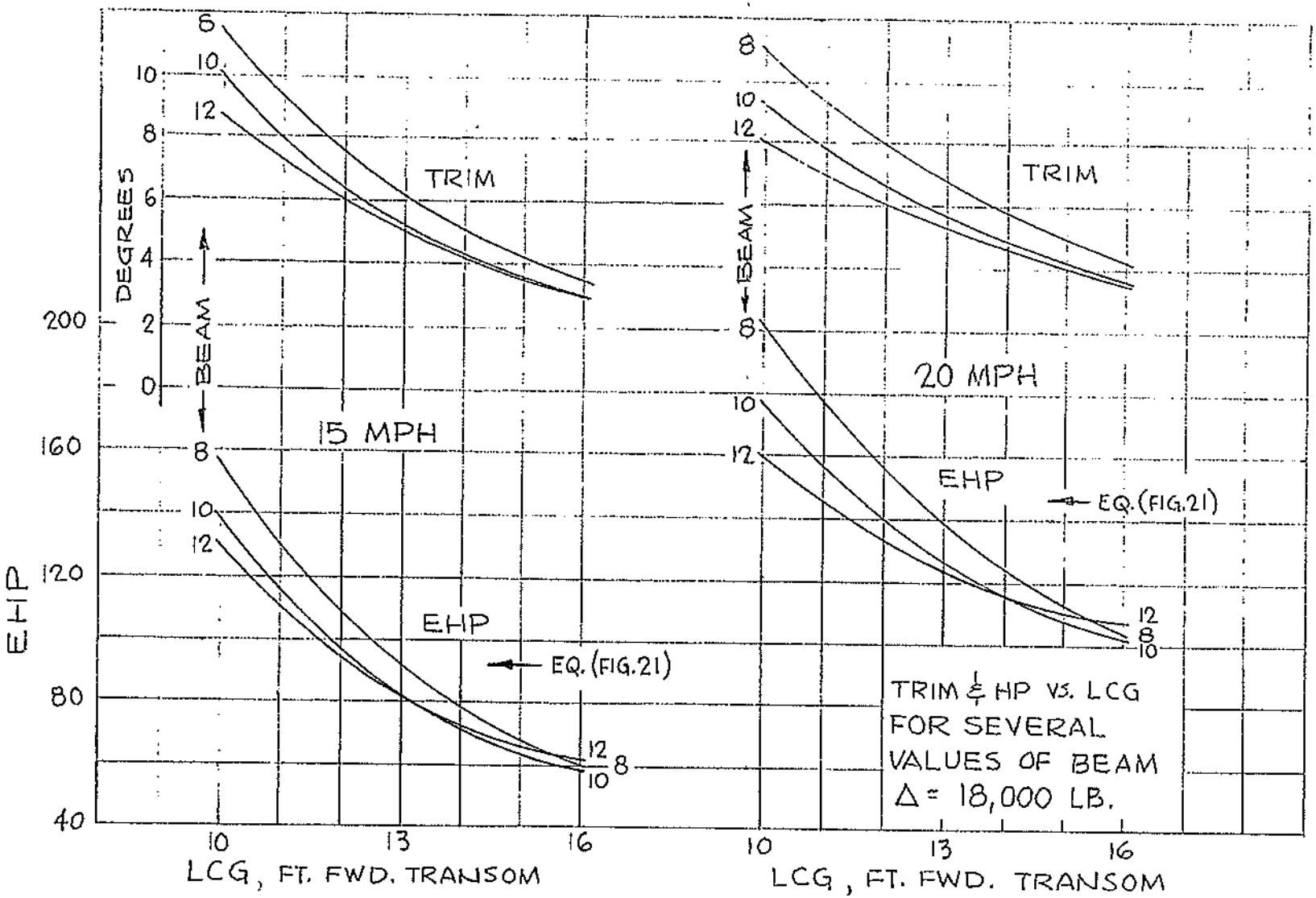

Figure 3.27. Trim and EHP vs LCG position for several beams, Δ = 18,000 lbs. and speeds of 15 and 20 MPH.

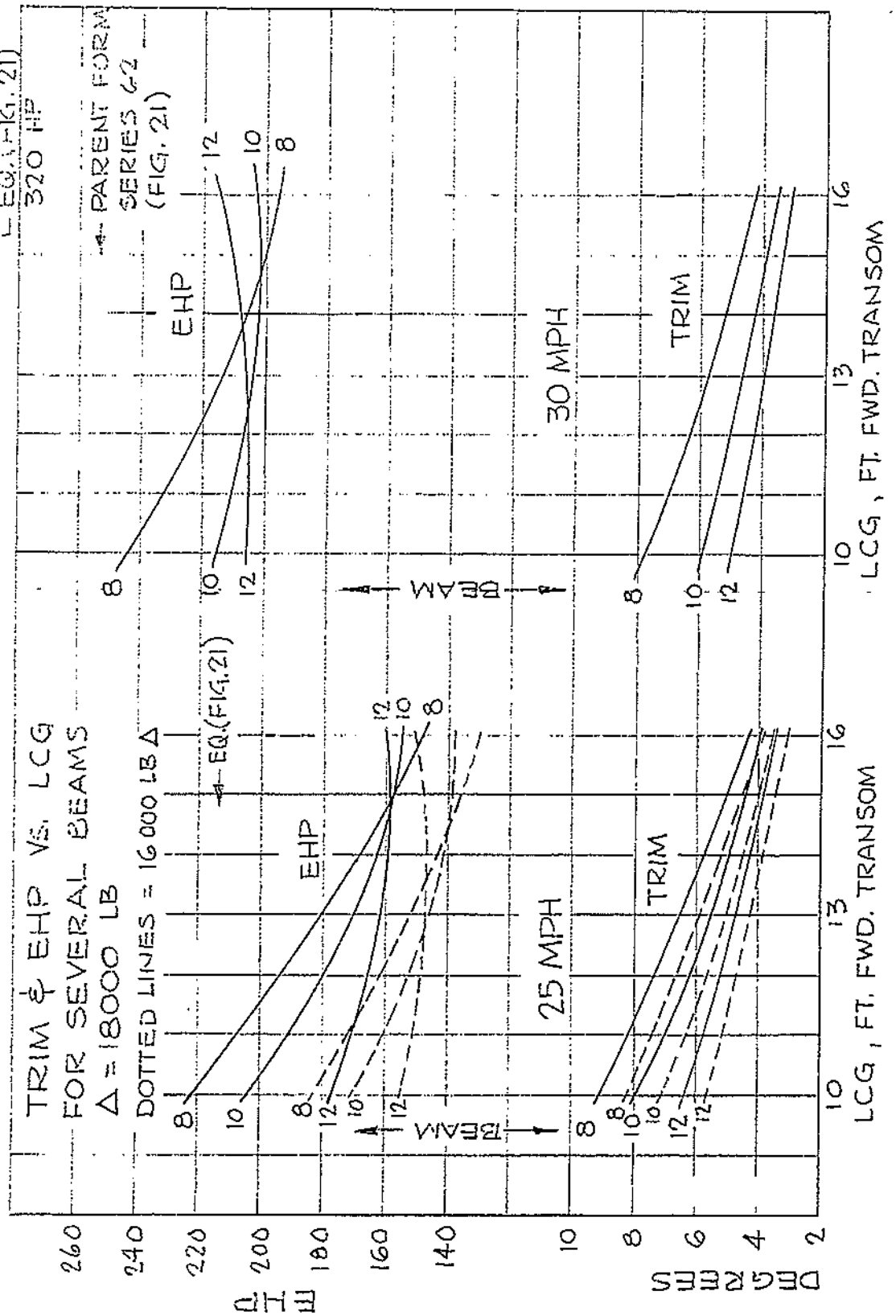

Figure 3.28. Trim and EHP vs LCG position for several beams, Δ = 16,000 lbs. for a speed of 25 MPH, and Δ = 18,000 lbs. for speeds of 25 and 30 MPH.

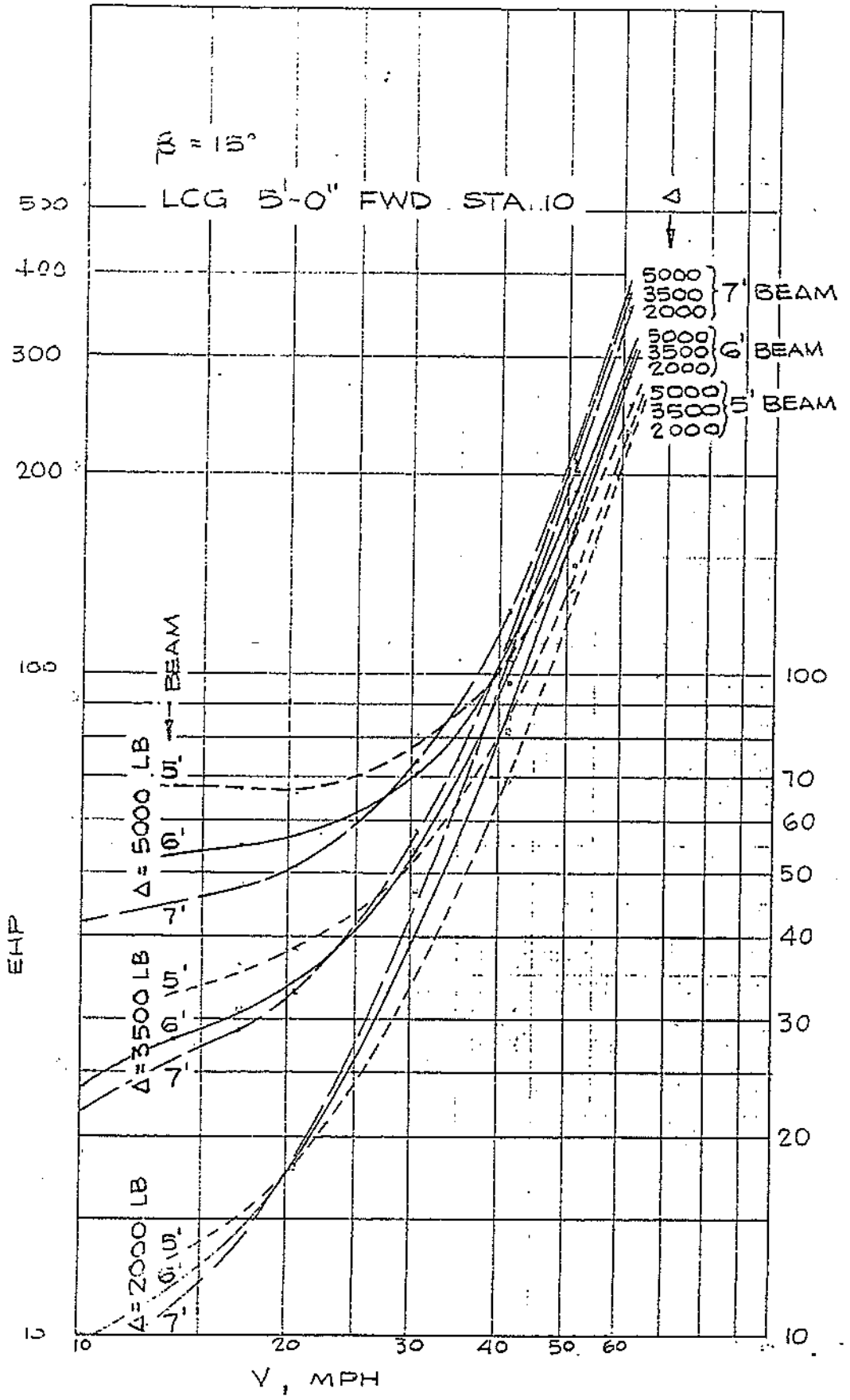

Figure 3.29. EHP vs speed in MPH for τ = 15°, several beams and displacements, and with LCG located 5 feet forward of station 10.

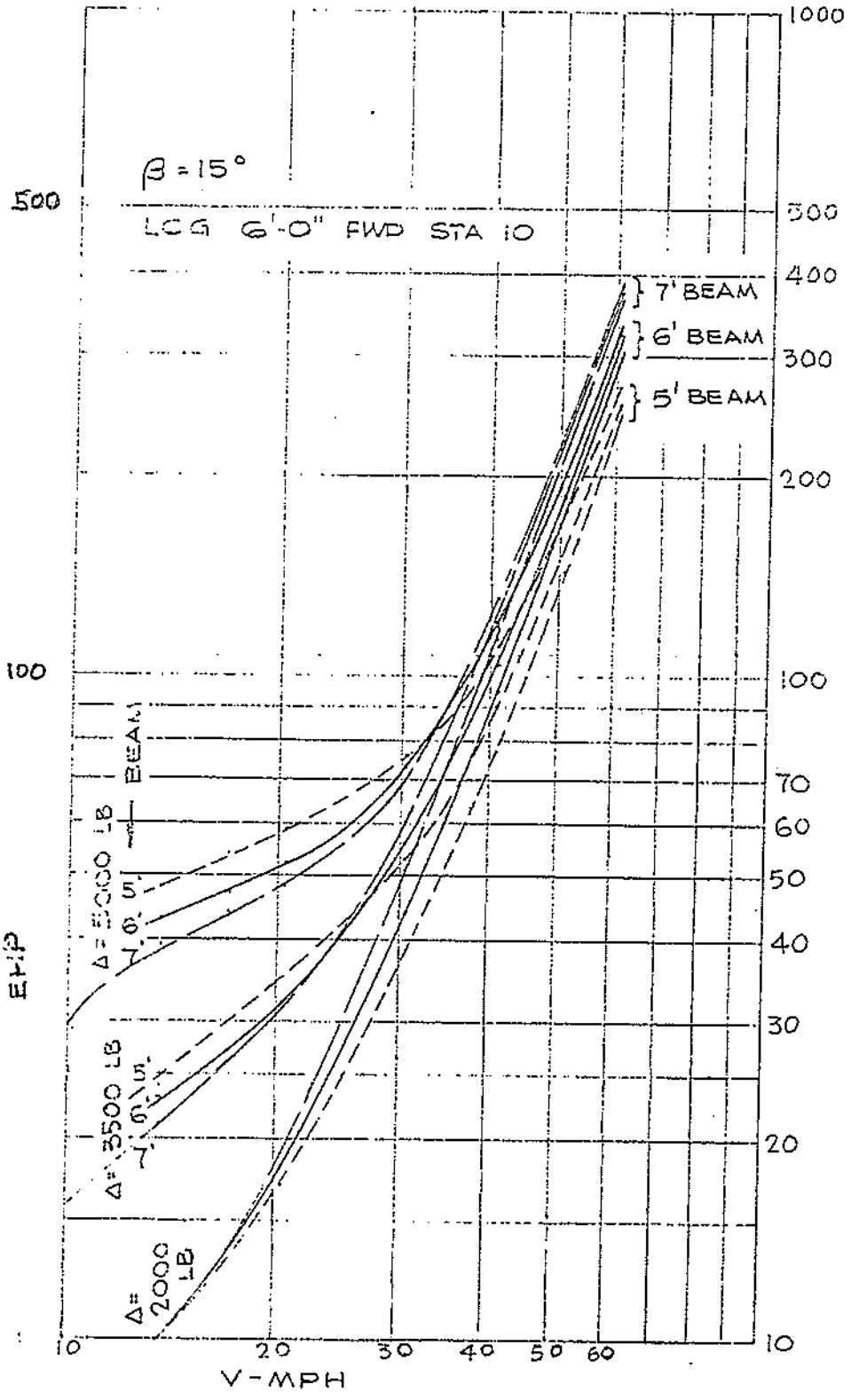

Figure 3.30. EHP vs speed in MPH for β = 15°, several beams and displacements, and with LCG located 6 feet forward of station 10.

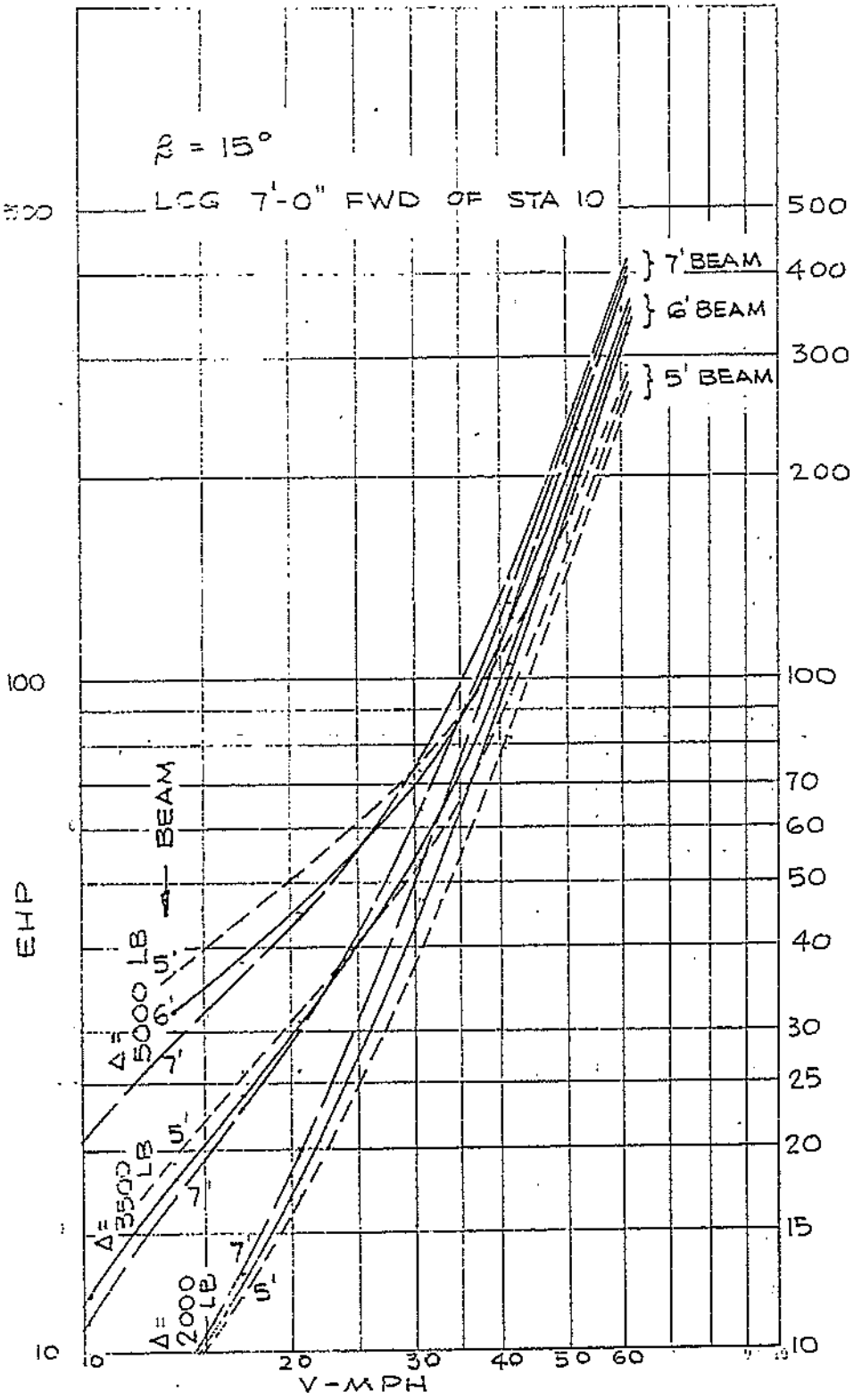

Figure 3.31. EHP vs. speed in MPH for τ = 15°, several beams and displacements, and with LCG located 7 feet forward of station 10.

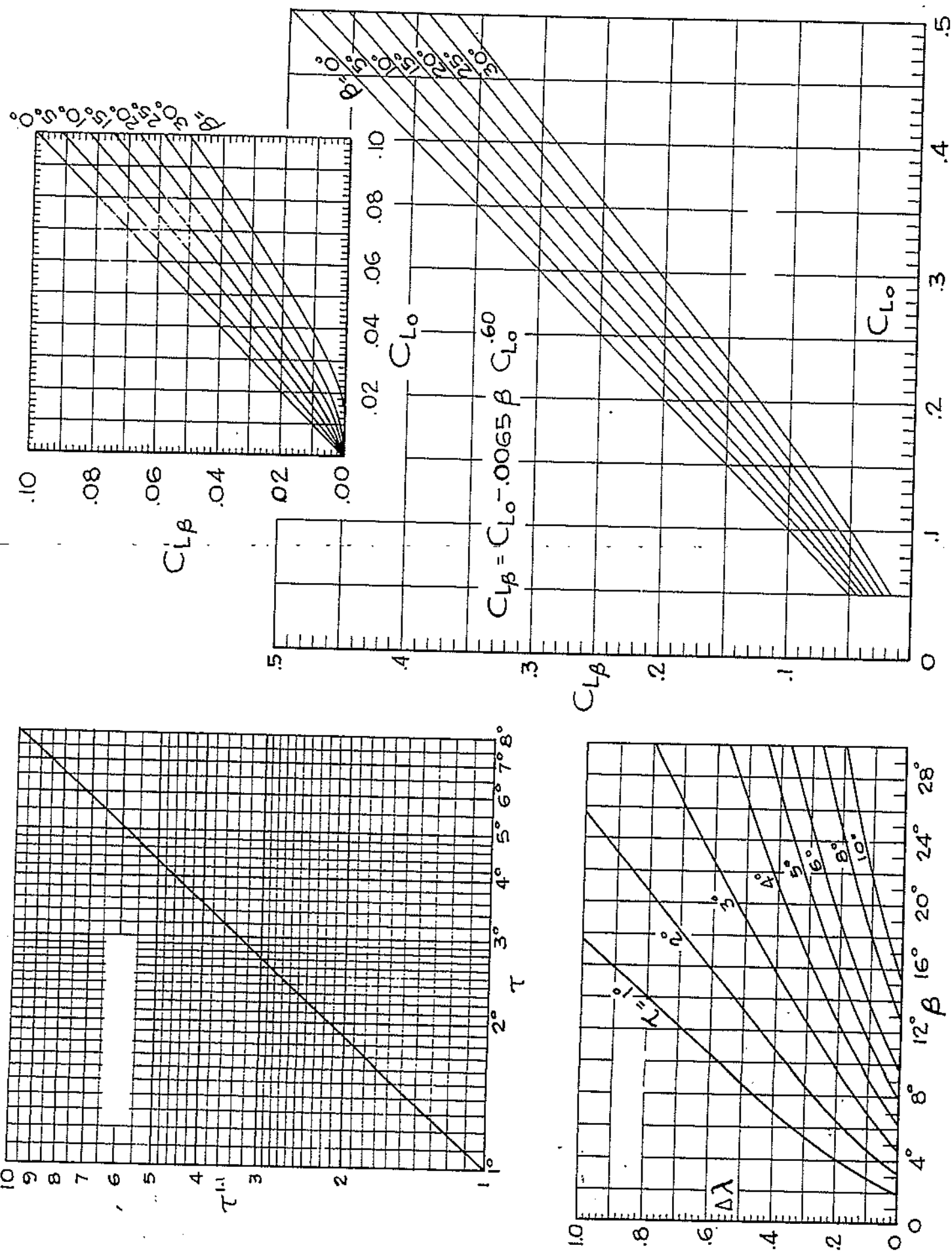

Figure 3.32. Various graphs for use with planing prism data

B. Savitsky Long Form. This is the basic method of Reference 1, which does not make the simplifying assumptions of the "Short Form". As noted above, it accounts for the effects of trimming moments due to the thrust line and the frictional drag. If the calculations are to be made by hand the method is too laborious. But with the use of a computer program it is an inexpensive and easy calculation to make.

It is not necessary to know anything about computers or programming to make use of this service. There are a number of men who are in a position to do computer work for the designer. The designer can send in one page of input data and get back dozens or hundreds of pages of output data. The computer service can handle all data preparation, key punching, etc. Figure 3.33, is a sample form that might be filled out. Actually no form is necessary. The information can be phoned in. Referring to Figure 3.33, water density, kinematic viscosity, and roughness allowance will almost always be constant for all conditions. Usually vertical center of gravity, shaft angle, depth of skeg, rudder clearance, and skeg drag lever arm, are also constant. The thrust vector lever arm will vary only with l.c.g. The designer can specify as many values of any of the factors as he chooses. For example, if 3 seights, 3 beams, 5 l.c.g.'s, and 2 deadrise angles are to be investigated at 5 speeds, the total number of cases will be 3x3x3x2x5 = 270.

The naval architect who handles the author's computer work has revised the basic NAVSEC program to make the output easier to use. A sample output sheet is shown in Figure 3.34. It will be noted that the input for each case is shown on the output sheet; this is helpful for the convenient use of the output sheets. The output data are given in great detail: the trim angle, total drag and all components of drag, EHP, wetted area, wettel keel length, wetted chine length, draft at center of transom, and the porpoising limit parameter. For those cases where the wetted chine length becomes negative the program has been corrected to handle it as a chines dry case.

C. Flap Effect. As mentioned before, Reference 71 gives a complete calculation method for the lift and center of pressure of planing surfaces including the effect of transom flaps. The method is too laborious for practical hand calculations, even though six of the functions have been pre-calculated and tabulated in the report. However, the increment of lift and trimming moment due to the flaps is a separate and simple calculation which can, for the present, be applied to the basic lift calculations done according to Savitsky's method.

In cases where the trim of the unflapped model is too high the designer may wish to determine the required size and deflection of flaps to produce a certain reduction in trim. At present his can only be done in Brown's method by trial and error. One possible procedure is as follows:

1. Calculate the lift and center of pressure of the

Figure 3.33

COMPUTER PROGRAM

INPUT FORM

PRISMATIC PLANING HULL DESIGN CALCULATIONS

DATE

TITLE

WATER DENSITY (lb-sec^2/ft^4)

KINEMATIC VISCOSITY (ft^2/sec)

ROUGHNESS ALLOWANCE

HULL WEIGHT (lbs)

LONGITUDINAL C.G. (ft)

VERTICAL C.G. (ft)

AVERAGE BEAM (ft)

DEADRISE ANGLE (deg)

HULL VELOCITY (knots)

THRUST VECTOR LEVER ARM (ft)

SHAFT ANGLE (deg)

TRIM ANGLE (deg)

DEPTH OF SKEG (ft)

RUDDER CLEARANCE (ft)

SKEG DRAG LEVER ARM (ft)

HYDRODYNAMIC DESIGN OF PRISMATIC PLANING HULLS APRIL 4, 1969
COMPUTER PROGRAM ADAPTED FROM NAVSHIPS 0900-006-5310

ARTHUR'S BOAT WORKS INC. - DESIGN NO. 124 BY JOSEPH KOELBEL

CASE NUMBER 188

I N P U T D A T A

DENSITY OF WATER	1.93840 LB.(SEC.**2)/FT.**4
KINEMATIC VISCOSITY	0.122850E-04 FT.**2/SEC.
ROUGHNESS ALLOWANCE	0.00040
HULL WEIGHT	10000.0 POUNDS
LONGITUDINAL C. G.	12.000 FEET FROM TRANSOM
VERTICAL C. G.	2.500 FEET FROM KEEL
AVERAGE BEAM	10.000 FEET
DEADRISE ANGLE	15.000 DEGREES
HULL VELOCITY	30.000 KNOTS
THRUST VECTOR LEVER ARM	2.750 FEET
SHAFT ANGLE	0. DEGREES
SKEG DEPTH	0. FEET
RUDDER CLEARANCE	0. FEET FROM TRANSOM
SKEG DRAG LEVER ARM	0. FEET

O U T P U T D A T A

SPEED COEFFICIENT	2.824 (GREATER THAN 1)
LIFT COEFFICIENT (DEADRISE SURFACE)	0.040
HULL FRICT. DRAG LEVER ARM ABT C.G.	1.830 FEET
TRIM MOMENT ABOUT CENTER OF GRAVITY	0.202801E 03 FOOT POUNDS
TRIM ANGLE (TAU)	2.859 DEGREES
TOTAL HULL DRAG	1892.636 POUNDS
FRICTIONAL DRAG	1105.614 POUNDS
SPRAY DRAG	287.553 POUNDS
SKEG DRAG	0. POUNDS
PRESSURE DRAG	499.470 POUNDS
EFFECTIVE HORSEPOWER	174.353 H. P.
WETTED AREA, SOLID	175.500 FEET**2
WETTED KEEL LENGTH	25.490 FEET
WETTED CHINE LENGTH	8.414 FEET
DRAFT, AFT AT CENTER OF TRANSOM	1.272 FEET
MEAN WETTED LENGTH TO BEAM RATIO	1.695 (LESS THAN 4)
PORPOISING LIMIT PARAMETER	0.142

PROGRAM PPH-1 ALFRED I. RAFF, NAVAL ARCHITECT

Figure 3.34. Typical prismatic planing hull computer program output.

unflapped model using the same wetted length but the new, lower trim angle.

2. Find a flap size and deflection which will have a lift increment equal to the loss in lift due to the reduction in trim.

3. Check the resulting center of pressure location.

4. Try a new wetted length (using the same desired trim angle), longer if the c.p. was too far aft, shorter if the c.p. was too far forward. With the longer wetted length the hull lift will be greater, requiring less lift from the flap and therefore the c.p. will move forward. The opposite will occur with a shorter wetted length.

5. Continue until the equilibrium wetted length is found. If the increments of wetted length and flap size and/or deflection are chosen systematically the results of a few trials can be plotted and the equilibrium conditions read off.

In due course this whole procedure will be computerized and will then be entirely practical for design purposes. In the meantime, there is a simple approximation which will be good enough for most purposes. It is essentially a simplification of the first two steps of the above procedure with an adjustment to prevent the usual overestimation of the required flap size or angle. This will be given in detail during the lecture, and a sample calculation will be passed out.

The other method of flap calculation which has been mentioned is that of Angeli, Reference 72. This method may be somewhat limited in application because the flap effectiveness was evaluated on specific models of warped bottom boats. But the calculation method is certainly much simpler and easier to use. It is based on the use of a longitudinal stability index for the boat in the planing condition. From this, and the boat's dimensions, the required trimming moment is calculated. From this and the assumed point of application of flap lift the magnitude of the flap lift is calculated. Finally, from this and the assumed flap dimensions the flap deflection is calculated. It is hoped that this work, or some development of it will be made available in the near future.

Both of these methods are, in the opinion of the writer, still in the formative stages, but the approximation they make possible is an important step ahead in planing boat performance prediction.

3.4 MODEL TESTS

Prediction of performance from model tests is treated in References 3, 4, 5, 6, 7, 30, 64 and in Chapter 1. Particular

attention is drawn to the statements on pages 128 and 129 of Reference 5 regarding prediction of planing boat performance from tests of smal models. Many of the references cited in this chapter and in Chapter 1 are model test reports from which the designer can select those of comparable characteristics (the appropriate size-weight paramenter, length-beam ratio, section shape, etc.). Tests of sixteen of the models reported in these references have been grouped together and presented in a uniform manner in Reference 60, the SNAME Small Craft Data Sheets, which are available singly or in a set. Their use is explained in Reference 61, which also gives the reasons for choosing the system of coefficients used.

When making a performance prediction from tests of a model geometrically similar to the full size boat there is no particular problem. But if the resistance of a new design is to be predicted from test results of a model of different design, some precautions must be observed. In general, they stem from the need to have the features which affect the performance prediction the same for both the full size boat and the model. A couple of examples will help illustrate the point.

If the resistance of a boat is to be predicted from Series 63, it must be noted that the total resistance coefficient, C_T, is based on the wetted area and the wetted area is that of the bare hull. The models had no appendages. Since turbulence was stimulated on the models, the Schoenherr friction coefficient, C_F, for fully turbulent flow corresponding to the model Reynolds number can be subtracted from the total resistance coefficient to obtain the residual resistance coefficient, C_R, for the model. C_R is the same for the full size boat, but only if it is based on a comparable wetted area. The new design may have a skeg or S-frames or other features which influence the wetted area but which would not influence the wave-making. In fact, the basic assumption of this type of prediction is that the full size boat will have the same wave-making characteristics as the model. Therefore, in computing the residual resistance of the full size boat a fictitious wetted area equal to λ^2 times the model wetted area must be used. Here λ is the ratio of ship size to model size, for example (LWL_{ship}/LWL_{model}). The full size frictional resistance can be calculated from actual wetted area of the new design. Although there are other ways of handling the arithmetic, such as correcting the C_{R}ship for the difference in wetted area, the method outlined here is a satisfactory way to carry out the work and it provides a physical explanation which should illustrate the principle.

If a resistance prediction is to be made from Series 62 additional precautions have to be taken. The DTMB notation, used in the Series 62 report, as well as in all other planing model data published by the model basin is as follows:

A_p - projected planing bottom area, exclusing area of external spray strips, ft.^{2}

B_p - beam over chines, excluding external spray strips, ft.

I_p - length of planing bottom, ft.

∇ - volume of displacement, ft.^{3}

LCG - longitudinal center of gravity location

The loading of the model is expressed as the area coefficient $A_p/\nabla^{2/3}$.

If the new design is geometrically similar to the Series 62 model, there is no problem and the coefficients are satisfactory. But the hull form characteristics are based on the plan form of the chine, that is, parts of the hull which are out of the water, particularly at high speed, and have no influence on smooth water. planing behavior. For example, in a given design the bow overhang and flare, forward of amidships, could arbitrarily be filled out from the narrow slab-sided shape of the early plywood runabouts to the full flaring form of some recent fiberglass models without changing the chine beam aft, the weight or the l.c.g. The actual smooth water planing performance of the boat would not be affected but, because the chine area would be increased and the centroid of the chine area moved forward, both the loading and l.c.g. coefficients would be changed in the DTMB notation. Consequently, two different predictions would be made for what is essentially the same boat. Therefore, to make an accurate prediction certain characteristics must be the same for model and ship; the ratio LCG/b, $C_\Delta = \Delta/wb^3$, and $C_V = V/(gb)^{\frac{1}{2}}$. Perhaps the easiest way to accomplish this is to construct a fictitious Series 62 planform which has approximately the same length as the chine length of the new design, with some adjustments as shown in Figure 3.35, and the same average beam in the afterbody (at about sta. 7 or 8), and then calculate its area and spot in the position of its centroid. (The drawing does not actually have to be made because of the known relationships between I_p, B_p, A_p, and the centroid, but its easier to visualize this way.) Now the actual position of the new design's l.c.g. can be located relative to the centroid of the fictitious area A and the area coefficient can be calculated based on the new design's displacement and the fictitious area A_p. Resistance values for the new design can now be determined as if it were geometrically similar to the series design, but still requires a three way interpolation for length-beam ratio, area (or loading) coefficient, and l.c.g. position. For the higher speeds Reference 6 gives a simple prediction chart using the seaplane coefficients which makes the calculation easy. But for the lower speeds the model data must be used.

TABLE IV

DESIGN EXAMPLE FROM SERIES 62, REF. 25

CONSTANTS: Δ= 15,000 lb; ∇ = 234 ft^3; $\nabla^{2/3}$ = 38 ft^2; $\nabla^{1/3}$ = 6.15 ft

V = 65 fps; V^2= 4230; $F_\nabla = V/\sqrt{g\nabla^{1/3}} = 4.71$

LCG = 8% aft of centroid of A_p

		$A_p/\nabla^{2/3}$ = 7.0	$A_p/\nabla^{2/3}$ = 6.5	$A_p/\nabla^{2/3}$ = 5.5
L_p/B_{px} = 3.06	A_p , B_{pa}	266 ft^2 , 9.3 ft		209 8.25
	L_p , LCG	28.4 ft , 11.6 ft		25.2 10.3
	P/b , C_{Lb}	1.25 , .041		1.25 .052
	C_Δ , C_v	.292 3.74		.417 3.96
L_p/B_{px} = 3.5	A_p , B_{pa}	266 8.75	247 8.4	209 7.7
	L_p , LCG	30.7 12.5	29.4 12.0	27.0 11.0
	P/b , C_{Lb}	1.43 .046	1.43 .050	1.43 .060
	C_Δ , C_v	.350 3.86	.395 3.94	.512 4.11
L_p/B_{px} = 4.09	A_p , B_{pa}	266 8.05		209 7.14
	L_p , LCG	32.9 13.4		29.2 11.9
	P/b , C_{Lb}	1.67 .055		1.67 .070
	C_Δ , C_v	.450 4.02		.645 4.26

NOTE: $C_{Lb} = \Delta / 1/2\ \rho\ v^2 b^2 = 2\ C_\Delta / C_v^2$

LCG = p , ft. fwd. of transom

B_{pa} = b , ft.

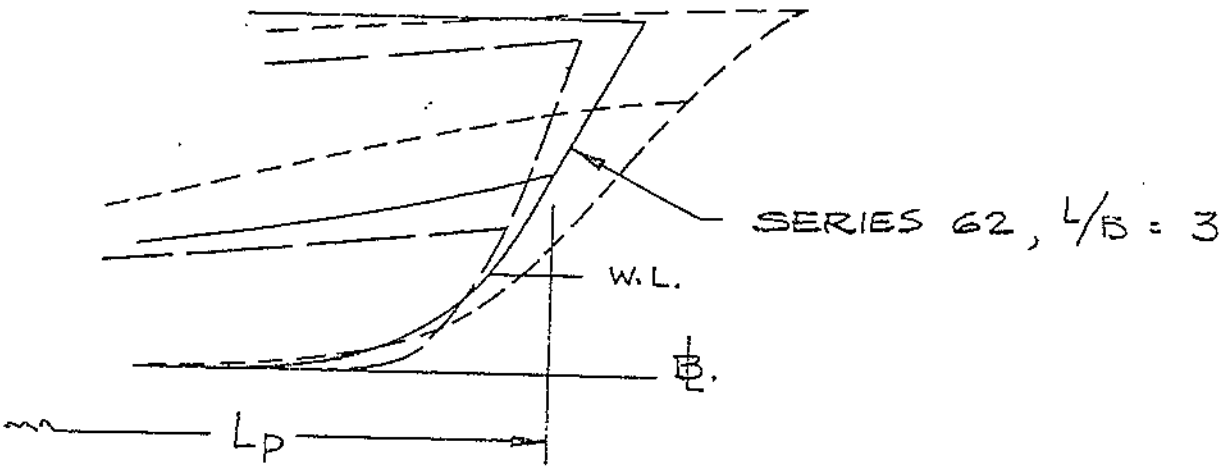

Illustration of how the bow of a design might vary without any significant effect on the smooth water planing characteristics. The forward end of L_p varies with chine height and bow overhang. A fictitious L_p must be chosen to define a Series 62 hull which will have an underwater form as much like the new design as possible, particularly in the afterbody, without regard to the dissimilarity in the chine planform. The average beam B_{PA} of the Series 62 hull should be taken equal to the average chine beam in the afterbody of the new design. $A_p = L_p \times B_{PA}$. For interpolation between length-beam ratios, use L_p/B_{PX} to be consistent with the models.

Figure 3.35: Various modifications of Series 62 bow.

It may be noted when making the interpolations for Series 62, that the models whose length-beam ratios and area coefficients bracket the new design will not have the same LCG/b, C_{Δ}, and Cv, as the new design. This is illustrated in Table IV. The interpolations, however, will give a resistance curve for a model with the correct coefficients. The values of resistance of the other models, if cross plotted, will show the trends with variation in these parameters. When making a performance prediction from tests of a single model, such as one of the SNAME Data Sheets, Reference 60, all the above recommendations must be observed. All the differences between the new design and the model must be considered and the necessary corrections and adjustments made. For any predictions from model tests it is necessary to be certain about how trim is defined and measured. For example, trim at any speed may be either the change from static trim or the angle of incidence of the mean buttock; in either of these cases the initial trim (at zero speed) of the mean buttock relative to the still water surface should be known to help relate the model to the full scale boat.

3.5 OTHER CALCULATIONS

The calculations referred to in Sections 3.1 through 3.4 pertain to the resistance of the hull only. Some specific models may have one or more appendages, and occasionally tests are for a fully appended model. It is necessary to calculate all the other components of resistance as well as that of the bare hull. These items are discussed in Sections 2.2.3 through 2.2.6.

3.5.1 Appendage Resistance

A. Keels and Skegs

Appendages of low aspect ratio, and which lie substantially in the flow lines of the boat in steady motion are considered to ha have only frictional resistance and their area is simply added to the hull wetted area.

B. Rudders and Struts

Appendages such as rudders and struts have both frictional resistance and form resistance. The following equation, adapted from Reference 9, for the usual range of t/c and type of section (not too blunt a leading edge and maximum t at 0.4 to 0.5c) can be used for struts and rudders:

$$D_{AP} = C_D \frac{\rho}{2} A_{PF} v^2$$

Where: D_{AP} - appendage drag

C_D - appendage drag coefficient based on planform area $= 2 (C_f + .0008) [(1.2 t/c) + 1]$

C_F - Schoenherr friction coefficient based on total wetted area of appendages, and Rn based on chord of appendage

$.0008$ - roughness allowance for short bodies
t/c - thickness to chord ratio of appendage
$[(1.2t/c)+1]$ - separation drag factor
A_{PF} - planform area, ft^2
v - speed, fps

Additional appendage drag information will be found in the references cited in Section 2.2.3. Reference 9 is especially useful.

C. Shafts

For exposed circular shafts inclined to the flow the drag is calculated on the basis of the drag coefficient for a cylinder and the component of velocity normal to the shaft. The effect of rotation is ginored. The formulas are:

$$D_S = C_D\, l d v^2 \sin^3 \theta$$
$$L_S = C_D\, l d v^2 \sin^2 \theta \cos \theta$$

Where:
D_S = drag of shaft in direction of flow
L_S = lift of shaft normal to flow
C_D = drag coefficient of circular cylinder = 1.2
l = exposed length of shaft, ft.
d = diameter of shaft, ft.
v = free stream velocity, ft./sec.
θ = angle of shaft inclination to flow

D. Boundary Layer

For those appendages close to the hull, such as scoops and strut palms, the effect of the boundary layer may be considered. The thickness of the boundary layer is given by the following formula (among others):

For $5 \times 10^4 < Re < 10^6$

$$\frac{\delta}{x} = 0.37\, Re^{-1/5}$$

For $10^6 < Re < 5 \times 10^8$

$$\frac{\delta}{x} = 0.22\, Re^{-1/6}$$

Where:
δ = thickness of turbulent boundary layer
x = distance from leading edge
Re = Reynolds Number vx/ν

References 3 and 4 give information on the thickness and velocity profiles of turbulent boundary layers. Reference 4 suggests that the average velocity can be taken as 0.75 times the free stream velocity.

There is an additional reduction in velocity under a planing boat due to the increased pressure under the hull. This is treated in References 1, 54 and 71. However, the magnitude of this reduction is

small and its extent from the surface is not well established. It is conservative to ignore this effect in planing boats. The phenomenon is the same as the change in local velocity around a displacement ship due to the pressure changes. This type of flow is known as potential flow and is treated in References 3 and 64.

E. Inlet Openings

The whole subject of inlet and outlet openings is treated at length in Reference 9. This will apply to cooling water inlets for the engines, outlets for underwater exhausts, air intakes wherever they are a definite projection on an otherwise streamlined structure.

It should be noted that an inlet can be flush with the skin and still have drag because of the energy required to accelerate the air or water up to the speed of the boat, assuming the fluid makes a 90° turn as it enters the boat, i.e. the intake pipe is normal to the skin.

To provide a guide to the importance of calculating cooling water inlet resistance an approximate analysis was made which reveals that the resistance amounts to one percent of the total resistance at about 40 knots. The cooling water requirements and drag coefficient are based on data collected by Mr. John C. Angeli. The flow rate used is a low average for diesel engines. Manufacturers' recommendations vary from about 3×10^{-4} to about 8×10^{-4} $ft^3/sec/BHP$. The acual rate for the specific engine should be used when available. substituting the values 3 and 8 into the derivation yields speeds at which the inlet drag equals one percent of the total drag of 33 knots for high flow rates and 54 knots for low flow rates. The derivation, using the low average flow rate is as follows:

The cooling water flow rate, Q, ft^3/sec is:

$$Q = 4.6 \times 10^{-4} \text{ BHP} \qquad (1)$$

Assuming a propulsive coefficient of 0.50:

$$\text{BHP} = 2 R_T v/550 \qquad (2)$$

For the typical inlet scoop with strainer the cooling water resistance, R_{CW}, lb, is:

$$R_{CW} = 0.6 \rho Q v \qquad (3)$$

Substituting (1) and (2) into (3) and with $\rho = (w/g) = 2$:

$$R_{CW} = 2 \times 10^{-6} R_T v^2 \qquad (4)$$

It is considered that although most resistance calculations are not accurate to anything like one percent, any known item of resistance should be calculated if it will be more than about one percent of the total. To solve for the speed at which R_{CW} becomes 1 percent

of R_T let $R_{CS} = 0.01\ R_T$ and substitute into (4)

$$0.01\ R_T = 2 \times 10^{-6}\ R_T\ v^2$$

$$v^2 = 5 \times 10^3$$

$$v = 70 \text{ fps} = 40 \text{ knots}$$

Therefore it seems that for boat speeds below 35 knots the cooling water scoops do not constitute a large increment of drag. The designer should use his own discretion depending on the accuracy of his data and of the remainder of his calculations.

3.5.2 Air Resistance

The calculation of air resistance is well covered in References 3, 4 and 9, and these should be consulted for detailed information. The air resistance is based on the above water frontal area and the speed of the boat through the air. The latter is the sum of the speed through the water and the wind speed. The frontal area should be divided into hull and superstructure. The hull area should consider the hull in its running attitude at the speed in question, but no credit should be taken for any blanketing of the superstructure by the bow. A good formula to use is that of G. S. Baker quoted in Reference 3:

For superstructure:

$$R_{air} = .004\ A\ V_k^{\ 2}$$

For the hull there is a reduction in drag coefficient because of the sharp bow:

$$R_{air} = .0012\ A_h\ V_k^{\ 2}$$

These can be combined and written:

$$R_{air} = .0012\ (3.3A_s + A_h)\ V_k^2,\ V_k \text{ in knots}$$

Formulas such as that given in Chapter 1 may also be used.

Except in extreme cases, air scoops should simply be considered in the frontal area and not calculated separately. An analysis similar to that for cooling water indicates that the resistance due to taking in the scavenging and combusion air of a typical diesel amounts to one percent of the total resistance at a speed of about 150 knots.

3.5.3 Rough Water Resistance Increment

A general discussion of rough water performance of power boats will be found in References 5, 20, 21, 25, 30 and 66. Some interesting results pertaining to a yacht hull and a trawler hull are given in Reference 75. Numerical data on some specific models will

be found in Reference 27 and 28 and other works listed in References 76 and 77. This subject will be treated in detail in Chapter 4. When making comparisons with model test data to approximate the rough water resistance increment, care must be taken in how this is done. For example, References 27, 28, 29 and 67 were used to estimate this increment for a 36-foot, 25 knot V-bottom design. The models all differed from the new in a number of ways. Depending on whether the comparison was made on a basis of equal L, $V/\sqrt{L}$, $V/\sqrt{B}$, or $F_{\nabla} = (v/g\nabla^{1/3})^{1/2}$, the resistance increment varied from .29 to .32, .35 to .38, .25 to .26, .17 to .33, etc. All the references were good for guidance. Reference 27 was chosen as most useful because results are given for two hull forms under identical conditions providing an opportunity to make some allowance for this parameter. In this type of comparison $V/\sqrt{L}$ was found to provide good results, whenever L/B was the same or could be interpolated. Because of the high displacement-length ratio of the particular design, F_{∇} was low and the resistance increment was lower than when using equal $V/\sqrt{L}$.

This is admittedly a very rough cut and does not properly account for all effects. But it indicates that the resistance increment will probably be between 25 and 35 percent of the smooth water resistance. This is for sea state 3 and a 36-foot boat. The relation between the sea state and the boat size should be the same for model and full scale. This kind of approach requires judgment and ingenuity.

If the rough water resistance is to be determined from a model test of the new design, then the matter becomes very simple. The frictional resistance is assumed not to change with wave height, so any change in resistance is Froude scaled (proportioned to displacement).

A great deal of recent work on a systematic series of models with bow shapes in rough water is reported in Reference 74 and Chapter 4.

3.5.4 Shoal Water Effects

A. Shoal Water Resistance

This can be a very important consideration in small craft design. Trials are often run in water shoal enough to affect the speed. The speed is not always reduced by shoal water but under many conditions it is increased. There also appears to be an optimum depth for least resistance and this depth varies with speed. At low speeds, however, there is always an increase in resistance and trim due to shallow water. This occurs because in the presence of the bottom, the water passing under the boat experiences an increase in aftward speed (because of the restricted area through which it moves) and consequently a reduction in static pressure. The reduction in pressure allows the stern to settle thereby increasing the trim angle and wave making resistance. The settling of

the stern further reduces the area through which the water flows, thereby increasing the aftward speed of the water and further reducing the pressure. This causes the stern to settle further. This sequence does not continue indefinitely because the increasing trim angle builds up dynamic pressure in the forward planing area and a new position of equilibrium is soon reached. Even in very shoal water where the relative reduction in area is greater, the increase in trim has a limit because the flow under the boat "chokes up". That is, the velocity reaches the maximum possible with the available pressure differential between the bow and the stern. Any additional water that must flow past the boat goes around the sides, causing a large alteration in wave pattern.

Fast boats which have no large projections below the hull, for example boats propelled by a jet pump, are an interesting case of shoal water effects. A 24-footer, for example, (with a static draft of 8 to 10 inches) traveling at a speed of about 20 knots experienced a sudden acceleration when the water depth changed rapidly from a few feet to a few inches. This occurred because the water became too shoal for any appreciable waves to form thus eliminating this component of resistance. The boat was in effect running on a smooth water-lubricated surface.

Reference 70 provides the only available information on shallow effects for planing type boats. A series 62 hull with representative proportions was towed in several water depths and several l.c.g. positions. The resistance, trim, and heave (C.G. rise) are given over a wide range of speeds for each of the model conditions. The shallow water effects become very apparent and sufficient information is given to make numerical evaluations for new designs. The key results are shown in Figures 1.8 and 1.9 of Chapter 1.

B. Design for Shoal Water

The average runabout is not the ideal shoal water boat. Most small jet propelled boats have the inlet on the centerline. When such a boat runs aground the inlet becomes blocked, thereby preventing the development of thrust. For shallow water operation there should be two inlets, one on each side of the keel. The bottom should have a small amount of deadrise so the inlets will be off the bottom when the boat is hard aground, thus providing a continuous supply of water to the propulsion pump. The same principle applies to tunnel stern boats, but is more difficult to put into practice. The boat should float at rest with the greatest draft forward of amidships so that when run aground at slow speed she will contact the mud on a small forward area, permitting the stern to be swung around and the boat headed back toward deeper water. This type of keel profile requires shallow skegs for both directional stability and steering. The skegs should be located outboard so they will not increase the draft of the hull. This type of design has been very successful in practice.

3.5.5 Stability

The stability of planing boats has been investigated in recent years. Reference 69, for example derives equations for planing characteristics of flat and deadrise surfaces in steady trimmed, rolled, and yawed attitudes, and these are compared with test results presented in Reference 55. Reference 69 also discusses the turning and stability of planing craft on the basis of long period period motions of infinitesimal amplitude. Unfortunately, test data necessary to evaluate the coefficients for practical ranges of values are not available. For example, the smallest trim angle investigated in Reference 55 is 6 degrees. There are no dynamic data available against which to check the stability equations. But this work is progressing and will eventually be reduced to a useable design tool.

A. Porpoising Stability

Virtually all that is known about this is referenced in Section 2.1.3. Basically it is a matter of calculating the porpoising parameter and checking to see if it falls above or below a line on a chart. Reference 1 gives results for prismatic surfaces of various deadrise angles, and Reference 6 gives results for Series 62 with 12-$\frac{1}{2}$ degrees deadrise.

B. Transverse Stability

This is a subject about which almost nothing is known. Some boats have a serious stability problem at high speed, occasionally leaning over on one half of the bottom. Some boats have been known to exhibit a sort of transverse porpoising, at speeds over 60 M.P.H. Some pleasure boats seem to be less stable while planing than when at rest, but there is perhaps a great deal of psychology in this. The case of one boat with rounded chines is discussed in Reference 25. A few of the pleasure boat builders have conducted experiments to find the roll angle versus roll moment for some boats but the results are proprietary. The ocean racing people have stability problems and have made many experiments to solve them but, naturally, have not published any design information. Devices that have been used include tapered wedges, the length and depth both increasing uniformly from the centerline toward the chine, and hydro-skis mounted variously from amidships to the transom. When on the transom, outboard, they are like long narrow trim flaps.

C. Directional Stability

This subject has been discussed above. See, for example, Section 2.3.2 D. There is practically no quantitative information available for small craft on directional stability, or course keeping. At the present time no meaningful calculations can be made.

3.5.6 Turning

This is another area in which there is very little information available. The best report seems to be Refernce 68 which gives the results of self propelled tests on a 76-foot by 21-foot by 4-foot twin screw, twin rudder, high speed, rough water boat. While the report can give only an approximation of turning radius for a design that differs from the one tested, there is a great deal of other valuable information in it. Tests were conducted to find:

a) increase in tactical diameter with speed
b) optimum rudder area
c) optimum aspect ratio
d) maximum effective rudder angle
e) optimum rudder position relative to propeller
f) best skeg shape and size
g) effect on turning of reversing one propeller

Additional information on turning and rudder design can be found in References 3, 4, 5, 10 and 64.

3.5.7 Unsymmetrical Planing Conditions

As pointed out at the beginning of Section 3.5.4 there is not yet a useable way to treat this subject numerically. The designer's own experience is his best help in producing a boat that will "handle well" under all conditions, "bank nicely" on turns, etc.

3.5.8 Hydrostatics

This is an area where, fortunately, there is no essential difference between a planing boat and a displacement boat. But, while the principles are identical, the treatment can be varied to suit the case. One of the boats, used as an example in the performance calculations, was to be marketed with a very wide range of powerplants from a single outboard to twin sterndrives, with varying fuel loads and arrangement plans, all of course in identical hulls. Therefore, after the hull lines were drawn for this boat it was necessary to see how it would float under a wide range of loading conditions. Because the usual lb./in. and MTI inch calculations are not accurate for large changes in draft or trim, a different method was devised. Bonjean Curves were calculated and plotted in the usual fashion. Then the displacement and l.c.b. were calculated at four mean drafts and four trims for each draft--one by the bow and two by the stern plus level trim. The displacement and center buoyancy for each combination of trim and draft were then plotted and curves of constant draft and trim were drawn through these points. This plot is shown in Figure 3.36. This seems like a lot of work but in many cases such as this one it saves a great deal of time. Instead of finding the flotation waterline by trial and error for each new configuration, it is necessary only to enter the chart with the and center of gravity and read immediately the mean draft and trim.

It was also desirable to know how stable the boat would be in each configuration. This was facilitated by calculating KM at each combination of trim and mean draft and making preliminary plots of KM against trim for each mean draft, and against mean draft for each trim. It was then possible to spot in points for even values of KM along the lines of constant trim and also along the lines of constant draft. Then like points were joined to produce the contours of constant KM shown by the dashed lines in the figure. Now for any displacement and L.C.G. the height of the metacenter above the keel, KM, can be read immediately. Subtracting KG, the height of the v.c.g. above the keel, from KM gives GM, the metracentric height. (The construction and use of Bonjean Curves is described Reference 4, which gives the British method, References 64 and 65.)

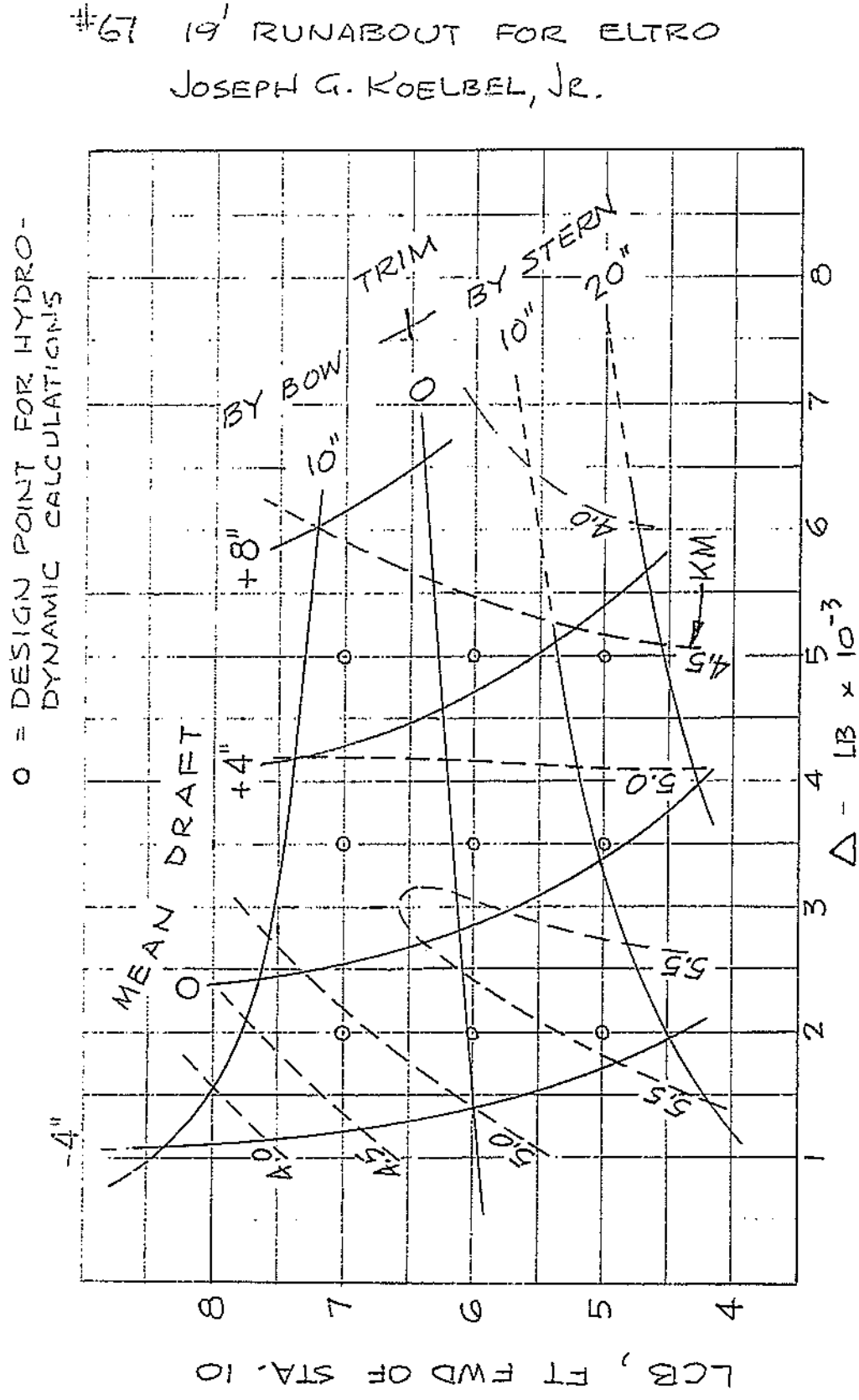

Figure 3.36. Mean draft, trim and KM as functions of LCB position and displacement for a 19 foot runabout.

SECTION 4: REFERENCES

Sources

DDC - Defense Documentation Center, Cameron Station
Alexandria, Virginia

DL - Davidson Laboratory, Stevens Institute of Technology,
711 Hudson Street, Hoboken, N. J. 07030

DTMB - David Taylor Model Basin, Naval Ship Research
and Development Center, Washington, D. C. 20007

NACA - National Aeronautics and Space Administration,
Washington, 25, D. C.

SBS - Sailing Book Service, 34 Oak Avenue,
Tuckahoe, N. Y. 10707

SNAME - The Society of Naval Architects and Marine Engineers
74 Trinity Place, New York, N. Y. 10006

SSCD - Society of Small Craft Designers, Viktor Harasty, Secretary
22 Second Avenue, Port Jefferson, N.Y. 11777

1. Savitsky, D., "Hydrodynamic Design of Planing Hulls", Marine Technology, Vol. 1, No. 1, SNAME

2. T and R Bulletin 1-25, SNAME

3. Saunders, H. E., "Hydrodynamics in Ship Design", Vol. I, II and III, SNAME

4. Barnaby, K. C., "Basic Naval Architecture", SBS

5. Phillips-Birt, D., "Naval Architecture of Small Craft", The Philosophical Library, SBS

6. Clement, E. P., and Blount D. L., "Resistance Tests of a Systematic Series of Planing Hull Forms", Transactions 1963, SNAME

7. Beys, P. M., "Series 63, Round Bottom Boats", Report 949, DL

8. Blount, D. L., "Resistance and Propulsion Characteristics of a Round Bottom Boat" (Parent Form of TMB Series 63), Report 2000, DTMB

9. Hoerner, S. F., "Fluid Dynamic Drag", S. F. Hoerner, 148 Busteed Drive, Midland Park, New Jersey

10. Van Lammeren, W.P.A., Troost, L., and Koning, J. G., "Resistance, Propulsion and Steering of Ships", The Technical Publishing Col, H. Stam-Haarlem-Holland, SBS

11. Hadler, J. B., "The Prediction of Power Performance of Planing Craft", Transactions 1966, SNAME

12. Clement, E. P., and Pope, J. D., "Stepless and Stepped Planing Hulls - Graphs for Performance Prediction and Design", Report 1490, DTMB

13. Clement, E. P., "Graphs for Predicting the Ideal High-Speed Resistance of Planing Catamarans", Report 1573, DTMB

14. Clement, E. P., "A Lifting Surface Apprach to Planing Boat Design", Report 1902, DTMB

15. Murray, A. B., "The Hydrodynamics of Planing Hulls", Transactions 1950, SNAME

16. Stoltz, J., Koelbel, J. G., Beinert, J., "How to Design Planing Hulls", Vol. 49 Ideal Series, Motor Boating, 959 Eighth Avenue, New York, N. Y. 10019

17. Clement, E. P., "Performance Limits of the Stepless Planing Boat and the Potentialities of the Stepped Boat", Symposium on Smallcraft Hydrodynamics, 1966, Southeast Section, SNAME

18. Shuford, C. L., "A Theoretical and Experimental Study of Planing Surfaces Including Effects of Cross Section and Planform", NACA Report 1355, Supt. of Documents, U. S. Govt. Printing Office, Washington 25, D. C.

19. Ashton, R., "Effect of Spray Strips on Various Power Boat Designs", Tech. Memo No. 99, D. L.

20. Van Mater, P. and Dormak, H., "Hydrodynamic Characteristics of Basic Planing Hull Types", Great Lakes Section, SSCD

21. McGown, S. C., "The Seaworthiness Problem in High Speed Small Craft", Jan. 24, 1961, N. Y. Metropolitan Section, SNAME

22. Clement, E. P., "Analyzing the Stepless Planing Boat", Report 1093, DTMB

23. Clement, E. P., and Kimon, P., "Comparative Resistance Data for Four Planing Boat Designs", Report 1113, DTMB

24. Clement, E. P., and Tate, C. W., "Smooth Water Resistance of a Number of Planing Boat Designs", Report 1373, DTMB

25. Koelbel, J. G., "The Detail Design of Planing Hull Forms", Symposium on Small Craft Hydrodynamics, 1966, Southeast Section, SNAME

26. Brown, P. W., "An Analysis of the Forces and Moments on Re-entrant Vee-Step Planing Surfaces", LR-1142, DL

27. Chey, Y., "Model Tests of a Series of Six Patrol Boats in Smooth and Rough Water", R-985, DL

28. Fridsma, G., "Model Tests of a Round Bottom Patrol Boat in Smooth and Rough Water", LR-1074, DL

29. Fridsma, G., "Comparative Tests on Model 2387 With and Without Bottom Camber in Smooth and Rough Water", LR-1153, DL

30. DuCane, P., "High Speed Small Craft", SBS

31. Hobbs, R., "Faster Boats", The Planimeter, July 1965, SSCD

32. Kimon, P., "The Planing Characteristics of an Inverted Vee Prismatic Surface with Minus 10 Degrees Deadrise", Report 1076, DTMB

33. Gilmer, T. C., "Model Tests of Some Fishing Launches", Fishing Boats of the World, II, SBS (See Ref. 66)

34. Yeh, H. "Series 64 Resistance Experments on High-Speed Displacement Forms", Marine Technology, July 1965, SNAME

35. Clement, E. P., "Merit Comparisons of the Series 64 High-Speed Displacement Hull Forms", Report 2129, DTMB

36. Skene, N. L., "Elements of Yacht Design", 1935, SBS (Out of print, may not be available)

37. Marwood, W. J., and Silverleaf, A., "Design Data for High-Speed Displacement-Type Hulls and a Comparison with Hydrofoil Craft", Third Symposium on Naval Hydrodynamics, ACR-65, Supt. of Documents, U. S. Govt. Printing Office, Washington 25, D. C.

38. Clement, E. P., "A Critical Review of Several Reports on Round Bottom Boats", Tech. Note 40, 1963, DTMB

39. Tate, C. W., "Model Tests of a Round-Bilge Boat with and without the Snadecki Longitudinal Strakes", Report 1281, DTMB

40. Harbaugh, K. H., "Smooth-Water Tests of Model 4943 Representing a 41-Foot Personnel Boat", Report 1735, DTMB

41. Clement, E. P., and Tate, C. W., "Model Test Results and Predicted EHP for an 86-Foot Personnel Boat, from Tests of Model 4675", Report 1288, DTMB

42. Clement, E. P., "Scale Effect on the Drag of a Typical Set of Planing Boat Appendages", Report 1165, DTMB

43. Carter, A. W., and Weinstein, I., "Effect of Forebody Warp on the Hydrodynamic Qualities of a Hypothetical Flying Boat Having a Hull Length-Beam Ratio of 15", Tech. Note No. 1828, NACA

44. Lippisch, A. M., and Colton, R. F., "Stepped Planing Boats", Unpublished Report (Panel H-12), SNAME

45. Clement, E. P., "Model Tests of a Stepped Planing Boat With an Adjustable Stern Stabilizer", Report 2414, DTMB

46. Clement, E. P., "Effect of Length-Beam Ratio on the Performance of a Stepped Planing Boat with an Adjustable Stern Stabilizer", Report 2552, DTMB

47. Clement, E. P., "The Planing Characteristics of a 15-Degree Deadrise Surface with Circular-Arc Camber", Report 2298, DTMB

48. Moore, W. L., "Cambered Planing Surfaces for Stepped Hulls - Some Theoretical and Experimental Results, Report 2387, DTMB

49. Clement, E. P., "The Design of Cambered Planing Surfaces for Small Motorboats", Report 3011, DTMB

50. Sherman, P., "Tests of a Planing Boat Model with Partial Hydrofoil Support", Report 1254, DTMB

51. Clement, E. P., "Effects of Longitudinal Bottom Spray Strips on Planing Boat Resistance", Report 1818, DTMB

52. Clement, E. P., "Reduction of Planing Boat Resistance by Deflection of the Whisker Spray", Report 1929, DTMB

53. Savitsky, D. and Breslin, J., "On the Main Spray Generated by Planing Surfaces", SMF Fund Paper No. FF-18, Institute of Aeronautical Sciences, N. Y., Jan. '58

54. Savitsky, D. and Ross, E. W., "Turbulence Stimulation in the Boundary Layer of Planing Surfaces, Part II, Preliminary Experimental Investigation", Report 444, DL

55. Savitsky, D., Prowse, R. E., and Lueders, D. H., "High-Speed Hydrodynamic Characteristics of a Flat Plate and 20° Dead Rise Surface in Unsymmetrical Planing Conditions", Technical Note No. 4187, NACA

56. Monk, E., Yachting Magazine, 50 West 44th Street, New York, N. Y. 10036, Jan. '58, p. 98

57. Clement, E. P., "Development and Model Tests of an Efficient Planing Hull Design", Report 1314, DTMB

58. Lord, L., "Naval Architecture of Planing Hulls", SBS

59. Koelbel, J. G., "A Comparison of Powering Methods", The Planimeter, Dec. 1961, SSCD

60. Small Craft Data Sheets, 1 - 16, SNAME

61. T and R Bulletin 1 - 23, "How to Use the SNAME Small Craft Data Sheets for Design and for Resistance Prediction", SNAME

62. Korvin-Kroukovsky, B. V., Savitsky, D., and Lehman, W. F., "Wetted Area and Center of Pressure of Planing Surfaces", Davidson Laboratory Report 360, Sherman M. Fairchild Publication Fund Paper 244, Institute of the Aeronautical Sciences, New York, N. Y.

63. Savitsky, D. and Neidinger, J., "Wetted Area and Center of Pressure of Planing Surfaces at Very Low Speed Coefficients", Davidson Laboratory Report 493, Sherman M. Fairchild Publication Fund Paper FF-11, Institute of the Aeronautical Sciences, New York, N. Y.

64. Comstock, J., "Principles of Naval Architecture", SNAME

65. Rabl, S. S., "Practical Principles of Naval Architecture", SBS

66. Traung, J. O., "Fishing Boats of the World", Vol. 1, 2, and 3, SBS

67. Savitsky, D., "On the Seakeeping of Planing Hulls", Symposium on Small Craft Hydrodynamics, 1966, Southeast Section, SNAME

68. Sugai, K., "On the Maneuverability of the High Speed Boat", Bureau of Ships Translation 868, AD 463211, DDC

69. Hsu, C. C., "On the Motions of High Speed Planing Craft", Hydronautics, Inc., Technical Report No. 603-1, AD 658151, DDC

70. Toro, A., "Shallow Water Performance of a Planing Boat", Symposium on Small craft Technology, 1969, Southeast Section, SNAME

71. Brown, P. W., "An Experimental and Theoretical Study of Planing Surfaces with Trip Flaps", April 1971, R-1463, DL

72. Angeli, J. C., "Evaluation of the Effect of Flaps on the Trim and Drag of Planing Hulls", April 11, 1970, Unpublished

73. Angeli, J. C., "Evaluation of the Quality of Planing Boat Designs", Feb. 18, 1971, Southeast Section, SNAME

74. Fridsma, G., "A Systematic Study of the Rough Water Performance of Planing Boats, Phase II, Irregular Seas", Feb. 1971, R-1495, DL

75. Numata, E., and Lewis, E. V., "An Experimental Study of the Effect of Extreme Variatons in Proportions and Form on Ship Model Behavior in Waves", 1957, R-643, DL

76. Koelbel, J. G., "Bibliography on Power Boat Design", Feb. 26, 1971, Report No. 120-1, to be Published by NAVSECNORDIV, Code 6660.03.

77. Koelbel, J. G., "Guide to Power Boat Design", Feb. 26, 1971, Report No. 120-2, to be Published wi h Reference 76 by NAVSECNORDIV, Code 6660.03

SMALL CRAFT BEHAVIOR IN A SEAWAY

by

Daniel Savitsky

Prepared for Conference
on
Small Craft Engineering
University of Michigan
Ann Arbor, Michigan

October 11-15, 1971

CONTENTS

BEHAVIOR IN A SEAWAY

by

Daniel Savitsky*

1) General

In past years hydrodynamic research on planing hulls has been mainly directed to problems of smooth water resistance and stability. As a result, there are now available to designers basic elemental planing data (Refs. 1-4, for example) and several laboratory developed hull series[5,6] which, when combined with the practical knowledge of the small boat naval architect, can produce excellent smooth water designs. The combination of these hydrodynamically efficient hulls with the presently available large horsepower engines has resulted in the evolution of high-performance, high-speed craft.

The modern, fast, planing hull, however, is mostly exposed to a rough water environment and, as is usually the case, a good smooth water boat is not necessarily a good performer in a seaway. Unfortunately, our present analytical capabilities for evaluating hull performance in a seaway are not sufficiently developed to quantitize rough water behavior. A summary of published small craft seakeeping studies available through 1968 appears in Ref. 7. That summary was necessarily a qualitative description relating the hydrodynamic characteristics of planing hulls in rough water to boat speed, trim, and hull section. Since publication of Ref. 7, new systematic seakeeping studies of prismatic hulls have been undertaken by the Davidson Laboratory, Stevens Institute of Technology (Refs. 8 and 9) which provide quantitative data useful to the small boat designer.

---

*Assistant Director
Davidson Laboratory, Stevens Institute of Technology

The objectives of a study of boat behavior in a seaway are to seek the following performance improvements in waves:

1. Power requirements
2. Craft motions
3. Impact loads on hull structure
4. Course-keeping ability

Items (2) to (4) can also be described as the ability of a craft to maintain speed within acceptable safety limits. In the present chapter, Item (4) will not be considered and the discussion will be limited to resistance increase, pitching and heaving motions, accelerations, and bottom pressures in head seas. The results of Refs. 8 and 9 are basically the source of technology for Items (1) and (2). Existing hydrodynamic impact theories (borrowed from the seaplane technology) and full-scale bottom pressure measurements on a PT hull form are used in the analysis of Item (3). These subjects together with a mathematical description of the sea surface are essentially the contents of the present chapter.

2) The Seaway

2.1 General

The logical starting point for this subject is a description of the sea from the point of view of the naval architect rather than the oceanographer. As typically described by Lewis[10], Bascom[11], Pierson, et al[12] simple regular waves are not representative of normal sea conditions, although they may approximate a smooth regular swell -- a condition often encountered after a storm has passed or as a result of a distant storm. The usual and more serious operational sea environments for a small craft are in areas where the sea is characterized by apparent great irregularity and incessant change of appearance. The sea is observed to be "short-crested" i.e., looking along a crest, it may seem that the crest disappears at a short distance, perhaps in a hollow or in another wave and other crests suddenly appear not far away.

A sample record of the ocean surface at a fixed point is shown in Figure 1. The record is typical of a short crested irregular sea where the wind has been blowing for some length of time. It is characterized by an appearance of great irregularity and confusion with wide fluctuations in the interval between crests (apparent or visible period $\tilde{T}_w$) and in the vertical distance between a successive trough and crest (apparent wave height $\tilde{h}_w$). It has been observed that over a large area of the sea and for periods of hours, the ocean surface may maintain a characteristic appearance which seems to defy precise description but which, nevertheless, is constant or "steady." At other times or places, the sea condition will be different but will still have a characteristic appearance. These observations suggest the feasibility of statistical description of the sea which will be discussed later.

Pierson, et al (Ref 12) have found that the short crested sea surface can be represented as an infinite number of infinitesimal regular sine waves superposed in a random fashion, so that all of the crests never coincide. As a practical matter the wave elevation at any instant may be considered as the sum of points on a large number -- instead of an infinite number -- of sine waves of very small amplitude. Usually, there are several trains of sinusoidal waves with different wave lengths, heights, directions, and relative phases present at the same time and their intersection creates a random or short crested diamond pattern. This process of superposition is graphically illustrated in Figure 2 where, for simplicity, several wave elements are represented. It is seen the addition of these and many other separate trains results in apparent confusion as represented by an actual photograph of the sea surface. The pattern becomes so complex that statistical methods must be used to analyze the waves and predict their height.

2.2 Regular Waves

Since an irregular wave can be represented by a summation of simple regular waves it is well to discuss the characteristics of these elemental waves. A simple regular wave train (Figure 3) can be described by its period (the time it takes two successive crests to pass a point), by its wave length (the distance between wave crests or troughs), and its height (the vertical distance between a trough and a succeeding crest). In the theory of simple gravity surface waves it is assumed that the crests are straight, infinitely long, parallel, equally spaced, and that the wave heights are constant. The wave form advances in a direction perpendicular to the line of crests at a constant velocity, C, referred

to as "celerity" to distinguish it from the water particle velocity, u, which is usually much smaller than C. The motions of such simple waves can be described in a plane perpendicular to the crest lines and are usually referred to as two-dimensional waves. Classical mathematical developments of the properties of simple harmonic (sinusoidal) gravity waves appear in many books on hydrodynamics (i.e., Refs 13, 14). These results are summarized herein following the discussion by Lewis in Ref 15.

2.2.1 Simple Gravity Waves in Water of Any Depth

The surface wave is the visible manifestation of pressure changes and water particle motions affecting the entire body of fluid -- theoretically to infinite depth. Since the wave form advances with celerity C, the wave elevation (as well as other properties such as orbital velocity and internal pressure) depends on time, t, as well as on the distances x and z. (See Figure 3 for definition of coordinate axis system.) Assuming the water to be inviscid and incompressible, the motion can be characterized by a velocity potential, φ, whose negative derivatives, with respect to x and z, define the horizontal and vertical velocity components, u and v respectively, of the individual fluid particles. From Ref 13, the velocity potential velocity potential for a two-dimensional wave in any depth of water is given by:

$$\varphi = \zeta_a C \frac{\cosh k(-z+h)}{\sinh kh} \sin k(x-C t) \qquad (1)$$

As shown in Figure 3, the origin of the coodinate system (x_o, z_o) is taken at the still water surface directly over a wave trough. Other notations are:

ζ_a = surface wave amplitude (half-height from crest to trough)

λ = wave length

h = depth of water

C = wave front velocity or celerity

k = the wave number; $2\pi/\lambda$

t = time

g = acceleration of gravity

The horizontal and vertical velocity components of the individual water particles for simple waves for finite depth water are:

$$u = -\frac{\partial \varphi}{\partial x} = -k\,\zeta_a C\,\frac{\cosh k(-z+h)}{\sinh kh}\cos k(x-Ct) \tag{2}$$

$$v = -\frac{\partial \varphi}{\partial z} = k\,\zeta_a C\,\frac{\sinh k(-z+h)}{\sinh kh}\sin k(x-Ct) \tag{3}$$

To determine these wave particle velocities, it is necessary to derive an expression for the wave celerity C. Using the free surface boundary conditions which state that (1) the vertical velocity of the water particles must be the same as the vertical velocity of the surface itself and (2) that the atmospheric pressure acting on the free surface is uniform, there is obtained, after linearization to waves of "small amplitude," the following simplified relation for conditions at $z = 0$.

$$\frac{\partial^2 \varphi}{\partial t^2} + g\frac{\partial \varphi}{\partial z} = 0 \tag{4}$$

Substituting equation (1) into (4) results in the following expression for the wave celerity:

$$C = \sqrt{\frac{g}{k}\tanh kh} \tag{5}$$

To obtain the shape of the free surface of the wave it is necessary to use Bernoulli's equation for time dependent flow with gravity force, $g\zeta$,

and uniform atmospheric pressure. The linearized (small wave heights compared to wave length) Bernoulli equation is

$$- g\zeta = \frac{\partial \varphi}{\partial t} \tag{6}$$

Substituting equation (1) into (6) results in the surface wave elevation ζ (at $z = 0$)

$$\zeta = \zeta_a \cos k(x - ct) \tag{7}$$

This equation shows the surface profile to be a cosine curve which is a function of time when observed at a fixed point x_o or a function of distance at a particular instant t_o.

The total velocity, U, of a fluid particle in the wave follows from a combination of equations (2) and (3):

$$U^2 = u^2 + v^2 \tag{8}$$

For the case of water of limited depth, h, it is found that the path of the particle is elliptical and is defined by the equation

$$\frac{\xi^2}{\alpha^2} + \frac{\zeta^2}{\beta^2} = 1 \tag{9}$$

Where ξ and ζ are the horizontal and vertical displacements of a particle from its initial still water position and α and β are the semi-axes of the ellipses:

$$\alpha = \frac{\zeta_o \cosh k(h-z)}{\sinh kh}$$

$$\beta = \frac{\zeta_o \sinh k(h-z)}{\sinh kh} \tag{10}$$

These equations show that the particles move in ellipses with a constant

distance, $2\zeta_o/\sinh kh$, between their foci, but with vertical and horizontal semi-axis which diminish with depth. At the bottom, the vertical semi-axis is zero and the water particles oscillate horizontally between foci.

2.2.2 Simple Gravity Waves in Deep Water

For very deep water, (i.e. large h ; in practice $h > \lambda/2$) the basis for the previous development continues to be applicable but there is a substantial simplification in the final mathematical results due to the fact that the ratio

$$\frac{\cosh k(-z+h)}{\sinh kh}$$

approaches e^{-kz} . The expression for the velocity potential is:

$$\varphi = \zeta_a C\, e^{-kx} \sin k(x - Ct) \tag{11}$$

Hence the horizontal and vertical velocity components of a water particle at any point in deep water are given by:

$$u = -\frac{\partial \varphi}{\partial x} = -k\,\zeta_a C\, e^{-kz} \cos k(x - Ct) \tag{12}$$

and

$$v = -\frac{\partial \varphi}{\partial z} = k\,\zeta_a\, C e^{-kz} \sin k(x - Ct) \tag{13}$$

The total velocity of a fluid particle is then

$$U = \sqrt{u^2 + v^2} = k\,\zeta_a\, C\, e^{-kz}(\cos \omega t - i \sin \omega t) \tag{14}$$

where ω = circular frequency = $2\pi/T_w$

It is seen that the water particle velocity is represented by a vector whose magnitude at the water surface = $k\,\zeta_a C$ and which rotates at the angular velocity, ω , in radians per second making a complete revolution in the period of the passing wave. The path of the particle at

the surface is a circle of radius ζ_a. The absolute value of the velocity vector and the radius of the circular path of the particle diminish with depth as e^{-kz}. At a depth of one-half the wave length the orbital velocities and path of the fluid particles are reduced to a value of approximately 4% of those at the water surface.

The surface wave profile ζ_o (for z = 0) is equal to:

$$\zeta_o = \zeta_a \cos k(x - Ct) \tag{15}$$

which is identical to shape of the surface profile for waves in water of finite depth (Eq. 7).

The wave celerity for deep water is obtained from equation (5) for the case when $h > \lambda/2$:

$$C = \sqrt{g/k} = \sqrt{g\lambda/2\pi} \tag{16}$$

A more convenient form for the equation of a simple harmonic wave can be obtained by using circular frequency $\omega = 2\pi/T_w$. The period T_w is the time required for the wave to travel one wave length, and hence, the relationship between wave length and period in deep water follows from equation (15).

$$T_w = \frac{\lambda}{C} = \frac{\lambda}{\sqrt{g\lambda/2\pi}} = \sqrt{\frac{2\pi\lambda}{g}} \tag{17}$$

Hence circular frequency:

$$\omega = \frac{2\pi}{T_w} = \sqrt{\frac{2\pi g}{\lambda}} = \sqrt{kg} = kC = 14/\lambda^{1/2} \tag{18}$$

Recalling Eq (15), when observed at a fixed point x = o :

$$\zeta_o = \zeta_a \cos\omega t \tag{19}$$

Alternatively, if the wave profile examined t = ,

$$\zeta_o = \zeta_a \cos kx \tag{20}$$

The maximum slope of the wave surface is obtained by differentiation of Eq (20) and solving for its maximum value.

$$\left.\frac{d\zeta_o}{dx}\right|_{max} = \theta = k\zeta_a = 2\pi \frac{\zeta_a}{\lambda} = \frac{\pi H}{\lambda} \tag{21}$$

Summarizing the major characteristics of the wave in feet-second units:

Wave velocity	$V_w = 2.260\sqrt{\lambda}$
Wave length	$\lambda = 5.118\sqrt{T_w}$
Wave period	$T_w = 0.442\sqrt{\lambda}$
Wave slope	$\theta = \pi H/\lambda$

The energy in a train of regular waves consists of kinetic energy associated with the orbital motion of water particles and potential energy due to the weight of water, ρg , and its elevation or depression with respect to the still water level. For one wave length, λ , the kinetic energy per unit breadth of wave is:

$$E_k = \frac{1}{2} \int_o^\lambda \varphi \frac{\partial \varphi}{\partial z}\, dx$$

For a simple cosine wave this is:

$$E_k = \frac{1}{4} \zeta_a^2 \rho g \lambda \tag{22}$$

The potential energy is:

$$E_p = \frac{1}{2} \rho g \int_o^\lambda \zeta_o^2\, dx$$

for a cosine wave at $t = 0$

$$\zeta_o = \zeta_a \cos kx$$

so that

$$E_p = \frac{1}{4} \zeta_a^2 \rho g \lambda \tag{23}$$

Thus it is seen that the potential and kinetic energies in wave motion are equal and the total energy per unit wave length is:

$$E = E_k + E_p = \frac{1}{2} \rho g \zeta_a^2 \lambda \quad (24)$$

or the energy per unit area of sea surface is:

$$E = \frac{1}{2} \rho g \zeta_a^2 \quad (25)$$

2.2.3 Simple Gravity Waves in Very Shallow Water

In very shallow water, when $h < \lambda/25$, classical solutions of the wave propagation problem show that:

$$\text{Wave celerity} = C = \sqrt{gh} \quad (26)$$

The waves are non-dispersive, i.e. the wave speed is independent of wave length. Further, the water particle motions consist only of horizontal oscillations given by the following

$$u = A e^{ih(x - Ct)} \quad (27)$$

where A is the maximum value of u.

For details on the solution of this problem the reader is referred to classical tests on hydrodynamics. This type of wave will not be further considered in the present chapter.

2.3 Irregular Waves and Sea Spectrum

In order to study ship motions in irregular seas, it will be instructive to consider in some detail the concepts typified by the Pierson-Neumann theory of the analysis of ocean waves (Ref 12 and 16) as summarized by Lewis (Ref 15) and Marks (Ref 17) amongts many notable contributors to this field. As previously discussed, the basis is the concept of representing the irregular sea state by a very large number (theoretically infinite) of small amplitude (infinitesimal) sine waves

of different wavelengths, amplitudes and directions, with each individual component having length, period and speed characteristics as developed in section 2.2 for the case of deep water waves. The case for waves in water of finite depth (offshore) or in very shallow water (surf) is still to be developed. The phase relation between the various deep water wave components is taken to be completely random. With these considerations then, any seaway can be characterized by an "energy spectrum" which indicates the relative importance "amount of energy" in each of the large number of different wave components which combine to produce the observed irregular pattern (Figure 2).

Several typical fixed point sea spectra are shown in Figure 4 (as taken from Ref 18) where relative wave energy is plotted against circular frequency, $\omega = 2\pi/T_w$. Such spectra have a variety of shapes depending upon local wind velocity, duration, fetch, and other storm areas from which a superposed swell may travel. Fixed point wave records give no indication of the direction of wave components, consequently are referred to as one-dimensional spectra. Considering an idealized typical spectrum, such as shown in Figure 5, the function $S_\zeta(\omega)$ is a quantity such that any increment of area under its graph, when multiplied by a suitable constant, represents the wave energy in that incremental band of frequencies. Thus the total energy in an increment of frequency, $\delta\omega$, at the central frequency, ω_n, of that increment is:

$$\rho g \left[S_\zeta(\omega_n)\, \delta\omega \right] \qquad (28)$$

The function $S_\zeta(\omega)$ is referred to as the spectral density. The total energy of the wave system is the sum of all the component energies over the entire frequency range.

$$\rho g \int_0^\infty S_\zeta(\omega)\, d\omega \tag{29}$$

The foregoing integral, which represents the area under the spectrum, is referred to as E. Thus the total energy is $\rho g E$.

It has been shown that the energy per unit surface area in a simple harmonic wave is proportional to the square of the amplitude and is equal to $\frac{1}{2} \rho g \zeta_a^2$ (Eq 25). It thus follows from Eq. (28) that the square of the amplitude ζ_{an} of a wave (ω_n) having the same energy as all the wave components in a band of frequencies represented by $\delta\omega$, with central frequency ω_n is:

$$\frac{1}{2} \rho g \zeta_{an}^2 = \rho g S_\zeta(\omega_n) \delta\omega$$

so that

$$\zeta_{an}^2 = 2 S_\zeta(\omega_n) \delta\omega \tag{30}$$

which is twice the incremental area shown in Figure 5. As $\delta\omega \to 0$, it is clear that there will be an infinite number of frequency components, all of which have infinitesimal amplitudes, required to represent the spectrum.

To visualize this concept, it is convenient to assume as an approximation that all of the wave components are traveling in the same direction, i.e., that the point spectrum represent a long crested sea such as is generated in a model towing tank. Then the elevation of the sea surface, $\zeta(t)$, as a function of time can be expressed as the limit of a sum of individual harmonic waves:

$$\zeta(t) = \lim_{\substack{\omega_n \to \infty \\ \delta\omega \to 0}} \Sigma \left[2 S_\zeta(\omega_n) \delta\omega \right]^{1/2} \cos \left[\omega_n t + \varepsilon(\omega_n) \right] \tag{31}$$

where ω_n is the circular frequency and $\varepsilon(\omega_n)$ is the random phase of each component in relation to an arbitrary reference. The radical

$$\left[2S_\zeta(\omega_n)\,\delta\omega\right]^{1/2}$$

represents the amplitude of each wave element as previously explained.

As a result of practical experience it has been found that 15 to 20 wave elements can provide for a satisfactory representation of a sea spectrum which will have essentially the same statistical properties as the spectrum with an infinite number of wave element components.

In the study of ship behavior in irregular waves it is more convenient to use an amplitude spectrum $2S_\zeta(\omega)$ obtained by doubling all the energy spectrum ordinates. Incremental areas will then represent directly the component wave amplitudes as $\delta\omega \to 0$, on the approximate component amplitudes if $\delta\omega$ is finite. The area under the spectrum is then $2E$.

It is emphasized that the component wave elements are not directly visible either at sea, in a model tank, or in a wave record. However, the energy spectrum defining these components can be obtained from a wave record by applying the techniques of generalized harmonic analysis if the full scale test record is at least 15-20 minutes long and if the sea conditions remain stationary. This involves a numerical autocorrelation process and a Fourier transform which are carried out quickly with modern digital computers. The mathematical details of the autocorrelation procedure are beyond the scope of this presentation and the interested reader is referred to Ref 14 for further details. Suffice it to say that standard computer programs for producing energy spectra from surface wave amplitude time histories do exist and are available at most computer centers.

The fundamental importance of a wave spectrum is that it provides the complete statistical characterization of the sea. Since the phase lags, $\epsilon(\omega)$, in the equation of the sea surface are random, it introduces an element of probability into the wave representation which permits the application of available results obtained from probability theory. One of the most important statistical characteristics of an irregular wave profile is that the distribution of heights for equal time intervals on a given wave record closely follows the normal or Gaussian distribution of statistics as shown in Figure 6. This observation permits the direct determination of the characteristics of the sea that are of primary interest to the boat designer. First, statistical theory shows that the "variance" or mean square value σ^2 of a wave record (average of the sum of the squares of deviations from the mean value measured at equal intervals of time) is equal to the area E under the energy spectrum, or one-half the area under an amplitude spectrum.

$$\sigma^2 = E = \int_0^\infty S_\zeta(\omega)\, d\omega = \frac{1}{2} \int_0^\infty 2\, S_\zeta(\omega)\, d\omega \qquad (32)$$

Thus, if the sea spectrum is known, the mean square value is also known from the spectral area.

Various statistical values of visible wave propteties can also be obtained from the spectrum by utilizing another statistical property observed in irregular wave profiles, i.e. the peak-to-trough wave heights of a record are found to follow closely a "Rayleigh" distribution, Figure 7. From statistical theory, the following useful relations are associated with a Rayleigh distribution. Recalling that E is the area under an energy spectrum and that is the area under an amplitude spectrum:

Average apparent wave height, crest-to-trough:

$$\tilde{h}_w = 2.5\sqrt{E} = 1.77\sqrt{2E} \tag{33}$$

Average of the 1/3 and 1/10 highest wave:

$$(\tilde{h}_w)_{1/3} = 4.0\sqrt{E} = 2.83\sqrt{2E}\ ;\ (\tilde{h}_w)_{1/10} = 5.1\sqrt{E} = 3.6\sqrt{2E} \tag{34}$$

The greatest heights expected on the average in different numbers of successive wave encounters, N, are as follows.

N	$(h_w)_{max}$
100	$6.5\sqrt{E} = 4.56\sqrt{2E}$
1000	$7.7\sqrt{E} = 5.46\sqrt{2E}$
10000	$8.9\sqrt{E} = 6.28\sqrt{2E}$

Other visible characteristics that are obtainable from a statistical evaluation of spectrum are such important results as, average apparent period; average apparent wave length; wave length of maximum energy; etc. Thus the spectrum of the seaway which specifies the invisible components of the wave patterns, also defines the properties of the visible pattern which are of immediate interest. Further details are given in Ref 17.

The discussion to this point has been concerned only with the simple spectrum of the sea at a fixed point -- a one-dimensional spectrim. This can be thought of as describing a long crested irregular sea. A more complete representation is given by a two-dimensional spectrim $S_\zeta(\omega,\theta)$ which describes the directions (θ) as well as frequencies of the wave components and accounts for the short-crestedness of a typical sea. An angular integration of this spectrum will yield the one-dimensional spectrum as would be obtained from a record taken

at a fixed point. For the purposes of this presentation, however, only the long crested irregular sea will be considered. The reader is referred to Ref 15 for further details on two-dimensional spectra.

Typical Sea Data

So far, the discussion of spectra has been concerned mainly with definitions and interpretations. For practical use, the designer requires quantitative data on the energy in a spectrum; the range of elemental wave component covered, the wave length for maximum energy; and finally the relation between the spectrum and wind speed. A number of formulations have been made for families of spectra using wind velocity as the main parameter. Neumann (Ref 11) developed one of the first accepted point wave spectra for fully arisen seas. A summary of the pertinent sea characteristics associated with the Neumann spectra is given in Table 1 which was prepared by Marks at DTMB. Included in Table 1 is a relation between wind speed and definition of sea state as recently accepted by naval architects. Sea state 4, for example, is associated with a wind speed of 19 knots; a significant wave height of 6.9 ft. A significant range of wave periods between 2.8 and 10.6 seconds. A wave period of maximum energy of 7.7 seconds and an average wave length of 99 ft.

It is interesting to note from Table 1, that as sea state increases, significant spectral energy exists over a wider band of wave lengths; and that this band width shifts to longer wave lengths. Further, the point of maximum energy in the spectrum shifts to longer waves and the significant wave height increases as the sea state increases.

Recently Pierson and Moskowitz (Ref 18) examined 460 available sea spectra and selected 54 spectra which satisfied specified weather

criteria. These selected spectra were grouped into five wind speeds: 20, 25, 30, 35 and 40 knots and are shown plotted in Figure 8. Using this spectral family, Pierson (Ref. 18) developed the following analytical formulation for ideal one-dimensional sea spectra for fully developed seas.

$$S_\zeta(\omega)d\omega = \frac{\alpha g^2}{\omega^5} e^{-\beta(g/V_w\omega)^4} d\omega \qquad (35)$$

where:

$S_\zeta(\omega)$ = spectral ordinate in cm^2-sec

ω = frequency in radians/sec

α = 8.10×10^{-3}

β = 0.74

g = acceleration of gravity, cm/sec^2

V_w = wind speed in cm/sec

As shown in Figure 8, the agreement between Eq. (35) and the actual measured spectra is reasonably good.

The continuing analysis of wave records, which are becoming available in larger numbers, together with advances in the theory of wave generation and decay, will greatly increase the reliability of spectral formulations. The ATTC and ITTC are continuously reviewing wave spectra developments in an attempt to provide realistic information to the designers It is recommended that the small boat naval architect accept their results as they become available in the future.

3) Behavior of Planing Craft in a Seaway

3.1 General

Although well-developed and acceptable technology exist for computing the rough water behavior of displacement ships (as summarized in Ref. 15), these procedures are not entirely applicable to planing craft which operate over a considerably wider range of speed coefficients. in the at-rest condition, the planing craft is, of course, entirely supported by buoyant forces. As the speed increases, dynamic forces are developed which lift the craft and correspondingly reduce the buoyant force. Finally, at speed-length ratios of approximately 5 or 6, the craft is supported almost entirely by dynamic forces; the draft is very small; and the buoyant forces are practically nil.

As will be subsequently shown, the pitch and heave behavior of the planing boat at speed-length ratios less than approximately 2.0 behaves in accordance with the linear theory of seakeeping, as developed for the displacement ship.

Because many small craft do indeed operate in the low speed-length ratio regime, either because of operational requirements or due to progressive overloading without corresponding power increases, the linear theory of seakeeping is applicable and should produce results useful to to the planing craft designer for speeds up to and somewhat beyond the hump speed range. Accordingly, the essentials of the linear theory of seakeeping will be presented herein.

As stated in the introduction to this chapter, the analysis will be confined to head sea operation in long-crested seas with emphasis on heave, pitch, added resistance and accelerations.

3.2 Elements of Linear Theory of Seakeeping

The principle of linear superposition first developed for ships by St. Denis and Pierson (Ref. 19), states that the response of a ship in

an irregular sea can be represented by a linear summation of its responses to the elemental simple wave components that compose the sea. The significance of this powerful principle is that, by superimposing essentially sinusoidal responses of a craft to the simple component waves that make up an irregular sea (section 2.3), the craft motions in the irregular sea can be predicted if the energy spectrum of the sea is known. This also involves the assumption that responses to a particular wave length are directly proportional to wave height--which, in the case of planing craft, appears to be approximately true for heave and pitch at a speed length ratio less than about 2.0. It would be useful at this point to illustrate the fundamentals of this technique by evaluating a typical pitching response for a displacement ship in irregular seas by following the example given by Lewis in Ref. 15.

3.2.1 Transformed Wave Energy Spectrum

Figure 9 shows how the process of superposition can be carried out beginning with a typical point amplitude wave spectrum assumed to represent a long-crested sea as previously discussed in section 3.1. Since wave encounter frequencies must be considered in a study of craft motions, this stationary point wave spectrum must be transformed to the spectrum that would be obtained by a wave meter moving at ship speed, V, through the water. In the case of head sea operation, it is clear that the frequency of wave encounter must be larger than the stationary frequencies and smaller for the case of following seas. Mathematically, the relationship between stationary frequency, ω, to frequency of encounter, ω_e, is given by:

$$\omega_e = \omega \pm \frac{\omega^2}{g} V \qquad (36)$$

where the (+) sign refers to the head sea condition and the (-) sign to the following sea condition.

Equation (36) transforms the abscissa scale of the point energy spectrum. Since the total energy in the sea must remain constant, regardless of

transformations, the ordinates of the transformed spectrum must also be altered so that integrated areas under the original stationary spectrum must equal the area under the transformed spectrum. This is accomplished by the following procedure, considering the head sea case, from Eq. (36)

$$\omega_e = \omega\left(1 + \frac{\omega}{g} V\right)$$

differentiating:

$$d\omega_e = d\omega + \frac{2\omega\, d\omega}{g} V \tag{37}$$

since, the total energy in a given spectrum does not change with transformation, we have from Eq. (32)

$$E = \int_0^\infty S_\zeta(\omega)d\omega = \int_0^\infty S_\zeta(\omega_e)d\omega_e$$

hence:

$$S_\zeta(\omega)d\omega = S_\zeta(\omega_e)d\omega_e$$

and

$$S_\zeta(\omega_e) = S_\zeta(\omega)\,\frac{d\omega}{d\omega_e}$$

From Eq. (37), the quantity $d\omega/d\omega_e$, which is the Jacobian $J(\omega_e)$ of the transformation between the ω and ω_e domains, is

$$\frac{d\omega}{d\omega_e} = \frac{1}{1 + \frac{2\omega V}{g}} \tag{38}$$

For head seas, the correspondence between these two frequencies is one to one, hence the Jacobian never vanishes. Substituting Eq. (36) into (38):

$$J(\omega_e) = \left[1 + \frac{4V}{g}\,\omega_e\right]^{-1/2} \tag{39}$$

The moving wave spectrum (encounter frequency domain) is then obtained from the stationary energy spectrum by multiplying the ordinate $S_\zeta(\omega)$ by the Jacobian $J(\omega_e)$ at each frequency, and plotting these

at the corresponding encounter frequency. The resulting spectrum obtained in the ω_e domain then is that which would be obtained by an observer moving with the craft into a head sea. Figure 9a illustrates the wave spectra transformed to head seas speeds of 7.97 kts and 11.27 kts.

In following seas

$$\omega_e = \omega(1 - \frac{\omega V}{g})$$

so that the encounter frequency is parabolic about the line $\omega V/g = 1/2$; becomes negative for $\omega V/g > 1$; and is zero at $\frac{\omega V}{g} = 1$. There are realistic interpretations of the negative frequency of encounter but these will not be discussed herein.

3.2.2 Response Amplitude Operators

It is now necessary to consider the response of a ship to individual sinusoidal waves. For the present illustrative example, a relationship between pitch and wave amplitude must be established for a range of wave lengths. This can be obtained by model tests in a towing tank where the model is towed at a speed corresponding to the full scale speed, V , for a range of wave frequencies ω which, when combined with V , produce a range of encounter frequencies, ω_e , corresponding to the range of frequencies in the transformed spectra such as shown in Fig 9a. This model test data will provide a ratio of say pitch amplitude to wave amplitude (θ_a/ζ_a) which, for a linear system, is independent of wave amplitude for a given wave length. These data should then be plotted in a special form for appropriate combination with the transformed wave energy spectrum. The proper presentation of these data is as follows.

As previously explained, an incremental area under the wave amplitude spectrum $2S_\zeta(\omega_e)$ represents the squared amplitude of a component wave as $\delta\omega_e \to 0$. The theoretically infinite number of component waves

can be approximated by a finite number of component waves if a reasonably small frequency increment, $\delta\omega_e$, is selected. The central frequency of each band can be represented by $(\omega_e)_n$; where n varies from 0 to a large finite number. The single amplitudes of the various equivalent wave components are then represented by the square roots of the areas of the individual rectangle, $2S_\zeta(\omega_n)\delta\omega$. Considering any one of the components, say $\omega_e = 0.8$, the pitching motion it produces can be determined from the relationship between pitch and wave amplitude at that frequency as obtained from the previously described model test. Since the area of the rectangle corresponding to $\omega_e = 0.8$ represents the square of the wave amplitude, it is also convenient to square the ratio of pitch amplitude to wave amplitude. This value $(\theta_a/\zeta_a)^2$ is plotted in Fig 19b and is designated "response amplitude operator" or simply RAO.

3.2.3 Spectrum of Craft Motions

The determination of the motion spectra of a marine craft in irregular seas is now simply obtained by multiplying the wave amplitude spectrum $2S_\zeta(\omega_e)$ at $\omega_e = 0.8$ (for the present example) by the squared RAO at the $\omega_e = 0.8$ wave component. The area of the rectangle at $\omega_e = 0.8$ in the pitch amplitude spectrum plot, Figure 9c, then represents the square of the amplitude of pitch produced by this wave component or approximately by the band of wave frequencies $\delta\omega_e$.

Suppose that the relationship in regular waves between pitch and wave amplitude is known from model tests or from calculations for a number of frequencies and the squared value is designated $Y_{\theta\zeta}(\omega_e)$. These values can be plotted and a smooth response amplitude curve can be drawn through the points for a particular ship speed, as shown in Fig. 9.

In general a smooth pitch amplitude spectrum curve can be obtained. Mathematically expressed

$$2S_{\theta}(\omega_e) = 2S_{\zeta}(\omega_e)Y_{e\zeta}(\omega_e)$$

The significance of the pitch response spectrum is that it completely defines the pitching behavior of the ship in the irregular seas. The same sort of information that is obtained from a wave spectrum can be obtained for pitching from the pitch spectrum; i.e., average pitch amplitude, average of the 1/10 highest pitch amplitudes, or highest pitch amplitude expected in a given number of cycles (see section 3.1). For example, designating the area under the amplitude spectrum of pitch by R, the average amplitude of pitch is $0.886\ R^{1/2}$. Figure 9 shows the response spectra of two geometrically similar ships, one 250 ft long and the other 500 ft, at the same Froude number.

The application of the same statistical relationships to a ship response spectrum as to a wave spectrum is justified by numerous analyses of model and ship records in irregular seas. These have shown that ship responses, such as pitching and heaving, are, over a reasonable interval of time, approximately stationary, random processes, and fortunately for simple treatment have the same "Gaussian" character as do wave records. Furthermore, the visible amplitudes or heights (peak to trough) of the ship or model response record do, like the wave record, follow closely a Rayleigh (or "random walk") distribution.

Spectra can be similarly obtained for many ship responses other than pitch. It is necessary only that the response to regular waves be approximately sinusoidal, with amplitudes linearly proportional to wave amplitude and dependent only on wave frequency at any particular ship speed and heading to the regular waves. Hence, the following responses

can be treated in this manner: pitch; heaving; vertical motion at any point (combined pitch and heave); vertical velocity at any point; vertical acceleration at any point; vertical motion, or velocity of any point relative to the sea surface.

3.2.4 Interpretation of Wave and Motion Spectra

It is clear from the foregoing discussions that there are peaks of amplitude in the motions of pitching and heaving in regular waves. when plotted against either speed or wave length. These peaks are governed predominantly by the following factors.

a) Relative wave-ship proportions.

b) Tuning factor, which is the ratio of natural periods of craft oscillation to period of wave encounter.

c) Magnification factor, determined by the degree of damping present.

When the craft speed in a given wave is such that synchronism is approached (tuning factor equal to 1.0). particularly severe motions will be obtained. Depending upon the craft design there may be different synchronous speeds for pitch and heave motions. At this resonant condition not only are the amplitudes of motion large, but the phase relations between the craft motions and the encountered waves are usually unfavorable, i.e., as the bow pitches down into the wave crest and reaches its highest point at the wave trough. Hence water is easily shipped over the bow and high relative velocities between bow and wave make for an uncomfortable slapping action. Thus near synchronous conditions will result in serious motions, but for a craft in regular waves, the motions can be reduced greatly by small changes in course or speed which will change the encounter frequency sufficiently to be out of resonance with the natural periods of oscillation of the craft.

In irregular seas it is much more difficult to avoid synchronism with all of the existing wave components and consequently, synchronous motions are of predominant importance. The bands of wave components in the seaway which are near synchronism will at times be in phase with one another producing several violent oscillations of the craft, and will at other times be out of phase, producing comparatively steady conditions. It is obvious then, in the design of a craft for a specified speed and operational sea states, that a brief computation be made to assure that requirements do not result in any of the natural oscillation periods of the craft being at resonance with that wave frequency which contains maximum energy in the transformed wave spectra. For the case of an existing craft required to operate in an unfavorable sea it is generally possible to avoid serious motions by reducing speed to the point where synchronism occurs with wave components containing small energy content. A change of course, on the other hand, usually results only in synchronism with other wave length components with high energy content. Of course, for very high speed planing craft, the encounter frequency becomes so large for any moderate sea state, that the craft will most likely avoid synchronism with all of the wave components and thus experience relatively mild motions. This does appear to be the case for planing craft where the motions at high speeds are usually less than in the lower hump speed regime. Unfortunately, as will be subsequently demonstrated linearity of motions do not exist at the high speeds so that the principle of superposition cannot be applied.

4) Behavior of Planing Craft in a Seaway

4.1 General

A series of constant beam, constant deadrise models of varying length (Figure 10) was tested by Fridsma (Ref. 8) to define the effect of deadrise, trim, load, speed, length-beam ratio, and wave proportions on the resistance, motions, and accelerations of a planing craft in waves. Of particular importance was a separate study to determine the applicability of linear superposition effects to the case of planing craft. For this investigation, tests were made in regular waves over a range of wave heights while keeping all other test conditions constant. The following conclusions were reached concerning linearity of results with wave height.

a. Linearity is, in general, a function of speed and wave length.

b. Impact accelerations and added resistance in waves are generally non-linear at all speeds and vary as some power function of wave height.

c. In the displacement range of speeds, $V/\sqrt{L} \leq 2$, the heave and pitch motions are linear with wave height. At higher speed length ratios, the motions are non-linear with the greatest non-linearity associated with the pitch motions.

It appears then, that the linear superposition theory, which is so successfully used in seakeeping studies of displacement ships in irregular waves, has only limited application to the planing craft. Thus to totally characterize the motions, added resistance, and acceleration for small craft through speed length ratios as high as 6, it is necessary to obtain test data within the specific irregular sea state of interest. As long as the system remains non-linear, observations made in one particular sea

state cannot be quantitatively extrapolated to other sea states.

As a consequence of this finding, the systematic model test program in regular waves was extended to include a thorough evaluation of the motions and loads of planing craft in a series of irregular seas for speeds up to a speed length ratio of 6.0. The results of this study (which utilized the models shown in Figure 10) are presented by Fridsma in Ref. 9 which contains a detailed design procedure for estimating the added resistance, heave and pitch motions, and impact accelerations at the bow and center of gravity as a function of hull geometry, hull loading, speed and sea state. This design procedure is included in the present set of notes.

4.2 Basic Model Studies

In the systematic model studies conducted by Fridsma, tests were made at speed length ratios of 2, 4, and 6; at beam loading coefficients of $C_{\Delta}=\Delta/wb^3$ = 0.38 to 0.72; and for LCG positions at from 54 to 68 percent of the hull length aft of the stem. The models were tested in Pierson-Moskowitz sea spectra having significant wave heights of 0.22, 0.44, and 0.66 beams. The deadrise angles were 10°, 20°, 30° and the length beam ratios were 4 and 5.

Tests were conducted at constant speed rather than constant thrust since an investigation of surge freedom at speed length ratios greater than 2.0 showed that for planing hulls, freedom in surge had little effect on the motions, accelerations and added resistance in a seaway (Ref. 9). The length of test run for each combination of hull geometry, operating condition, and sea state was such as to assure at least 75 individual wave encounters. This provides a satisfactory sample for statistical analysis

of the data.

4.3 Statistical Analysis of Motions and Accelerations

The processing of data obtained from tests in irregular seas requires the use of statistical methods to determine the relations between average values and say 1/10 highest and 1/3 highest as desired. For linear systems, the time history of the random motions was previously described as a narrow band spectrum having a zero mean Gaussian distribution for its elevations and a Rayleigh distribution for its wave height. Statistical relations describing the motions are thus given in terms of the standard deviation previously described.

Since the planing boat behaves in a non-linear fashion over the greater part of its operating range, these spectral analysis techniques cannot be used. Fridsma (Ref. 9) has defined the probability functions for the case of motions and accelerations of planing craft. It was found that the motion amplitudes about the mean may be described by a probability function given by the so-called "distorted Rayleigh function." The peak accelerations were found to follow a simple exponential distribution. It is a one parameter distribution which is uniquely determined from the average values. For instance, the 1/10 highest accelerations are equal to 3.3 times the average acceleration. A complete description of these mathematical formulations is given in Ref. 9. For the present purposes, the prediction procedure will be limited to the average 1/10 highest pitch and heave motions; the average value of added resistance in waves; and the average and 1/10 highest values of the impact accelerations.

The heave and pitch motions are defined to be the amplitude of the crest relative to the mean heave and trim position; the impact acceleration is the amplitude of the crest relative to the "at-rest" position and taken to be zero "g". The added resistance is the resistance increment due to operation in waves and is to be added to the smooth water resistance to obtain the total resistance in waves.

The heave motions are non-dimensionalized in terms of beam, b , as is the significant wave height $H_{1/3}$ for the specified sea state.

5) Design Procedure

The ultime goal for this study is to enable designers and those interested in planing craft to use the information gathered in Ref. 9 in a practical and meaningful way. Working charts, with appropriate correction factors, (Figs. 11-24) were constructed so that the results could be immediately applicable to the prediction of full scale performance of planing hulls. Some details of the effects of individual parameters can be gleaned from the charts and equations; but this is discussed in the next section in a more generalized way. In this section the reader will be shown how to use these charts, and what corrections are applicable, as well as a number of worked examples.

To enter the charts and determine a prediction for a given boat, seven quantities must be known; namely, displacement, overall length, average beam, average deadrise, speed, smooth water running trim and the significant wave height of the irregular sea. Since realistic boats do not normally have a constant beam or deadrise, it is suggested that these quantities can be averaged over the aft 80% of the boat. It is understood that the designer has recourse to smooth water prediction methods (Ref. 1) which will enable an estimate to be made for the resistance, trim, and rise of the center of gravity as a function of forward speed.

The non-dimensional parameters are calculated next, such as C_Δ, L/b, $V/\sqrt{L}$, and $H_{1/3}/b$.

In using the charts, the designed should be careful not to make gross extrapolations. The charts are accurate within the ranges of test data. A reasonable amount of extrapolation has been built into the charts beyond the limits of the test data; and the results continue to be reliable. It is when parameters go far beyond the test ranges that one must be careful. The guide below should be helpful in establishing the limits of the use of the charts.

Parameter	C_Δ	L/b	C_Δ/L/b	τ	β	$H_{1/3}/b$	$V/\sqrt{L}$
Range	.3-.9	3-6	.06-.18	3°-7°	10°-30°	to 0.8	to 6

5.1 Added Resistance in Waves (Figs11 and 12)

The chart in Fig11 is entered with a given trim and deadrise. $(R_{AW}/wb^3)_{max}$ and $(V/\sqrt{L})^*_{max}$ are read off for the three sea states. An interpolation for the correct sea state can be made immediately; or the added resistance can be obtained as a function of wave height. For a given $V/\sqrt{L}$ or a series of speeds, the ratio V/V^*_{max} is calculated, and $R_{AW}/R_{AW_{max}}$ obtained from Fig 12. The added resistance is found by multiplying the resistance ratio of Fig 12 by the $R_{AW}/wb^3)_{max}$ obtained from Fig 11. The result, however, is true for a $C_\Delta = 0.6$ and $L/b = 5$, and must be corrected by means of the following formulas

$$(R_{AW}/wb^3)_{final} = (R_{AW}/wb^3)_{charts} \times E\ (C_\Delta,\ L/b,\ V/\sqrt{L},\ H_{1/3}/b)$$

ADDED RESISTANCE CORRECTIONS

$V/\sqrt{L}$	E	Equation
2	$1 + \left[\frac{(L/b)^2}{25} - 1\right] \Big/ (1+.895(H_{1/3}/b - 0.6))$	(1)
4	$1 + 10\ H_{1/3}/b(C_\Delta/L/b - .12)$	(2)
6	$1 + 2\ H_{1/3}/b\left[.9(C_\Delta - .6) - .7(C_\Delta - .6)^2\right]$	(3)

For the particular values of C_Δ and L/b, calculate E and plot as a function of $V/\sqrt{L}$. Read off E at the $V/\sqrt{L}$ of interest to correct the added resistance value.

* $(V/\sqrt{L})_{max}$ or V/V_{max} are associated with the speed at which $(R_{AW})_{max}$ occurs.

5.2 Motions (Figs 13-17)

The design procedure for the motions are incorporated on five charts. These charts will give the correct values for the 1/10 highest motions (crests) at the specified load, length/beam ratio, and sea state but for a trim of 4° and deadrise of 20°. Corrections for trim and deadrise are then applied to obtain the final values. Figures 13, 14 and 15, and 16 and 17 are for speed length ratios of 2, 4, and 6 respectively. Interpolation for speed will be done as a last step.

Enter Figs 13-17 at a specified sea state for the particular C_{Δ} of interest. Values of the heave and pitch will be obtained for each of the three speeds. This must be done for both $L/b = 4$ and 5. Interpolate for correct L/b by a straight line approximation. The results must be corrected by means of the following formulas

$$(h_{1/10}/b)_{final} = (h_{1/10}/b)_{charts} \times F(\tau, V/\sqrt{L}) \times G(\beta, V/\sqrt{L})$$

MOTION CORRECTIONS

	Formula	Equation
Trim	$F = 1 + \frac{V/\sqrt{L}}{24}(\tau - 4^{\circ})$	(4)
Deadrise	$G = .56 + .11V/\sqrt{L} + .11(\frac{\beta}{10})^{2}(1 - \frac{V/\sqrt{L}}{4})$ $= 1 \qquad V/\sqrt{L} \leq 4$ $= G \qquad V/\sqrt{L} \geq 4$	(5)

After applying trim and deadrise corrections, plot the heave and pitch values against $V/\sqrt{L}$ and interpolate for correct speed. Repeat procedure for other sea states.

5.3 Accelerations (Figs 18-24)

Seven (7) charts are presented to obtain the average C.G. (Figs 18 20) and bow (Figs 21-24) accelerations. Individual plots are provided for each speed ($V/\sqrt{L} = 2, 4, 6$) and length/beam ratio ($L/b = 4, 5$). Accelerations are obtained for the correct load, at a specified sea state. After interpolation for L/b, corrections are applied for trim and deadrise.

Enter Figs 18-20 and obtain values of the C.G. acceleration at each of the three speeds for a given $H_{1/3}/b$ and C_Δ. Do for both L/b = 4 and 5. Repeat in Figs 21-24 for bow acceleration. Plot the acceleration against $(L/b)^2$ and interpolate for correct length/beam ratio.

The results are corrected for trim and deadrise by the following formula

$$\eta_{final} = \eta_{charts} \times \left[\frac{\tau}{4^\circ}(5/3 - \frac{\beta}{30^\circ}\right] \qquad (6)$$

A bow acceleration correction is applied for increased deadrise (warp) at the bow by taking 85% of the final values.

With corrections applied, interpolate results for given speed and repeat procedure for other sea states.

5.4 Worked Examples

No. 1: Determine the added resistance, motions, and accelerations for the model condition: $\beta = 20^\circ$, $\tau = 4^\circ$, L = 45", b = 9", Δ = 18.95 lb, V = 13.06 fps, $H_{1/3}$ = 4"

a) The parameters are calculated

$wb^3 = (62.4)(.75)^3 = 26.3$

$L/b = 45/9 = 5$

$C_\Delta = \Delta/wb^3 = 18.95/26.3 = .72$

$V/\sqrt{L} = \frac{13.06}{1.689}/\sqrt{45/12} = 4$

$H_{1/3}/b = 4/9 = .444$

$1/C_\Delta = 1/.72 = 1.39;\ 1/C_\Delta^2 = 1/(.72)^2 = 1.93$

$C_\Delta/L/b = .72/5 = .144$

b) Added resistance

For $\beta = 20^\circ$ and $\tau = 4^\circ$, from Fig 11

	$H_{1/3}/b$ .2	.4	.6
$(V/\sqrt{L})_{max}$ =	4.0	4.2	4.2
$(R/wb^3)_{max}$ =	.025	.043	.051
$(V/V_{max}) = 4/(V/\sqrt{L})_{max}$ =	1.00	.95	.95
From Fig 12, (R/R_{max}) =	1.00	.99	.98
Therefore $R/wb^3 = R/R_{max} \times (R/wb^3)_{max}$ =	.025	.0425	.0500
From Eq. (2), E =	1.050	1.096	1.145
$(R/wb^3)_{final} = E \times (R/wb^3)_{charts}$ =	.0262	.0465	.0573

From a plot of R/wb^3 vs. $H_{1/3}/b$, the value at $H_{1/3}/b$ of 0.444 = .0493.
In model pounds the resistance is .0493 x 26.3 = 1.29 lb.
The actual measured value was 1.28 ib

c) Motions

From Fig 14, the 1/10 highest heave motions at $1/C_\Delta = 1.39$ and $H_{1/3}/b = .444$ is $h_{1/10}/b = .240$ at L/b = 5.

Similarly the pitch = 4.6° (Fig 15).

There is no correction for trim or deadrise.

This compares with the measured values of 2.10 in. of heave and 4.6 deg. of trim.

d) Accelerations

The C.G. acceleration from Fig 19 at L/b = 5, $1/C_\Delta^2 = 1.93$, and $H_{1/3}/b = .444$ is .52 g . The bow acceleration from Fig 23 is found similarly and is = 1.70 g . These are the final values since the correction factors are unity. Therefore to nearest 1/10 of a g . $\ddot{\eta}_{cg} = 0.5$ g and $\ddot{\eta}_{bow} = 1.7$ g . This compares well with the measured values of 0.4 and 1.7.

No. 2: Determine the performance of an actual planing hull. In DL R-1153 Model 2387-1 was tank tested in irregular seas. From the lines plan, the beam and deadrise is averaged over the aft 80% of the boat $\bar{\beta} = 18^{\circ}$, $\bar{b} = 11.2'$. The boat displaces 55,000 lb, has an overall length of 52 ft and its trim is 5.2° when running at 29 knots in smooth water. The model of this boat was tested in a Sea State 3 and 5, equivalent to significant wave heights of 3.8 and 8.5 ft respectively. The performance is evaluated on the work sheets that follow .

The added resistance in waves is plotted vs. $H_{1/3}/\bar{b}$ and the values at 0.34 and 0.76 recorded; namely, $R_{AW}/w\bar{b}^3 = .037$ (SS 3) and .054 (SS 5). This compares rather well with the actual measured values of .025 and .052 taken from DL Report 1153.

The 1/10 highest heave amplitude can be calculated in full scale feet by multiplying through by the average beam. Thus the 1/10 highest heave amplitudes in full scale feet is 2.2. This compares well with the measured value of 1.6 ft. Repeating the procedure for Sea State 5 yields for the 1/10 highest heave amplitudes 5.2 ft (predicted) versus 4.8 ft (measured). The pitch motions were not measured in the tests on Model 2387-1.

The bow acceleration must be compared at the same longitudinal station. Since the accelerometer on Model 2387-1 was mounted 25% LBP aft of the forward perpendicular, a linear correction was applied between the C.G. and bow locations. The final average bow acceleration at 25% LBP is therefore 1.3 g . The 1/10 highest acceleration is simply 3.3 times the average. After going through a similar procedure for a Sea State 5, the following comparison between predicted and measured accelerations can be made.

		η_{cg}		η_{bow}	
		average	1/10 highest	average	1/10 highest
SS 3	Predicted	0.6	2.0	1.3	4.3
	Measured	0.6	1.7	1.3	3.5
SS 5	Predicted	1.0	3.3	2.1	6.9
	Measured	-	-	2.6	6.5

Both for the C.G. and bow accelerations the predictions are in good agreement.

PLANING HULL PERFORMANCE

WORK SHEET

I. TABULATE GIVEN INFORMATION

Δ , Displacement, lb
L , Overall length, ft
$\bar{b}$, Average beam, ft
$\bar{\beta}$, Average deadrise, deg
V , Speed, kts
τ , Smooth Water running trim, deg
$H_{1/3}$, Significant wave height, ft

Δ	L	$\bar{b}$ *	$\bar{\beta}$ *	V	τ	$H_{1/3}$
55,000	52	11.2	18	29	5.2	3.8
						8.5

*Averaged over aft 80% of boat

II. CALCULATE PARAMETERS

wb^3 = 89,800
$1/C_\Delta$ = 1.64
$1/C_\Delta^2$ = 2.7
$C_\Delta L/\bar{b}$ = .133

	C_Δ	$L/\bar{b}$	$\bar{\beta}$	$V/\sqrt{L}$	τ	$H_{1/3}/\bar{b}$
Limits	.3-.9	3-6	10-30	0-6	3-7	0-.8
	.61	4.6	18	4.0	5.2	.34
						.76

III. AODEO RESISTANCE

A. At given $V/\sqrt{L}$, τ, $\bar{\beta}$ perform the following:

1. Obtain values of $(V/\sqrt{L})_m$ from Fig. 11
2. Obtain values of $(R_{AW}/wb^3)_m$ from Fig. 11
3. Calculate $V/\sqrt{L}/(V/\sqrt{L})_m$
4. Obtain $R_{AW}/(R_{AW})_m$ from Fig. 12
5. Multiply Lines 2x4 to get R_{AW}/wb^3
6. E corrections - Eqs. (1)-(3)
7. Multiply Lines 5x6 - Final values
8. Interpolate for given $H_{1/3}/b$

B. Repeat procedure for other speeds

Line	$H_{1/3}/\bar{b}$		
	.2	.4	.6
1	3.6	3.6	3.6
2	.0235	.040	.047
3	1.11	1.11	1.11
4	.96	.96	.96
5	.0226	.0384	.0451
6*	1.025	1.051	1.076
7	.0232	.0404	.0486

*It will be necessary to plot E vs. $V/\sqrt{L}$ and interpolate for given speed.

WDRK SHEET (continued)

IV. HEAVE AND PITCH MOTIONS

A. At given $H_{1/3}/\bar{b}$ obtain 1/10 highest values at $\tau = 4^{\circ}$, $\beta = 20^{\circ}$

1. Obtain heave or pitch from
2. Figs 13-17
3. Interpolate for correct $L/\bar{b}$
4. F. - Trim correction, Eq (4)
5. G. - Deadrise correction, Eq. (5)
6. Final values - multiply lines 3x4x5
7. Interpolate for given speed

B. Repeat procedure for other $H_{1/3}/b$

			Heave	Pitch
Line	$L/\bar{b}$	$V/\sqrt{L}$		
			4	4
1.	4		.155	4.0
2.	5		.170	4.0
3.	$L/\bar{b}$=	4.6	.164	4.0
4.			1.18	1.18
5.			1	1
6.			.194	4.7°

V. ACCELERATIONS

A. At given $H_{1/3}/b$ obtain avg cg and bow accelerations at $\tau = 4^{\circ}$ and $\beta = 20^{\circ}$

1. & 2. Obtain η_{cg} from Figs 18-20
3. Interpolate for correct $L/\bar{b}$
4. Obtain η_{bow} from Figs 21-24
5.
6. Interpolate for correct $L/\bar{b}$
7. Trim-Deadrise Correction, Eq. (6)
8. Multiply Lines 3x7 for η_{cg}
9. Multiply Lines 6x7 for η_{bow}
10. Bow warp = .85 η_{bow}
11. Interpolate for given speed

B. Repeat procedure for other $H_{1/3}/b$

		$V/\sqrt{L}$		
Line	$L/\bar{b}$	2	4	6
1	4		.30	
2	5		.56	
3	$L/\bar{b}$		.44	
4	4		.95	
5	5		1.90	
6	$L/\bar{b}$		1.40	
7			1.38	
8			.61	
9			1.93	
10*			1.64	

*May vary with bow shape

6) Effect of Design Variables on Seakeeping

The design charts previously presented are not only useful for making estimates of the loads and motions of specific planing hulls in a seaway but can also be used to identify those hull parameters which have a significant effect upon seakeeping.

6.1 Effect of Trim Angle

The mean running trim angle is of particular importance in effecting seakeeping performance. For identical loading conditions and speed, the smooth water trim is essentially equal to the mean trim in rough water. A decrease in trim angle is accompanied by reductions in pitch motions, heave motions, added resistance, and impact accelerations. This is especially the case for speed length ratios greater than 2.0. Specifically, impact accelerations are nearly linearly related to trim angle so that a 50% reduction in trim should result in a similar reduction in "g" loading. The motions and added resistance are somewhat less than linearly dependent upon trim angle - but still significantly reduced with decrease in trim.

It appears then that some means of trim control be incorporated into a design. This can be accomplished either by trim flaps or shift in ballast. The size of the trim flaps and/or the amount of ballast shift to attain a desired trim change can be determined by the analytical procedures described in Refs 1 and 2.

6.2 Effect of Deadrise Angle

All other conditions being equal (trim, speed and loading), the impact accelerations in a seaway decrease nearly linearly with increasing deadrise angle. The motions and added resistance in waves are only slightly dependent upon deadrise.

It must be noted however that, if the loading, LCG, and beam of the boat are held constant, the smooth water running trim will increase. This will consequently mitigate some of the beneficial effects of increased deadrise. Thus, some form of trim control is desirable to attain the full benefits of high deadrise.

6.3 Effect of Loading

Impact accelerations decreased nearly linearly with increasing loading coefficient, $C_{\Delta} = \Delta/wb^3$. Further, at speed length ratios greater than 2.0, the motions and added resistance are slightly reduced as the loading coefficient is increased.

This result implies that, for a given hull length, a narrow beam is most preferable for good seakeeping performance. Unfortunately, a reduction in beam results in an increased trim angle which may mitigate some of the beneficial effects of increased loading. Proper attention to LCG position or trim control can assure attainment of the advantages of high beam loading.

6.4 General Conclusions

a) Pitch and heave motions increase with increasing sea state and are generally greatest when the combination of craft speed and wave length result in wave encounter frequencies which are equal to the natural heave and pitch period of the craft.

b) Motions appear to be maximum for wave lengths of the order 2-3 times the hull length and are substantially reduced in wave lengths less than 1.5 times the hull length.

c) In an irregular sea, large motion responses to those wave components having the greatest energy are to be expected - especially if these represent synchronous response with the natural heave and pitch period of the craft.

7) Pressure Distributions During Impact

A knowledge of bottom impact pressures is required for structural design. Research on this problem is currently underway and, hopefully, procedures for accurately predicting these pressures will soon be developed. For the present purposes, consideration will be given

a) to theoretical pressure distributions for a two-dimensional wedge, and

b) to a presentation of the Heller-Jasper technique currently used to estimate bottom pressures.

The two-dimensional case will illustrate the general characteristics of the planing pressures and their dependence upon trim, velocity, and deadrise. The Heller-Jasper results will present current procedure for estimating design bottom pressures.

7-1 Pressure Distribution For a Two-Dimensional Chines Dry Wedge

The equivalence between a planing surface and a two-dimensional wedge penetrating a fluid surface in a plane normal to the water surface is the basis for this analysis. To obtain the pressure distribution on this wedge, vonKarman[20] simulated the wedge penetration by the potential flow about the lower surface of a submerged flat plate moving normal to itself and expanding in width at a rate equal to increasing beam of the two-dimensional wedge. This is referred to as the "expanding plate" analogy and is illustrated below:

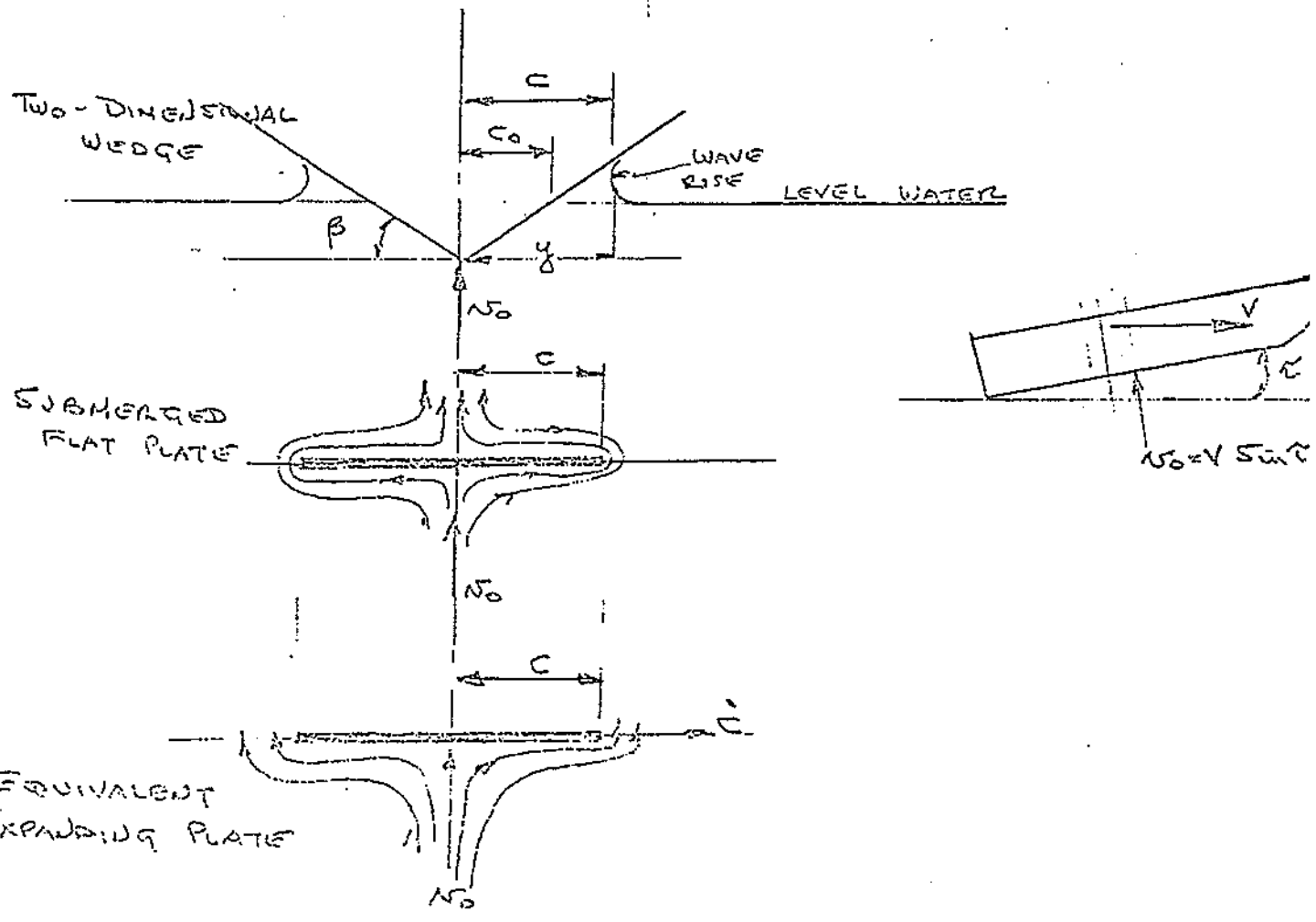

From potential flow theory for the flow about a submerged flat plate.

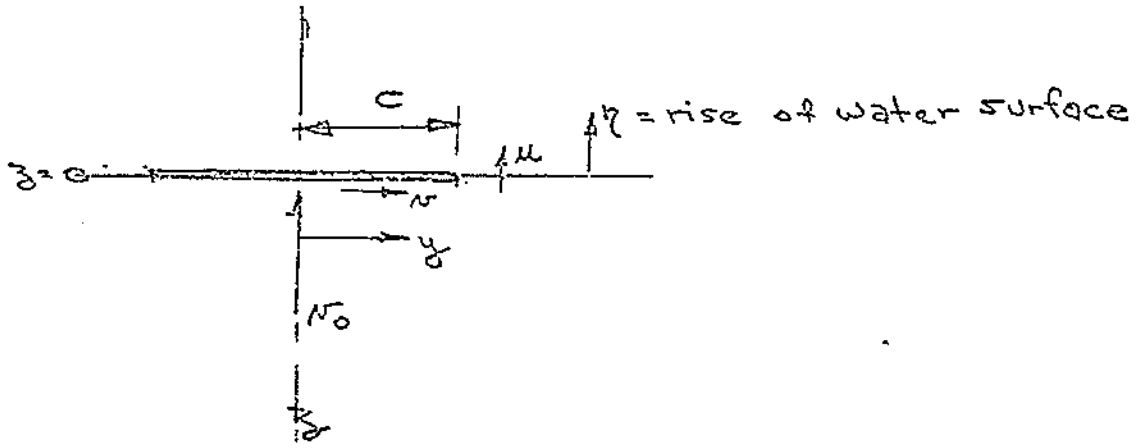

On the plate:

$$\varphi = \pm v_o (c^2 - y^2)^{1/2} \tag{1}$$

$$v = \frac{\mp v_o y}{(c^2 - y^2)^{1/2}} \tag{2}$$

Outside plate, at $z = 0$

$$u = v_o \frac{y}{(y^2 - c^2)^{1/2}} \tag{3}$$

7.1.1 Computation of Rise of Water Surface

At $z = 0$ the rise of the water surface during time, t, is obtained by integrating equation (3)

$$\eta = \int_o^t u \, dt = \int_o^t v_o \frac{y}{(y^2 - c^2)^{1/2}} \, dt \tag{4}$$

the time variable, t, is inconvenient and can be eliminated by noting that the half width, c, increases with time:

$$t = t(c)$$

$$dt = \frac{1}{\frac{dc}{dt}}\, dc = \frac{1}{\dot{c}}\, dc \tag{5}$$

where $\dot{c}$ is the rate of expansion of the plate. The water surface rise is now expressed:

$$\eta = \int_o^c \frac{v_o}{\dot{c}} \frac{y}{(y^2-c^2)^{1/2}}\, dc \tag{6}$$

Regard y as a fixed quantity and vary the wetted width, c, to approach y in the sense of the expanding plate analogy. For a simple deadrise wedge, penetrating a fluid surface at a constant velocity, $\dot{c}$ is also a constant. Thus, integrating (6);

$$\eta = y \frac{v_o}{\dot{c}} \sin^{-1} \frac{c}{y} \int_o^c \tag{7}$$

At the instant when the rise of a surface water particle is such as to bring it into contact with the wedge:

$$\eta = y \tan\beta$$

$$y = c$$

Evaluating the limits in the integrated equation for η

$$y \tan\beta = \frac{y v_o}{\dot{c}} \frac{\pi}{2}$$

and finally $$\dot{c} = \frac{\pi}{2} \frac{v_o}{\tan\beta} \tag{8}$$

For the simple deadrise wedge, $\dot{c}$ is a constant for constant v_o:

$$\dot{c}_o = \frac{v_o}{\tan\beta} \tag{9}$$

so that from (8) and (9) it can be shown that

$$c = \frac{\pi}{2} c_o \tag{10}$$

which is the wave rise for a planing deadrise surface in the chines dry area. This relation has been experimentally verified by numerous model tests (Ref 1).

7.1.2 Pressure Distribution for Wedge in Chines Dry Area

For the case of a submerged plate of constant width in a uniform flow normal to the plate, the pressures are simply obtained from the Bernoulli equation

$$p + \frac{\rho v^2}{2} = \text{constant} = p_\infty + \frac{\rho v_o^2}{2}$$

where:

p, v, denote pressure and velocity on the plate

p_∞, v_o, denote pressure and velocity at infinity

From the previous section then:

$$p - p_\infty = \frac{\rho v_o^2}{2} \left(1 - \frac{y^2}{c^2 - y^2}\right) \tag{11}$$

at $y = 0$ (keel)

$$p - p_\infty = \frac{\rho v_o^2}{2}$$

which is the stagnation pressure.

For the non-steady flow represented by the expanding plate analogy to the penetrating wedge, the half-breadth, c, of the plate increases with time so that the velocity potential, φ, is also variable. Thus the general form of Bernoulli equation is required.

$$\frac{p}{\rho} = -\frac{\partial \varphi}{\partial t} - \Omega - \frac{v^2}{2} + F(t) \tag{12}$$

where:

Ω = extraneous force, assumed to be zero

$F(t)$ = Bernoulli constant (so-called)

$F(t)$ is evaluated at infinity where $\frac{\partial \varphi}{\partial t} = 0$

Thus:

$$F(t) = \frac{v_o^2}{2} + \frac{p_\infty}{\rho} \tag{13}$$

Recalling that, on the plate:

$$\varphi = -v_o(c^2-y^2)^{1/2}$$

$$v = \frac{v_o y}{(c^2-y^2)^{1/2}}$$

c = variable width

y = point fixed on plate

v_o = variable (as in impact)

Equation (60) can now be written:

$$\frac{p}{\rho} = \sqrt{c^2-y^2}\,\frac{dv_o}{dt} + \frac{v_o^2 c}{\lambda\sqrt{c^2-y^2}} - \frac{v_o^2 y^2}{2(c^2-y^2)} + \frac{v_o^2}{2} \tag{14}$$

where $\lambda = v_o/\dot{c}$

For the case of constant penetration velocity (v_o) as in planing, $dv_o/dt = 0$ and

$$p = \frac{\rho v_o^2}{2}\left[\frac{2c}{\lambda(c^2-y^2)^{1/2}} - \frac{y^2}{c^2 y^2} + 1\right] \tag{15}$$

The first term on the right hand side of the above equation is the pressure due to the expansion of the wetted width, c ; the second term is that due to flow along the surface of the plate; and the third is

the stagnation pressure. These three terms are separately plotted in Fig 25 along with their summation. It is seen that the pressure at the keel is greater than the original stagnation pressure and that the peak pressure, which is considerably higher than the keel pressure, occurs near the outer edge of wetted width. Various characteristics of the pressure distribution are obtained from Eq 15 and are summarized below.

Pressure at Centerline (keel)

$$p = \frac{\rho v_o^2}{2} \left(\frac{2}{\lambda} + 1\right)$$

Position of Zero Pressure $(y)_{p=0}$

$$(y)_{p=0} = c \left(1 - \frac{\lambda^2}{8}\right)$$

Maximum Pressure $(p)_{max}$

$$(p)_{max} = \frac{\rho v_o^2}{2} \left(\frac{1}{\lambda^2} + 2\right)$$

Position of Maximum Pressure $(y)_{p_{max}}$

$$(y)_{p_{max}} = c\sqrt{1 - \lambda^2}$$

As an example, consider a constant deadrise wedge:

$$\beta = 22\text{-}1/2^o$$

$$\tan\beta = .413$$

$$\lambda = \frac{v_o}{\dot{c}} = \frac{\dot{c}_o \tan\beta}{\dot{c}} = \frac{2}{\pi} \tan\beta = 0.263$$

Then:

a) Keel pressure: $\frac{\rho v_o^2}{2}\left[\frac{2}{\lambda} + 1\right] = 8.6 \frac{\rho v_o^2}{2}$

which is considerably higher than the keel pressure for a non-expanding plate.

b) Maximum Pressure: $\frac{\rho V_o^2}{2}\left(\frac{1}{\lambda^2} + 2\right) = 16.4\,\frac{\rho V_o^2}{2}$

which is nearly twice the keel pressure.

c) Position of Maximum Pressure:

$$(y)_{P_{max}} = c\sqrt{1 - \lambda^2} = .965c$$

d) Position of Zero Pressure:

$$(y)_{p=0} = c\left(1 - \frac{\lambda^2}{8}\right) = .99c$$

For deadrise angles less than approximately 15^o-20^o, compressibility effects become important so that the above formulations lose their applicability. Chuang (Ref 21) presents a tabulation of pressure coefficients for deadrise angles less than 15^o. For flat plate surfaces, the maximum pressure at the leading edge of the planing surface is $\frac{1}{2}\rho V^2$ for all trim angles where V is the forward planing velocity.

The previous discussions were only intended to illustrate the general characteristics of planing pressures and their dependence upon trim, velocity, and deadrise. Ideal two-dimensional models were used and these were restricted to the chines dry area of the hull. For complete pressure distribution over hull bottoms as obtained in model tests of both planing and impacting surfaces, the reader is referred to the works of Smiley (Refs 22 to 24), and others. These results and many others, should eventually be summarized in a form beneficial to the small craft designer.

7.2 Design Bottom Loads (Heller-Jasper)

The design procedure formulated by Heller-Jasper (Ref. 25) is semi-empirical and is based upon extensive full-scale experimental pressure and load data obtained from extensive rough water tests of an aluminum motor torpedo boat of the following dimensions:

Weight	=	109,000 lb	B = 15'
LWL	=	75'	d = $3'-2\frac{1}{2}''$
β_{av}	=	20^{o}	

The boat was extensively instrumented with pressure gauges, strain gauges, and accelerometers. It was run in the roughest water at the highest speed considered safe for the operating personnel. Waves from 4 to 6 feet in height with length-beam ratio of about 20 were encountered.

The primary objective of these full-scale tests was to determine the local loading of plating panels and frames. Pressure gauges were so located as to permit determination of the transverse as well as longitudinal distribution of bottom pressure during impact. It was found that, as the boat planes over a wave, the point of initial impact occurs at the hull, but at a longitudinal location which depends on the relative attitude of the boat and wave at time of impact. The bottom area subjected to impact pressures then increases with time, moving along the keel and spreading laterally as more of the bottom is wetted. The maximum impact force (and acceleration) is attained after initial impact. The peak local pressure at any given section, at any instant of time, is located near the instantaneous water line according to the theoretical analysis in Section 7.1.

An examination of the full-scale pressures indicated that the transverse load distribution over the entire girth from keel to chine could be reasonably approximated by a versed sine function. Furthermore, the pressure peak appears to traverse the girth during each impact. The longitudinal distribution of pressure indicated that the maximum values occur between 25 and 50% of the length from the bow. There was a linear

reduction to 50% of the peak value at the bow and to 25% at the stern. In addition, rigid-body impact accelerations varied linearly from bow to stern.

It is found that the maximum effective pressure for the entire boat does not occur when the accelerations are greatest. The maximum linear acceleration of the center of gravity occurs at the instant at which the total pressure force on the boat is a maximum. In the semi-empirical design procedure developed by Heller and Jasper, it is assumed that the maximum impact force occurs at the time when the entire half girth G is immersed and that maximum effective pressure occurs when the wetted width extends over only about one-third of the distance from keel to chine, G/3.

Heller and Jasper used the experimental longitudinal and transverse pressure distributions and develop empirical relations between maximum g loading and design pressures for bottom plating transverse framing, and longitudinal framing. These expressions are summarized below.

a) Peak Pressure (P_{01})

$$P_{01} = \frac{3}{G}\left[\frac{3}{2}\frac{W}{L}\left(1 + \frac{\ddot{y}_{CG}}{g}\right)\right]$$

where:

G = girth, transverse distance between keel and chine

W = weight of craft

L = length of craft

$\ddot{y}_{CG}$ = impact acceleration at CG determined by model tests or computational method by Fridsma (Ref. 9)

g = acceleration of gravity

b) Maximum Effective Pressure ($\bar{p}$)

$$\bar{p} = P_{01} \times \text{Dynamic Load Factor}$$

Dynamic Load Factor = 1.1

c) Equivalent Static Pressure for Design of Bottom Plating (p)

$$p = \bar{\bar{p}} + p_h$$

p_h = hydrostatic pressure for craft at rest

This formulation applies to panels between 25% and 50% of the length forward of the stern and for panel widths less than 10% of the half-girth. For other panel locations and sizes, the reader is referred to Reference 25.

d) Bottom Pressure for Longitudinal Framing (p_L)

$$p_L = \bar{\bar{p}} \times .38 \div p_h$$

This formulation applies to bottom frames at approximately midship. For other longitudinal frame locations refer to Reference 25.

e) Bottom Pressure for Transverse Frame (p_T)

$$p_T = \bar{\bar{p}} \times .67 + p_h$$

The work of Heller and Jasper contains considerably more detail relative to structural design of planing hulls. The reader is strongly urged to become familiar with this reference prior to undertaking a new design.

REFERENCES

1. Daniel Savitsky, "Hydrodynamic Design of Planing Hulls," MARINE TECHNOLOGY, Vol. 1, No. 1, October 1964.

2. P. Ward Brown, "An Experimental and Theoretical Study of Planing Surfaces with Trim Flaps," Davidson Laboratory, Stevens Institute of Technology SIT-DL-71-1463, April 1971.

3. E.P. Clement and J.O. Pope, "Graphs for Predicting the Resistance of Large Stepless Planing Hulls at High Speeds," DTMB Report 1318, April 1959.

4. C.L. Shuford, Jr., "A Theoretical and Experimental Study of Planing Surfaces including Effects of Cross Section and Plan Form," NACA Report 1355, 1958.

5. K.S.M. Davidson and A. Suarez, "Tests of Twenty Related Models of V Bottom Motor Boats--EMB Series 50," DTMB Report R-47, March 1949.

6. E.O. Clement and D.L. Blount, "Resistance Tests of a Systematic Series of Planing Hull Forms," Trans. SNAME, Vol. 71, 1963.

7. Daniel Savitsky, "On the Seakeeping of Planing Hulls," MARINE TECHNOLOGY, Vol. No. 2, April 1968.

8. Gerard Fridsma, "A Systematic Study of the Rough Water Performance of Planing Boats," Davidson Laboratory, Stevens Institute of Technology SIT-DL-69-1275, November 1969.

9. Gerard Fridsma, "A Systematic Study of the Rough Water Performance of Planing Boats - Irregular Waves, Part II. Davidson Laboratory, Stevens Institute of Technology SIT-DL-71-1495, March 1971.

10. Edward V. Lewis, "Lecture Notes on Ship Behavior at Sea," Summer Seminar at Stevens Institute of Technology, June 1956.

11. Willard Bascom, "Ocean Waves," Scientific American, August 1959.

12. W.J. Pierson, Jr., G. Neumann, and R.W. James, "Practical Methods for Observing and Forecasting Ocean Waves by Means of Wave Spectra and Statistics," U.S. Hydrographic Office Publication 603, 1955.

13. Horace Lamb, "Hydrodynamics," Cambridge, England, 1924.

14. B.V. Korvin-Kroukovsky, "Theory of Seakeeping," SNAME, New York, N.Y., 1962.

15. E.V. Lewis, "Principles of Naval Architecture," SNAME, New York, N.Y., 1967.

16. W.J. Pierson, Jr. and W. Marks, "The Power Spectrum Analysis of Ocean Wave Records," Trans. AGU Vol. 33, 1952, p. 834.

17. Wilbur Marks, "The Application of Spectral Analysis and Statistics to Seakeeping," SNAME, T & R Bulletin No. 1-24.

18. L. Moskowitz, W.J. Pierson, and E. Mehr, "Wave Spectra Estimated from Wave Records Obtained by OWS Weather Explorer and OWS Weather Reporter, New York University, College of Engineering Research Division, 1962, 1963.

19. M. St. Denis, and W.J. Pierson, Jr., "On the Motions of Ships in Confused Seas," Trans. SNAME 1955.

20. Th. von Karman, "The Impact of Seaplane Floats During Landing," NACA TN 321, 1929.

21. S. Chuang, "Impact Pressure Distributions on Wedge-Shaped Hull Bottoms of High Speed Craft," NSRDC R-2953, August 1969.

22. R.F. Smiley, "Water Pressure Distributions During Landings of a Prismatic Model Having an Angle of Deadrise of 22½ Degrees," NACA TN 2816, November 1952.

23. R.F. Smiley, "An Experimental Study of Water Pressure Distributions During Landings and Planing of a Heavily Loaded Rectangular Flat-Plate Model," NACA TN 2453, September 1951.

24. R.F. Smiley, "A Theoretical and Experimental Investigation of the Effects of Yaw on Pressures, Forces, and Moments During Seaplane Landings and Planing," NACA TN 2817, November 1952.

25. S.R. Heller, Jr. and N.H. Jasper, "On the Structural Design of Planing Craft," Transactions of Royal Institute of Naval Architects, July 1960.

TABLE I

WIND AND SEA SCALE FOR FULLY ARISEN SEA

SEA-GENERAL			WIND[3]					SEA[3]							
DESCRIPTION[1]	(BEAUFORT) WMO FORCE	DESCRIPTION	RANGE (KNOTS)	SEA STATE	WIND VELOCITY (KNOTS) AVERAGE	WAVE HEIGHT FEET (AVERAGE 1/10 HIGHEST) SIGNIFICANT	SIGNIFICANT RANGE OF PERIODS (SECONDS)	PERIODS OF MAXIMUM ENERGY OF SPECTRUM T (AVERAGE OF 10%)	T (AVERAGE OF 10%)	WAVELENGTH (AVERAGE WAVE LENGTH) (NAUTICAL MILES)	WAVE VELOCITY (KNOTS)				
See Beaufort table.	0	Calm			0	0	0	0	-	-	-	-	-	-	
Ripples with the appearance of scales are formed, but without foam crests.	1	Light Air	1 - 3	0	1	0.03	0.08	0.10	up to 1.2 sec	0.7	0.5	10 in.	1	1.4 - 1.6	
Small wavelets, still short but more pronounced; crests have a glassy appearance, but do not break.	2	Light Breeze	4 - 6		5	0.19	0.59	0.77	0.6-1.4	1.0	1.4	5.3 ft	8	19 min	
Large wavelets, crests begin to break. Foam of glassy appearance. Perhaps scattered white horses.	3	Gentle Breeze	7 -10	1	8.3	0.5	1.0	1.2	0.8-1.8	3.4	2.7	30	7.8	1.7 hrs	
					10	0.86	1.4	1.8	1.0-4.0	4	2.7	27	10	1.4	
Small waves, becoming longer; fairly frequent white horses.	4	Moderate Breeze	11-16	2	12	1.4	2.2	2.8	1.0-5.0	4.8	3.4	40	14	2.8	
					13.3	1.6	2.9	3.7	1.4-2.8	5.4	3.9	53	24	4.3	
					14	2.0	3.3	4.2	1.5-2.3	3.6	1.0	39	28	5.2	
				3	16	2.9	4.6	5.6	3.0-8.8	6.5	6.4	71	40	8.4	
Moderate waves, taking a more pronounced long form; many white horses are formed. (Chance of some spray).	5	Fresh Breeze	17-21		18	3.8	6.1	7.6	3.3-10.0	7.2	5.4	90	55	8.2	
				4	19	4.3	6.9	8.3	3.4-10.6	7.3	5.4	99	63	8.5	
					20	5.0	8.0	10	3.0-11.3	8.1	5.3	111	77	10	
Large waves begin to form; the white foam crests are more extensive everywhere. (Probably some spray).	7	Strong Breeze	22-27	5	22	8.4	10	13	3.4-12.2	8.0	5.5	130	100	12	
					24	2.9	11	16	3.7-13.5	9.3	6.3	160	130	14	
					24.3	8.2	15	21	3.8-13.6	9.3	7.0	164	140	15	
				6	26	9.8	15	20	4.0-14.5	10.3	7.4	188	180	17	
Sea heaps up and white foam from breaking waves begins to be blown in streaks along the direction of the wind. (Spindrift begins to be seen).	7	Moderate Gale	28-33		22	11	18	23	4.5-15.5	11.3	7.9	217	230	20	
					30	14	22	28	4.2-16.9	11.1	8.6	250	280	25	
					30.5	14	22	29	4.8-17.0	12.4	8.7	255	290	24	
					33	16	26	33	5.0-17.5	12.9	9.3	285	330	27	
Moderately high waves of greater length; edges of crests begin to spindrift. The foam is blown in well marked streaks along the direction of the wind. Spray affects visibility.	8	Fresh Gale	34-40	7	34	19	30	38	5.3-18.3	13.4	9.7	321	420	30	
					36	22	35	44	5.8-19.3	14.5	10.3	363	500	33	
					37	23	37	46.7	6-20.5	14.9	10.5	326	530	37	
					38	25	40	50	6.8-20.0	15.4	10.7	398	600	38	
					40	26	43	53	6.5-21.2	16.1	11.4	444	710	43	
High waves. Dense streaks of foam along the direction of the wind. Sea begins to roll. Visibility affected.	8	Strong Gale	41-47	8	43	31	50	61	7-23	17.0	13.0	492	810	47	
					44	36	54	25	7-24.7	17.7	12.5	534	960	52	
					46	40	61	81	2-25	18.6	13.3	590	1110	52	
Very high waves with long overhanging crests. The resulting foam is in great patches and is blown in dense white streaks along the direction of the wind. On the whole the surface of the sea takes a white appearance. The rolling of the sea becomes heavy and shock-like. Visibility is affected.	10	Whole Gale*	48-55		49	44	51	70	2-27.5	19.4	13.0	630	1250	63	
					52	42	78	97	7-5-27	20.2	14.7	700	1420	69	
					51.5	52	51	104	2-28.5	20.6	13.7	726	1360	53	
				9	52	51	62	110	8-18.5	21.0	14.8	750	1410	65	
					54	59	91	131	7-29.3	21.8	15.4	810	1650	61	
Exceptionally high waves (small and medium-sized ships might for a long time be lost to view behind the waves). The sea is completely covered with long white patches of foam lying along the direction of the wind. Everywhere the edges of the wave crests are blown into froth. Visibility affected.	11	Storm*	56-63		56	64	105	135	7-5-31	22.8	16.1	910	2103	86	
					59.5	75	116	142	10-32	24	15.0	885	2505	101	
Air filled with foam and spray. Sea completely white with driving spray; visibility very seriously affected.	12	Hurricane*	64-71		> 64	> 85[1]	> 125[1]	> 164[1]	10-1351	1161	1161	~	~	~	

*For twelve winds [and] above, whole gale and storm] require those used for rarely sustained over [duration] fully arisen.

a)A heavy [illegible] means that the values tabulated are at the centre of the [twelve] ranges.

b)For such [illegible], the sea confused. The crests blow at the water and ale etc.

3)Manual of Sea Volume II, Admiralty London, H.M. Stationery Office, 1951, pp.

3)Practical met observing and forecasting Ocean Petterssen, Second James, N.Y. McGraw College of Engineering 1951.

This table compiled by Wilbur Marks, Davis Polhemus Hotel Boston

FIGURE 1

TYPICAL OCEAN WAVE RECORD AT A FIXED POINT

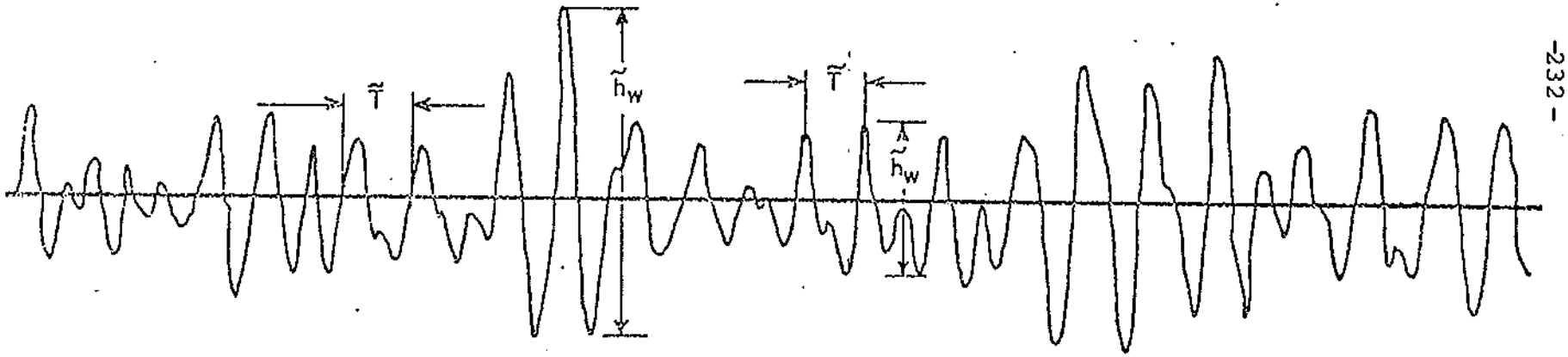

FIGURE 2

SUPERPOSITION OF REGULAR WAVES TO FORM IRREGULAR SEA

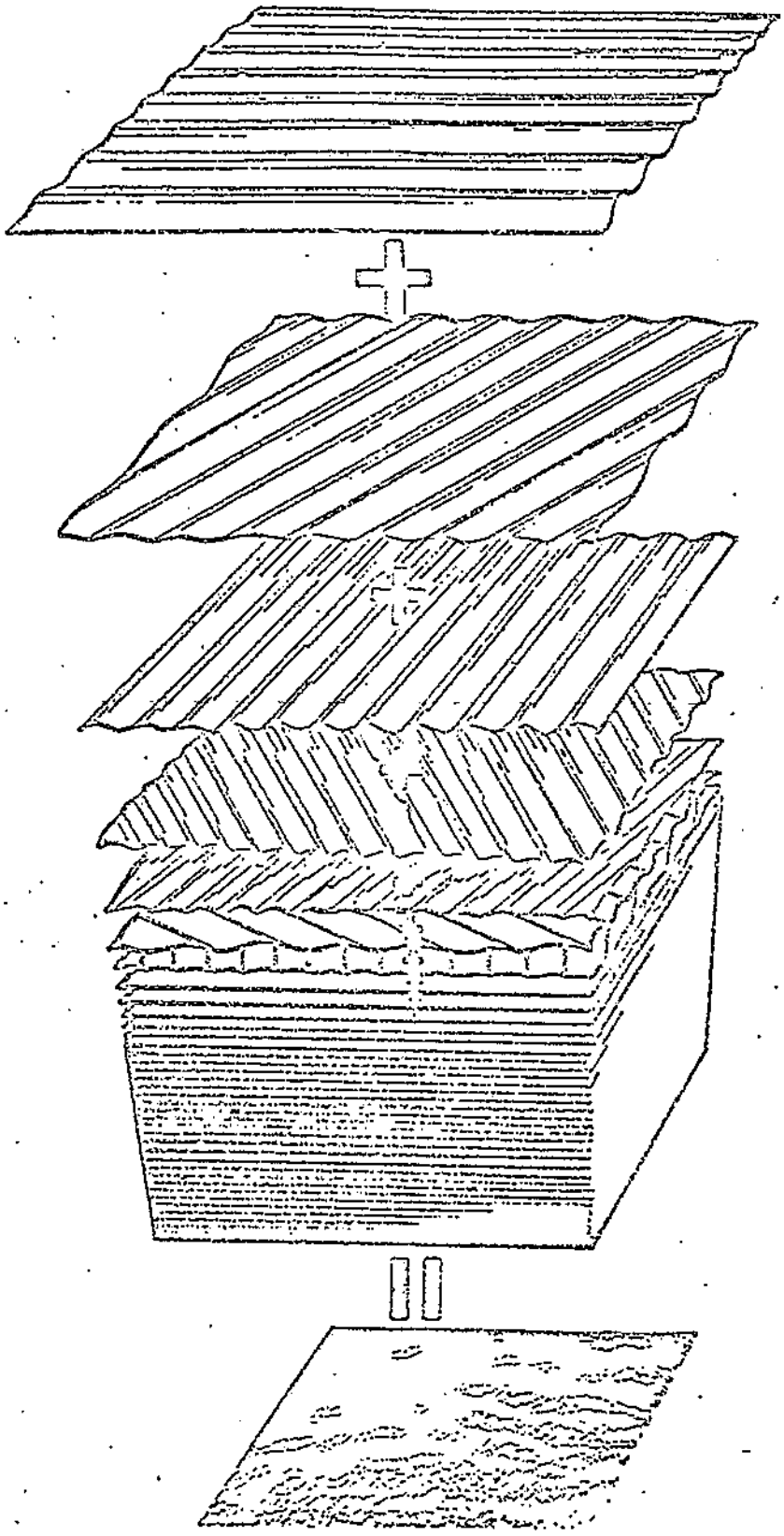

FIGURE 3

SIMPLE REGULAR GRAVITY WAVE

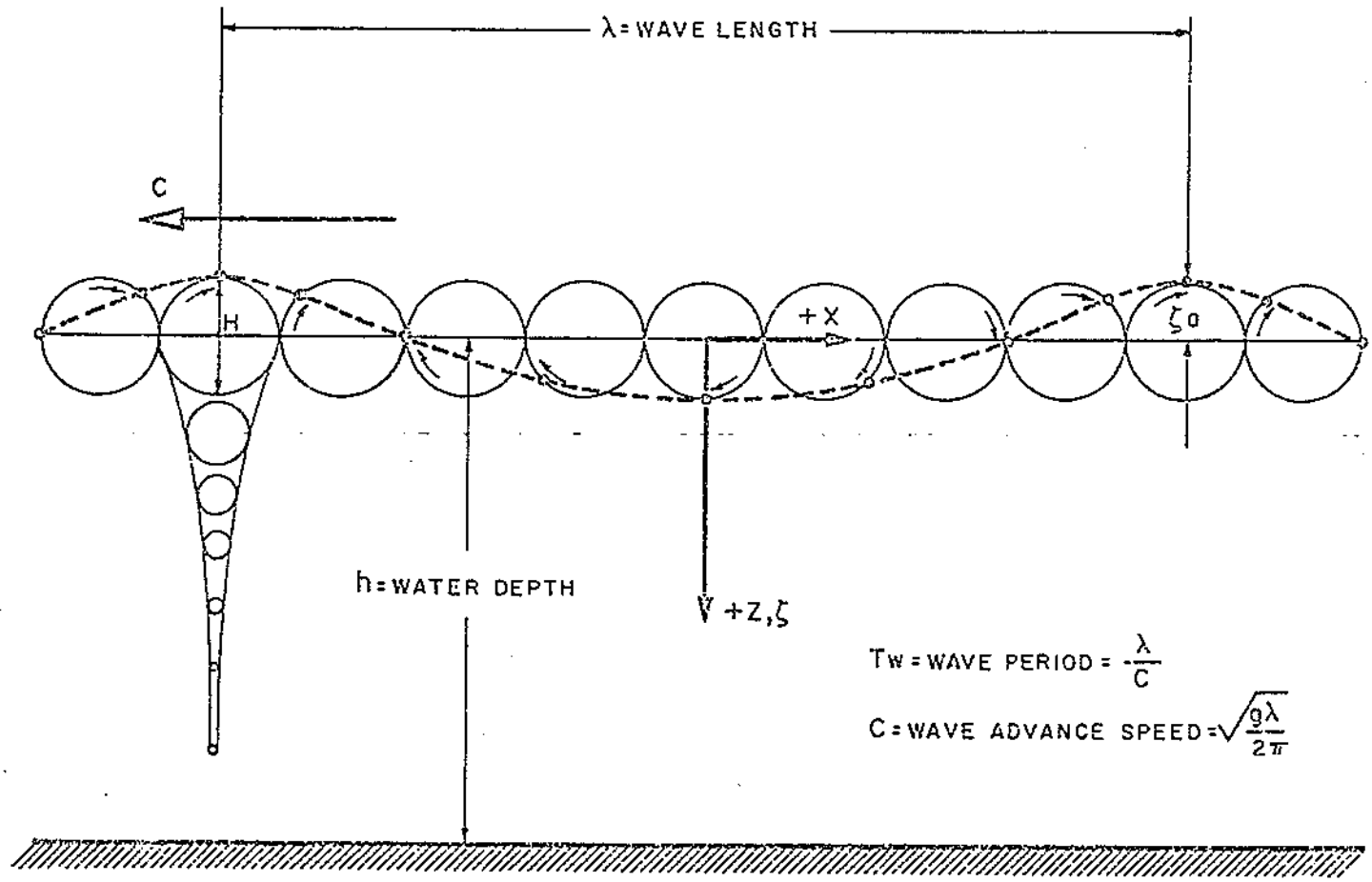

FIGURE 4

TYPICAL SEA SPECTRA (REF. 18)

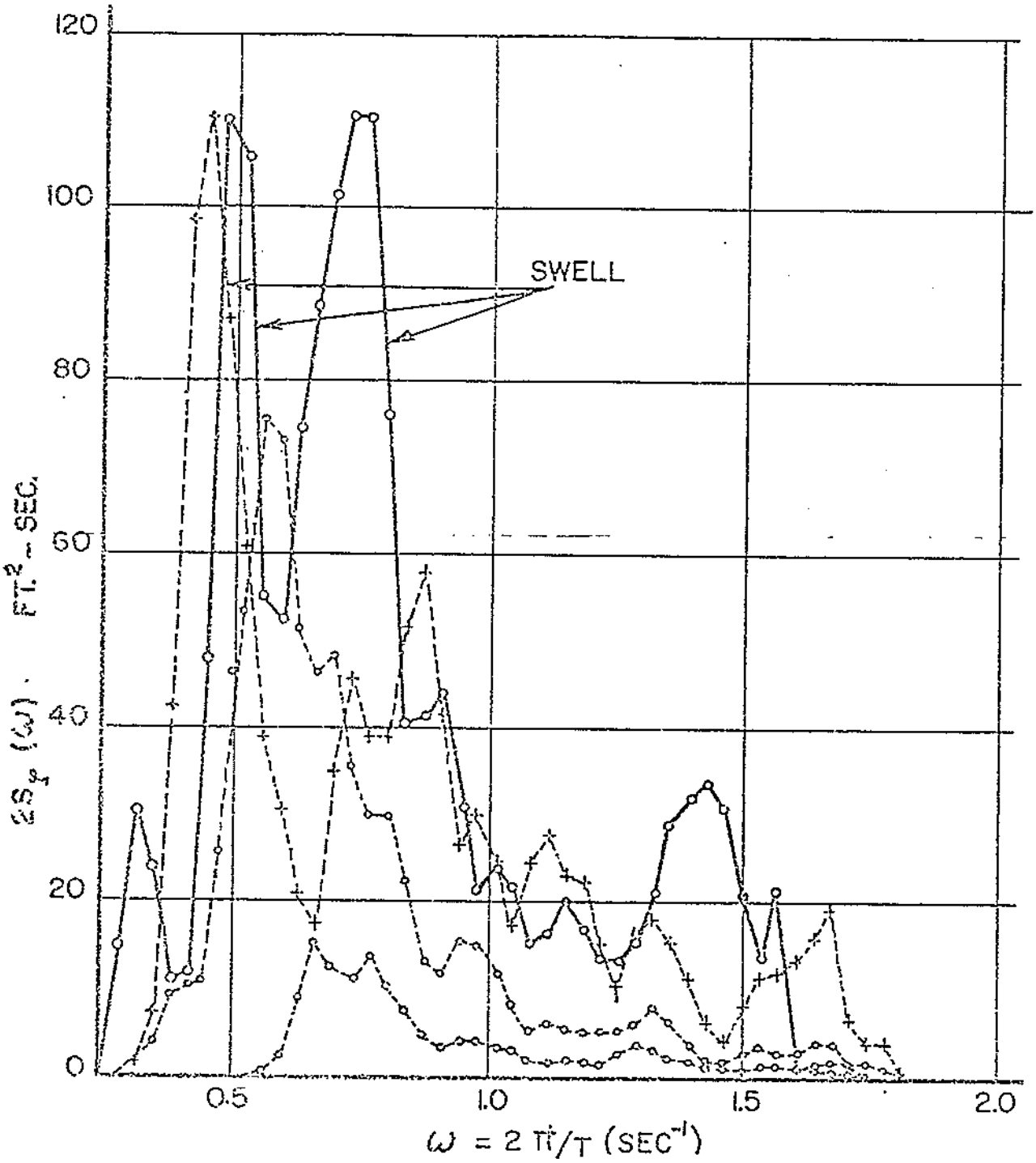

FIGURE 5
-236-

IDEALIZED TYPICAL ENERGY SPECTRUM

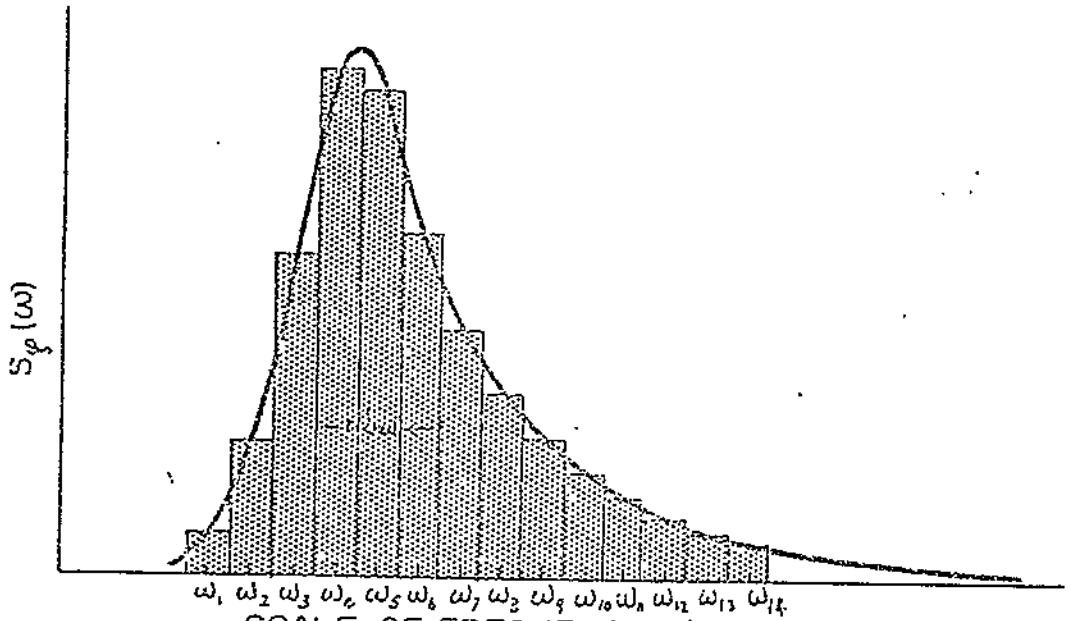

SCALE OF FREQUENCY. $\omega = 2\pi/T$

(a) SPECTRUM

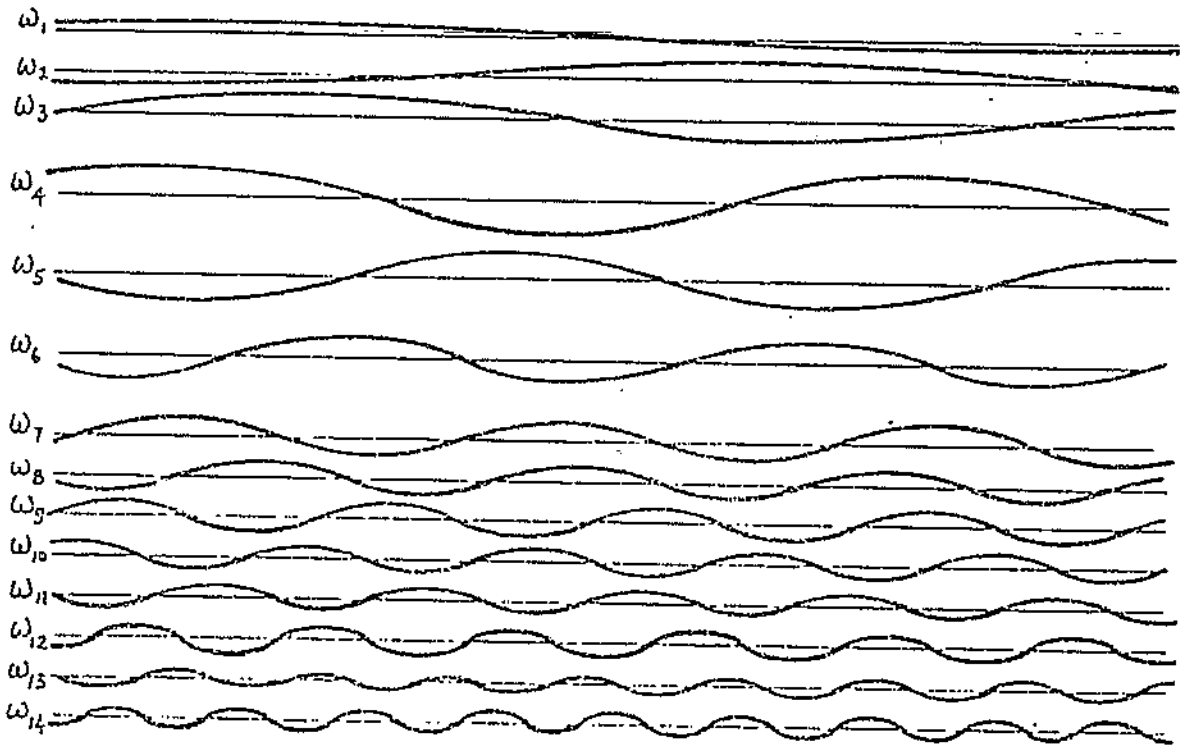

SCALE OF TIME OR DISTANCE

LENGTH OF EACH = $5.12\ T^2 = 200/\omega^2$ AMPL. = $\sqrt{2 S_\zeta(\omega_n)\,\delta\omega}$

(b) COMPONENT WAVES

FIGURE 6

FREQUENCY OF OCCURRENCE OF DEVIATIONS

FROM MEAN VALUE ON WAVE RECORD

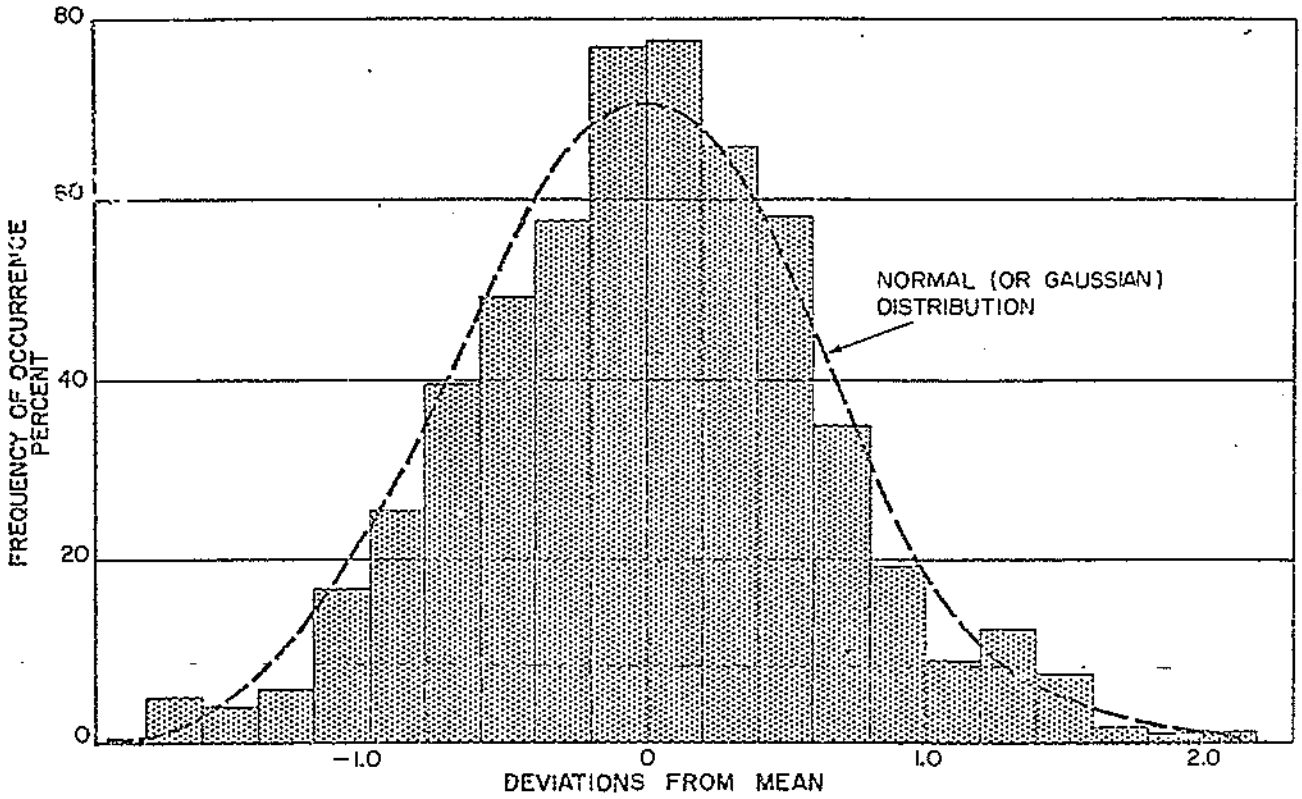

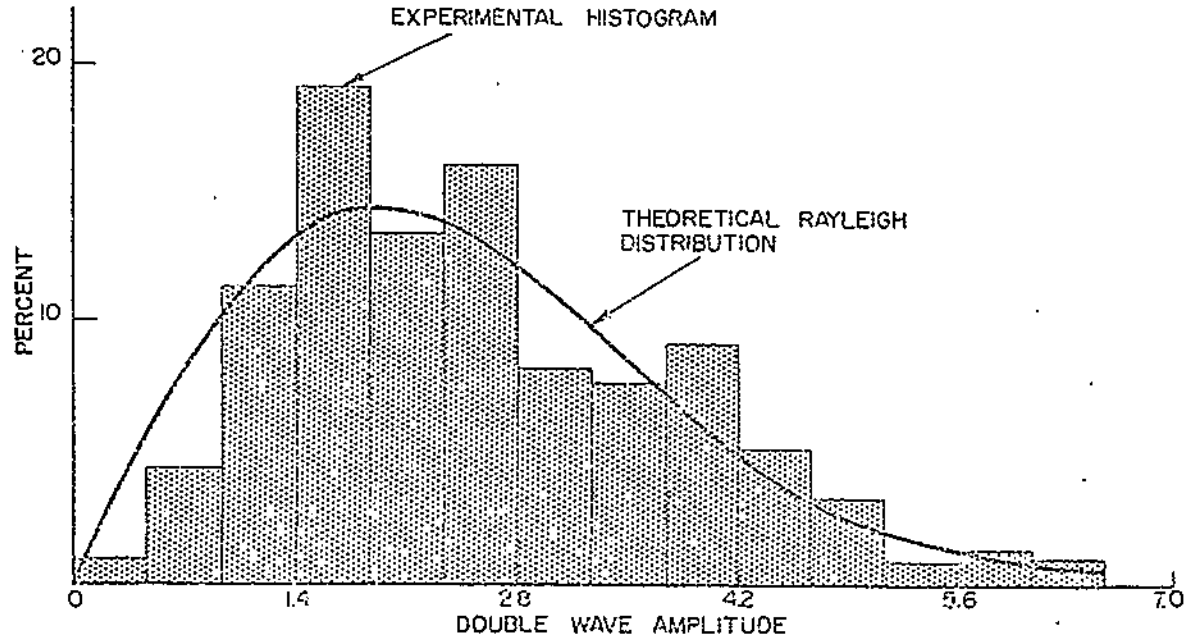

FIGURE 7

TYPICAL DISTRIBUTION OF WAVE COMPONENTS

IN IRREGULAR SEA RECORD

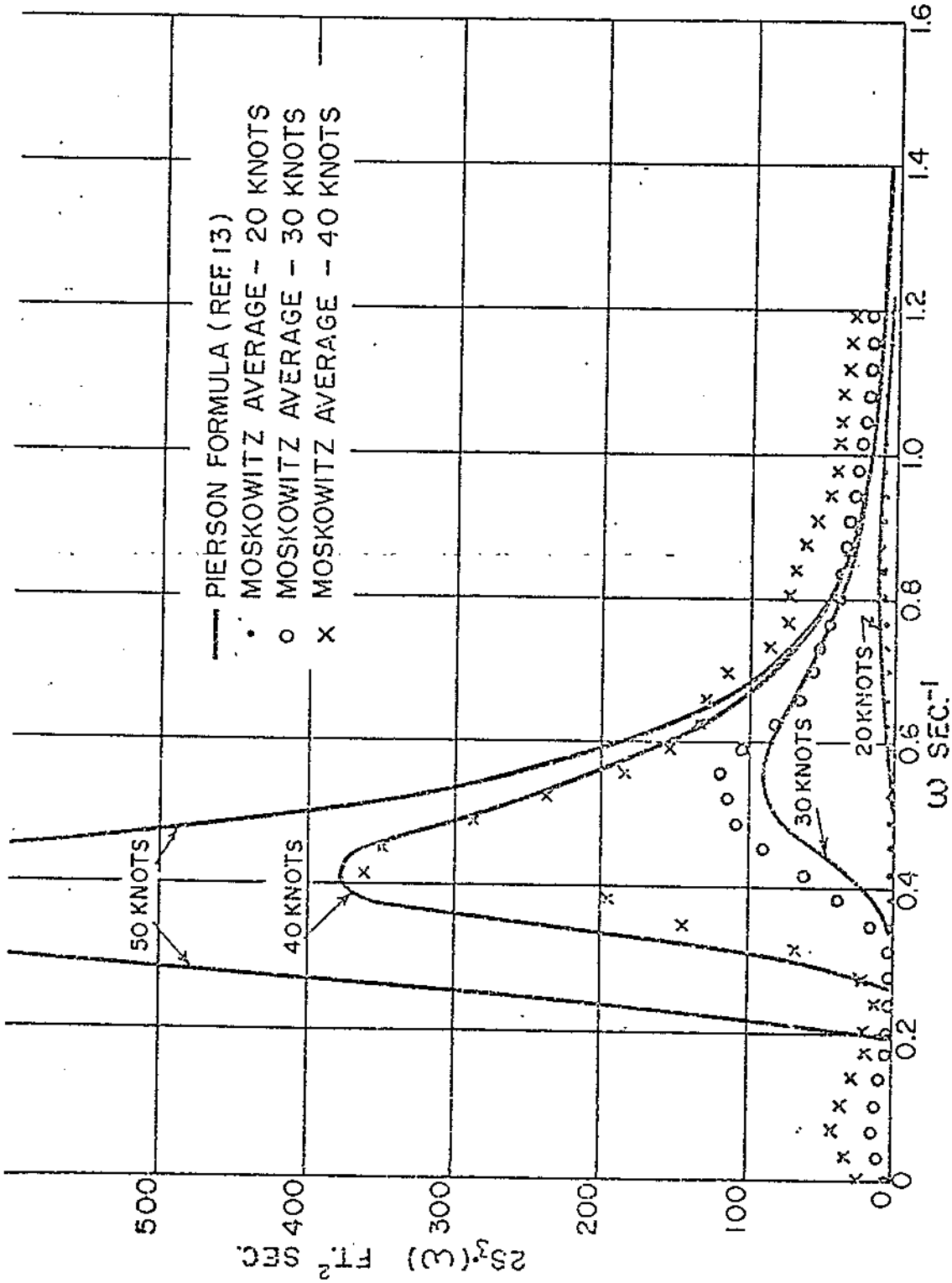

FIGURE . 8

FAMILY OF SEA SPECTRA

FIGURE 9

TYPICAL PITCHING RESPONSE TO IRREGULAR SEAS

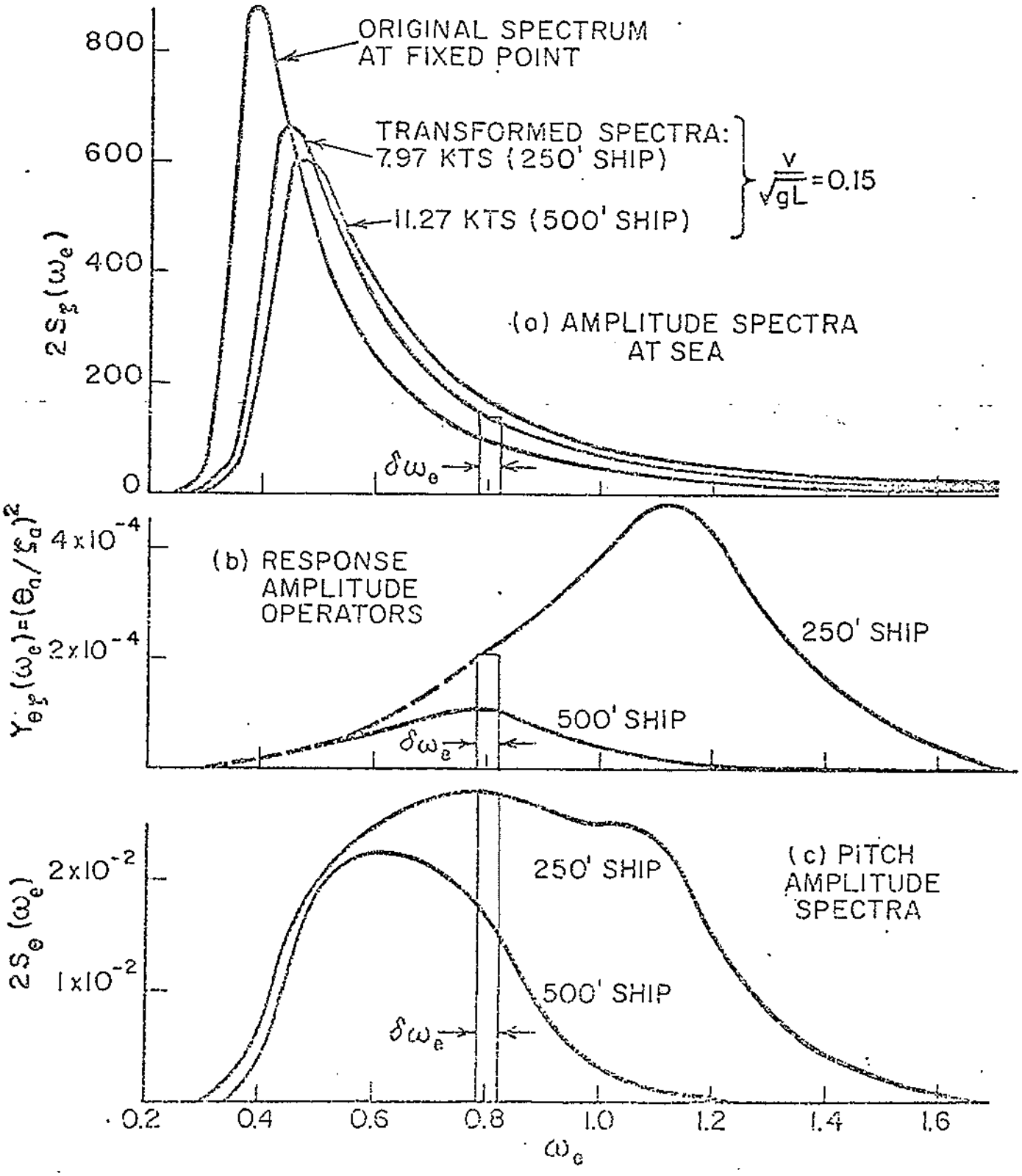

FIGURE 10
LINES OF PRISMATIC MODELS

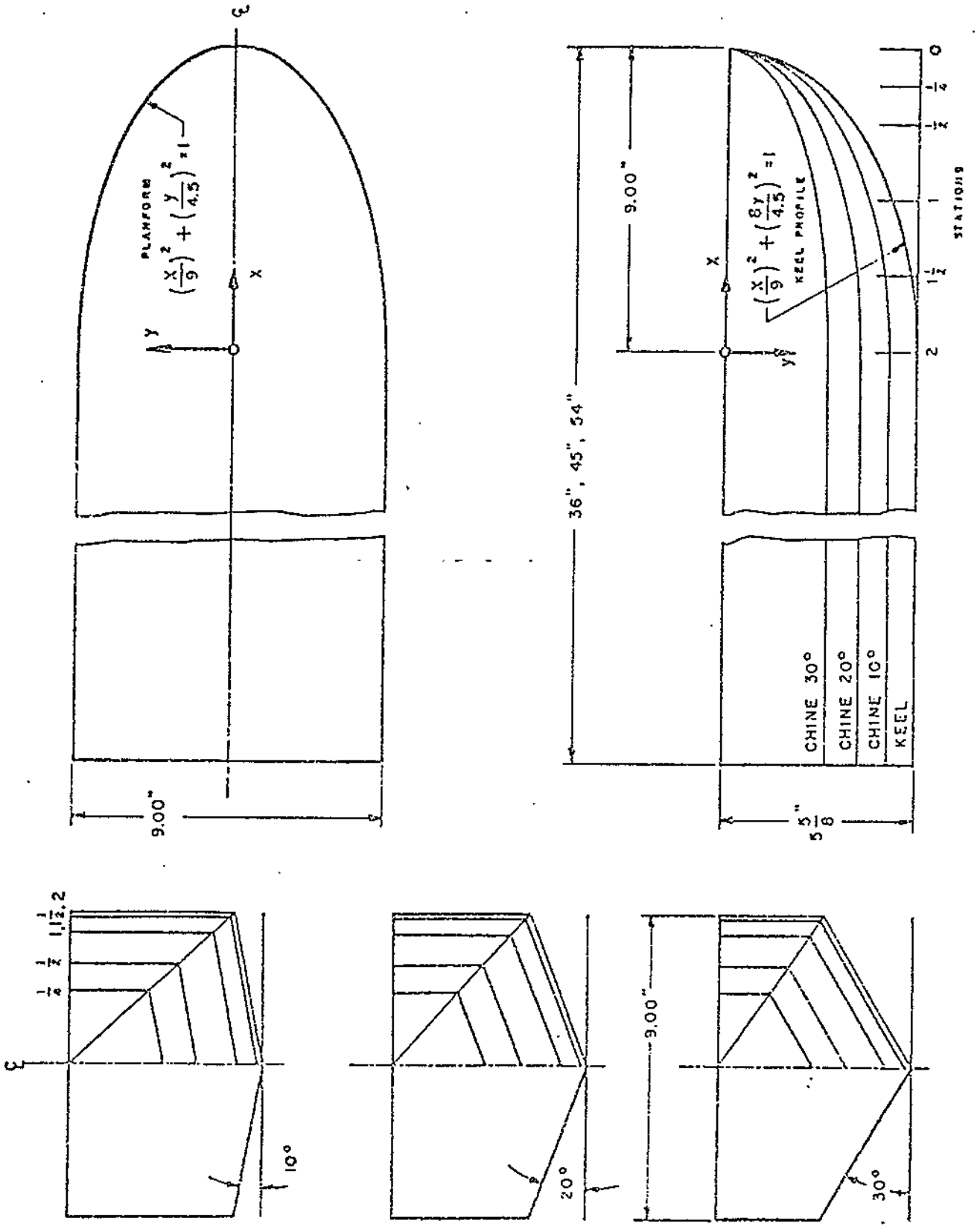

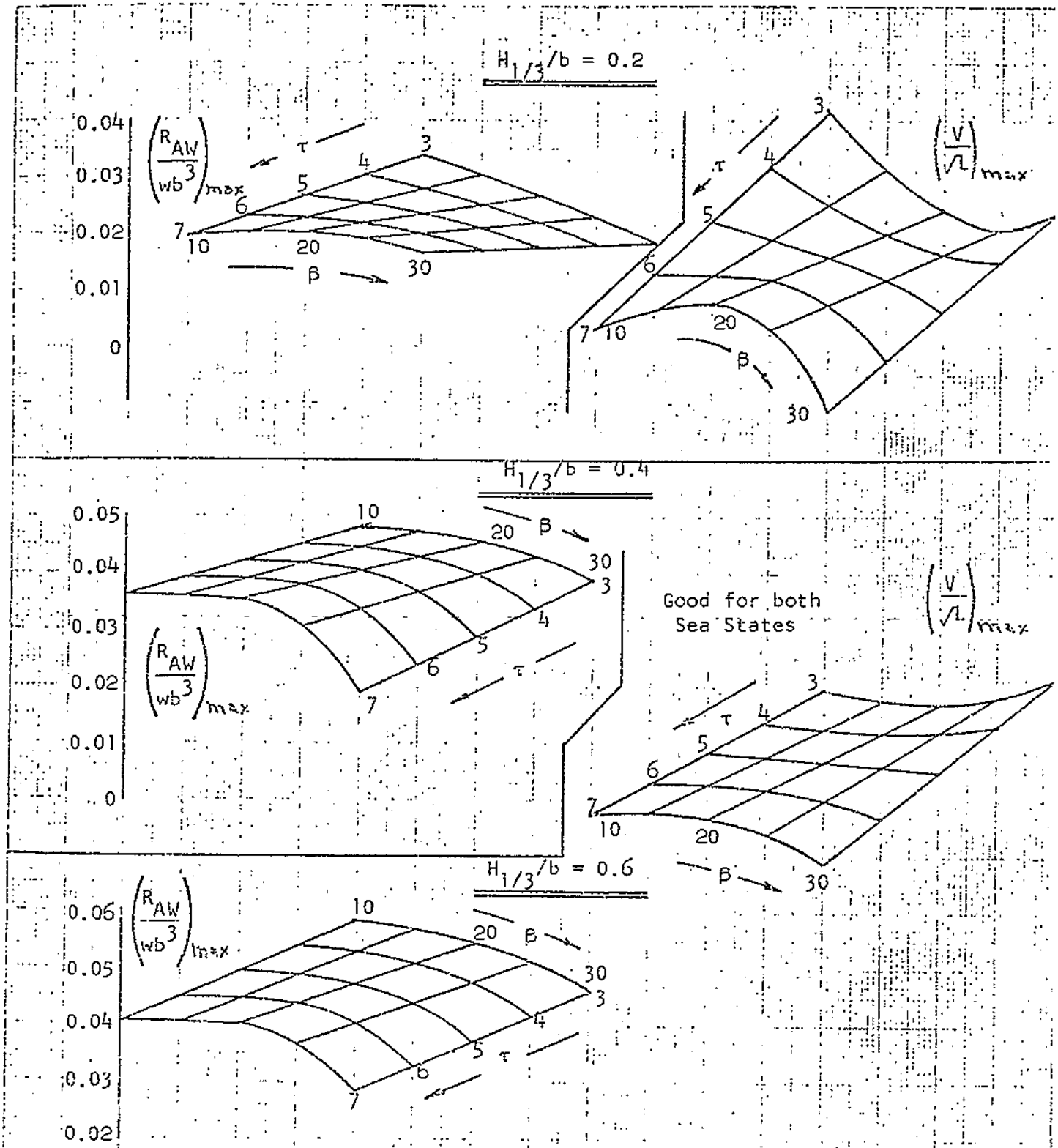

FIG. 11 MAXIMUM ADDED RESISTANCE AND SPEED FOR $C_\Delta = 0.60$ AND $L/b = 5$

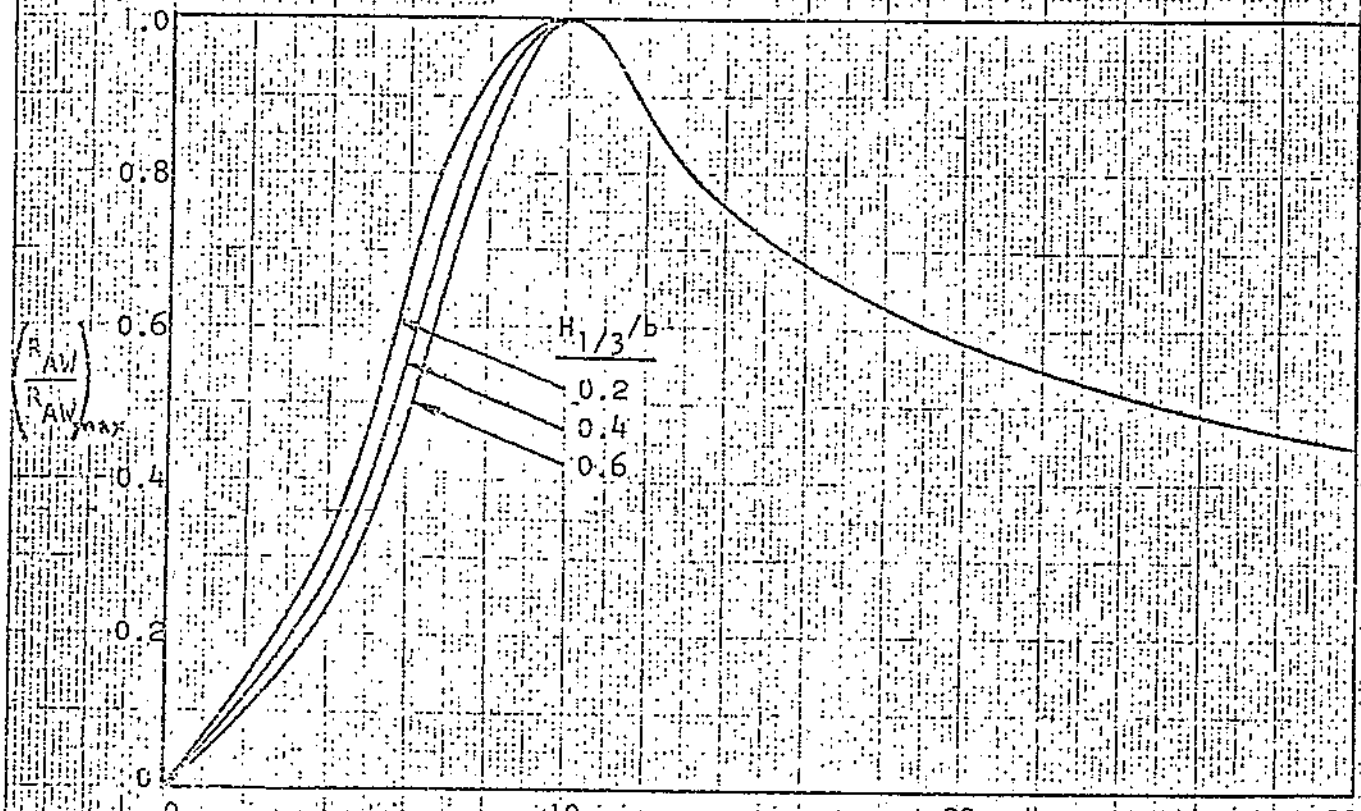

$$\frac{R_{AW}}{wb^3} = \left(\frac{R_{AW}}{R_{AW_{max}}}\right) \times \left(\frac{R_{AW}}{wb^3}\right)_{max} \times E(V/\sqrt{L},\ C_\Delta,\ L/b,\ H_{1/3}/b)$$

FIG. 12 GENERALIZED ADDED RESISTANCE PLOT FOR $C_\Delta = 0.60$ AND $L/b = 5$

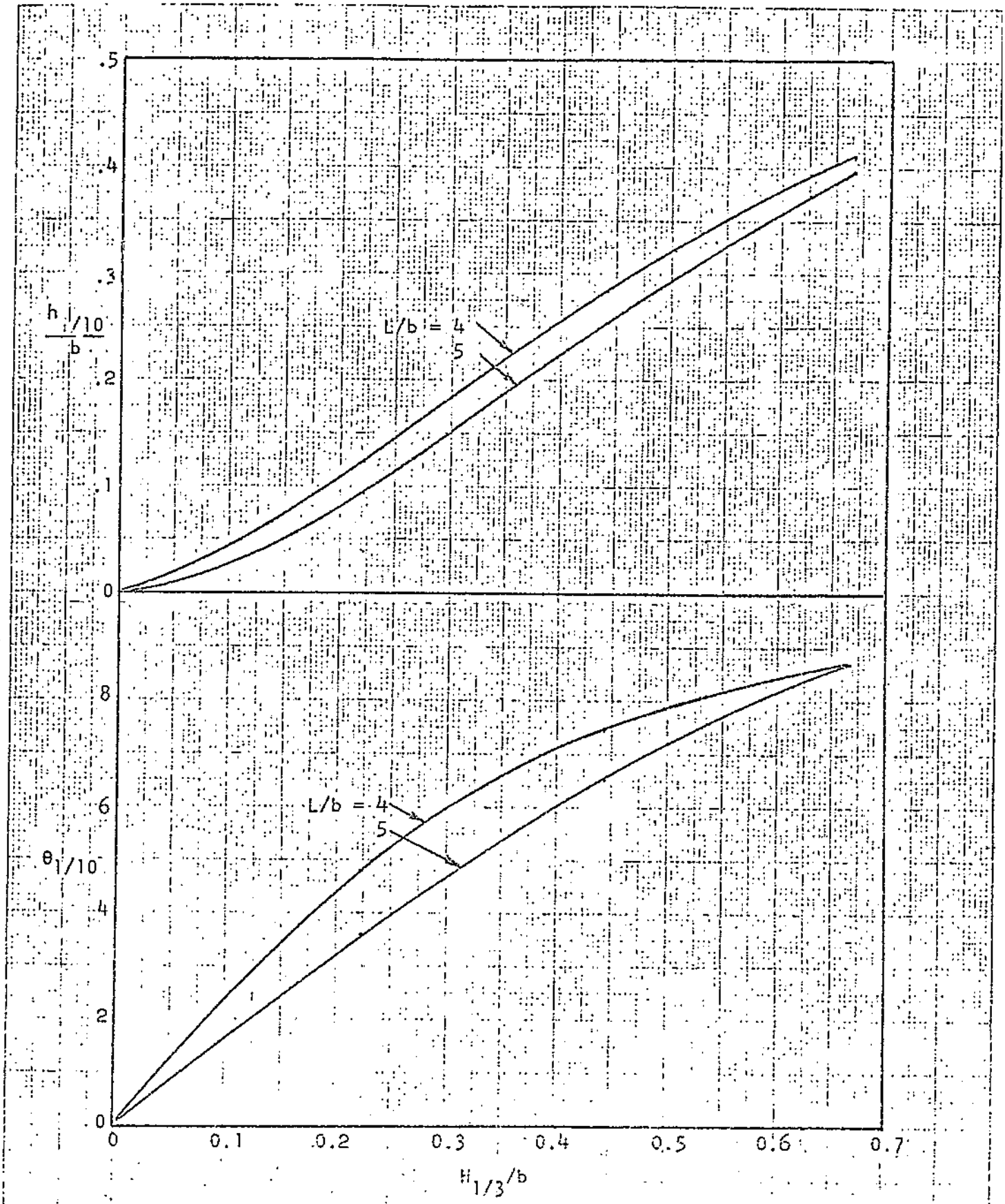

FIG. 13 1/10 HIGHEST MOTION AMPLITUDES AT V/$\sqrt{L}$ = 2

($\tau = 4^{\circ}$, all C_{Δ}, all β)

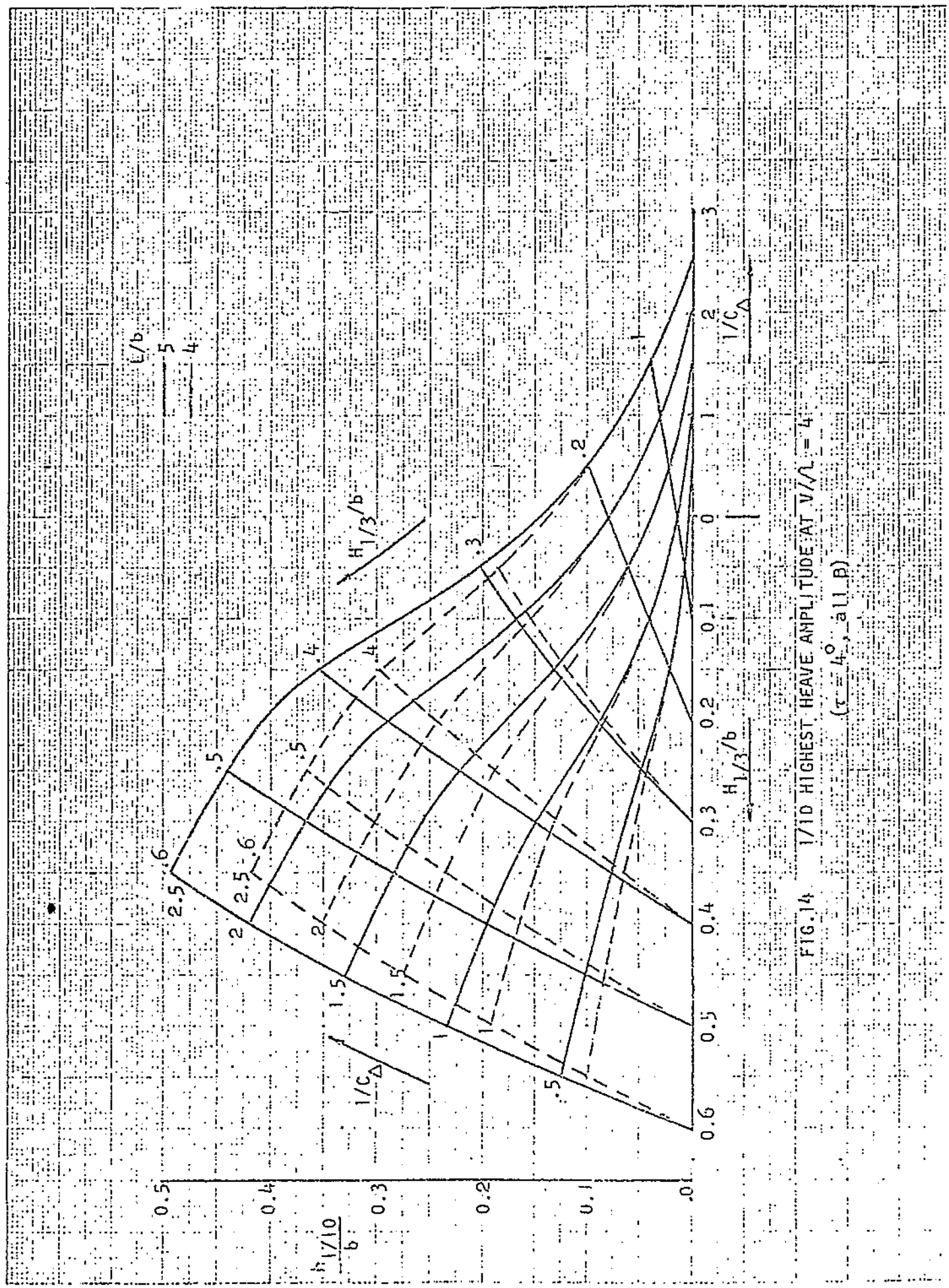

FIG.14 1/10 HIGHEST HEAVE AMPLITUDE AT $V/\sqrt{L} = 4$
($\tau = 4°$, all β)

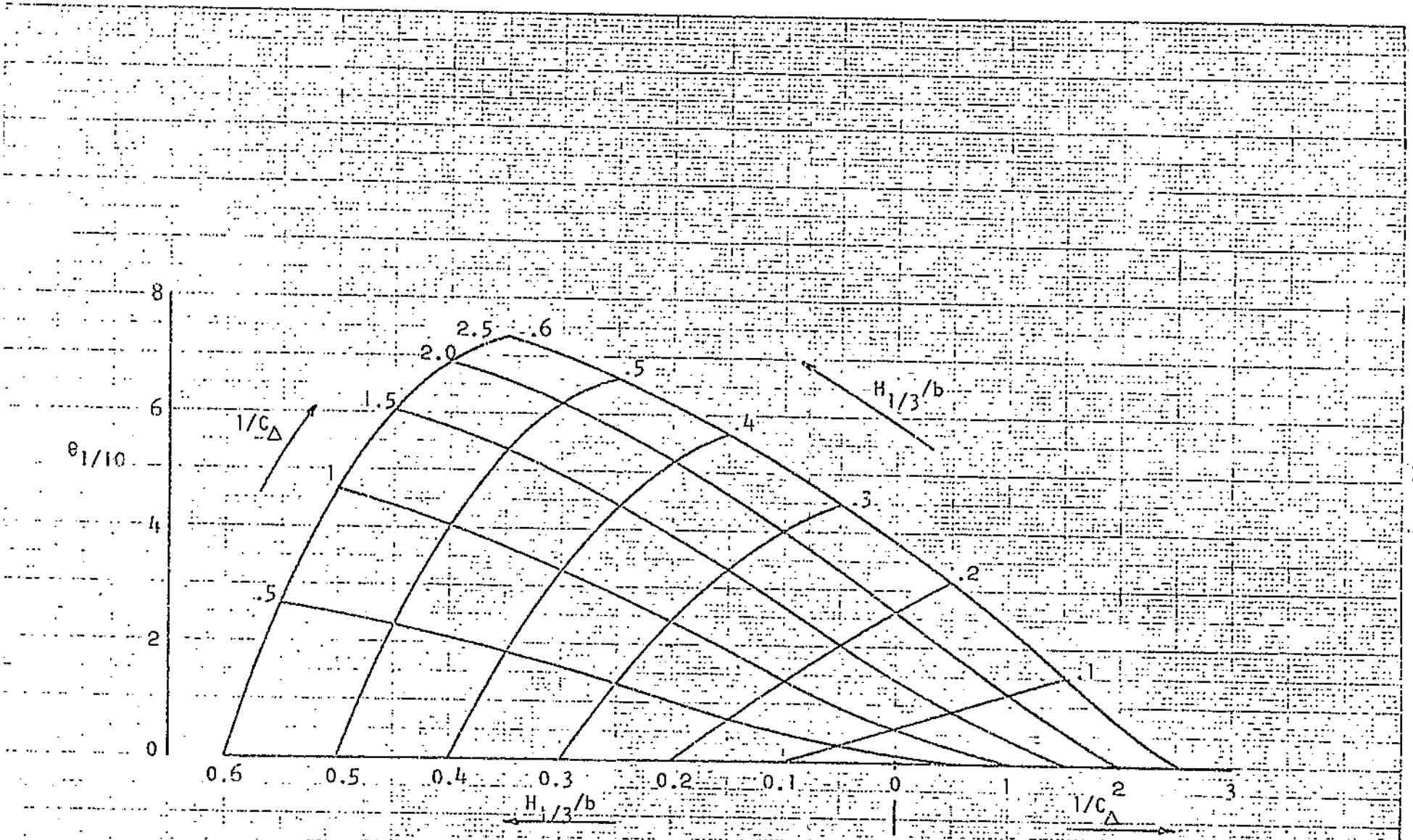

FIG. 15 1/10 HIGHEST PITCH AMPLITUDES AT V/√Lr = 4

($\tau = 4^{\circ}$, all β, L/b = 4 & 5)

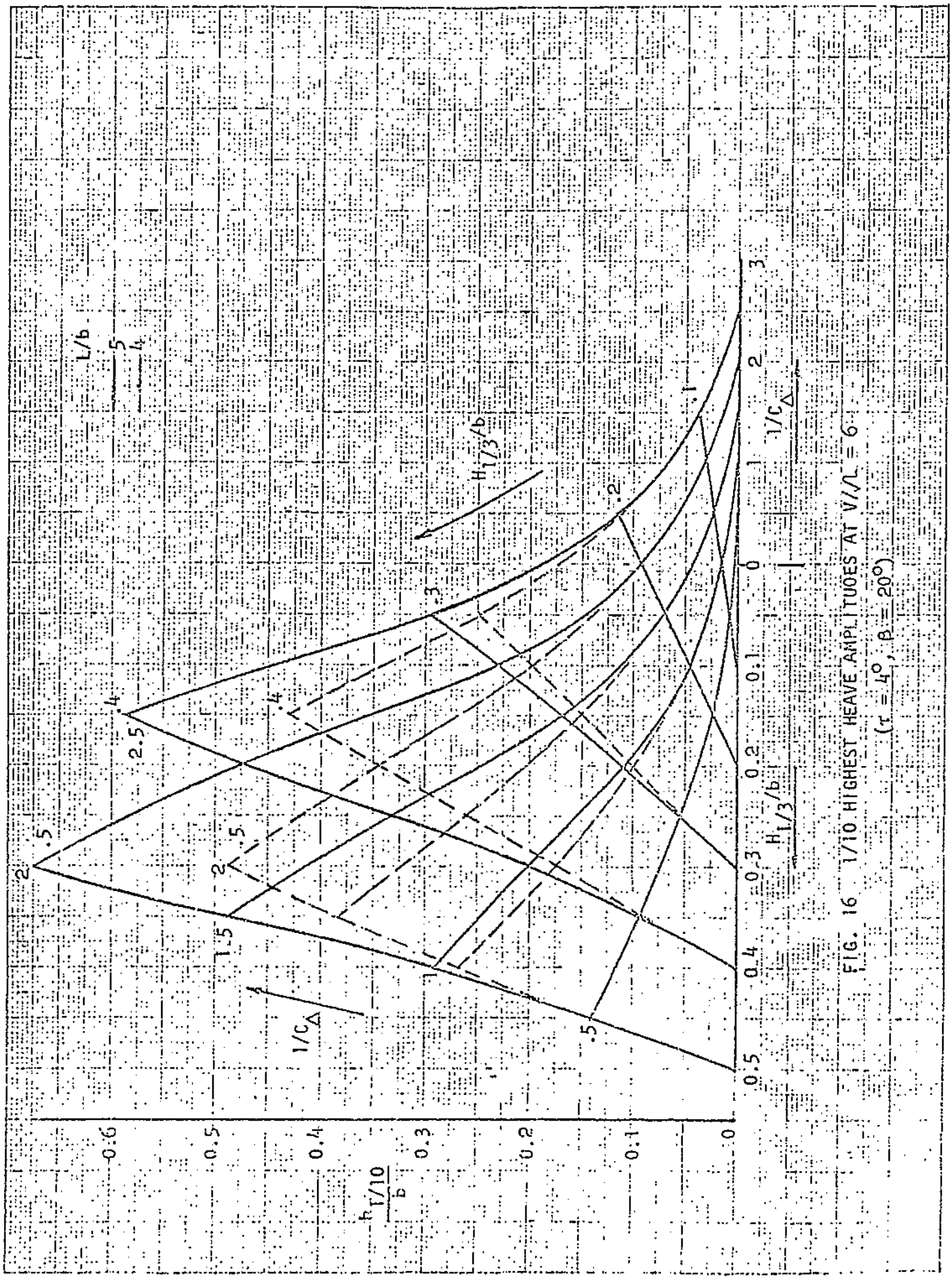

FIG. 16 1/10 HIGHEST HEAVE AMPLITUDES AT $V/\sqrt{L} = 6$
($\tau = 4^\circ$, $\beta = 20^\circ$)

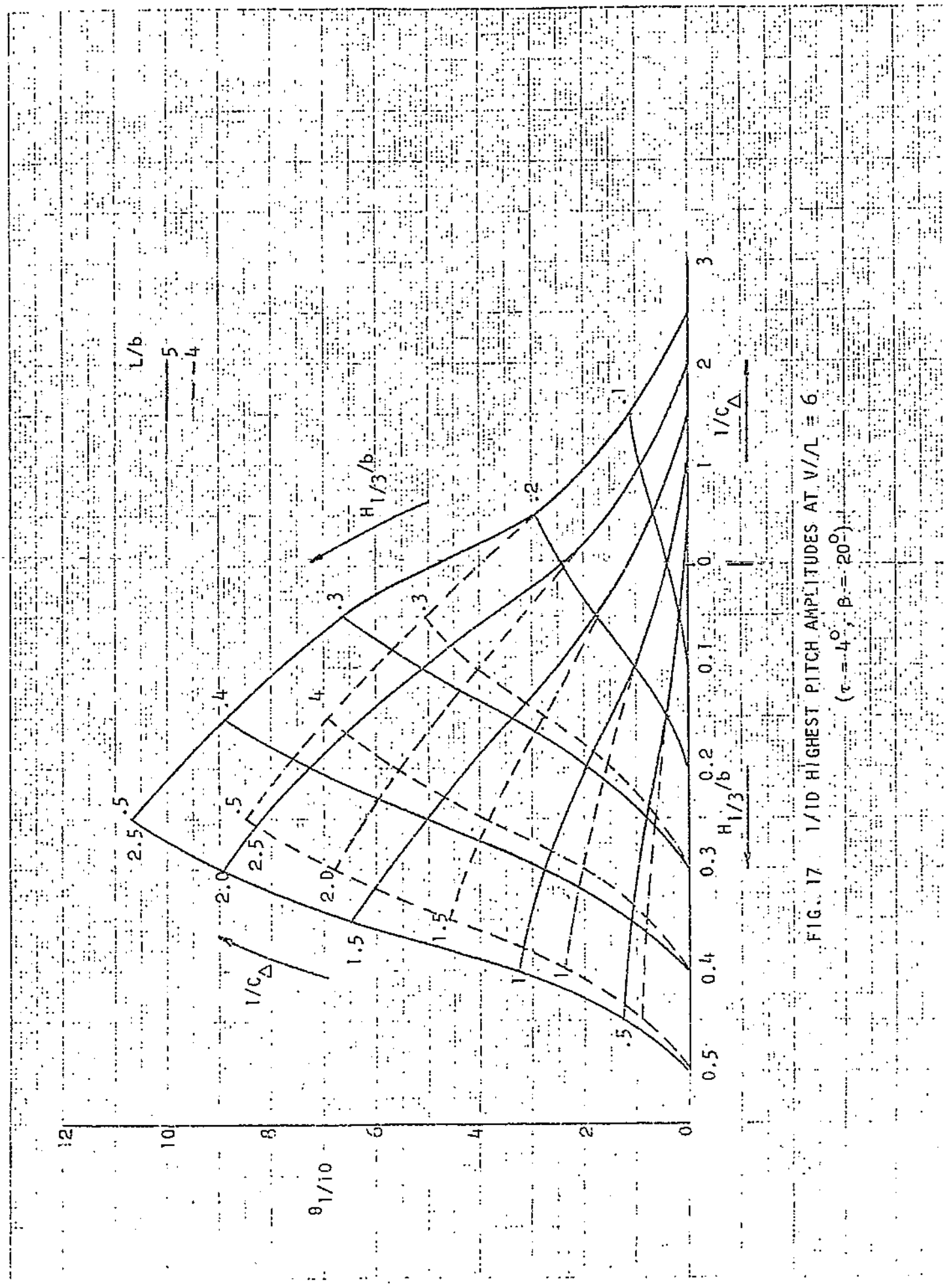

FIG. 17 1/10 HIGHEST PITCH AMPLITUDES AT V/√L = 6
($\tau = 4^{o}$, $\beta = 20^{o}$).

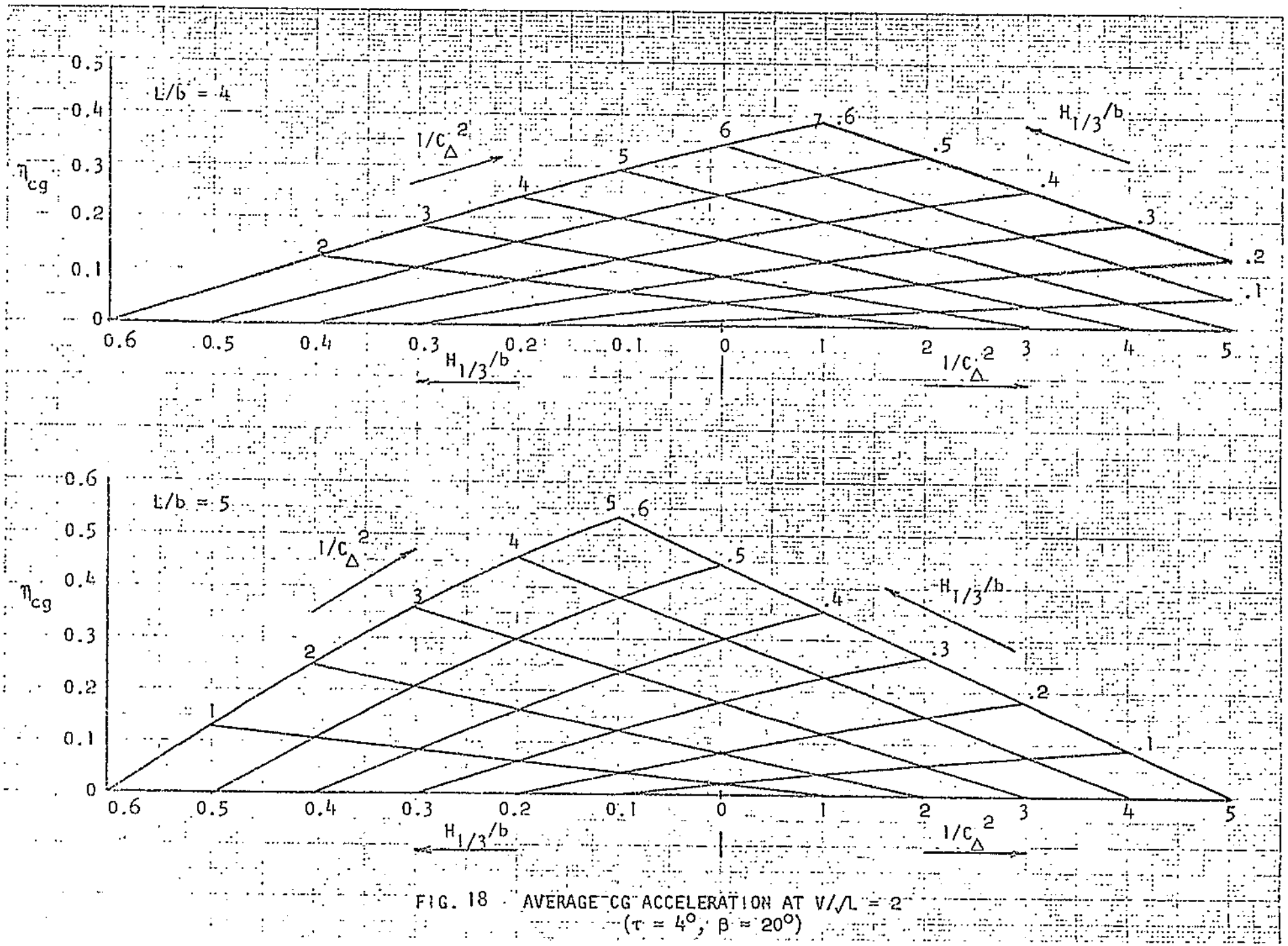

FIG. 18 AVERAGE CG ACCELERATION AT $V/\sqrt{L} = 2$
($\tau = 4^\circ$, $\beta = 20^\circ$)

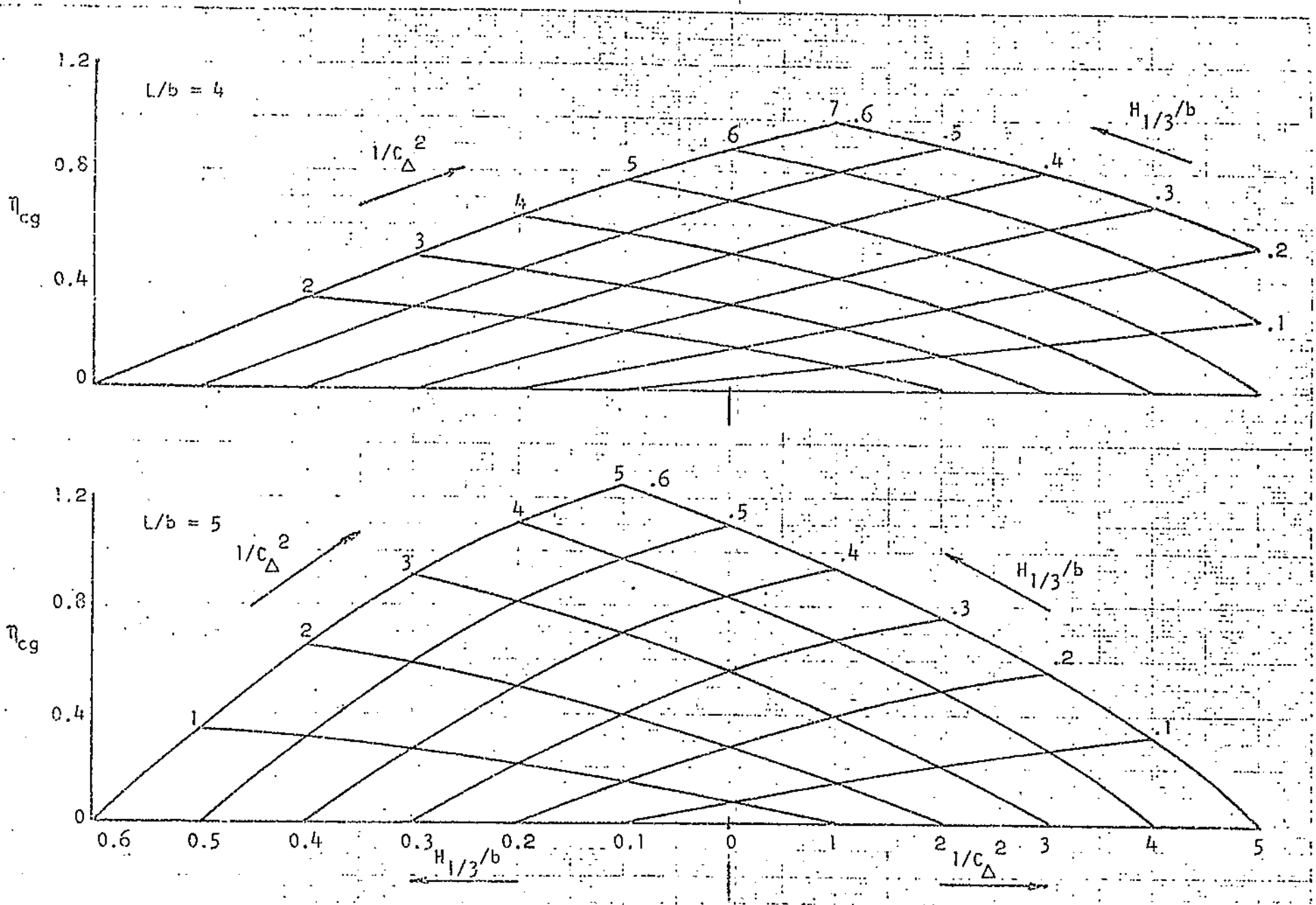

FIG. 19 — AVERAGE CG ACCELERATION AT $V/\sqrt{L} = 4$
($\tau = 4^\circ$, $\beta = 20^\circ$)

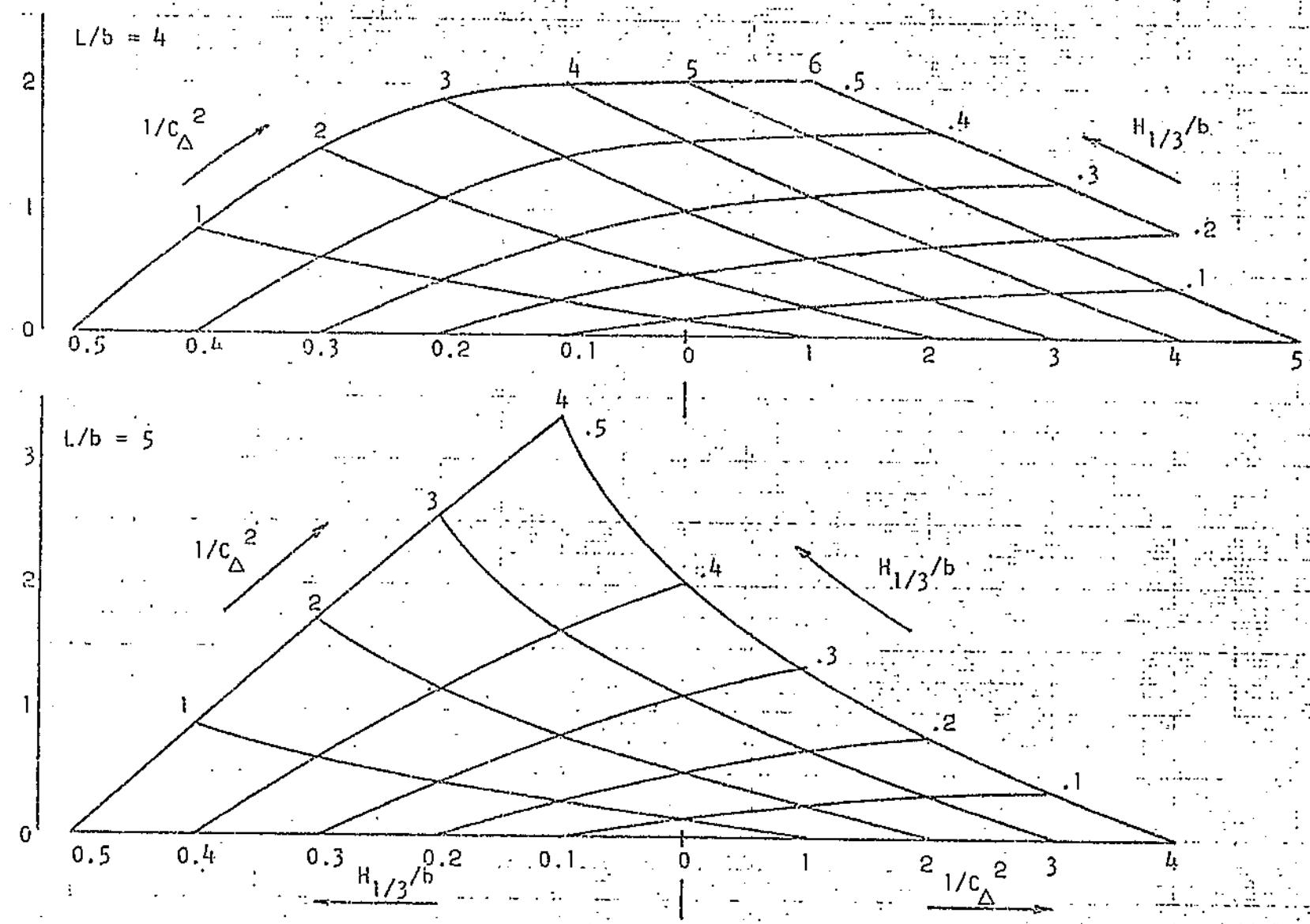

FIG. 20 AVERAGE CG ACCELERATION AT $V/\sqrt{L} = 6$
($\tau = 4^\circ$, $\beta = 20^\circ$)

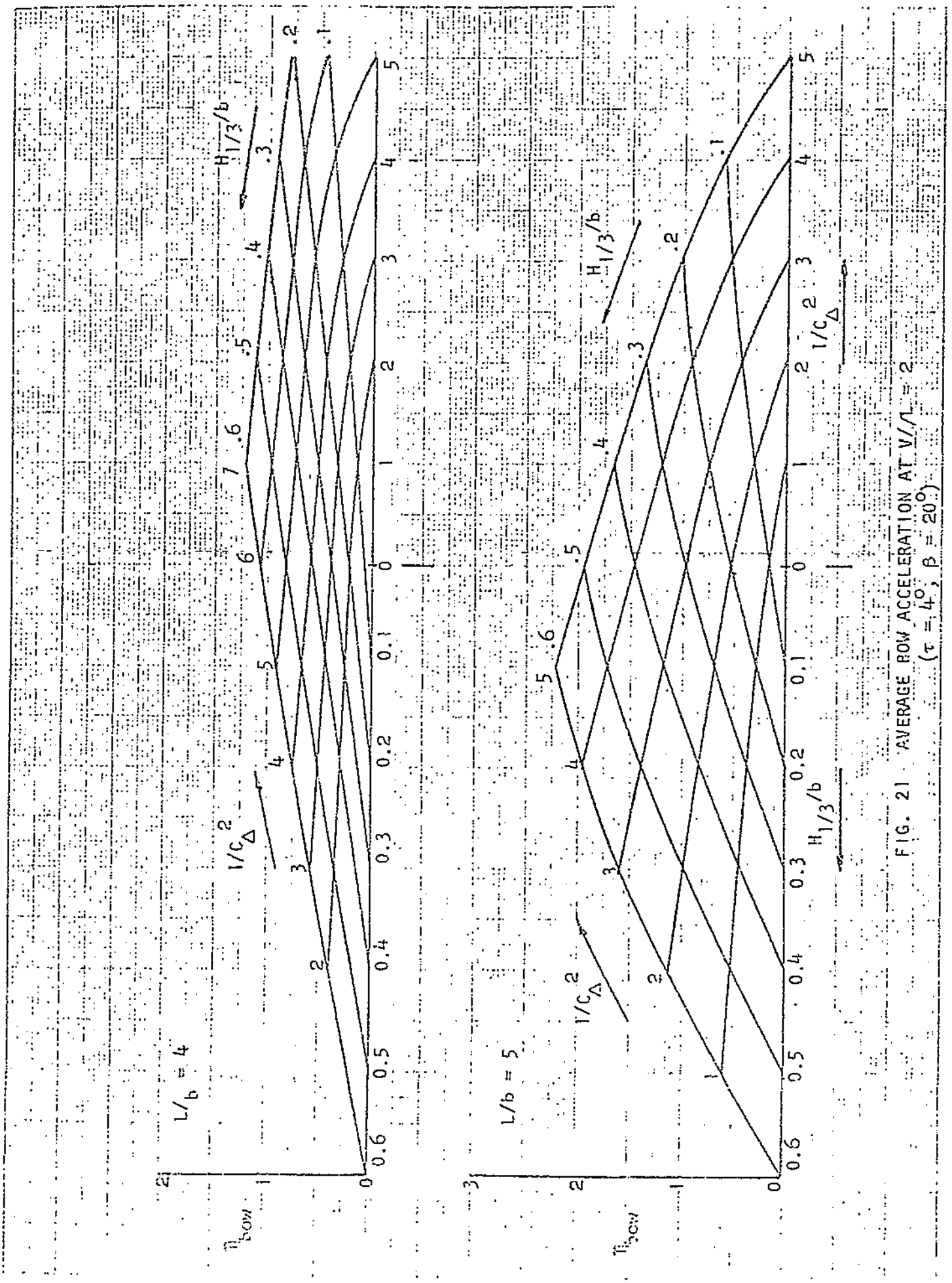

FIG. 21 AVERAGE BOW ACCELERATION AT $V/\sqrt{L} = 2$
($\tau = 4^o$, $\beta = 20^o$)

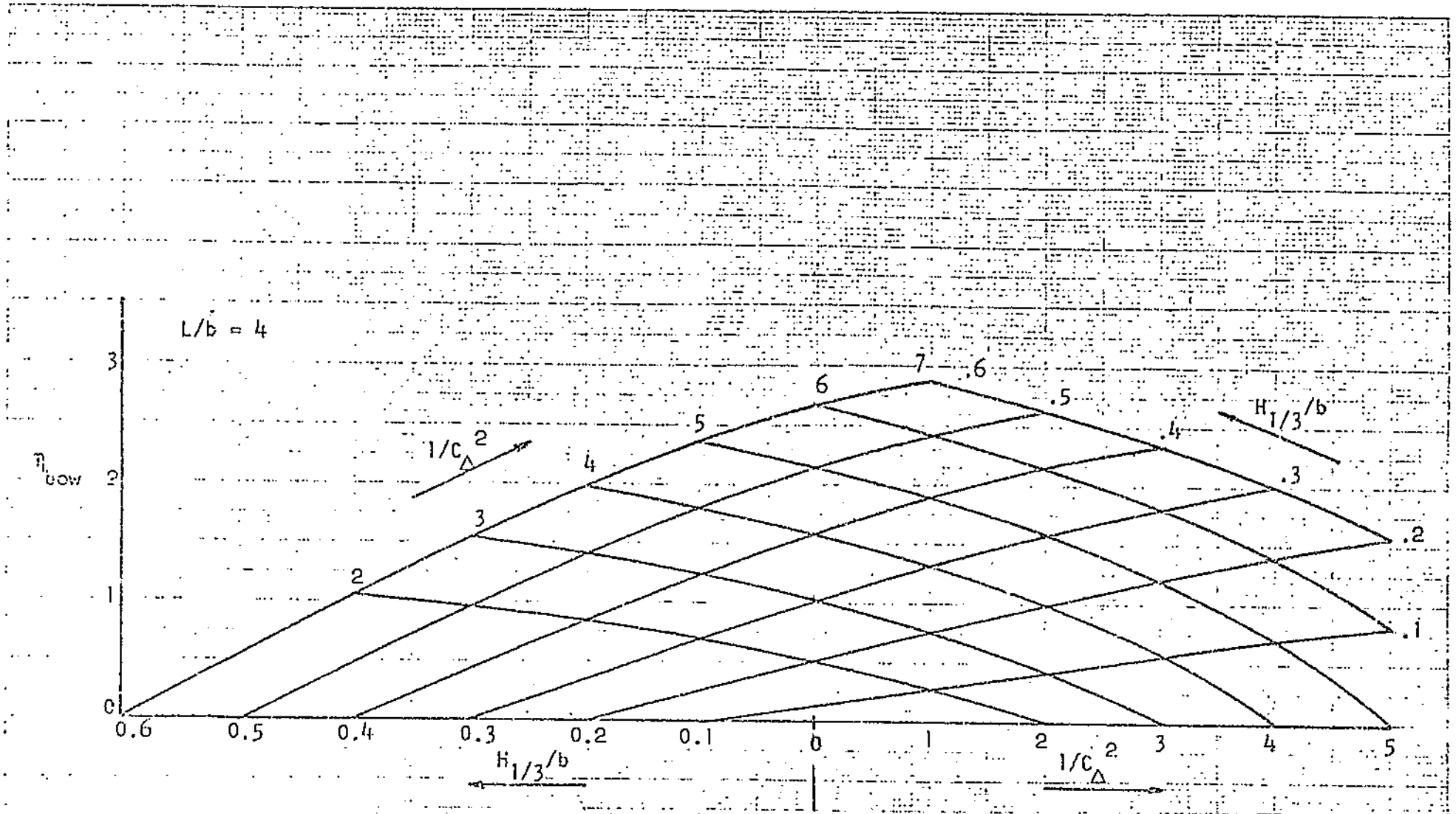

FIG. 22 AVERAGE BOW ACCELERATION AT $V/\sqrt{L} = 4$
($\tau = 4^\circ$, $\beta = 20^\circ$)

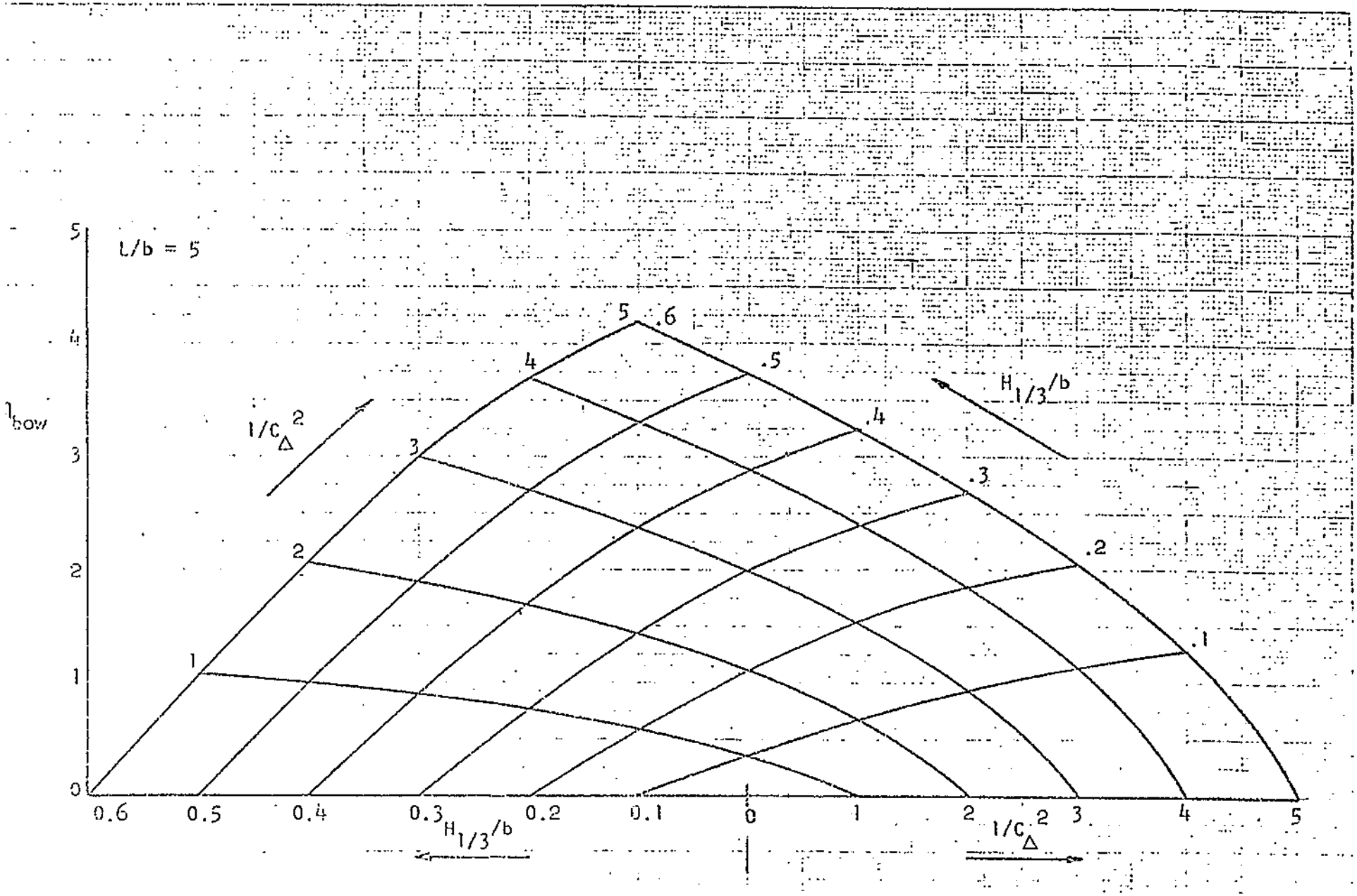

FIG. 23 AVERAGE BOW ACCELERATION AT $V/\sqrt{L} = 4$
($\tau = 4^\circ$, $\beta = 20^\circ$, $L/b = 5$)

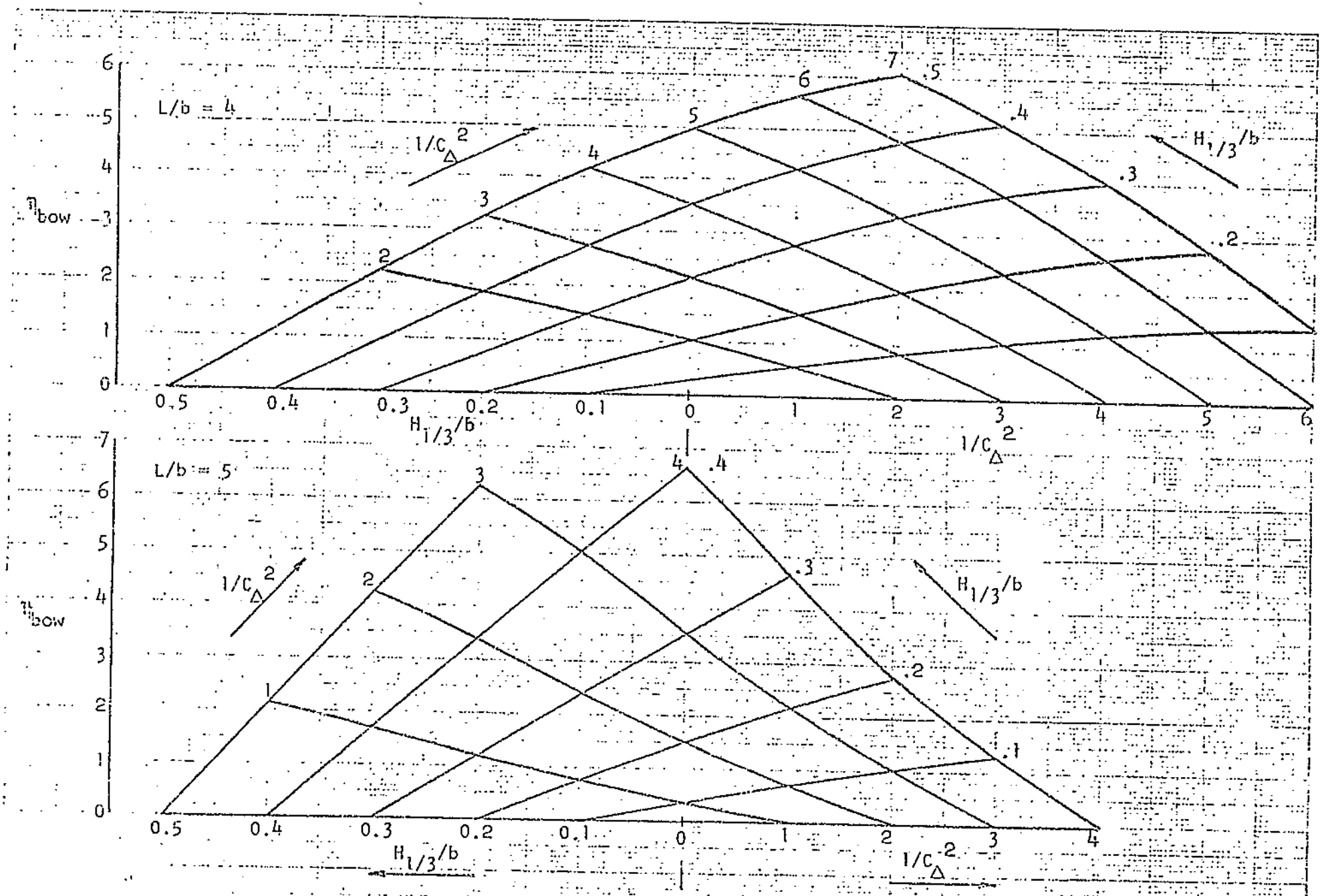

FIG. 24 - AVERAGE BOW ACCELERATION AT $V/\sqrt{L} = 6$
($\tau = 4^\circ$, $\beta = 20^\circ$)

FIGURE 25

PRESSURE DISTRIBUTION FROM EXPANDING PLATE ANALOGY

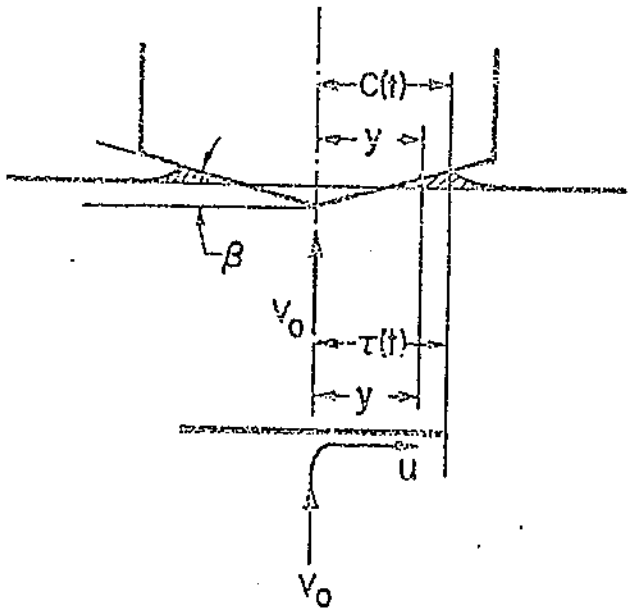

VELOCITY TANGENT TO PLATE

$$u = V_o \frac{y}{\sqrt{C^2 - y^2}}$$

VELOCITY POTENTIAL FOR PLATE

$$\phi = -V_o \sqrt{C^2 - y^2}$$

GENERAL BERNOULLI EQUATION

$$\frac{p}{\rho} = -\frac{\partial \phi}{\partial t} - \frac{U^2}{2} + F(t)$$

PRESSURE EQUATION

$$p = \frac{\rho V_o^2}{2}\left[\underbrace{\frac{2C}{\frac{V_o}{\dot{C}}\sqrt{C^2 - y^2}}}_{(1)} \underbrace{- \frac{y^2}{(C^2 - y^2)}}_{(2)} + 1\right] \quad (3)$$

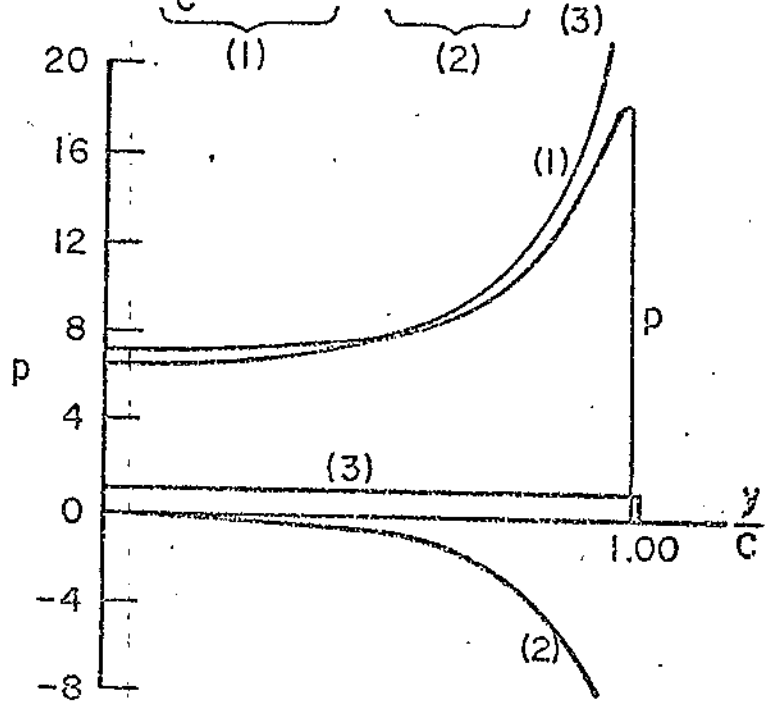

INTRODUCTION

The subject of waterjet propulsion has for many years been controversial and mysterious to most small craft designers. This lecture and paper are intended to place waterjets in their proper perspective, to clear up misconceptions, and to present useful information and application data for small craft engineers.

It should be emphasized that waterjets offer no miraculous solutions to the marine propulsion problems. Instead, they are to be considered one of many special tools that can be fruitfully applied in appropriate cases to produce the best craft system for a particular function.

Brief summaries are given of the state of the art and fundamentals of waterjet propulsion. Detailed discussion of application and related issues and special problems is offered.

This paper is intended essentially to be a condensation of rather comprehensive lecture material that will preserve key points and reference material for later use.

PRACTICAL APPLICATION OF WATERJET PROPULSION

Howard R. Apollonio

Jacuzzi Bros., Inc.

Presented at the University of Michigan
Continuing Engineering Education Center
1971 Small Craft Engineering Short Course
October 11-15, Ann Arbor, Michigan

CONTENTS

STATE OF THE ART SUMMARY

In the last decade intensive evolution of waterjets from an experimental oddity to a serious alternative to established propeller systems has taken place.

Key issues that have been resolved in this period have been those of providing performance to match or exceed that of existing equipment with proven reliability at a reasonable cost. A wide variety of applications provided background data and the basis for improved development. These include pleasure craft, workboats and military vessels.

In a rather short period of time, numerous competing waterjet manufacturers rose and fell, leaving only a handful remaining in 1971, whose strength has grown significantly. In the United States, Jacuzzi Bros., Inc. and Berkeley Pump Company have the only volume production. Berkeley spcializes in pleasure craft propulsion, whereas Jacuzzi has been successful in both that and the industrial-duty markets in the U. S. and overseas. Hamilton Ltd. has branches in Australia, New Zealand and Canada, plus an active licensee in England, Dowty Turbocraft. Another licensee, Buehler Corp., in the U. S., was active in the 1960's, but never achieved market success and became inactive in 1971. It is interesting to note that successful domestic manufacturers were well established builders of conventional pumps before entering the waterjet business.

The successful domestic waterjets are based upon mixed flow pumping elements, and all models bear marked similarity to one another in inlet and control configuration. The Hamilton jets contain axial flow pump elements, one, two or three in tandem, and are also quite similar to one another. All of these waterjets are represented by a few models designed for volume production and substantial flexibility to meet various needs. They all feature short flush inlets and integral control mechanisms for steering and vectoring of thrust ahead and astern. A typical mixed flow waterjet is shown in Figure 1.

Market acceptance of waterjet propulsion was understandably slow initially, but in a decade has grown significantly in scope and volume. Marine propulsion is generally a "show me" market, where a new development must demonstrate its ability to operate competitively with existing systems, in addition to special advantages it has. Waterjets have done this in enough areas to render then a significant alternative to propeller systems.

Waterjets conspicuously offer the advantages that accrue to complete absence of underwater appendages: shallow draft, maneuverability and safety. Frequently available direct coupling to popular engines, combined with integral forward to reverse shifting is attractive for having eliminated the need for clutches and gearboxes. The ability to operate at full power at any speed has occasional advantages. In addition, waterjets can be constructed to give outstanding reliability, ruggedness, excellent craft control, exceptional forward acceleration, and adaptability to certain auxiliary pumping functions.

Disadvantages that waterjets exhibit include low propulsive efficiency at low boat speeds, occasional fouling with debris, and sometimes high weight and cost as a tradeoff against propulsive efficiency at modest boat speeds.

Waterjet propulsion has been most widely utilized in pleasure craft, where investment costs are low and innovation is popular. These have been inboard configuration craft 14 to 30 feet LOA, with 100 or more horsepower gasoline engines, for speeds of 25 knots and above. Domestic jets feature close-coupled inboard/outboard type mounting to provide advantages in weight distribution and accomodation space. Deep and medium vee prisimatic hulls give the best overall performance at high speed with jets, combining good seakeeping, directional stability, and freedom from aeration of the inlets.

Waterjet units of nominal 12 inch diameter comprise the bulk of pleasure craft units. These are derived from deep well turbine pumps, whose high pressure low flow rate characteristics relegate them to efficient speed and power regimes of 30 knots and above, at 200 or more horsepower. As installed power rises the jets are proportionately less expensive than vee drive and inboard/outboard systems, based on boat manufacturers overall propulsion system costs. They are comparatively much more reliable (the 12 inch jets virtually never fail in this service, whereas boat dealers often cite a lucrative repair business on propeller drives as a key factor in their opposition to jets). At lower power, the fixed configuration of the popular waterjets disadvantages them in cost with respect to inboard/outboards that are mass-produced in the smaller sizes.

Jacuzzi has introduced a new 12 inch jet for the lower speed and power regime, however, to help fill this gap. Its price is competitive, and it has demonstrated propulsive performance comparable to that of inboard/outboards in most installations.

The considerable activity in pleasure craft has given rise to many advancements in waterjet technology. This has included: high speed and high acceleration inlet development, accurate, effective control systems, new boat handling techniques,component life and reliability data, corrosion and cavitation data, and information on interactive hydrodynamics.

Extensive application of waterjet propulsion to industrial duty and military vessels has been a rather recent development. These applications generally represent substantial investment and risk, demanding schedules, and a hostile environment. Here it is mandatory that the fundamental requirements for high propulsive efficiency and reliability be met. Conservatism and slow acceptance of new developments is understandable in people who depend upon boats for life and livelihood.

The first truly convincing demonstration of waterjets' capability to meet these needs was that of the U. S. Navy's PBR riverine warfare craft. Some 1000 Jacuzzi 14 inch jet units were put into this service. Their record shows an attractive combination of performance, reliability, ruggedness and servicability under severe operating conditions, to augment obvious shallow draft advantages.

Subsequently, these waterjets have been applied to a variety of workboats and yachts driven by small diesel engines, with 200 to 300 horsepower at 2800-3000 RPM. These jet units are best suited to boat speeds of 25 to 50 knots.

Two other Jacuzzi units deserve mention in demonstrating what has been accomplished with waterjet propulsion. A 20 inch model, for 250 to 500 SHP at 1800-2300 RPM offers a wide range of favorable propulsive efficiency, at 20 to 50 knots, and makes an economical combination with diesel and small gas turbine engines. A crewboat fleet in Maracaibo, Venezuela has run 12 of these units at 260 and 400 SHP for some 3000 hours to date. They are expected to run 4-5000 hours between overhauls. No difficulties whatever have been encountered. The only maintenance required has been lubrication of the thrust bearings at each 100 hours.

A 36 inch waterjet has been developed for even longer service and outstanding reliability. It is designed to match gas turbines at 1000-3000 SHP, or diesels at 600-1000 SHP. Properly applied, this unit

will give exceptional propulsive efficiency over a very wide range of boat speeds. It is being seriously considered for major programs in patrol boats, landing craft, crewboats and passenger ferries.

Two special waterjet applications deserve mention. One is the Boeing hydrofoil "Tucumcari" which has been carefully optimized throughout, for outstanding performance and reliability. It is propelled by twin centrifugal waterjet pumps in parallel, built by Byron Jackson, and powered by a 3200 SHP gas turbine. This waterjet installation has demonstrated that the advantage of simplified power transmission can be combined with excellent performance for this type of application. It has been in service for 3 years.

Another special application is similar, this time in an experimental 100 ton surface effect ship built by Aerojet General Corp. and presently udergoing builders trials. Its two waterjets were built by Aerojet General, and feature two mixed flow pumps (stages) in tandem, running at different shaft speeds for resistance to cavitation when accelerating. Their advantage to the craft is the same as for "Tucumcari", above. These units are powered by multiple gas turbines at up to 6000 SHP to each jet. Initial tests have been fully successful.

Racing of the 12 inch pleasure craft jets has provided interesting and valuable data on effects of extreme speed and power. Associated inlet phenomena (cavitation, drag, etc.) have been of particular interest. A spedical Berkeley jet in a 17 foot hull powered with 1500 SHP has run consistantly over 100 knots in quarter mile drags and holds a record of 125 mph at the time of this writing.

HYDRODYNAMIC FUNDAMENTALS

Waterjet propulsion generically refers to propulsion of vessels by internally mounted pumps with appropriate ducting. This arrangement of the actuator component of the system leads to the fundamental differences with respect to propeller systems, as will be shown below.

A pump by itself can be a highly efficient device for transmitting mechanical energy to a fluid, with efficiencies of 80-90% readily attainable. This results from carefully controlled flow conditions, minimal tip losses, and recovery of rotational energy behind the impeller. As the impeller rotates it governs inflow rate and energy transfer precisely, regardless of the source of fluid (in the absence of cavitation and separation). Scaling laws (so-called "affinity laws") as follow are readily applicable when a given orifice such as a nozzle controls discharge flow:

$$Q \propto N \quad , \quad H_p \propto N^2 \quad , \quad SHP \propto N^3$$

Under these conditions, efficiency remains constant. An illustration of pump and nozzle flows is shown in Figure 2. The "affinity laws" at the pump remain in effect regardless of boat speed, and actually control inlet flow velocity.

A waterjet pump as a propulsion device produces thrust by means of applying a momentum change to the fluid passing through it. A propeller does this also, but with a different relationship to the driven vessel. The energy that a pump imparts to the fluid takes the form of pressure or head, denoted H_p. This pressure is converted to velocity in a nozzle via Bernoulli's Theorem. At zero boat velocity this thrust would theoretically be:

$$T_s = \dot{m} V_j = \rho q V_j \qquad (1)$$

Equation (1) expressing T_j instead of T_s also represents the reaction force of the waterjet unit against the hull, in order to satisfy requirements for equilibrium across the nozzle discharge. This, however, is not true propulsive thrust which is the result of interrelationship of fluid forces around the craft system.

In the case of a moving boat, a control volume around the entire craft should be visualized as in Figure 3.[1] A streamtube of flow through the propulsion device enters with a velocity, V_o, and momentum, $m \cdot V_o$. The mass of water entering the system is internally forced to depart at V_j with momentum $m \cdot V_j$. Since the momentum of the incoming water does no useful work, it must be deducted from $m \cdot V_j$ in order to identify net propulsive thrust. This thrust then is the product of the rate of mass flow and the difference in velocities into and out of the control volume:

$$T = \dot{m} (\Delta V) = \rho q (V_j - V_o) \qquad (2)$$

Note that this relationship is quite independent of the driven vehicle. Curves of T vs V_o can readily be constructed for a waterjet of a particular configuration whose pumping characteristics are known and be accurately applied to all manner of vessels.

The catch to this apparently simple procedure is in determining V_j. The pressure at the nozzle represents the sum of energy changes within the control volume superimposed upon the available energy at V_o. Therefore, duct losses, elevation changes and amendments to pump head must be taken into account.[2] In summary,

$$H_n = H_p + V_o^2/2g - H_e - H_L \qquad (3)$$

---

[1] A propeller's control volume, on the other hand, should be separate from the boat, because the propeller is an external propulsion device.

[2] e.g. losses due to cavitation

The term H_L usually defies computation, and must be predicted from past experience -- i.e., model test or nozzle probe data for various waterjets. Pump head, H_p, is identified from the affinity laws Conveniently for testing, the difference between H_n and H_p is the aggregate of all energy transformations in the system, regardless of the mechanism of their occurrence. The terms $(V_o^2/2g-H_e-H_L)$ collectively represent a quantity called "ram pressure" or "ram pressure recovery", H_R, which is commonly expressed as a percent of $V_o^2/2g$. Some writers also refer to this quantity as inlet efficiency, η_i. Values of 50% to 80% ram pressure recovery are attainable at $H_e = o$ (planing hulls) depending upon inlet size, boat speed and boundry layer flow. Trends of ram pressure recovery depend primarily upon inlet velocity ratio, $IVR = V_i/V_o$, where V_i is taken at the mean streamline in the inlet entrance. Other significant influences include entrance geometry, boat trim, yaw, and cavitation number. Inlet model data is shown in Figure 4 with shape and IVR varied. Full scale tests of the elliptical configuration at 20 inch i.d. showed excellent correlation with prediction.

It should be noted that interpretation of H_p and H_R may vary according to how H_p is defined. As a matter of convenience in collecting pump test data some manufacturers, for instance, use a value of pump head and efficiency that includes inlet and discharge losses in the laboratory test stand. Their H_p contribution is then low by this factor, but H_R is high for a particular set of waterjet nozzle data, compared with a breakdown that includes pure pump element data.

With a pump operating at near constant efficiency (above), momentum considerations become the controlling factor in waterjets' propulsive efficiency. This is reflected in the term jet efficiency, η_j, defined in terms of jet velocity ratio, $\mu = V_o/V_j$, and system loss coefficient, ζ:

$$\zeta \cong (V_o^2/2g-H_e-H_L)/V_o^2/2g \cong 1-\eta_i \quad : \quad (4)$$

$$\eta_j = \frac{2\mu(1-\mu)}{1-\mu^2(1-\zeta)} \qquad \text{(see Figure 5 and derivations in references 1,2,\&3)} \qquad (5)$$

This term relates thrust energy output to energy imput from the pump:

$$\eta_j = T \; V_o / \rho g \; H_p \; q \qquad (6)$$

Thrust propulsive efficiency, or thrust efficiency is then comprised of:

$$\eta_T = T\ V/550 \cdot SHP = \eta_j\ \eta_p \text{ , where} \quad (7)$$

$$\eta_p = \rho g H_p q/550 \cdot SHP \quad (8)$$

The shape of a thrust efficiency vs boat speed curve is then governed by η_j . In particular, this means that a given shaft speed of or power into a waterjet gives a certain velocity, which when related to boat speed yields relationships of η_T vs V_o similar to the curves of η_j vs μ . At different power levels then, different boat speeds are optimum, and vice versa, with a particular waterjet.

The type of pump used in a waterjet propulsion unit determines the jet velocities attainable at various shaft speeds and input SHP. These types range from high pressure, low flow centrifugal to low pressure, high flow axial flow pumps. A parameter called specific speed, N_s, is used to describe basic pumping parameters:

$$N_s = N\ \ Q^{.5}/H_p^{.75} \quad (9)$$

Pump efficiency attainable as a function of type, via N_s, is plotted in Figure 6. In practice, pump efficiencies in waterjet units range approximately as follows:

$0.70 < \eta_p < 0.85$ for axial and centrifugal types

$0.75 < \eta_p < 0.90$ for mixed flow types

Pump selection and evaluation for suitability can be carried out simply by checking jet efficiency and velocity at V_o, translating V_j to head, H_{jet} and H_p, and working out pump type or shaft speed at a given SHP from equations (8) and (9) and Figure 6. Rather straightforward optimization procedures can be derived from these relationships. See Application Fundamentals , below.

The problem of cavitation can influence the choice of pump type and the performance of any type of pump. Cavitation on the impeller is most likely to occur at low boat speeds combined with high shaft speed and velocity into the impeller (high flow rate). Under these conditions local static pressure is low compared to dynamic pressure drop across the blades. As boat speed increases static pressure builds up due to ram pressure recovery and the extent of cavitation diminishes, provided that the inlet is sized to allow adequate difference between ram pressure and dynamic pressure into the impeller. This phenomenon bears the same importance in waterjet applications that propellers' cavitation does in their applications.

Two parameters, cavitation number and suction specific speed, are commonly used to evaluate pump cavitation conditions. The former is more accurate and the latter is more convenient.

Cavitation number, the ratio of local static to dynamic pressure, is computed at the blade tip:

$$\sigma = (H_a + V_o^2/2g - H_e - H_L)/(V_{ie}^2 + \omega r_{ie}^2)/2g \qquad (10)$$

Significant cavitation occurs at $0.10 < \sigma < 0.15$, depending also upon pump type and the pump's Q/N ratio. Axial flow pumps are most resistant to cavitation; and centrifugal pumps are least resistant, generically. Partial, but ususally acceptable cavitation occurs at higher values. Performance changes due to cavitation are generally gradual in axial and mixed flow and abrupt in centrifugal pumps.

Suction specific speed relates cavitation to pumping parameters and static pressure at the impeller:

$$N_{ss} = N\, Q^{.5}/(NPSH)^{.75}, \text{ where} \qquad (11)$$

$$NPSH = H_a + V_o^2/2g - H_e - H_L \qquad (12)$$

Continuous operation at N_{ss} = 13,000 has been accomplished with mixed flow pumps without serious effects. Values of N_{ss} around 16,000 should be feasible at somewhat reduced efficiency and component life. Cavitation usually becomes noticible around N_{ss}=8000.

When noticible cavitation is encountered in continuous operation erosion resistant materials such as titanium or 17-4 stainless steel must be used for the impeller to maintain acceptable life. Both of these have given excellent results.

Means of reducing cavitation effects on overall performance include:

minimizing shaft speed;

maximizing static pressure via inlet diffusion;

use of multiple stages (pump elements in tandem), where the first stage or inducer cavitates but provides enough pressure to the next stage to minimize cavitation;

splitting a thrust requirement between several waterjet units to reduce the demand on each.

Cavitation of the inlet entrance can occur at extremes of boat speed. The inlet can be choked upon abrupt acceleration (drag racing situations and inlets optimized for very high speed via low entrance area). More significantly, inlets can sustain losses or create drag due to cavitation and separation internally at the leading edge and externally at the trailing edge. The former is usually the result of poor design of the transition from the hull, and the latter occurs at very low inlet velocity ratios. Both phenomena can be designed out of the system as evidenced by the success of many craft operating at 70 to 100 knots. The process is essentially empirical due to an absence of analytical data.

Inlet design usually becomes a compromise between hydrodynamic function and reduction of size, weight, and space occupied. Common inlets for planing hulls are configured with an abrupt aft lip and a well radiused forward lip leading from the hull into the duct to achieve clean streamline shaping. The duct proceeds upward at a 30 to 35° angle with respect to horizontal, and then bends into the impeller eye. Diffusion of flow to raise static pressure inside can be accomplished internally or externally, depending upon the desired inlet velocity ratio, the impeller eye velocity, and the expected boat velocities. Special cross sectional shapes are employed to preserve high inlet efficiency over a suitable range of velocity ratios. A removable grill is fitted over the inlet entrance to exclude debris that cannot be expected pass through the pump.

Hydrofoil inlets pose a special problem in that they

must be built integrally with foil supporting struts. This leads to compromises between internal efficiency, weight, and external drag. Considerable experience with these inlets, however, has led to very successful designs.

It seems contradictory to speak of "appendage drag" for a propulsion system with no appendages; however, when inlets are placed in a hull, interactive forces of some kind must result. The magnitude rather than the existance of these forces then becomes the key issue. Prediction of inlet induced forces by potential theory offers substantial promise, but complications arising from three dimensional effects have made progress slow. Studies of these phenomena have been undertaken at the Naval Ship Research and Development Center and the Technische Universität Berlin. Several years can be expected to pass before realistic results can be obtained and transformed into useful design data. Meanwhile, experience and simple hypotheses remain the useful tools at present.

Experience with a wide variety of planing craft indicates consistantly that hull resistance is not significantly altered by addition of flush inlets that operate properly with respect to waterjet unit performance. No discrepancies have been found in Jaccuzzi's experience between measured or predicted thrust and bare hull resistance properly estimated by model test or series data, in a range of inlet velocity ratios from 0.5 to 1.0 at non-cavitating inlet conditions. This simply implies that whatever induced forces are present fall within the band of uncertainty of the resistance estimate. Apparent inlet drag has been exhibited at extremes of IVR, at speeds above 50 knots and at hump resistance conditions below 20 knots. Approximate trends in these effects are illustrated in figure 8, for the inlets above, exclusive of boat trim effects.

Several hypotheses are offered to explain these inlet/hull interactive phenomena. First, noticible inlet forces appear to have the most influence on hull resistance via trim effects that are small over a wide range of inlet velocity ratios and/or boat speeds - e.g. lift at low IVR and sinkage aft at high IVR, causing increased frictional resistance or an increased induced (trim) drag component, respectively. Induced trim effects may be beneficial however, as well as detrimental. Secondly, these effects can be explained in terms of momentum changes at the inlet insofar as vertical forces are produced; whereas horizontal forces cancel. Horizontally the waterjet can be thought of as a pipe wherein a force applied at one end is transmitted to the other; whereas vertically it acts as a reaction elbow to fluid forces applied at its entrance. Third, inlet forces resolved normal to the hull bottom represent

local alterations to normal planing pressures, but the small relative areas and pressure changes involved render this effect minimal. Note that tremendous suction forces are not present for the simple reason that water will force its own way into an inlet with little persuasion from a pump. Fourth, parasitic drag of an inlet results from separated flow from inlet to hull. Stable flow in this region has been observed and analytically predicted to IVR's as low as 0.5.

Occasionally arguments are forwarded for scoop type projecting inlets on planing hulls to improve ram pressure recovery. However, the gain in H_R is usually more than offset by parasitic drag of this true appendage that adds both friction and potential forces.

In the case of hydrofoil craft, projecting inlets are unavoidable. Pitot type intakes are employed at the ends of foil supporting struts, and are properly sized by and related to comprehensive tradeoffs between exterior skin friction and potential forces, internal duct system losses, entrained water weight, jet efficiency, and attainable pump efficiencies. Techniques for accurately determining external inlet drag are available from aircraft nacelle design data.

MECHANICAL DESIGN

Successful waterjets have been plain and simple machines with specific refinements to insure life and proper function. The rotating element is analogous to that of a propeller system: a shaft and rotor (impeller) supported by a radial bearing at each end and a thrust bearing forward. Watertight sealing of the shaft penetration of the casing is successfully accomplished by face seals, lip seals, or a packing gland, depending upon intended applications of the unit. Alignment of these components is accomplished precisely by routine machining and assembly of the casing and supporting parts at the factory. The boatbuilder is thereby relieved of the most difficult portions of propulsor installation when waterjets rather than propellers are used. Proper design and construction of the rotating components can insure for them smooth, trouble-free operation over long durations of time.

Control systems integral to the waterjet are based upon vectoring of the jet discharge stream. Steering is effected by horizontal deflection of the jet; and reversing is accomplished by diversion of flow into an auxiliary duct that discharges in a forward direction beneath the boat hull. The most successful control systems employ a tube, (steering deflector) gimbaled around the nozzle for steering. The tube provides full turning of the stream with minimal breakup and loss. Beneath this tube at its discharge end a duct (reverse chute) is fitted to provide reversing thrust when a gate valve (reverse gate) is lowered over the end of the steering deflector. The reverse gate can be held at any position in its travel to provide desired proportions of reverse to forward thrust, for precise boat control at any throttle setting. The most effective maneuvering of a jet boat results from this type of shifting at a constant high idle shaft speed, allowing instant application of low to high thrust in any direction. Actuation of the control components can be with any conventional systems that provide the necessary force and travel. Morse push-pull cables are widely used, for example. This alternative to gear and clutch control represents an attractive feature of waterjets by eliminating a drive train component.

Casing parts are designed for watertight integrity, servicability, minimum weight, ease of construction, and proper hydrodynamic flow. Weight saving design however, must often be sacrificed to castability, especially where cost is important; and these parts consequently possess tremendous strength. Fabrication and considerable machining of casing parts can be done for premium cost lightweight waterjet units. Where high wear occurs on parts, or lightening for handling in the service of subassemblies is desired, casing parts are split and bolted together. Inlets are a good example of the latter consideration, where a portion (grill housing) becomes part of the hull and mates to the rest of the pump via a machined, gasketed flange.

The problem of corrosion exerts the dominant influence upon selection of materials for waterjet construction. Early experience with cast aluminum made this constraint quite clear. This desireably inexpensive, lightweight material could not be successfully coated to prevent its rapid deterioration in sea water; and results of its use led to many hard feelings. Recent experience has produced promising results for anodized, impregnated, and coated aluminum parts of substantial size; but these are not yet conclusive. As an alternative, ni-resist, a nickel alloy ductile iron has been used with excellent corrosion resistance at a reasonable price. For higher strength and cost, 300-series stainless steels are very satisfactory. Many other materials hold promise but are not in common use as a result of higher price, poor availability, etc. In highly stressed or cavitation critical areas, titanium and 17-4 PH stainless steel are used. Titanium offers a bonus of low density and the best known corrosion resistance. Its price is now very competitive with 17-4 PH and high copper and nickel alloys.

The economies of casting and mass production, coupled with high tooling costs for new models serve to explain why waterjet propulsion is available only in a limited number of configurations. Consequently it becomes impractical to optimize waterjets for each of their many potential applications.

FUNDAMENTAL CONSIDERATIONS FOR APPLICATION

Many people consider waterjet propulsion units to be mystical "black boxes" that may do fine things, but are not to be completely trusted. Once the mystery is removed, however, as the preceding sections have attempted to do, faith can be restored and the "black box" concept becomes attractive. That is, the waterjet becomes a handy package or module that is simple to design into a craft, install, connect, and operate. At a given input power, the unit operates at a particular shaft speed and produces a readily known amount of thrust. Its life and service requirements are usually well defined. It is simply bolted into place at the bottom and transom as a unit, to which drive shaft and control connections are quickly made Appropriate detailed data and installation and operating instructions as required are readily available from responsible manufacturers.

The Applications sections of this paper outline when and where waterjets should be considered reasonable alternatives to existing systems. A description follows of the performance and characteristics that are available, what constraints are applied to these, and how the waterjets can be integrated with their vessels. Two sections follow to answer these questions. The first presents basic parameters and the second deals with detailed considerations.

Waterjet propulsion should be considered a valid alternative to propeller systems when they can offer at least comparable propulsive efficiency, except in certain special applications where a performance penalty is acceptable. The range $\eta_D \cong \eta_t = 0.45$ to 0.55 is considered comparable in this context, generally speaking. Experience has shown that boat speed is the key variable controlling waterjets' propulsive efficiency. Speeds of 20 knots or a minimum true planing speed represent a practical lower limit. Below that, either cavitation, low jet efficiency, or low basic pump efficiency of high specific speed pumps (see figure 6 and Hydrodynamics above) limit overall efficiency attainable. Centrifugal

pumps operate at up to specific speed, $N_s = 2,000$. Mixed flow pumps are characterized by $2,000 < N_s < 10,000$. Axial pumps operate at N_s greater than 10,000. The most commonly used pump type is single stage mixed flow of specific speed around 3500 or 7000. The limits for a given waterjet depend essentially upon the power that it must absorb. Both jet velocity and cavitation number vary markedly with power and shaft speed, and place limits in a continuum. There can be no single power rating of a waterjet, unlike an engine, for this reason. For example, a unit may be very efficient at 20 knots with 200 SHP, but require 30 knots or more to be efficient at 600 SHP. Upper limits on speed are less clearly defined for lack of boats that need to run that fast. Jet efficiency effects are fairly obvious, i.e., low head, high specific speed pumps are not suitable for very high speed. Other pump types will operate best at high speed, with its attendant suppression of cavitation. Ordinary production inlets run satisfactorally up to about 50 knots boat speed; then special redesign should be employed for a higher speed. Thrust/speed curves and cavitation data furnish necessary information for the foregoing considerations.

Comparable overall cost is another key parameter that should be met in considering alternative propulsion devices. In the event that a wide discrepancy occurs between initial costs, significantly lower maintenance costs or operating costs (due to higher propulsive efficiency) should be demonstrated in order to justify the more expensive system. As a general rule, waterjets' relative costs drop as power level increases. The designer should obtain price quotations from manufacturers and installed cost and maintenance data from experienced users to answer these questions.

Maintenance and service must be considered initially also. Any system can be engineered to minimize requirements, but experience provides the real answers. Routine maintenance and service requirements of waterjets and simple propeller systems tend to be very similar. Vulnerability to damage is very different between internally and externally mounted components, and may be a deciding factor.

When the foregoing requirements are met, waterjets can then be compared on the basis of their special advantages. Inherantly these include: shallow draft operation, safety, protection of working parts, virtually no vibration or gyroscopic forces, and ease of installation and incorporation into design. When appropriately applied, waterjets can offer high propulsive efficiency, low cost, elimination of gearboxes, low maintenance and service requirements, and exceptional maneuverability, acceleration, and stopping.

Some applications even arise where only waterjets are practical, due to extremely shallow or debris laden water.

Waterjets should not be applied to sustained high power operation at low speed (except in very special cases), to aerated portions of a hull, to directionally unstable hull forms, or to installations where the pump cannot be immersed at startup.

A range of waterjet sizes exists on an off-the-shelf basis for planing craft installation at 100-3,200 SHP, continuous, and boat speeds to around 50 knots (70 knots with special inlets). These are available as complete units, or subassemblies in some cases. Their peak propulsive efficiency ranges from about 0.50 to 0.60, net, when properly applied. Complete operational data is usually available or can be projected from experience obtained elsewhere in their "families". The variety of configuration and performance characteristics is still somewhat limited by low demand at present, but is expanding rapidly. The following discussions will be addressed primarily to these waterjet types.

Prospects for optimization of waterjet propulsion systems are somewhat limited by practical considerations. It is a simple matter to design an optimum waterjet for a particular application when craft requirements are well defined, but producing them on this basis is both expensive and time consuming. Instead, the boat designer must usually select from alternatives that are designed for broad usage, optimizing by choice rather than design. As demand increases, choice will broaden, and this process will become more flexible. When optimization is employed, it usually begins with a given speed and power determining pump characteristics, via pressure derived from jet efficiency at an appropriate loss coefficient; then flow is calculated with an assumed pump efficiency. Reiteration of the process is then made by adjustments for the assumed variables, weight influence, shaft speed, and cavitation allowance. Mechanical design follows, influenced by particular considerations of service, control, feasible construction, weight, space, and successful earlier practice.

Performance estimation for vessels propelled by available waterjets is usually a simple matter with appropriate data furnished by the manufacturer. A curve of resistance vs speed can be projected upon curves of thrust vs speed such as figure 9, to immediately produce a set of speed and power data. Propulsive efficiency, range, fuel requirements, etc., can then readily be computed, if desired. At extremes of speed and

power consult the manufacturer for performance corrections. In this process as well as any other, accurate boat weight, resistance, etc., are requisite to a successful prediction. Substantial, realistic margins on vital quantities benefit waterjet and propeller applications alike, and are strongly advised. When resistance data is not available, waterjet manufacturers can make ball-park estimates of performance from weight, power, and speed requirements, just as boat designers can with propellers. Boat length, beam, deadrise, LCG, etc., should be cited also, in order to make estimates as realistic as possible.

The subject of matching engines to waterjets can be the first or second key step in unit selection. Waterjet units are available for direct coupling to virtually all popular domestic engines in the 100-500 SHP range. Matching these then is as simple as overlaying engine and waterjet SHP as RPM powering curves, as is shown in figure 11. As a rule of thumb, the uppermost impeller trims are the most efficient and resistant to cavitation. The engine manufacturer likewise sets preferences on shaft speed for continuous operation. The low limit for the engines shown can be taken at 2,150 RPM. Hence, instead of the desired "A" trim, impellers "E" and "M" would be selected in the example given. Note that waterjet powering curves remain essentially constant in spite of variations in boat speed. Also, the jet will probably operate at a higher shaft speed than a propeller will for a given power, as shown in figure 12. Impeller trims refer to geometrical modifications that can change an impeller's speed some 20% at constant power or change power absorbtion 50 to 100% at constant speed.

At powers above 500SHP, gas turbines are becoming most common as the prime movers for high speed craft in waterjets' favorable operating range. It is not practical to match pumps to their high shaft speeds. Hence reduction gearboxes are used, and these can be tailored to turn the most suitable impeller. More freedom of waterjet design for tradeoffs between performance, weight, and cost is allowed, compared with the direct-coupling case.

Waterjets and gas turbines, both being similar as turbomachines, make a desireable match for one another. Power and speed characteristics are similar, and transitions are very smooth. Vibration is practically nonexistant. Waterjets power requirements tend to closely follow the turbines' optimum operation line. Waterjets benefit any engine and prolong its life by being a smoothly operating load device that will not overload (even with debris inside).

A waterjet user should remain aware that the direction of shaft rotation in a pump is almost always clockwise facing aft from inlet toward discharge. He should also note that immersion of the pump should be sufficient to allow startup from rest (a static waterline at the pump centerline is sufficient), yet little enough that the inspection cover or an extension of it can be used without flooding the vessel.

APPLICATION DETAILS

Selecting the most suitable number of waterjet units for a vessel can be a simple or very trying process. Key considerations here are the availability of units, their weight, cost, and efficiency, the power, RPM, cost, and weight of available engines, and the amount of space available. Ideally, waterjets for a particular craft should be powered to produce the highest possible jet efficiency. Considerations of cost, weight, and life, or availability may make this impractical, however. One waterjet unit could be driven by two different engine sizes in a two or three shaft line installation at equal total power, and total thrust would vary as shown in figure 14. In this case both thrust and life are greatest with three at low speed, but thrust is highest at high speed with two. In another case three small units at high power for each might be compared with one or two larger units at high or low power for each, all combinations generating equal total thrust. The larger units' added cost or weight would have to be offset by deleting the third engine and/or by their operation at higher propulsive efficiency.

When large jets are feasible choices but direct coupling to desired large diesels is not possible, a variety of inexpensive, simple reduction gears is available.

The absence of underwater appendages has other ramifications than invulnerability for waterjet propelled vessels. Hull form must be depended upon for directional stability. Low forefoot profiles popular for propeller driven planing craft may cause wandering or spinning out at high speed with waterjets. Skegs are an effective solution to this problem. Prismatic - especially deep vee-hull forms are a better solution. These forms also steer precisely. Waterjet propelled craft can turn very rapidly, without excessive heel,

yet never trip in a turn. Turning radii of one to two boat lengths at maximum speed are commonly attainable. Jet boat control feels "slippery" to an inexperienced operator, primarily as the result of no appendages; but practice leads to equal and usually better boat control with the jets than with propeller systems.

The hull bottom form usually has little effect upon inlet performance, in spite of popular conceptions to the contrary. Skegs, keel coolers, and other protruberances upstream of inlets however, should be so located as to insure that streamline flow is reestablished ahead of the inlets. Aerated conditions arising from inverted vee forms, flat bottom hulls at high speed, or continual broaching of inlets must be avoided.

The location of waterjet units fully astern provides the opportunity for wide choice of LCG location and general arrangement by permitting the engine weight and bulk to be located aft as well as in its traditional location.

It should be added to the earlier discussion of waterjet control systems that manual actuators are usually sufficient for up to about 300 SHP industrial duty applications above that level, power assisted devices are required. These can be expected to become standard options for the appropriate waterjet units. Proper alignment of steering deflectors is at least as important as that of rudders. Adequate clearance must be allowed for operation of the reversing mechanisms.

The most precise low speed maneuvering with waterjets is obtained when throttle and shift can operate independantly of one another. This allows high thrust to be switched instantly from forward to reverse and in between. This arrangement may not be suitable for many operators however, who must use instead the integrated single lever arrangement. These still shift very quickly and can be very effective. The operator should be made aware that high idle or greater shaft speed is required for sufficient thrust with a jet, or else he will encounter sluggish response. A control with adjustable idle such as the Morse "MK" makes a good compromise.

In industrial duty waterjet applications it is usually necessary to protect the external control parts ("steering assembly") from impact with docks, pilings, other vessels, etc. This is accomplished by fitting a functional fender, step, or bustle around or above these parts, or by recessing the whole into the transom with just enough clearance for control functions.

Pleasure craft jets commonly are offered with either inboard or outboard mounting of the bulk of the unit to meet various needs for engine location. Inlet grill housings are available with various entrance shapes to fair with the many keel/garboard forms encountered in single unit installation. Industrial duty units are inboard mounted only, with flat grill housings. Occasionally needs for floating mounting arise, whereby the unit is supported at 3 or 4 points and fitted with flexible boots at inlet and discharge to isolate the unit from hull flexure.

Grills are available for any application in a variety of forms to cope with special debris problems such as rocks and certain weeds. Weeds that are admitted to the pump and will not pass through can be minced to do so by special weed cutters fitted to the inspection cover. Occasional debris will hang up in the impeller of a waterjet in spite of precautions, but this is very rare, especially in high specific speed units. (One high production unit has never had this happen.) When this does happen the pump loses thrust and torque and usually vibrates. Operation can be continued but is advised against. Clearing of the impeller through the inspection hole is quite simple. The engine must be stopped, of course, for safety's sake, during this operation.

Drive shafting for waterjets becomes a function of the configuration of the propulsion system, and the precision with which components are held in relation to one another. Routine gasoline and diesel installations use double universal jointed shafts to accomodate misalignment imposed by installation and working of the hull under way. The pump shaft cannot flex as readily as a long propeller shaft can, thus it must be protected by the coupling. Available drive shaft lengths range from 4-½ inches to several yards (with intermediate support as required.). Gas turbines over 500 SHP and their gearboxes are close coupled and carefully hard-mounted to the waterjets using gear type couplings that are very short and accomodate only small misalignment.

Corrosion problems of the waterjet itself are addressed in its design. However, some installations may impose galvanic corrosion problems. In fiberglass, wood, or concrete vessels waterjets may suffer if they are not electrically isolated from other machinery or electrical sources. Installations in aluminum or steel vessels pose few problems because the waterjet is compatable with or more cathodic than the hull. (except aluminum units in steel hulls.) Local isolation, coating of both jet and hull, and the bulk or size of the hull together protect the hull completely when it is more anodic.

SPECIAL APPLICATIONS

Racing is a natural offshoot of successful pleasure craft propulsion. There has been considerable racing activity with waterjets in California and Texas, and competition is very keen. All units used are modified from stock, for no special racing units have been built to date. Drag racing imposes the most severe requirements. Jet drag boats have exhibited perhaps the strongest initial acceleration of any existing form of transportation, responding instantly to full power. However, at the top end their performance fades as the result of improper inlet application. This deficiency will in time be corrected as demand warrents. The success of rather crude flow diverters at more than 100 knots promises great success for sophisticated forms. Cavitation must of course be present, but is hardly noticed in units that are properly prepared, and where boat speed changes rapidly. In marathon and circle racing the exceptional turning ability and acceleration of jet boats presents thrills and an edge over otherwise faster propeller driven craft. Special nozzle sizes to help suppress cavitation, relocation and trimming of nozzles to improve boat trim, and lightweight reduction gears have become important modifications to racing waterjets. The gearboxes permit use of "A" impellers with very high speed engines, for considerable advantage over heavily trimmed impellers.

Combination propulsion unit/fire pump waterjets have been steadily popular over many years. These are constructed from high pressure jet units with a valve and elbow placed between pump and nozzle, leading into a water main to hydrants and monitors. A compact, simple machinery arrangement results. Pure pumping units based on waterjet components have also been built.

Hydrofoil and air cushion craft represent the most conspicuous special industrial type waterjet applications.

Jets are uniquely suitable for these craft simply by elimination of the complex and notoriously unreliable drive trains to propellers. They have problems too, insofar as working fluid must be routed over long distances, incurring hydrodynamic losses, added drag, and weight penalties. Proper tradeoffs between key variables however, will result in highly successful system designs. See inlet and state-of-the-art discussions above. Waterjets for these vessels are non-optimum with respect to jet efficiency in the direction of high jet velocity. This is associated with low flow, intentionally low specific speed pumps to minimize duct size, weight, and drag influence.

A key problem in pump application to these craft is a prominant hump thrust requirement at low speed and inlet pressure. This leads to cavitation problems at the required power. Low specific speed pumping, multistaging, or a special inducer stage helps to alleviate the problem. See cavitation discussion, above. Usually these problems are not as severe as those of propellers in these applications.

Other low speed requirements should be mentioned in passing. There are a few applications for craft that operate at less than 15 knots yet must have extreme shallow draft. These are special tugs, barges, and military craft. Here specially adapted waterjets can be applied, at reduced power or life. Very high specific speed units are called for. Tugboats with a substantial deadheading or free running requirement can be designed to do so at high speed, then tow at substantial power with waterjets, circumventing the need for expensive, vulnerable controllable pitch propellers.

Other special applications are too limited to mention or have not been thought of yet. The near future will see considerable productive innovation in waterjet propulsion, and one day's special application will become the next's standard.

SUMMARY

Discussions of waterjet propulsion development, principles of operation, and considerations for application have been presented to familiarize the small craft engineer with this mode of propulsion in a usable sense.

A brief sketch was made of modern waterjet units, manufacturers, and key applications that have been made. It was concluded that refinements and accomplishments have established waterjet propulsion as a valid alternative to propeller systems when properly applied.

Basic hydrodynamic and mechanical characteristics of waterjet units were outlined for reference to clarify application considerations. Principles of hydraulic operation and jet thrust were pointed out to distinguish waterjet from propeller characteristics. Special considerations for cavitation and apparent appendage drag were described in detail. Propulsive efficiency characteristics were derived and shown to be competitive. Uniquely simple mechanical features were pointed out to indicate attainable quality, reliability, and ease of use.

Advice on waterjet application was presented first in perspective, then in detail. Criteria for selecting waterjet over propeller propulsion were defined. Issues of optimization and practical constraints were cited briefly. Techniques of boat performance estimation and matching waterjets to engines were spelled out. Special problems advantages, and tradeoffs with incorporating waterjets in boats were discussed in detail.

Finally, characteristics of special waterjet applications were described to illustrate some of the flexibility of this means of propulsion.

LIST OF SYMBOLS

g	acceleration of gravity, ft/sec^2
H_e	elevation head, ft
H_L	hydrodynamic head loss, ft.
H_n	head at the nozzle, ft
H_p	Head produced by pump, ft.
H_R	ram pressure recovery head, ft
$\dot{m}$	flow rate, slugs/sec
N	shaft speed of rotation, RPM
N_s	specific speed
N_{ss}	suction specific speed
NPSH	net positive suction head, ft
Q	flow rate, GPM
q	flow rate, ft^3/sec
R_A	appendage resistance, lbs
r_{ie}	radius of impeller entrance, ft
T	propulsive thrust, lbs
T_j	jet thrust, lbs
T_s	static or bollard thrust, lbs
V_{ie}	velocity at impeller entrance, ft/sec
V_j	jet discharge velocity, ft/sec
V_o	craft velocity, ft/sec

LIST OF SYMBOLS (Cont'd.)

ζ	hydrodynamic loss coefficient
η_a	"appendage efficiency"
η_j	jet efficiency
η_p	pump efficiency
η_t	thrust efficiency
μ	jet velocity ratio
ρ	fluid density, slugs/ft^3
σ	local blade tip cavitation number
ω	rotational speed, rad/sec

LIST OF FIGURES

REFERENCES

1 D. N. Contractor and Virgil E. Johnson,Jr., "Water Jet Propulsion". Paper No. 67-361 presented at AIAA/SNAME Advance Marine Vehicles Meeting, Norfolk, Virginia, May 22-24, 1967.

2 Hun Chol Kim, "Hydrodynamic Aspects of Internal Pump - Jet Propulsion", Marine Technology, Vol. 3, No. 3, January, 1966, pp. 80-98.

3 Claus F. L. Kruppa, "High Speed Propellers, Hydrodynamics and Design", The University of Michigan Continuing Engineering Education, October 9-11, 1967.

4 J. Arcand and D. R. Comolli, "Waterjet Propulsion for High-Speed ships". Paper No. 67-350 presented at AIAA/SNAME Advance Marine Vehicles Meeting, Norfold, Virginia, May 22-24, 1967.

5 John H. Brandau, "Aspects of Performance Evaluation of Water-Jet Propulsion Systems and a Critical Review of the State-of-the-Art". Paper No. 67-360 presented at AIAA/SNAME Advance Marine Vehicles Meeting, Norfolk, Virginia, May 22-24, 1967.

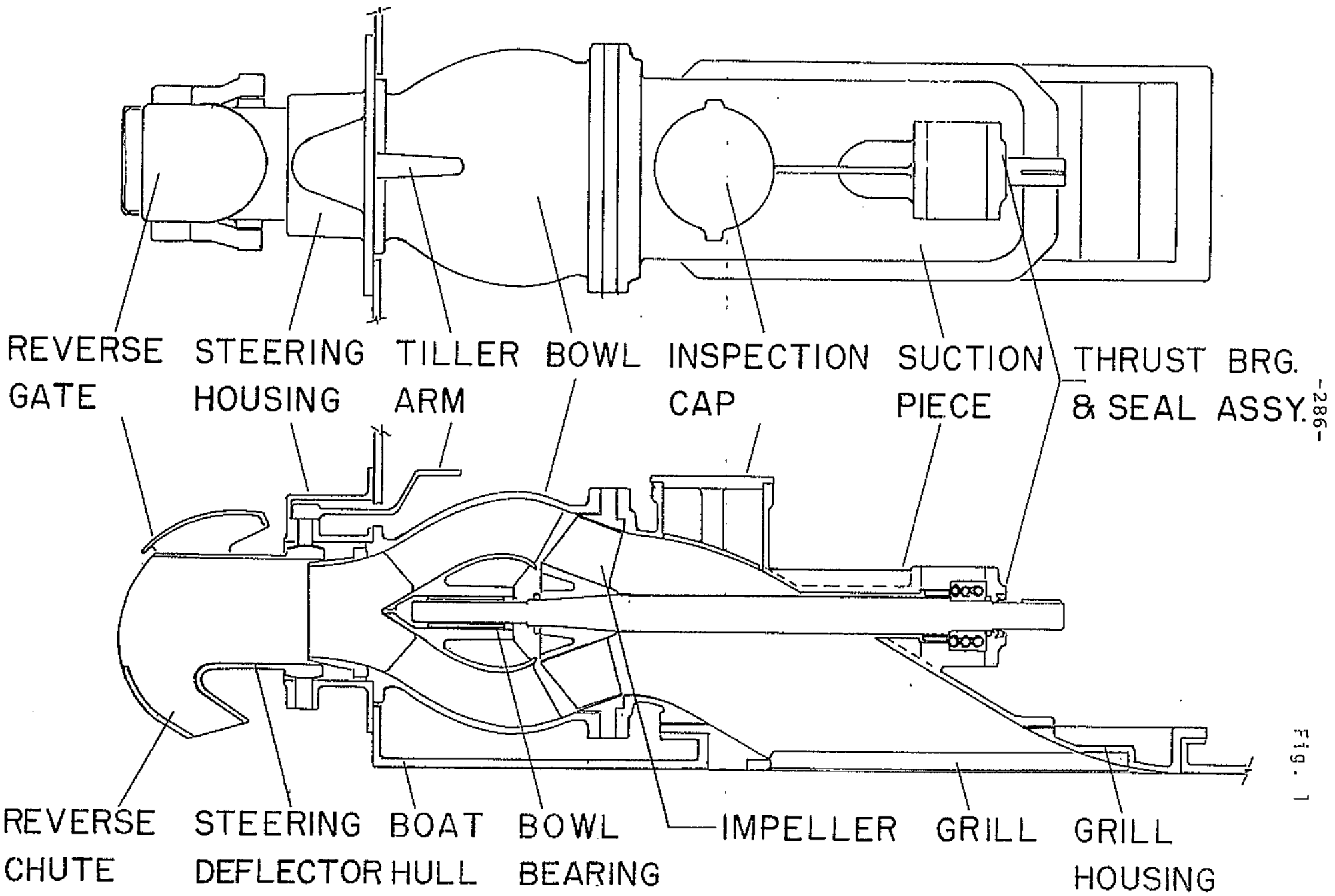
REVERSE GATE
STEERING HOUSING
TILLER ARM
BOWL
INSPECTION CAP
SUCTION PIECE
THRUST BRG. & SEAL ASSY.
REVERSE CHUTE
STEERING DEFLECTOR
BOAT HULL
BOWL BEARING
IMPELLER
GRILL
GRILL HOUSING

Fig. 1

Fig. 2

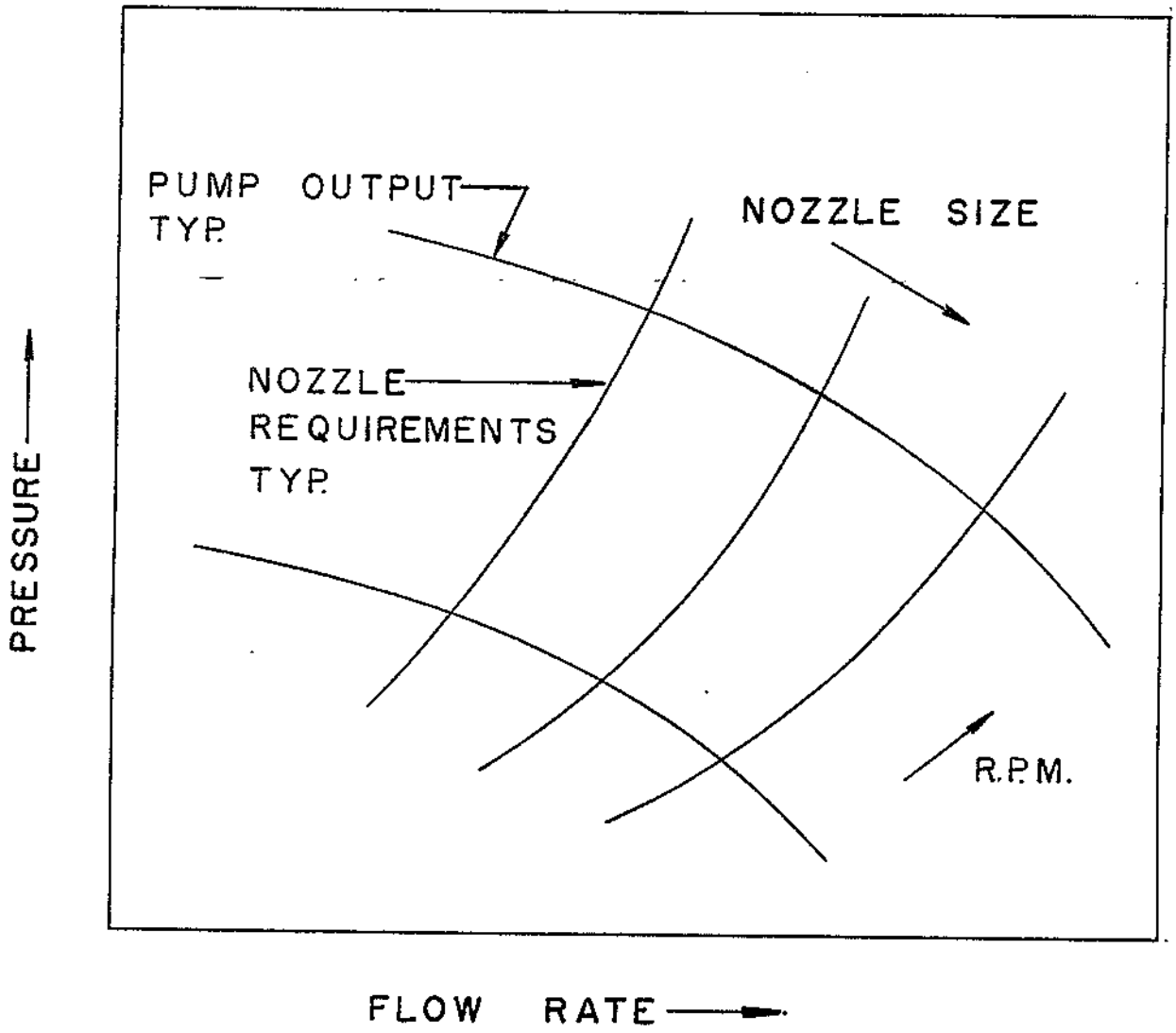
PUMP OUTPUT
TYP.
NOZZLE SIZE
NOZZLE
REQUIREMENTS
TYP.
R.P.M.
PRESSURE
FLOW RATE

Fig. 3

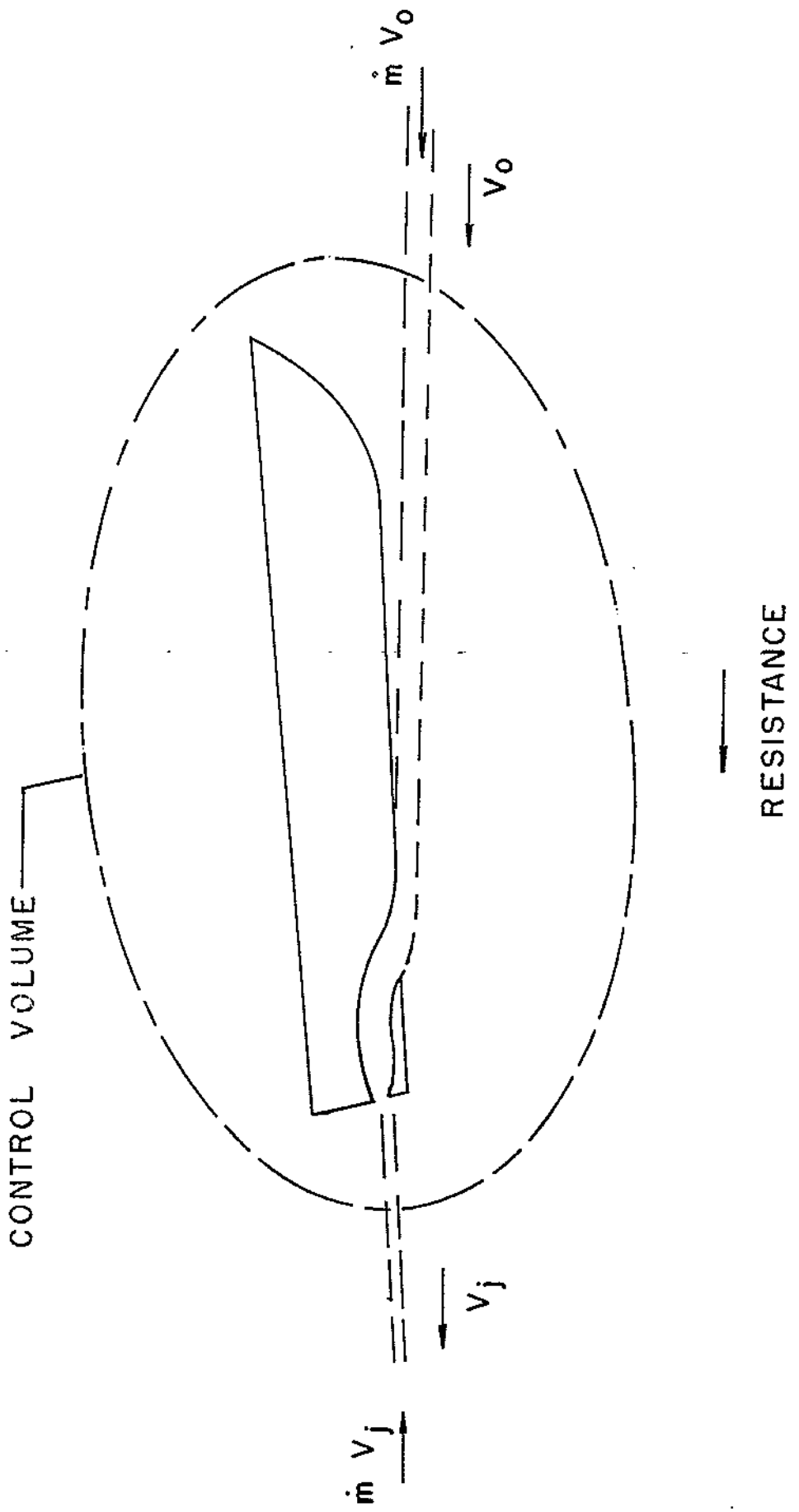

Fig. 4

COMPARISON OF RECTANGULAR AND ELLIPTICAL INLET RAM RECOVERY VARIATIONS WITH INLET VELOCITY RATIO

SYM	CONFIGURATION
⊡	RECTANGULAR
⊙	ELLIPTICAL – 0.3 IN. AFT LIP RADIUS

$$\eta_i = 1 - \frac{(P_{T_o} - \overline{P}_{T_i})}{P_{T_o}}$$

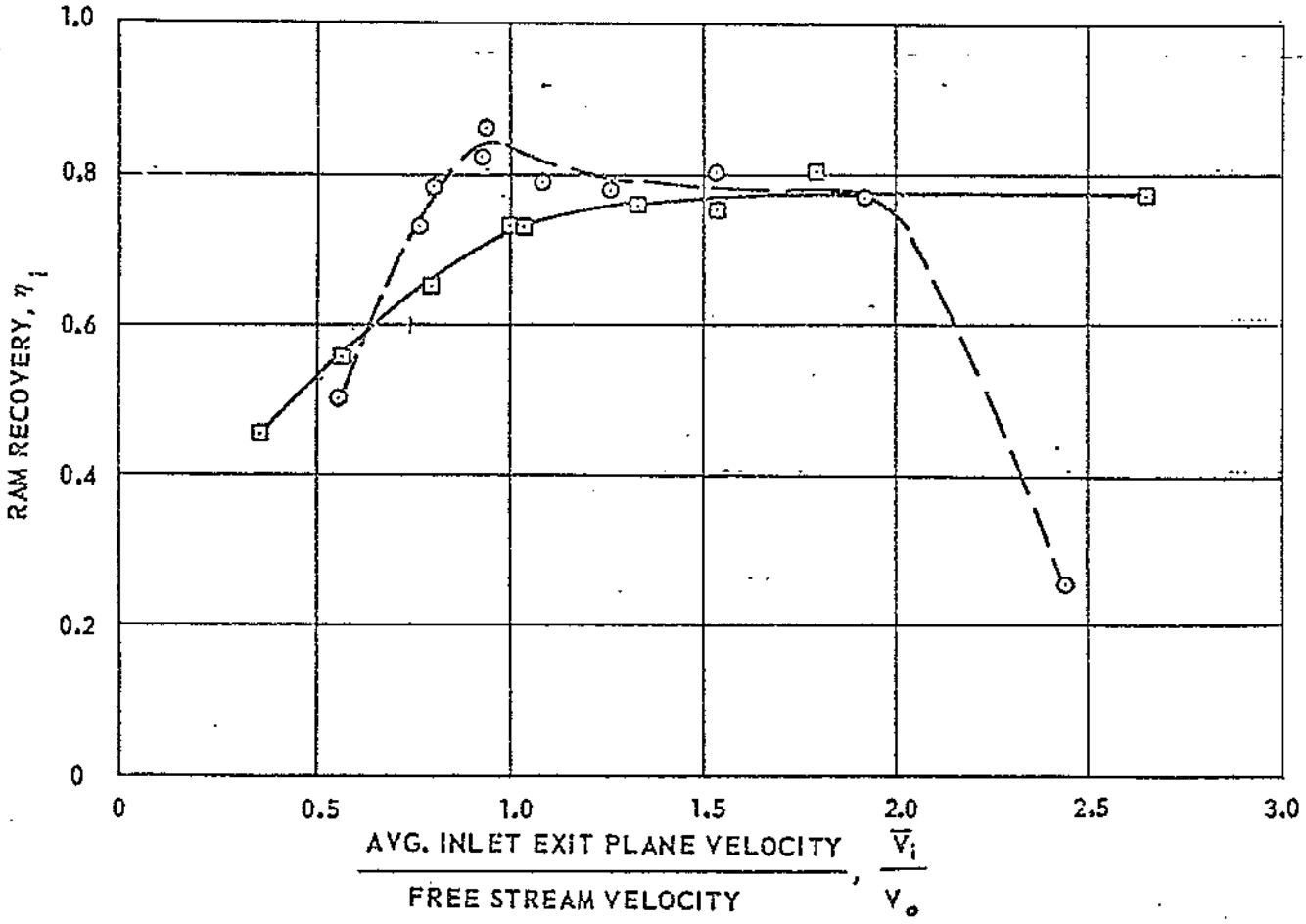

Fig. 5

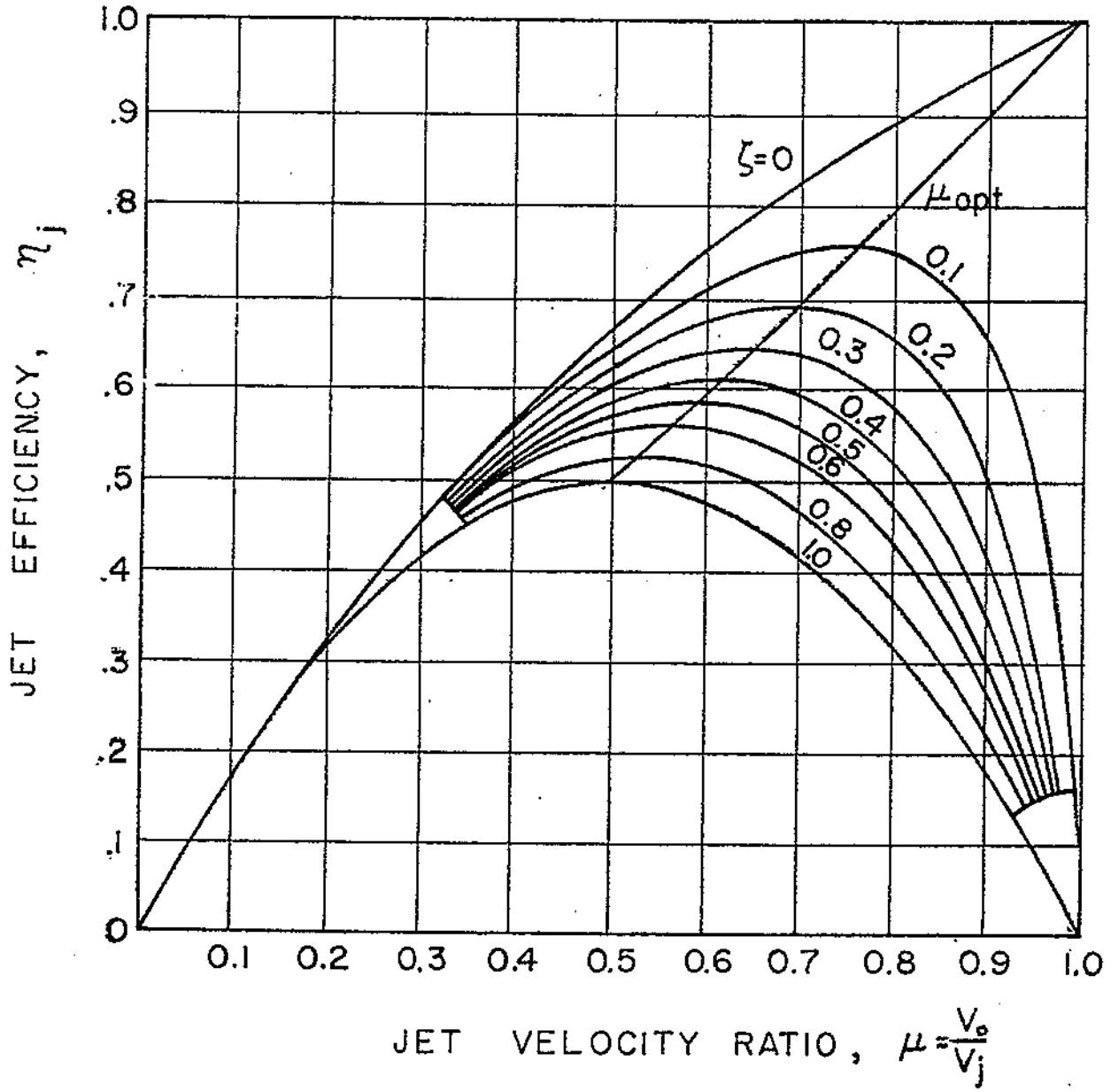
1.0
.9
.8
.7
.6
.5
.4
.3
.2
.1
0
ζ=0
μopt
0.1
0.2
0.3
0.4
0.5
0.6
0.8
1.0
0.1 0.2 0.3 0.4 0.5 0.6 0.7 0.8 0.9 1.0
JET EFFICIENCY, η_j
JET VELOCITY RATIO, $\mu = \frac{V_o}{V_j}$

Fig. 6

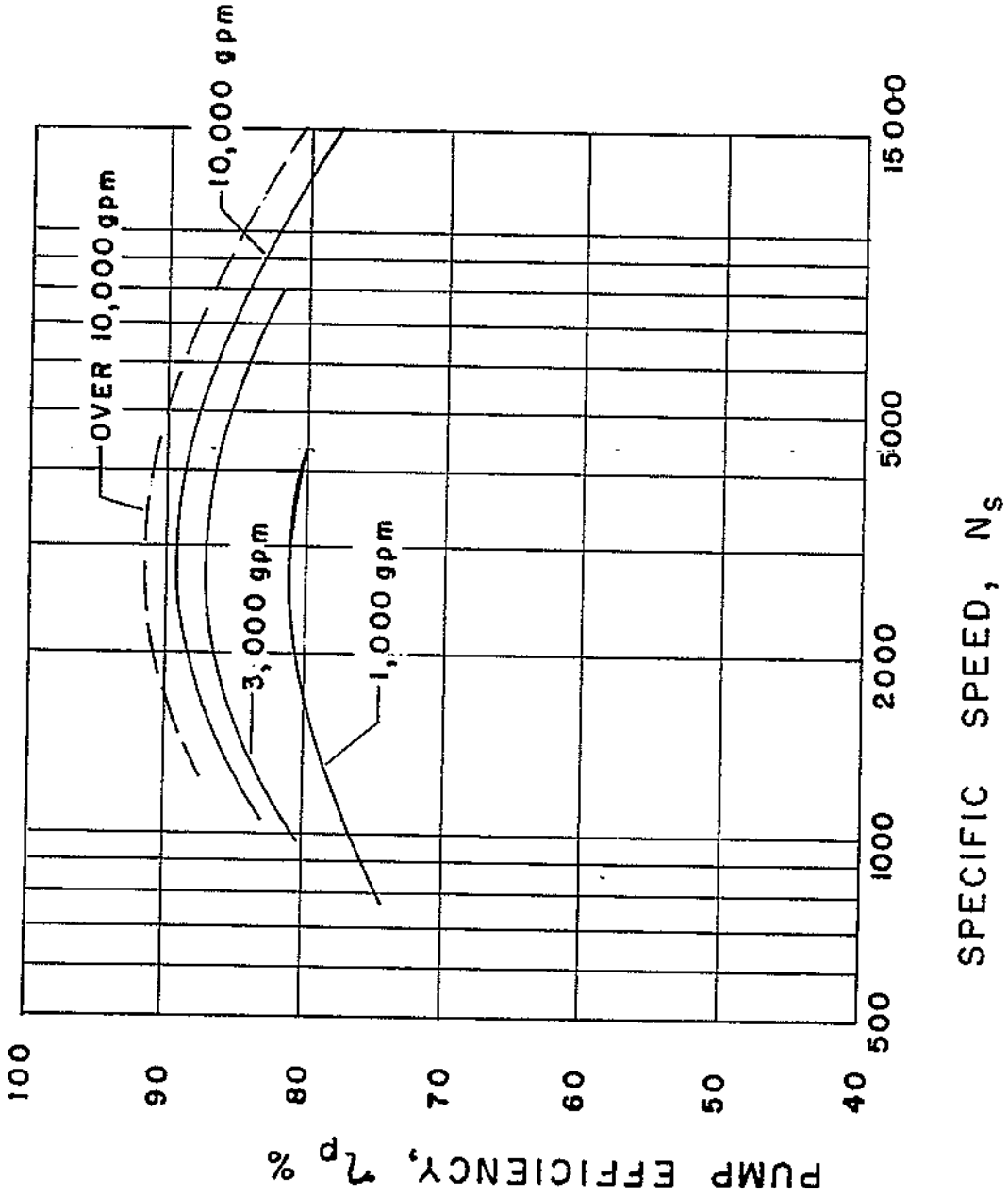
OVER 10,000 gpm
10,000 gpm
3,000 gpm
1,000 gpm
100
90
80
70
60
50
40
500
1000
2000
5000
15000
PUMP EFFICIENCY, η_p %
SPECIFIC SPEED, N_s

Fig. 7

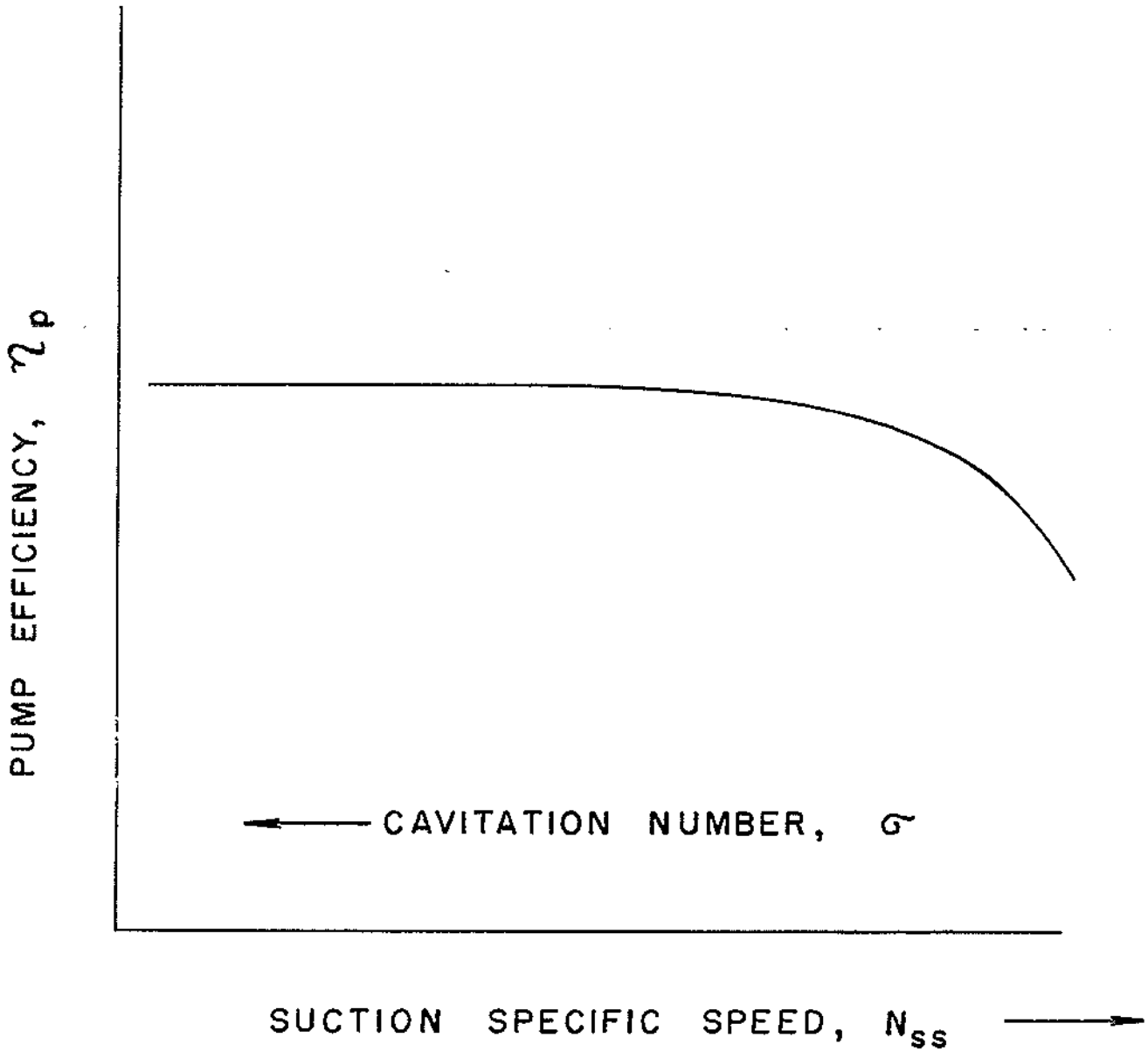
PUMP EFFICIENCY, η_p
CAVITATION NUMBER, σ
SUCTION SPECIFIC SPEED, N_{ss}

Fig. 8

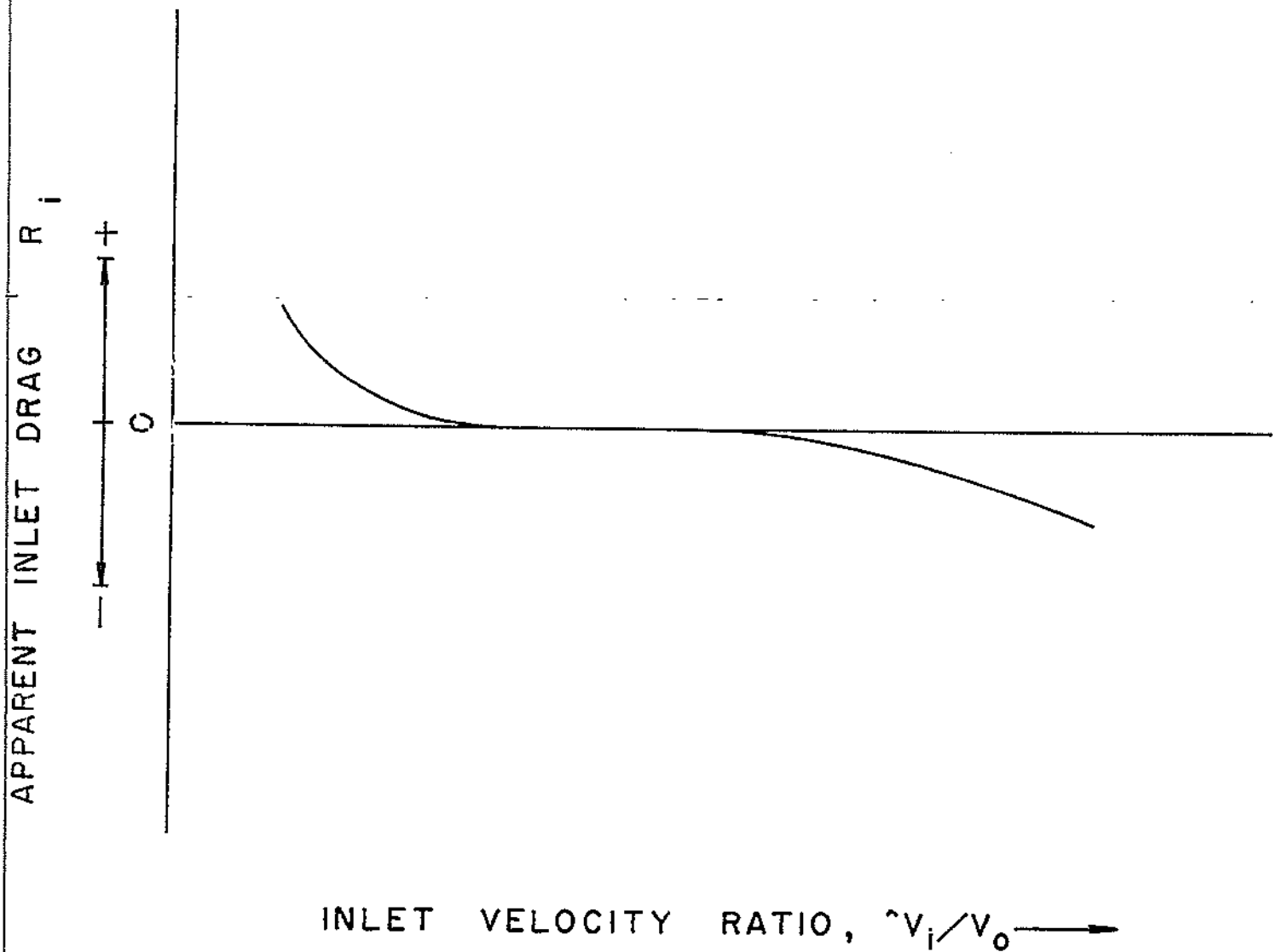

Fig. 9

ENGINEERING DATA SHEET I
DATE: 3-31-70
PAGE 9

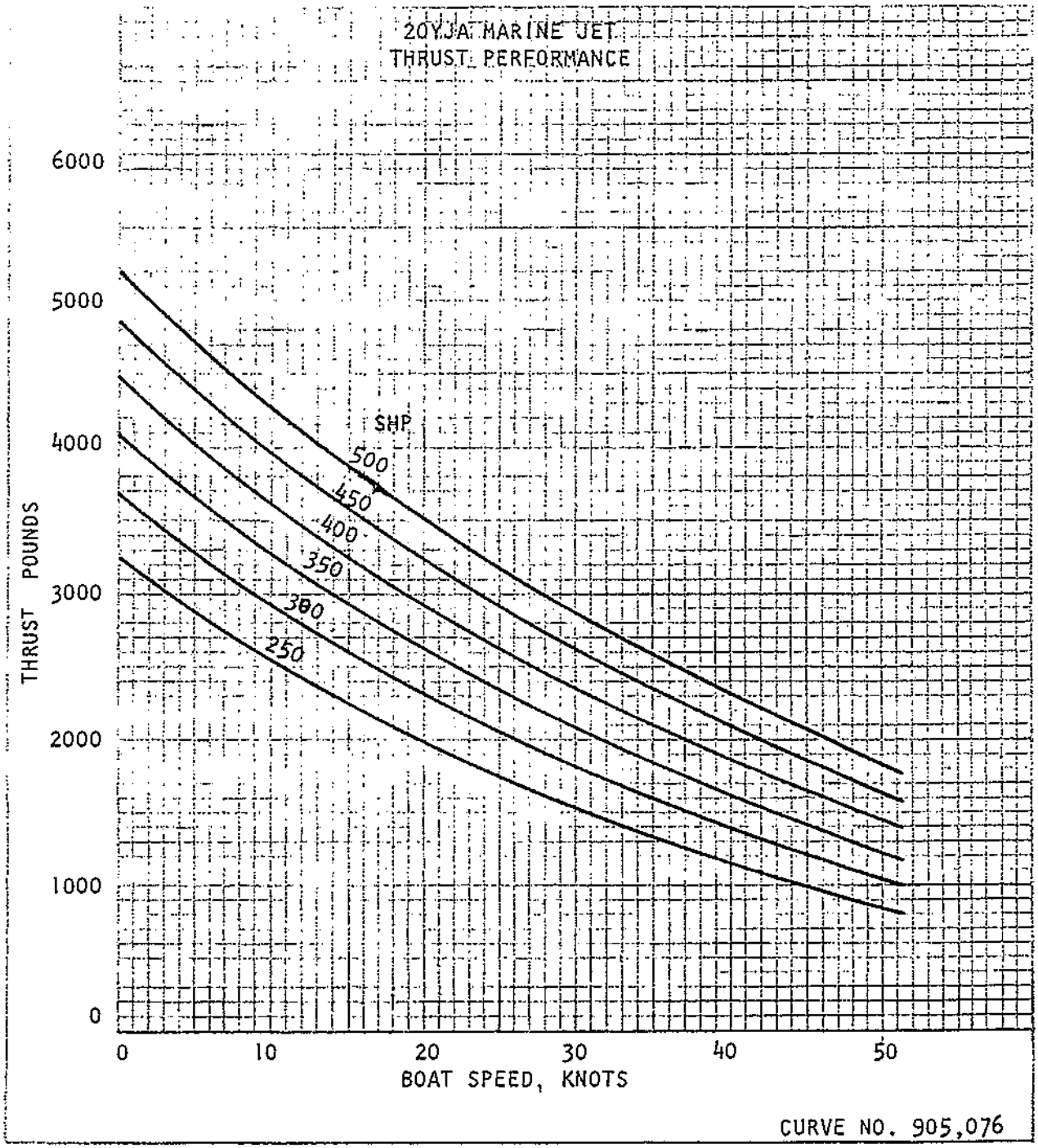

CURVE NO. 905,076

Fig. 10

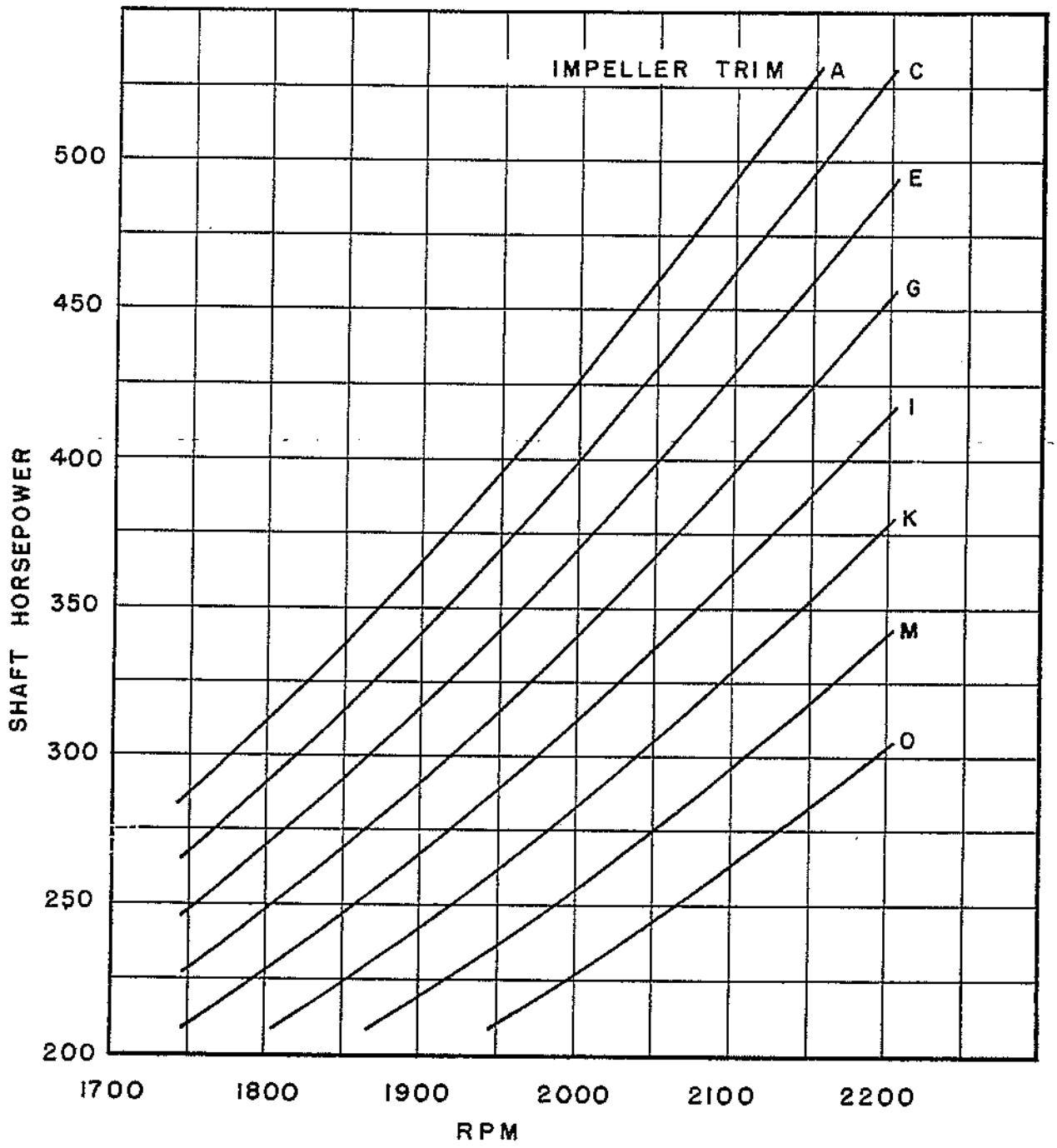
IMPELLER TRIM
A
C
E
G
I
K
M
O
500
450
400
350
300
250
200
SHAFT HORSEPOWER
1700
1800
1900
2000
2100
2200
RPM

Fig. 11

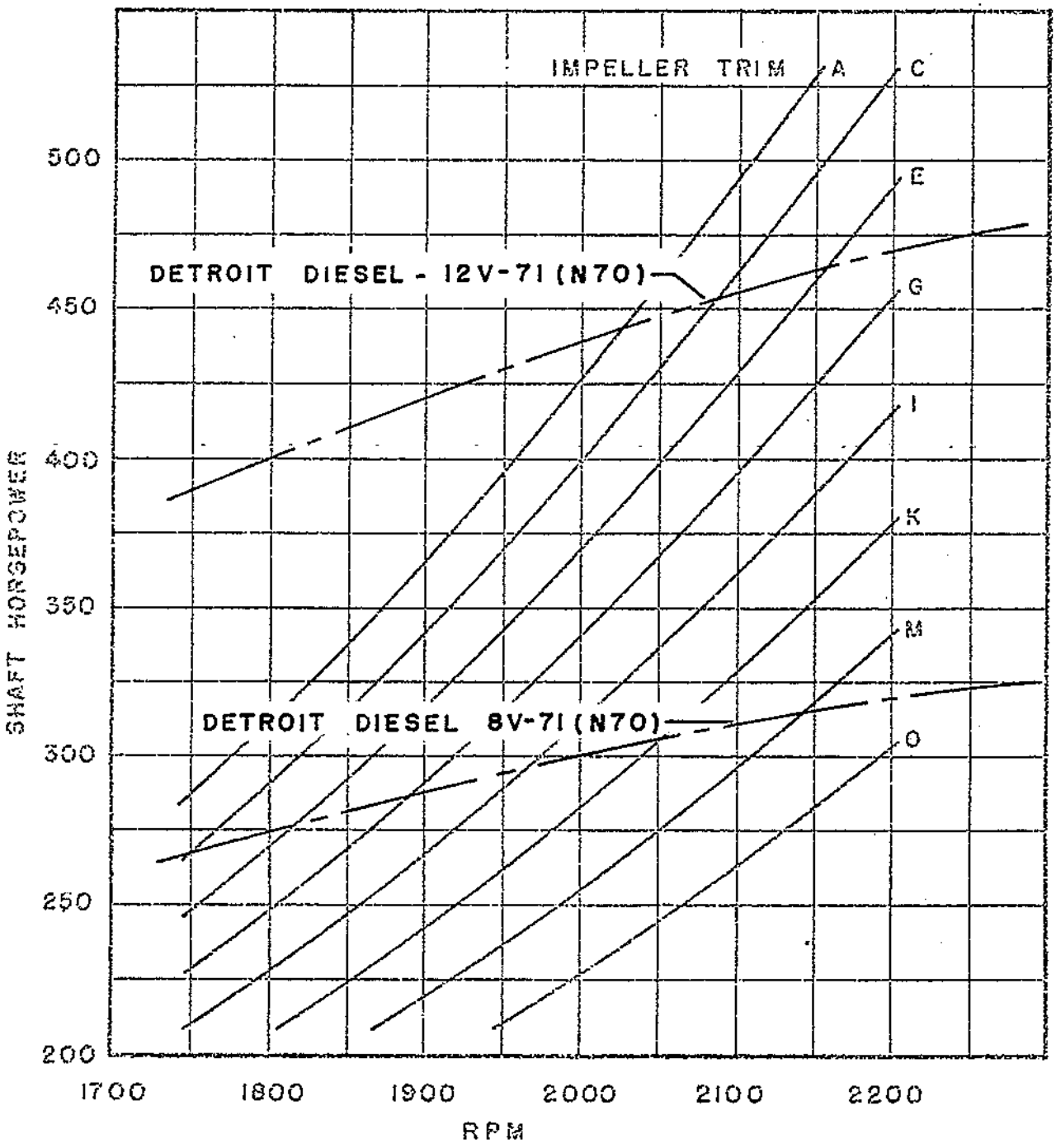
IMPELLER TRIM
A
C
E
G
I
K
M
O
DETROIT DIESEL - 12V-71 (N70)
DETROIT DIESEL 8V-71 (N70)
SHAFT HORSEPOWER
500
450
400
350
300
250
200
1700
1800
1900
2000
2100
2200
RPM

Fig. 12

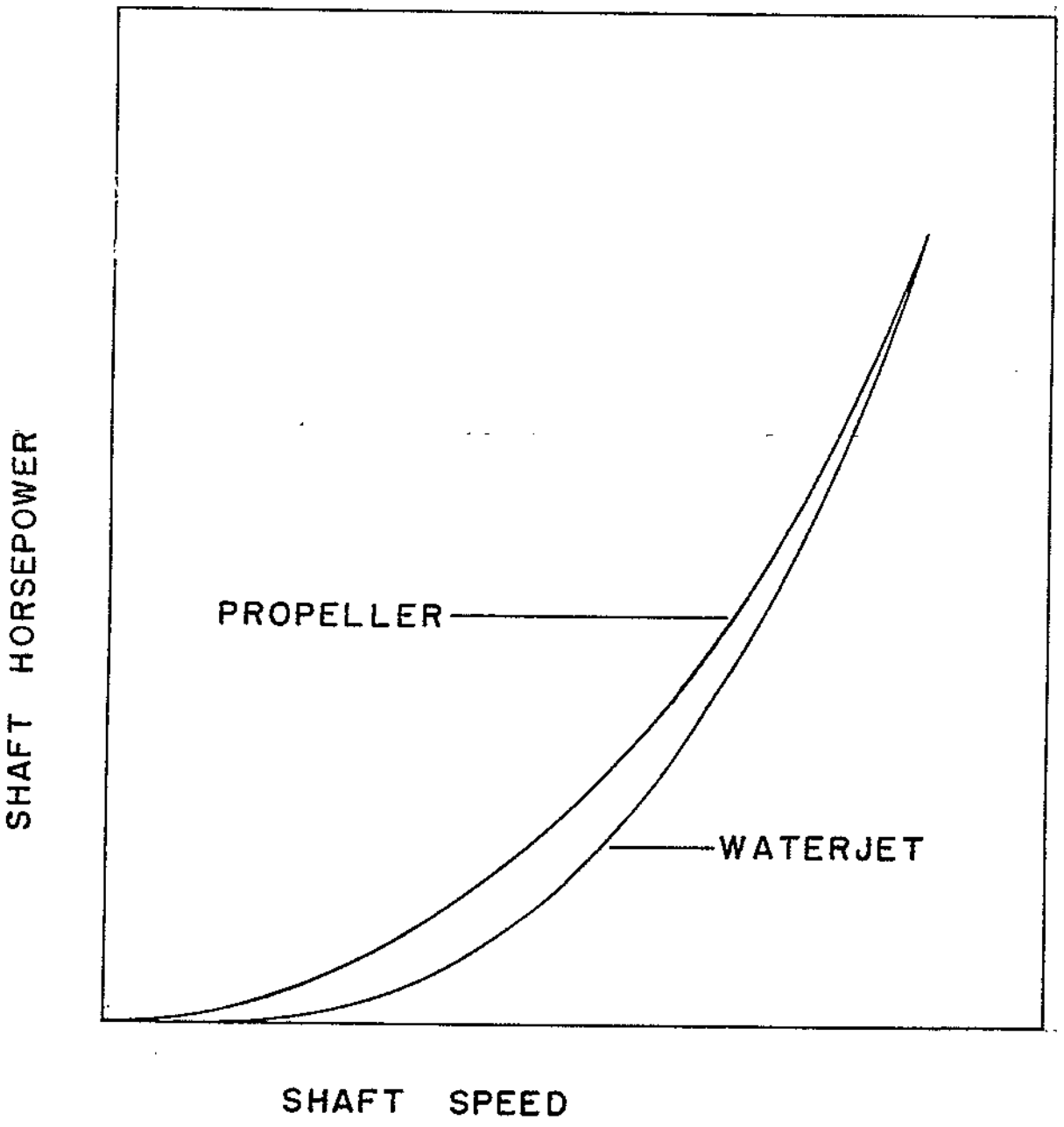

Fig. 14

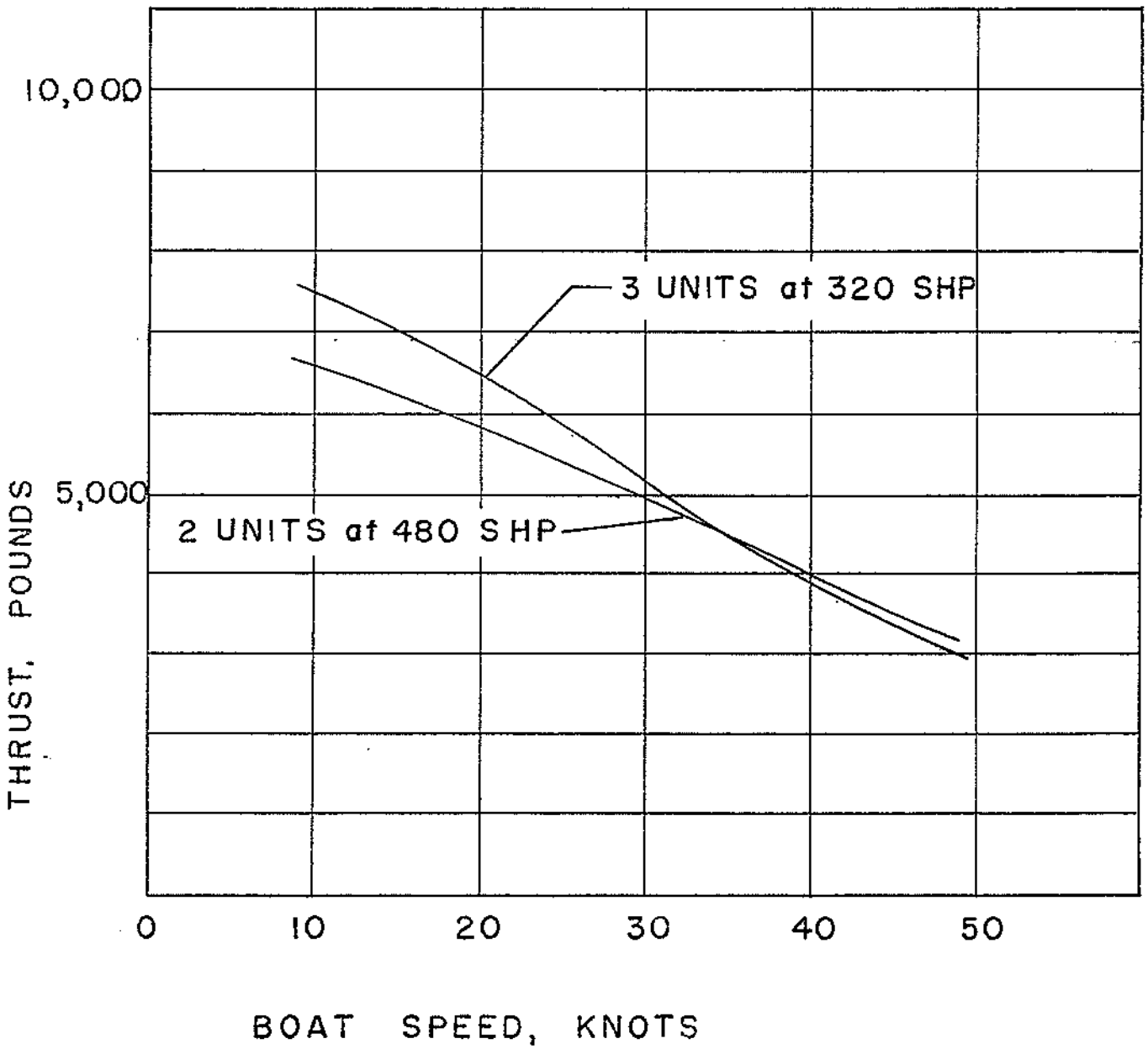
10,000
5,000
THRUST, POUNDS
3 UNITS at 320 SHP
2 UNITS at 480 SHP
0
10
20
30
40
50
BOAT SPEED, KNOTS

Fig. 15